UNRAVELING THE ROLE OF CELL WALL REMODELING FACTORS IN *ARABIDOPSIS* ROOT DEVELOPMENT



Priya Ramakrishna, BEng. MSc.

Thesis submitted to the University of Nottingham
for the degree of Doctor of Philosophy

September 2016

Abstract

Lateral roots are a key component of the plant root system architecture that help anchorage in soil and acquisition of water and nutrients. In the dicot *Arabidopsis*, lateral roots initiate post-embryonically from a specialised set of cells at the xylem pole of the pericycle cell layer termed 'founder cells (FC)', overlaid by three distinct tissue layers – endodermis, cortex, epidermis. The FCs undergo a coordinated series of asymmetric cell divisions (ACD) to form a primordium that grows and emerges through these overlying layers as a mature lateral root. Different auxin signaling modules, as well as tight regulation of the cell geometry are important during early organogenesis.

In this study, we were interested to identify molecular components that influence cell wall remodeling properties and cell geometry in the FC and regulates asymmetric cell division during early lateral root initiation. Transcriptomic analysis of FCs (De Smet et al., 2008) identified a candidate gene *EXPANSINA1* (*EXPA1*) of expansin superfamily, known for their unique ability to alter linkage between the cell wall polymers and cause wall loosening. *In vivo* expression studies showed that *EXPA1* is expressed in FCs prior asymmetric cell division. The mutant *expa1-1* exhibits perturbed ACD with a delay in kinetics of primordia from Stage I to II, loss in radial expansion of FCs in response to auxin which is important for organised formative divisions.

To understand if these defects are due to altered properties of the cell wall, and role of auxin in this process, we developed an optimised technique to study the chemical properties of the FC cell wall junctions based on confocal Raman spectroscopy. This showed altered interactions in *expa1-1* between the major cell wall polymers xyloglucans and pectins locally in the pericycle cell wall upon auxin treatment, that could influence cell geometry during early lateral root development. Additionally, sugar monomer analysis of digested whole roots showed interesting alterations in representative global wall sugar levels in the root which although diluted due to lack of tissue specificity warrants further study. In conclusion, the combination of molecular and biochemical analyses reveals that auxin dependent regulation of *EXPA1* plays an important role in lateral root FC and is required for organised asymmetric cell division.

Publications

Murphy E., Vu L.D., den Broeck L.V., Lin Z., **Ramakrishna P.**, van de Cotte B., Gaudinier A., Goh T., Slane D., Beeckman T., Inzé D., Brady S.M., Fukaki H. and De Smet I. (2016) RALFL34 regulates formative cell divisions in Arabidopsis pericycle during lateral root initiation. *Journal of Experimental Botany* **67**: 4863-4875.

Yue K., Sandal P., Williams E.L., Murphy E., Stes E., Nikonorova N., **Ramakrishna P.**, Czyzewicz N., Montero-Morales L., Kumpf R., Lin Z., van de Cotte B., Iqbal M., Van Bel M., Van De Slijke E., Meyer M.R., Gadeyne A., Zipfel C., De Jaeger G., Van Montagu M., Van Damme D., Gevaert K., Rao A.G., Beeckman T., De Smet I. (2016) Reciprocal regulation between ACR4 and PP2A-3 regulates formative cell divisions in the *Arabidopsis* root. *PNAS* **113**: 1447-1452.

Kajala K., **Ramakrishna P**., Fisher A., Bergmann D.C., De Smet I., Sozzani R., Weijers D. and Brady S.M. (2014) Omics and modelling approaches for understanding regulation of asymmetric cell divisions in *Arabidopsis* and other angiosperm plants. *Annals of Botany* 113: 1083-1105.

Ramakrishna P and De Smet I. (2014) Evolutionary Aspects of Auxin Signalling. In: Zažímalová E., Petrasek J., Benková E. (Eds.) Auxin and its role in plant development. *Springer Vienna* 13: 265-290.

Acknowledgements

"The journey is the reward"

The statement sums up my PhD experience in five simple words

I would like to express my sincere gratitude to my supervisors Professor Ive De Smet and Professor Malcolm Bennett for their support, guidance and encouragement that made this journey possible. I am grateful for the trust and confidence that was placed in me that motivated me to challenge myself and explore new ideas.

I am thankful to Tobias Baskin, Darren Wells and Graham Seymour for the interesting discussions that piqued my interest to learn more about the mysteries of the plant cell walls.

I also thank Evan Murphy for the interesting discussions and live-stream music in the lab that made time course experiments fun and feel not-so-time consuming. Tatsuaki Goh for introducing me to the wonders of 4D imaging of plants. I also thank my lab mates and all the people who have helped me in the lab and encouraged me to move forward.

I also thank Graham Rance for his help with the confocal Raman microscopy analysis and the Graduate School UNICAS sandpit award to carry out this interdisciplinary project.

I am very thankful to Ute Voss for the many brainstorming sessions we have had and for being a great friend. I also thank all the wonderful people I have met, the friendships built during this study that made this journey enjoyable.

Special thanks to my parents for their moral support and encouragement in their own sweet caring way. A big thank you to Kamaljit for cheering me along through this long journey.

I thank the University of Nottingham for the Vice Chancellors Scholarship for Research Excellence and the School of Biosciences for the financial support to undertake this research.

Contents

Abstract ..... **i**

Publications ..... **ii**

Acknowledgements ..... **iii**

Contents ..... **iv**

Abbreviations and acronyms ..... **ix**

List of figures ..... **x**

List of tables ..... **xiv**

Thesis structure **1**

CHAPTER 1. IMPORTANCE OF THIS RESEARCH 3

1.1. Motivation and significance **4**

1.2. References **8**

CHAPTER 2. ASYMMETRIC CELL DIVISION AND LATERAL ROOT FORMATION 9

2.1. Asymmetric cell division **10**

2.2. Asymmetric cell divisions during lateral root initiation (excerpt from review) **13**

2.2.1. Pre-initiation events 16

2.2.2. Anticlinal asymmetric division of pericycle cells 22

2.2.3. Periclinal asymmetric division of pericycle cells 24

CHAPTER 3. EXPANSINS AND CELL WALL REMODELING 25

3.1. Size and evolution of the expansin superfamily **27**

3.2. Plant cell wall structure **32**

3.3. EXPANSIN structure and action on wall **34**

3.4. The role of expansins in fundamental developmental events **40**

3.4.1. Root system architecture 42

3.4.2. Root hair formation 43

3.4.3. Leaf initiation 44
3.4.4. Stomatal opening/closing 47
3.4.5. Hypocotyl 47
3.4.6. Flower development and senescence 48
3.4.7. Pollen tube growth 50
3.4.8. Seed germination 50
3.4.9. Fruit 51
3.4.10. Secondary wall formation 53

3.5. Hormonal regulation of plant expansins 54

3.6. Future perspectives for expansin research 59

Aims and objectives: 61

CHAPTER 4. EXPANSINA1 IS IMPORTANT FOR ORGANISED CELL EXPANSION AND ASYMMETRIC CELL DIVISIONS DURING LATERAL ROOT INITIATION IN ARABIDOPSIS 62

4.1. Introduction 63

4.2. Results 64
4.2.1. Meta-analysis to identify cell wall remodelling genes active during lateral root initiation 64
4.2.2. EXPA1 is expressed in the pericycle during lateral root initiation 67
4.2.3. EXPA1 is regulated by auxin and is a secondary response downstream of SLR-ARF7-ARF19 module 69
4.2.4. In-vivo analysis of pEXPA1::nx3GFP on auxin treatment 72
4.2.5. EXPA1 is involved in pericycle cell expansion during lateral root initiation 73
4.2.6. Auxin-mediated pericycle cell expansion during lateral root initiation 78
4.2.7. Auxin mediated cell size changes in overlaying tissue layers 81

4.3. Discussion 83

4.4. Materials and methods 91
4.4.1. Plant material 91
4.4.2. Genotyping 91
4.4.3. Growth conditions and media 92
4.4.4. Phenotyping 92
4.4.4.1. Measurement of primary root length and lateral root density 92
4.4.4.2. Lateral root staging 93
4.4.4.3. Lateral root bending assay 93
4.4.5. Generation of transgenic lines 93
4.4.5.3. p35S::EXPA1 overexpressor line generation 93

4.4.6. qRT–PCR 94
4.4.7. Confocal Imaging 95
4.4.8. Cell measurements 95

4.5. Supplementary figures 97

4.6. Supplementary tables 98

4.7. References 110

CHAPTER 5. CONFOCAL RAMAN MICROSCOPY BASED IMAGING OF ARABIDOPSIS ROOT SECTIONS 113

5.1. Introduction 114
5.1.1. Plant Cell Wall Components 114
5.1.2. Primary cell wall interactions and plant growth 118
5.1.3. Confocal Raman microscopy 119
5.1.4. Principle of Raman spectroscopy 120

5.2 Results 122
5.2.1. Optimisation of sample preparation for Arabidopsis roots by confocal Raman microscopy 122
5.2.1.1. Embedding media optimisation 122
5.2.1.2. Embedding procedure 123
5.2.1.3. Vibratome sectioning 123
5.2.2. Optimised Confocal Raman imaging of Arabidopsis root sections . 124
5.2.2.1. Sample preparation 124
5.2.2.2. Data acquisition 125
5.2.2.3. Data analysis 126
5.2.3. Raman spectra of pure wall compounds for reference 127
5.2.4. Differences detected in Raman spectra of Arabidopsis roots 131
5.2.5. Advantages and disadvantages of the techniques 134

CHAPTER 6. A COMPARATIVE STUDY ON CELL WALL PROPERTIES OF ARABIDOPSIS ROOTS AND WALL MUTANT EXPA1-1 136

6.1. Introduction 137

6.2. Results 139
6.2.1. Monosaccharide compositional analysis of whole roots of Arabidopsis by HPAEC-PAD 139
6.2.1.1. *expa1-1* roots exhibit reduced levels of galactose compared to wildtype 141
6.2.1.2. Auxin treatment induces alterations in composition of cell walls of Arabidopsis roots 142

6.2.2. Chemical analysis of pericycle cell wall composition of expa1-1 by confocal Raman microscopy 144
6.2.2.1. Chemical composition of root xylem pole pericycle cell wall..... 145
6.2.2.2. Auxin induced differences in composition of root xylem pole pericycle cell wall..... 147

6.3. Discussion 149
6.3.1. Monosaccharide profile and wall composition 150
6.3.2. Raman spectrum based differences in chemical composition of the pericycle cell wall..... 153

6.4. Materials and methods..... 156
6.4.1. Sample preparation for hydrolysis 156
6.4.2. Saeman hydrolysis 156
6.4.3. HPAEC-PAD 156
6.4.4. Confocal Raman microscopy..... 157

6.5. Supplementary figures..... 158

6.6. References 160

CHAPTER 7. A ROLE FOR BHLH49 IN ARABIDOPSIS LATERAL ROOT DEVELOPMENT 162

7.1. Introduction..... 163

7.2. Results and discussion..... 165
7.2.1. bHLH49 is specifically activated in the lateral root founder cells at primordia initiation 165
7.2.2. bHLH49 is required during early stages of lateral root primordia formation 167
7.2.3. Role of auxin in regulation of bHLH49 and root growth 171
7.2.4. bHLH49 as a potential transcriptional regulator..... 173
7.2.5. bHLH49 mediated regulation of cell wall remodelling genes 175
7.2.5.1. In silico promoter analysis of RALFL34 and EXPA1 promoter . 176
7.2.5.2. Protoplast assay to test bHLH49 mediated regulation of RALFL34 and EXPA1..... 177

7.3. Discussion 179
7.3.1. bHLH49 and lateral root development..... 179
7.3.2. bHLH49-mediated transcriptional regulation 180
7.3.3. Auxin-mediated control of bHLH49 expression 182

7.4. Materials and methods..... 184
7.4.1. Plant materials..... 184

7.4.2. Growth conditions and media 184
7.4.3. Genotyping 184
7.4.4. Phenotypic analysis 184
7.4.5. qRT-PCR 184
7.4.6. Microscopic analysis 185
7.4.7. Transient activity assays 185

7.5. References 186

CHAPTER 8. CONCLUSIONS AND FUTURE WORK 188

8.1. Conclusions - Bringing it all together 189

8.2. Future perspectives 198

References 202

Appendices 232

Abbreviations and acronyms

FAO	Food and Agriculture Organisation (of the United Nations)
ACD	Asymmetric cell division
RSA	Root system architecture
LR	Lateral root
LRI	Lateral root initiation
LRF	Lateral root formation
LRP	Lateral root primordia
LRIS	Lateral Root Induction System
DAG	Days after germination
TAIR	The Arabidopsis Information Resource
GO	Gene Ontology
NAA	1-Napthalene acetic acid
NPA	1-N-Naphthylphthalamic acid
CHX	Cycloheximide
SD	Standard deviation
SED	Standard error of the difference
SEM	Standard error of the mean
ANOVA	Analysis of Variance
FACS	Fluorescence-activated cell sorting
HPAEC	High Performance Anion Exchange Chromatography
EXPA1	EXPANSINA1
RALFL34	RAPID ALKALINISATION FACTOR LIKE 34
bHLH	basic Helix-Loop-Helix
ACD	Asymmetric cell division
XPP	Xylem pole pericycle

List of figures

Figure 1.1. Infographic that explains the challenges we face in maintenance of food security (Source: ccafs.cgiar.org/bigfacts). 6

Figure 2.1. Schematic of an Arabidopsis plant indicating few developmental processes where asymmetric cell division occurs; embryo development- which occurs after fertilization of the flower in the silique (seed pod), symmetry breaking in the leaf epidermis during stomatal development and asymmetric cell division that gives rise to the ground tissue in the root Figure taken from (Petricka et al., 2009). 11

Figure 2.2. Schematic of key features and steps that are frequently observed during asymmetric cell division (ACD). ACD could give rise to unequally sized daughter cells (a) or equally sized daughter cells (b,c) Figure taken from (De Smet and Beeckman, 2011). 12

Figure 2.3. Schematic representation of the primary root of Arabidopsis thaliana indicating the developmental progression along (pre-initiation events) leading to Asymmetric Cell Division (ACD).. 15

Figure 3.1. A simplified schematic showing the evolution of the EXPANSIN superfamily. 29

Figure 3.2. A schematic of the EXPANSIN protein with its conserved domains. 36

Figure 3.3. A simplified model for EXPANSIN action in a plant cell.. 38

Figure 3.4. Expansins in plant growth and development. The schematic highlights the various processes in plant that contain expansin expression and/or activity. 41

Figure 3.5. Schematic showing a simplified regulatory network of auxin, brassinosteroids (BR), gibberellins (GA), ethylene and abscisic acid (ABA) signalling in regulation of EXPANSIN expression that controls developmental and stress responses in plants..... 56

Figure 4.1. Schematic that depicts identification of *EXPA1* following meta-analysis of various cell wall remodelling genes. See also Supl. Table 4.1. and 4.2. 65

Figure 4.2*. In vivo* expression analysis of *pEXPA1::n3xGFP*. *EXPA1* expression observed in lateral root founder cells. 68

Figure 4.3. 3DPG Col-0 seedlings analysed for EXPA1 levels by qRT-PCR.. 71

Figure 4.4. Comparison of expression profile of *pEXPA1::n3xGFP* expression in 3DPG roots that are untreated and imaged post gravitropic stimulus (a, c) and post 15hrs 10µM NAA treatment (b, d). 72

Figure 4.5. T-DNA insertion diagram of *expa1-1* with insert located 60bp upstream of the start site (ATG) in the 5′UTR region of the gene (a); qRT-PCR on *expa1-1* line

indicating the T-DNA line was a full knock-out of *EXPANSIN1* expression (b) (n=3 ±SE). 74

Figure 4.6. Schematic of lateral root bend assay (a); representative data of Col 0 and *expa1-1* analysed 18 hours post bend for early initiation defects (b); 42hrs post-bend for emergence defects (c)..... 75

Figure 4.7. Stage I primordia visualised in wildtype (a) and *expa1-1* background (b); Quantification of frequency of occurrence of defective primordia in Col 0 vs *expa1-1* (c)..... 77

Figure 4.8. Visualisation of lateral root initiation in roots of 3DPG seedlings that were imaged 12hrs gravitropic root bend in wildtype and *expa1-1*. Walls visualised using plasma membrane marker WAVE131YFP..... 77

Figure 4.9. Schematic of lateral root induction system (Himanen et al., 2004) (a); illustration of root confocal slice used for cell width measurements (b); representative 2D confocal slices of wildtype and *expa1-1* roots without auxin (+NPA, -NAA) and with auxin treatment (+NPA,+6hrNAA) root used for cell size measurements. 79

Figure 4.10. Box plot showing distribution of pericycle cell width for Col-0 (WAVE131YFP) and expa1-1 (*expa1-1*xWAVE131YFP). Seedlings were grown on 10µM NPA, and post treatment on 10µM NAA. 80

Figure 4.11. Box plots showing the distribution of cell length (a), width (b) and the ration of length/width (c) between Col-0 (WAVE131YFP) and *expa1-1* (*expa1-1*xWAVE131YFP) for pericycle (A), endodermal (B), cortical (C) and epidermal cells (D). and distribution of cortical cell length (d). Seedlings were germinated and grown on 10µM NPA and a batch post-treated with 10µM NAA for 6 hrs,. 82

Figure 4.11-1. Schematic of transverse section of the root with the two xylem poles in focus (A); View of the pericycle cell layers involved in asymmetric cell division from the side (B), the three-adjacent xylem pole pericycle cells are marked by the yellow asterix. 85

Figure 4.12 A. Schematic timeline of lateral root initiation with approximate times based on literature and observation..... 87

Supplementary figure 4.1. Expression pattern of *pEXPA1::nx3GFP* in the root tip. Cell wall visualised by propidium iodide staining..... 97

Supplementary figure 4.2. Box plot showing quantification of emerged lateral root densities of Col 0 and expa1-1 97

Figure 5.1: Schematic of polysaccharide structures found in plant cell walls..... 116

Figure 5.2. Schematic of light interactions with a surface (a); Schematic of Raman Effect that Raman spectroscopy is based on (b)..... 121

Figure 5.3. Schematic of confocal Raman instrument setup. 125

Figure 5.4. Raman spectra of commercially available cell wall compounds- cellulose, xyloglucan and pectin. Peaks assigned based on literature (Table 5.2) 129

Figure 5.5. Representative cross section of Arabidopsis root slice viewed under 100X magnification used for confocal Raman spectroscopic analysis. 131

Figure 5.6. Average Raman spectrum at the xylem pole pericycle cell junction of Col 0 roots under untreated (i.e. 10µM NPA grown) and post 6hr 10µM NAA treatment condition.. 133

Figure 6.1. Estimation of recovery of sugars following total acid hydrolysis (TAH)..140

Figure 6.2. Representative graph of 2 biological replicates of monosaccharide profiling of 10DPG roots of Col 0 and *expa1-1*. 141

Figure 6.3. Monosaccharide composition profile of 10DPG Col 0 and *expa1-1* roots under untreated (-NAA) and post 10µM NAA treatment (+6hr NAA) conditions. 143

Figure 6.4. Composition of Glucose (a) and Galactose (b) in 10DPG roots of Col 0 and *expa1-1* under untreated (-NAA) and post 10µM NAA treatment (+6hr NAA) conditions. 143

Figure 6.6. Average Raman spectrum at the xylem pole pericycle cell junction of Col 0 and *expa1-1* roots under untreated conditions (i.e. 10µM NPA grown). 146

Figure 6.7. Average Raman spectrum at the xylem pole pericycle cell junction of Col 0 and *expa1-1* roots under untreated (i.e. 10µM NPA grown) and post 6hr 10µM NAA treatment condition.. 148

Supplementary figure 6.1. Chromatogram of monomeric sugar standards analysed by HPAEC-PAD analysis. 158

Supplementary figure 6.2. Representative chromatogram of the separated sugars in untreated wildtype Col 0 (A) and *expa1-1* mutant (B); 6hr 10µM NAA treated roots of Col 0 (c) and *expa1-1* (D). 159

Figure 7.1. Expression profile of *pBHLH49::nx3GFP* visualised in the lateral root. Stage I (a,b), Stage II (c), and later stage primordia (d).. 166

Figure 7.2. Expression profile of *pBHLH49:BHLH49::sYFP* visualised in the lateral root. 167

Figure 7.3. qRT-PCR that shows *bhlh49-1* as a knockout line. 169

Figure 7.4. Box plots that show the distribution of primary root length (a) and lateral root density/cm of the root (b) in Col-0 and *pRPS5a::bHLH49* (n=2); Representative DIC images of close Stage I primordia and unusually positioned lateral roots in the overexpressor *pRPS5a::bHLH49* line (c).. 170

Figure 7.5. qRT-PCR of 3DPG Col-0 roots analysed for bHLH49 levels. Auxin treatment response time series (a); Expression profile in response to 10µM NAA, 10µM CHX and NAA+CHX 0, 2 and 6 hours post induction (n=2, ±SE) (b); bHLH49 expression in auxin response mutants (n=2, ±SE) (c). 172

Figure 7.6. FACS profile of bHLH49, RALFL34 and EXPA1 from the transcript profiling dataset of pericycle cells induced by auxin to form lateral roots (De Smet et al., 2008) (a); Expression profile of bHLH49 and bHLH76 in lateral root transcriptomic time course dataset in log2 scale (Voß et al., 2015) (b). 175

Figure 7.7. In silico promoter analysis of EXPA1 (2.1Kb) and RALFL34 (1.2Kb) promoter that marks the E-box and G-box sites generated using CLC Genomics Workbench, Qiagen. 176

Figure 7.8. Luciferase (LUC) activity upon co-expression of pRALFL34::LUC and GUS (control) or bHLH49 in protoplasts (a) and the same for pEXPA1::LUC (b). 178

Figure 8.1. Phylogenetic tree of EXPA family of genes. 192

Figure 8.2. Schematic of root zones used in the study by Wilson et al., 2015 for multiohmic analysis of roots to identify cell wall remodeling genes (A); Epitope intensities for different root zones with results for each antibody (B) (Wilson et al., 2015). 196

Figure 8.3. Schematic model for role of EXPA1 in lateral root formation 198

List of tables

Table 3.1. A summary of EXPANSIN gene families identified 30

Table 4.1. List of genes selected based on differential regulation by hormones in available micro-array datasets from Genevestigator (Hruz et al., 2008)..... 66

Supplementary Table 4.1. List of 406 putative cell wall remodelling genes differentially expressed in the pericycle during lateral root initiation 98

Supplementary Table 4.2. List of cell wall remodelling genes selected from overlay with transcript profiling dataset of FACS sorted auxin-induced pericycle cells 108

Table 5.1. Polysaccharide composition of cell wall with their primary monomer units based on literature..... 119

Table 5.2. Table of bands of Raman spectra assigned to cell wall polysaccharides based on literature..... 130

Table 7.1. List of genes identified by Yeast One Hybrid analysis of RALFL34 (400bp) promoter (Murphy et al., 2016). 174

Thesis structure

The thesis is divided into three main parts:

Part I introduces the different aspects of the research undertaken in detail. **Chapter 1** sets the scene and provides a broad perspective on the global significance of the research and the motivation to undertake this work. **Chapter 2** is directed at the specific developmental area of study that is the focus of the PhD. The chapter introduces the process of lateral root formation with emphasis on the importance and role of asymmetric cell division in the process. It has been presented here as an excerpt from a joint review paper published in the *Annals of Botany* (Kajala et al., 2014) which broadly covers asymmetric cell division in key developmental processes. **Chapter 3** introduces the expansin superfamily and their role in plant cell wall remodelling in diverse developmental processes, with focus on root development.

Part II forms the bulk of the thesis and covers the main research findings with each chapter structured into a brief introduction, results, discussion and the methods. **Chapter 4** in this part describes the role of *AtEXPANSINA1* in coordinating asymmetric cell division during lateral root formation with functional characterisation, spatio-temporal expression and cell size studies. **Chapter 5** describes an optimised protocol for confocal Raman imaging of *Arabidopsis* roots. **Chapter 6** describes findings from monomeric sugar profile analysis and confocal Raman microscopy on *Arabidopsis* root sections to study cell wall compositional differences in the wall mutant *expa1-1* in response to auxin treatment. The research output from this chapter is part of research

undertaken with funding from an interdisciplinary grant awarded by the Graduate School. **Chapter 7** describes a role for a transcription factor bHLH49 in lateral root development.

The thesis is concluded in **Part III** with general discussion of the key results. **Chapter 8** in this part, draws together key conclusions from the experimental chapters and discusses potential future work that arises from the findings of the current research.

Chapter 1. Importance of this research

1.1. Motivation and significance

Plants are fascinating beings. They adapt, survive and thrive among us in their own exotic way, yet what we do not know about them far outweighs what we do know and understand about this interesting kingdom of lifeform. The existence of plants is critical for humankind given how much we depend on plants from the basic necessities of life in the form of food, clothing, shelter, to the complex chemicals derived from them to support the modern world of medicine, biorefineries, etc., and not to forget, their importance to maintain the quality of our environment.

A broad knowledge of the science of plants is the foundation of crop technology that over the centuries has evolved in order for farmers to adopt and adapt the farming techniques to optimise the quality and yield from crops. The knowledge is key to face some of the challenges that lie ahead of us. The 'Green Revolution' in the 1960s increased cereal yields greatly through efforts in breeding for rice, wheat and then other crops, to produce high-yielding dwarf varieties that were more responsive to nutrient availability in soil and less susceptible to lodging (Norman Earnst. Borlaug, 1970). This was accomplished through the combined use of these new varieties with mechanisation, crop protection chemicals and chemical fertilisers. However, there have been side effects on the environment arising from misuse of fertilisers and pesticides and increased vulnerability to pests and diseases due to loss in traditional varieties. For the future that demands more food it is important to keep in mind to protect the environment and enable sustainable use of resources. The perspectives for 2050 by Food and Agriculture Organisation (FAO) estimates that the

agricultural productivity has to increase by 60 percent by 2050 in order to meet the demand for food associated with the forecasted growth in population (FAO, 2009) (**Figure 1.1**). Zero Hunger is also one of 17 Global Goals that make up the 2030 Agenda for Sustainable Development in the United Nations Development Programme (UNDP, 2016) and the FAO has recognised research and development as being one of the key drivers for agricultural productivity (FAO, 2014).

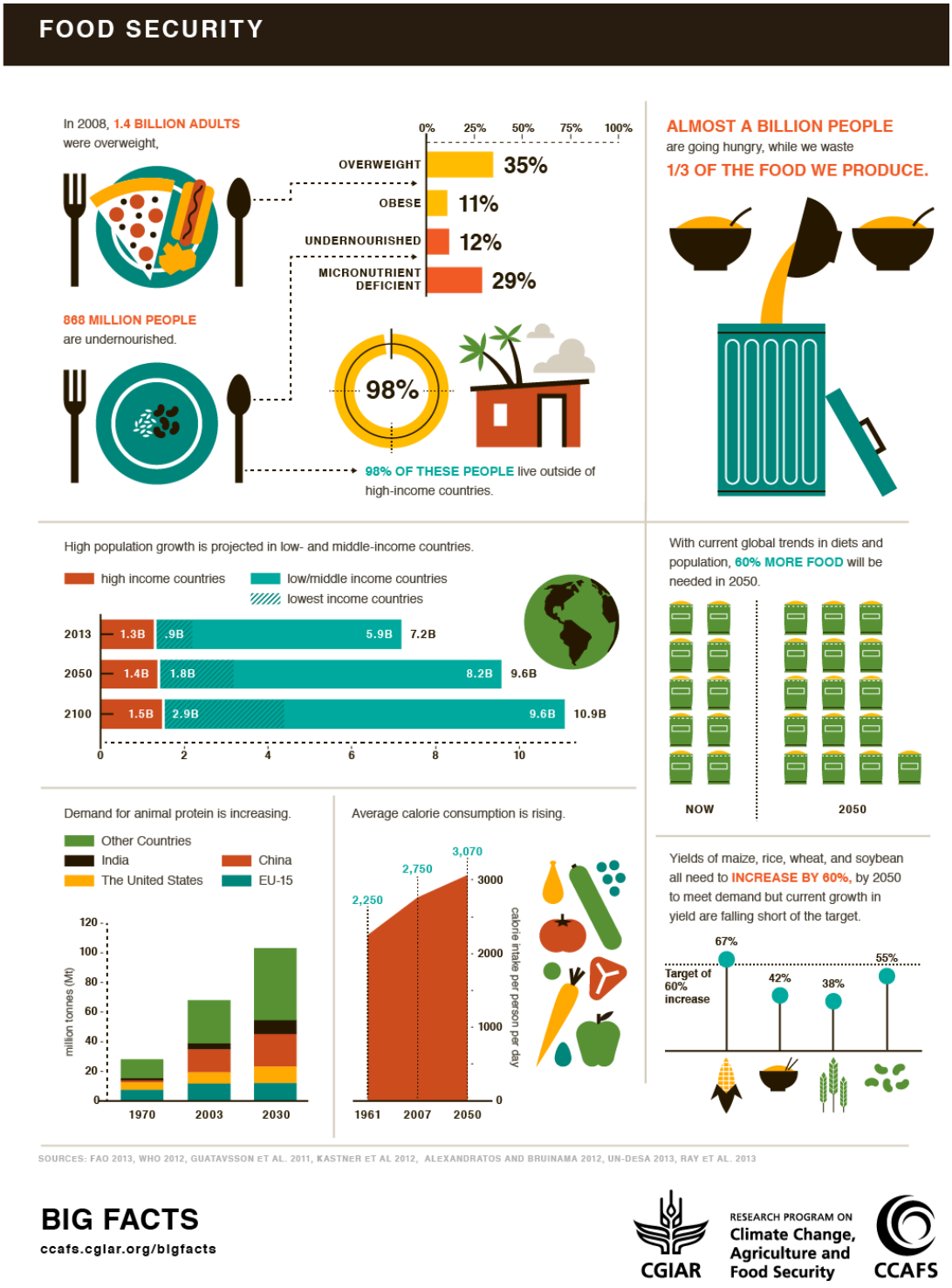


Figure 1.1. Infographic that explains the challenges we face in maintenance of food security (Source: ccafs.cgiar.org/bigfacts).

We need a new green revolution that draws upon the advances in technology and better crop management systems to grow crops that are tolerant to low soil fertility and cope with fluctuating extreme weather conditions. It has been proposed that the Second Green revolution will be through redesigning of the plant root architecture to enhance nutrient acquisition, making plants tolerant to infertile soils while at the same time boosting yield (Lynch, 2007; Herder et al., 2010). Efforts have begun to focus on the lines of 'to produce more from less'. Roots can be looked at as the hidden veins of the plant that spread through the soil looking for minerals and nutrients that the plants require to sustain and develop while also providing anchorage. The plant roots are extraordinary in their ability to sense their environment, navigate through different soils layers, adapt themselves depending on the availability of the nutrients that they require and provide the plant with the resources needed to survive. Hence, the idea of a Second Green Revolution with the roots being the center of focus would help make agriculture less dependent on fertilisers and resilient against insecure water supply and fluctuating weather conditions. It points to the importance of understanding the mechanisms behind development of roots and understand their interaction with the soil and environment to be able to achieve this goal.

In this respect, my PhD is aimed to attain a better understanding of the fundamental process of lateral root formation using a model plant *Arabidopsis thaliana* to uncover a cell-specific network that controls lateral root initiation. Lateral roots grow down and outward in the soil to generate the three-dimensional root network required by plants to acquire water, mineral and nutrients. Their formation has been described in depth in **Chapter 2**. The lateral

roots have a marked effect on size and vigor of crop plants and their adaptation to various soils. In *Arabidopsis* and most dicots, lateral roots initiate post-embryonically from a specialised set of xylem pole pericycle cells termed 'Lateral Root Founder Cells' through a coordinated series of asymmetric cell divisions that are important for organised lateral root formation. However, very little is known about the molecular components in the pericycle that play a role in mediating these divisions. In order to uncover this, we need a better understanding of how growth and division of individual pluripotent pericycle cells are coordinated? How the root is restructured to accommodate a newly developing lateral root? The PhD aims to addresses these questions and gain a better understanding of the asymmetric cell divisions and lateral root formation. The developmental plasticity of the root is explored at various levels – transcriptional, translational and focuses on the contribution of cell wall composition and organisation in the formation of a lateral root.

1.2. References

FAO. (2009). FAO's Director-General on How to Feed the World in 2050. Population and Development Review **35,** 837-839.

FAO. (2014). The State of Food and Agriculture.

Herder, G.D., Van Isterdael, G., Beeckman, T., and De Smet, I. (2010). The roots of a new green revolution. Trends in Plant Science **15,** 600-607.

Lynch, J.P. (2007). Roots of the Second Green Revolution. Australian Journal of Botany **55,** 493-512.

Norman Earnst. Borlaug. (1970). The green revolution, peace and humanity.

UNDP. (2016). UNDP support to the implementation of the 2030 agenda for sustainable development.

Chapter 2. Asymmetric cell division and lateral root formation

Chapter 2 is an introduction to the process of asymmetric cell division during lateral root initiation in *Arabidopsis thaliana* which is the primary focus of the PhD research undertaken. It has been presented here as an excerpt from a joint review paper published in the *Annals of Botany* (Kajala et al., 2014)[$]. The review broadly covers the current knowledge in the asymmetric cell division process that is fundamental to development of different parts of the plant and the application of omics technology to aid increased understanding of the field. The chapter is updated with recent findings subsequent to publication of the review.

Author contributions:

Main contribution in the paper is towards the section on lateral root formation

- Literature review, construction of the section and written by Ramakrishna P
- Supervision by De Smet I.

[$] Title:	Omics and modelling approaches for understanding regulation of asymmetric cell divisions in arabidopsis and other angiosperm plants
Authors:	Kajala, Kaisa **Ramakrishna, Priya** Fisher, Adam Bergmann, Dominique C. De Smet, Ive Sozzani, Rosangela Weijers, Dolf Brady, Siobhan M.
Year:	2014
Journal:	Annals of Botany
DOI:	10.1093/aob/mcu065
URL:	http://aob.oxfordjournals.org/content/early/2014/05/12/aob.mcu065.abstract

2.1. Asymmetric cell division

Asymmetric cell divisions are formative divisions that generate daughter cells of distinct identities and are fundamental for multicellular organisms. The asymmetric divisions define the fundamental development of a plant enabling establishment of organ polarity, tissue patterning, maintenance of stem cell pools and morphogenesis (De Smet and Beeckman, 2011). These divisions also play a vital role in post-embryogenic organogenesis which is a feature distinct to plants over animals, for instance in lateral root initiation (Malamy and Benfey, 1997, De Smet et al., 2008), branching of shoot via shoot apical meristem (Lee and Clark, 2013), development of stomata (Peterson et al., 2010) (**Figure 2.1**).

Cell divisions generating daughter cells with different fates are not always spatially asymmetric. An asymmetric cell division can produce daughter cells of different sizes or produce initially identical cells with fates that differ as a consequence of subsequent cell interactions. The asymmetry in fate can be coordinated either via an intrinsic asymmetric division wherein there is unequal segregation of identity determinants (due to an intrinsic signal or competitive segregation of determinants, or post-translational protein modifications); or through an extrinsic one (‘niche-controlled’) wherein the division plane is oriented to position daughter cells in distinct local environments thereby exposing them to different intercellular identity-determining signals (Kajala et al., 2014) (**Figure 2.2**).

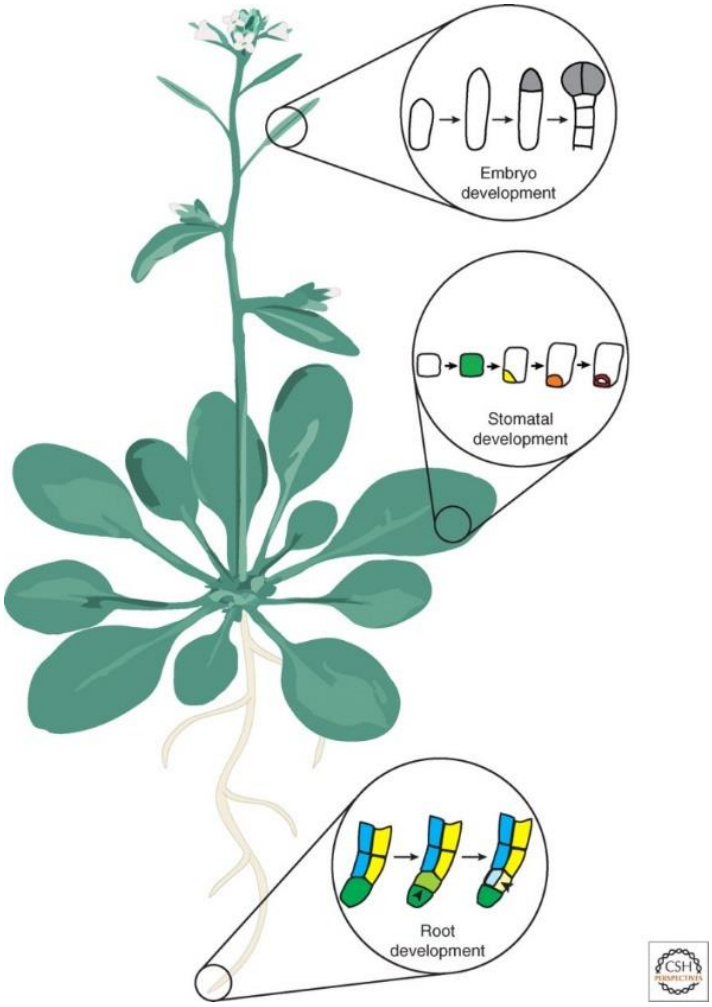


Figure 2.1. Schematic of an Arabidopsis plant indicating few developmental processes where asymmetric cell division occurs; embryo development- which occurs after fertilization of the flower in the silique (seed pod), symmetry breaking in the leaf epidermis during stomatal development and asymmetric cell division that gives rise to the ground tissue in the root Figure taken from (Petricka et al., 2009).

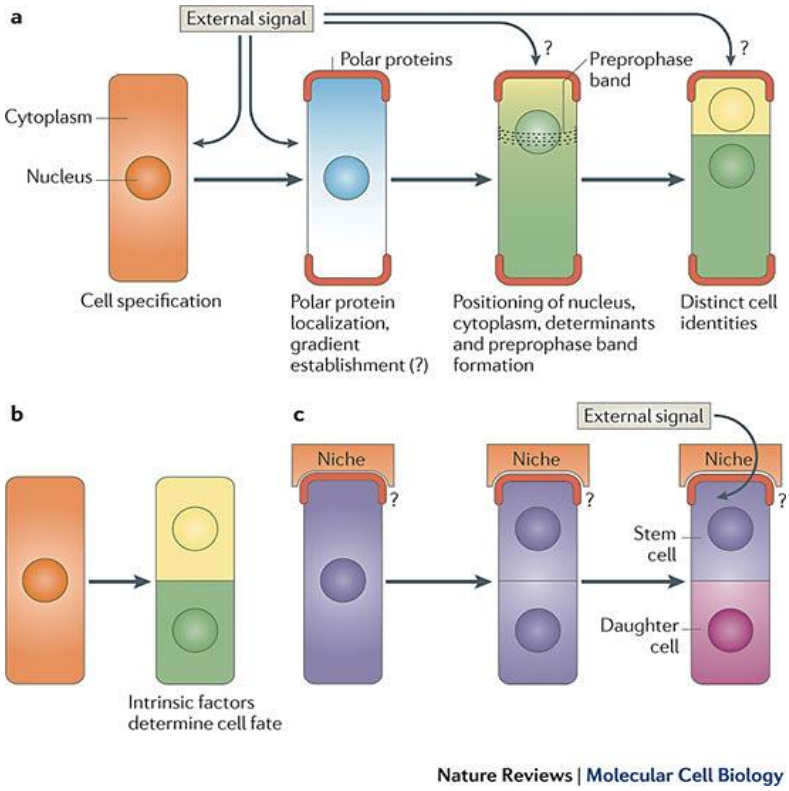


Figure 2.2. Schematic of key features and steps that are frequently observed during asymmetric cell division (ACD). ACD could give rise to unequally sized daughter cells (a) or equally sized daughter cells (b,c) Figure taken from (De Smet and Beeckman, 2011).

For instance, in *Arabidopsis thaliana*, cell-to-cell contact with neighboring cells is critical in maintaining stem cell pools in root meristems. The root stem cell divisions seem to form daughter cells of equal size, which in some instances can for a short time have similar molecular composition (Willemsen et al., 2008) and strongly dependent on external positional control for maintenance of stem cell identity (De Smet and Beeckman, 2011). There are many instances in plant development where the physical symmetry as well has been linked to the determination of new cell fates (De Smet and Beeckman, 2011), for example formation of the male germ line in flowering plants during which haploid microspores divide asymmetrically to form a large vegetative cell and a small generative cell that subsequently divides symmetrically to produce

two sperm cells (Borg et al., 2009); the first zygotic division in plants giving rise to apical and basal cell lineages (Mayer et al., 1993) and others. Another instance, which is also the main focus of this study are the asymmetric cell divisions that take place during initiation of lateral roots in the model plant *Arabidopsis thaliana*.

2.2. Asymmetric cell divisions during lateral root initiation (excerpt from review)

Lateral roots provide an important means by which plants can increase their absorptive area and their capacity to exploit soil resources. They are one of the major determinants of root system architecture; aid uptake of water and nutrients from the soil, provide mechanical support and anchorage, and help plants respond to biotic and abiotic stresses (Péret et al., 2009, De Smet, 2012). In *Arabidopsis thaliana,* a limited number of pericycle cells in front of a xylem pole will undergo coordinated asymmetric, anticlinal cell divisions – referred to as lateral root (LR) initiation – to form unequal sized daughter cells expressing different markers (De Smet et al., 2008). This is followed by a 90° shift in the axis of division upon which the small daughter cells divide periclinally in an outward manner to form a core of cells with different identities (Malamy and Benfey, 1997; Dubrovsky et al., 2001) (**Figure 2.3**). Through a series of cell divisions and differentiation steps, generating cell diversity and tissue patterns, a LR primordium is formed that eventually emerges through overlaying tissues of the primary root, generating a new apical meristem which in turn controls the further growth of the LR (Malamy and Benfey, 1997; Swarup et al., 2008b; Péret et al., 2009; De Smet and Beeckman, 2011; De Smet, 2012b; Goh et al., 2012b; Lavenus et al., 2013b; Lucas et al., 2013). Intriguingly, the interaction of the LR

primordium with overlaying tissues rather than the precise pattern of cell divisions influences its shape (Lucas et al., 2013). Establishment of correct cell identities on asymmetric cell division is preceded by coordinated pre-initiation events such as priming, cell cycle progression, founder cell establishment, symmetry breaking, nuclear migration and auxin response that leads onto the actual asymmetric divisions that form the lateral root primordia and in turn lateral root and these are discussed in detail in the further sections.

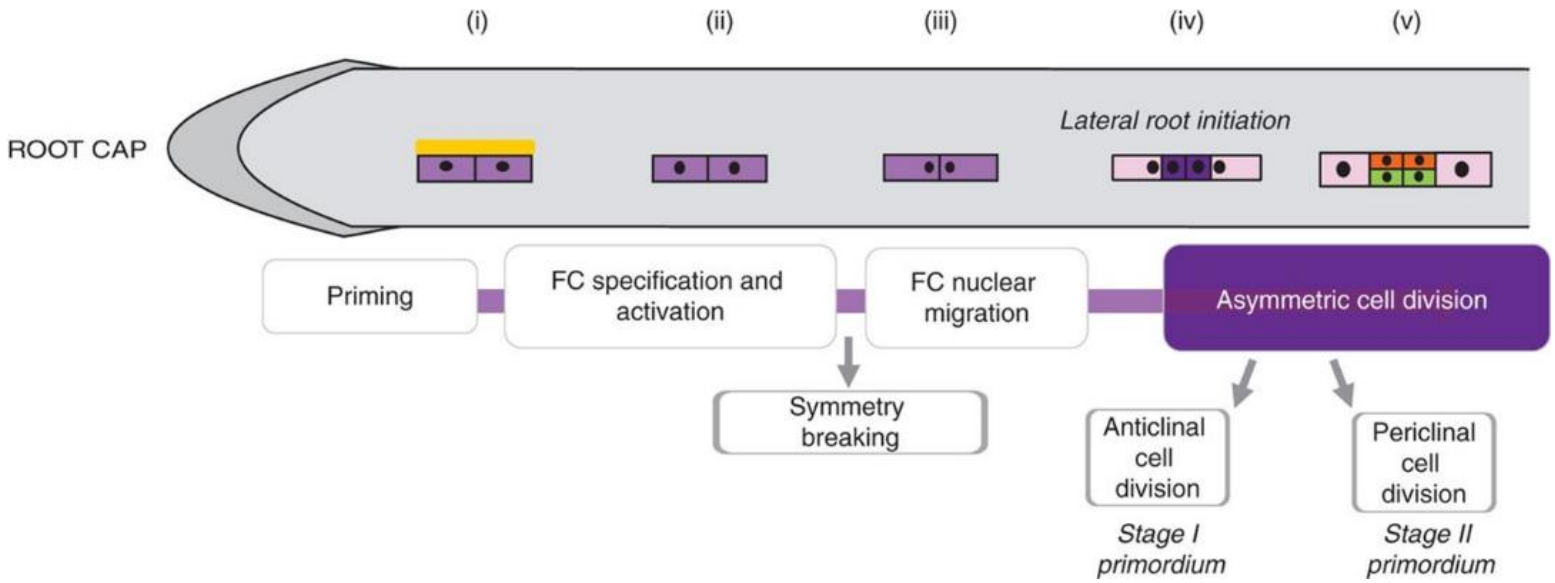


Figure 2.3. Schematic representation of the primary root of *Arabidopsis thaliana* indicating the developmental progression along (pre-initiation events) leading to Asymmetric Cell Division (ACD). (i) Priming in basal meristem where an auxin maxima (yellow) in the protoxylem cells alongside oscillating gene expression in the region leads to formation of pre branch sites in the adjacent xylem pole pericycle cells (XPP); (ii) These XPP cells have the competence to form lateral roots (LR) and they pass through a developmental window to be specified as founder cells (FC); (iii) The nuclei of FC migrate towards the common cell wall indicates preparation to undergo ACD; (iv) Anticlinal ACD of FCs in the differential zone of root giving rise to two small daughter cells (dark purple) and two larger flanking cells (light purple) - Stage I primordium; (v) 90° shift in axis of division with the central core of small daughter cells dividing in an outward manner giving rise equally sized daughter cells with different identities (the red and dark blue blocks), also representing stage II primordium.

2.2.1. Pre-initiation events

Developmental decisions on the distribution of LRs take place in the distal zone of the root tip in the basal meristem region. Studies using *DR5::GUS* time series (De Smet et al., 2007; De Rybel et al., 2010b) and *in vivo,* real-time visualisation of *DR5::LUCIFERASE* expression together with genome-wide gene expression studies (Moreno-Risueno et al., 2010b), suggest that periodic auxin response along with oscillating waves of gene expression function as an endogenous 'clock-like' mechanism for the formation of prebranch sites that are future sites of LR primordia and LRs giving rise to a regular pattern of LRs along the primary root (De Smet et al., 2007; Moreno-Risueno et al., 2010b; Van Norman et al., 2013) (**Figure 2.3-i**). The expression of more than 3400 genes oscillates either in phase or in antiphase with the *DR5* reporter and both these phases are required for LR positioning along primary root (Moreno-Risueno et al., 2010b).

Auxin is one of the key regulators of each step of LR development, and disrupting auxin transport or response affects LR density, positioning and patterning (Celenza et al., 1995; Laskowski et al., 1995; Tian and Reed, 1999; Casimiro et al., 2001; Benková et al., 2003; Tatematsu et al., 2004; De Smet et al., 2006a; De Smet et al., 2007; Muto et al., 2007; Dubrovsky et al., 2008; Laskowski et al., 2008; Mravec et al., 2008; Swarup et al., 2008b; Uehara et al., 2008; Péret et al., 2009; De Smet et al., 2010; Overvoorde et al., 2010a; Lavenus et al., 2013b; Marhavy et al., 2013). Other hormones too influence LR development either independently or by interfering with auxin-regulated processes (De Smet et al., 2006a; Fukaki and Tasaka, 2009; Lavenus et al., 2013b). For instance, cytokinins affect both LR initiation and development (Li

et al., 2006a; Laplaze et al., 2007; Bielach et al., 2012); with auxin and cytokinin having antagonistic activities during the early phase of LR formation. Interestingly, cytokinin response is repressed in the priming and initiation region of the root with ectopic overproduction in the basal meristem being inhibitory to LR initiation (Bielach et al., 2012). In a recent marker-based chemical biology approach, the root branching non-auxin like molecule naxillin was identified (De Rybel et al., 2012). The chemical promotes auxin response specifically in the basal meristem region where founder cell identity is established and could function as a beneficial tool to unravel the molecular networks surrounding priming and founder cell identity establishment.

Following an auxin response of protoxylem elements in the basal meristem region of the primary root, the adjacent XPP cells get primed, providing them with the competence to form a LR (De Smet et al., 2007; Parizot et al., 2008; Moreno-Risueno et al., 2010b; Parizot et al., 2012). Under *in vitro* growth conditions, the primary root displays a root waving pattern. The left-right positioning of the LRs along the primary root axis correlates with the root curvature with the LRs forming on the convex side of the root bends (Fortin et al., 1989; De Smet et al., 2007; Ditengou et al., 2008; Laskowski et al., 2008; Lucas et al., 2008). Gravisimulated or manual bending of the root induces a mechanical strain which exhibits activation in local competence of XPP cells caused by changes in local auxin distribution and signalling (Ditengou et al., 2008; Laskowski et al., 2008; Laskowski, 2013). However, expression of the auxin-responsive *ARABIDOPSIS HISTIDINE PHOSPHOTRANSFER PROTEIN 6* (*AHP6*) suggests that an auxin response maximum may occur in protoxylem adjacent pericycle cells before this stage (Bishopp et al., 2011).

GATA23 is the earliest known marker for LR development that was identified by meta-analysis of various available LRI transcriptomic data sets (De Rybel et al., 2010b; Parizot et al., 2010). *GATA23* is specifically expressed in XPP cells before the first asymmetric division. The *GATA23* RNAi line shows clear reduction in the number of stage I and II primordia and an overall decrease in the number of emerged and non-emerged primordia, while overexpression showed increased founder cell specification observable by high occurrence of ectopic primordia (De Rybel et al., 2010b). An AUXIN/INDOLE-3-ACETIC ACID28 (AUX/IAA28)-dependent auxin signaling mechanism controls *GATA23* expression in the basal meristem regulating LR founder cells specification prior to LRI and root branching patterns (**Figure 2.3-ii**) (Brady et al., 2007; De Rybel et al., 2010b; Yadav et al., 2010). Small signalling peptide RALF34 is suggested to act upstream of GATA23 and have an important role in regulation of asymmetric cell division in the pericycle (Murphy et al., 2016).

Subsequent to priming, these XPP cells pass through a developmental window for LR initiation, wherein at minimum auxin concentration, the XPP cells have maximum probability to become specified founder cells (**Figure 2.3-ii**) (Dubrovsky et al., 2008; Dubrovsky et al., 2011a). The endodermis has recently been shown to be involved in assisting the transition from founder cell state to LR initiation phase via an auxin reflux pathway between the endodermal cells and the founder cells. This is achieved through laterally localised *PIN3* expression in overlaying endodermal cells reinforcing auxin movement to founder cells. The *pin3* mutant exhibits a dramatic delay in the onset of LR initiation following founder cell specification (Marhavy et al., 2013). PIN7 is also known to affect the frequency of founder cell specification with mutation in *pin7*

affecting the number of primordia being initiated (Benková et al., 2003; Marhavy et al., 2013). GNOM/FEWER ROOTS is also involved in establishment of an auxin response maximum possibly through PIN mediated auxin gradient establishment in LR founder cells (Geldner et al., 2004; Okumura et al., 2013). Taken together, auxin accumulation through AUX1−PIN based transporter activity and their positive feedback and cross-regulation controls LR patterning (Laskowski et al., 2008). When local auxin maximum concentration is reached, the cells proceed onto LR initiation phase (Dubrovsky et al., 2008; Benková et al., 2009). Cytokinins also affect this process by repressing many PIN proteins thereby preventing proper auxin gradient establishment required for re-specification of LR founder cells (Li et al., 2006a; Laplaze et al., 2007). Recent studies suggest that cytokinin may aid as a positional signal for the formation of new LR primordia (Chang et al., 2013).

Following the increased auxin response in LR founder cell pairs several AUX/IAA–ARF factors interact leading to the migration of nuclei towards the common cell wall which is one of the morphological features of LR founder cells preparing for asymmetric cell division (**Figure 2.3-iii**) (De Smet et al., 2007; De Rybel et al., 2010b). The SOLITARY ROOT (SLR)/IAA14–ARF7–ARF19 module regulates this synchronous migration of the founder cell nuclei towards the common cell wall just prior to LR initiation (De Smet et al., 2007; Dubrovsky et al., 2008; De Rybel et al., 2010b; Goh et al., 2012b). The *slr-1* and *arf7 arf19* mutants when treated with excess auxin show abnormal nuclear migration and asymmetric cell division (De Rybel et al., 2010b). LR initiation closely follows the nuclear migration in the differentiation zone (Dubrovsky et al., 2011a).

Control of cell cycle activity is essential for lateral root founder cells to undergo asymmetric cell division, and the lack of which leads to either no divisions or uncontrolled proliferative divisions without proper organ formation (Beeckman et al., 2001; Himanen et al., 2002b; DiDonato et al., 2004; Vanneste et al., 2005b; De Smet et al., 2010; Jurado et al., 2010; Sanz et al., 2011). It is essential that the cells remain in a mitotically competent state prior to asymmetric cell division (ACD), which is suggested to be maintained by the *ABERRANT LATERAL ROOT FORMATION 4* (*ALF4*) encoded nuclear protein (with the *alf4* mutant displaying no lateral root initiation) (Beeckman et al., 2001; DiDonato et al., 2004; Dubrovsky et al., 2008). The transition of XPP cells from G1-to-S and ensuing cell cycle progression is stimulated by auxin and these 'primed' cells reactivate cell cycle when they reach the lateral root initiation zone (Casimiro et al., 2003), emphasising the fact that activating cell cycle-related genes alone is not sufficient to initiate a new LR (Vanneste et al., 2005b). Blocking of early auxin response (in a gain-of-function *slr* mutant) or transport (using transport inhibitor *N*-1-naphthylphthalamic acid - NPA), results in the absence of lateral root initiation (Casimiro et al., 2001; Himanen et al., 2002b; Vanneste et al., 2005b). Gain-of-function mutations in SLR/IAA14 (Fukaki et al., 2002a; Fukaki et al., 2005a; Vanneste et al., 2005b) and IAA28 (Rogg et al., 2001; Dubrovsky et al., 2009; De Rybel et al., 2010b), negatively regulate LR formation through the inactivation of ARF7 and ARF19, which are necessary for activation of LRI genes. The *slr* mutants are agravitropic and show a complete lack of lateral roots (Fukaki et al., 2002a) and the *arf7 arf19* double mutants exhibit fewer LRs owing to inhibition of auxin-induced pericycle cell division that is required for LRI (Wilmoth et al., 2005; Okushima et al., 2007a;

Dubrovsky et al., 2009). ARF7 and ARF19 together activate LATERAL ORGAN BOUNDARIES-DOMAIN16/ASYMMETRIC LEAVES2-LIKE18 (LBD16/ASL18) and LBD29/ASL16 (Okushima et al., 2007a), with *LBD16* being expressed specifically in the LR founder cells before the first asymmetric cell division. LBD16/ASL18 along with other related LBDs regulate the establishment of asymmetry of the founder cell (Goh et al., 2012b). The E2Fa transcription factor is an essential component that regulates the asymmetric cell division during lateral root initiation (De Smet et al., 2010; Berckmans et al., 2011). *E2Fa* expression is regulated by the LBD18−LBD33 dimer that is, in turn, regulated by the auxin signalling pathway (Berckmans et al., 2011). The auxin mediated G1-to-S transition is inhibited by INTERACTOR OF CYCLIN-DEPENDENT KINASE (CDK)/KINASE-INHIBITORY PROTEIN (KIP)-RELATED PROTEIN (ICK/KRP) family of proteins, with the *krp2* mutants showing increased lateral root density. Formation of complex of ICK2/KRP2 with CDKA;1–CYCD2;1 leads to increased activity of CDKA;1–CYCD2;1 and consequently increased LR density (Himanen et al., 2002b; Ren et al., 2008; Sanz et al., 2011). Other D-type cyclin (CYCD) subunits- *CYCD4;1* and *CYCD3;1* genes are also known to be involved in LR initiation (Himanen et al., 2002b). In addition, A2-type cyclins (CYCA2s) are involved in early G2-to-M transition of cell cycle during LRI and a triple *cyca2;234* mutant shows a delay in the expression of mitotic regulators, while the auxin signalling and G1-to-S regulatory genes remained unaffected (Vanneste et al., 2011). S-PHASE KINASE-ASSOCIATED PROTEIN 2A (SKP2A) a cell cycle F-box protein, is involved in positive regulation of cell division during LRI observed by the overexpression of SKP2A increasing the number of lateral root primordia. Auxin binds directly with SKP2A, regulating

the proteolysis of cell cycle repressing transcription factors in a TIR1-AFB independent pathway. Overexpression of SKP2A in the *tir1* mutant background induced lateral root initiation and *skp2a* mutants show auxin-resistant root growth phenotype (Jurado et al., 2008; Jurado et al., 2010). A close homolog, SKP2B contrastingly involved in negative regulation of cell division in founder cells. *skp2b* mutants displaying higher number of Stage I and II primordia suggesting its involvement in the first asymmetric cell division (Manzano et al., 2012). Finally, in addition to auxin, cytokinins act directly on LR founder cells blocking G2-M cell cycle transition (Li et al., 2006a).

2.2.2. Anticlinal asymmetric division of pericycle cells

The founder cells undergo the first formative anticlinal asymmetric cell division giving rise to two small daughter cells and two larger flanking cells (**Figure 2.3-iv**). The latter undergoes another round of asymmetric cell division to form a core of small daughter cells and flanking large cells (stage I primordium) (De Smet et al., 2008). This pattern of asymmetric cell division occurs simultaneously in two to three pairs of adjacent pericycle cell files (Kurup et al., 2005). PLETHORA 3 (*PLT3)*, *PLT5*, *PLT7* transcription factors (TFs) are expressed in specified LR founder cells before the first asymmetric cell division. The triple *plt3*,*plt5*,*plt7* mutant display altered rhizotaxis with LR primordia often grouped in longitudinal or radial clusters with only a few emerged lateral roots, but higher LR density. The PLTs function downstream of ARF7 and ARF19 and influence rhizotactic patterning of LRs (Hofhuis et al., 2013). The small daughter cells are characterised by the differential expression of several genes. For example, *ARABIDOPSIS CRINKLY4* (*ACR4*), a receptor-like kinase that

identified through an integrated systems biology approach involving transcript profiling of auxin-activated XPP cells in a highly synchronised time-course subjected to fluorescence-activated cell sorting (De Smet et al., 2008). This led to a list of differentially expressed genes potentially involved in LR initiation with high spatial and temporal resolution, which were further subjected to stringent filters in order to identify key components solely associated with asymmetric cell division. *ACR4* was one of the main candidates identified via these filters (De Smet et al., 2008). *ACR4* promotes formative cell divisions in the pericycle, cell identity specification of small and large flanking cells after the first anticlinal asymmetric cell division and suppression of cell divisions in pericycle cells surrounding the LR (De Smet et al., 2008).

Following the first asymmetric division, the small daughter cells exhibit an auxin maximum (Benková et al., 2003) which is around the same time when BDL/IAA12-MP/ARF5–dependent signalling occurs (De Smet et al., 2010). The BDL/IAA12−MP/ARF5-dependent auxin response helps patterning of the LR downstream of SLR/IAA14−ARF7−ARF19 with the hemizygous gain-of-function *bdl* mutants (*ProBDL:bdl*^{hem}) and weak loss-of-function *mp*^{S319} mutants showing abnormalities in pericycle divisions and irregularly positioned lateral roots (De Smet et al., 2010). Interestingly, presence of ARF7–ARF19-independent LR formation is revealed by REDUCED LATERAL ROOT FORMATION, a cytosolic protein with a cytochrome b_5-like heme/steroid binding domain (Ikeyama et al., 2010). This is observed by the *rlf-1* mutation having an inhibitory effect on anticlinal cell division of the founder cells thereby affecting LR initiation. However, auxin-inducible expression of *LBD16/ASL18* and *LBD29/ASL16* genes remains unaffected in the *rlf-1* mutant.

Some *ROOT GROWTH FACTOR* (*RGF*)/*GOLVEN* (*GLV*)/*CLE-LIKE* (*CLEL*) genes, encoding for small signalling peptides, are expressed in stage I primordia (Fernandez et al., 2013b; Fernandez et al., 2013a). *CLEL6* or *CLEL7* affect the regular pattern of asymmetric cell division leading to LR primordium formation (Meng et al., 2012).

2.2.3. Periclinal asymmetric division of pericycle cells

Subsequent to the anticlinal divisions, the cell division plane shifts by 90° for the next formative, but periclinal cell division, with the cells dividing in an outwards manner occurs forming a second layer (stage II primordium) (**Figure 2.3-v**) (Malamy and Benfey, 1997; De Smet et al., 2008). The End199 GUS marker line precisely reflects expression of *SCARECROW (SCR)* and shows distinction between the inner and outer layer of cells in the stage II primordium and is also one of the earliest observed instance of differential expression between the cell layers (Malamy and Benfey, 1997). Strict control of cell division orientation is required for *de novo* organogenesis and shape formation. Several proteins are known to be implicated in the process (De Smet and Beeckman, 2011; Rasmussen et al., 2011). Recently α Aurora kinases (AUR1 and AUR2) which were also identified in the systems approach mentioned above for ACR4 (De Smet et al., 2008), have been indicated to influence the mechanism by which the switch in the plane of division occurs during asymmetric cell division in LRs. The *aur1-2 aur2-2* double mutants exhibit randomly oriented cell divisions instead of distinct cell layers during primordia development and change in growth dynamics, but the dome shape of the LRP remained unaffected (Van Damme et al., 2011; Lucas et al., 2013).

Chapter 3. Expansins and cell wall remodeling

Chapter 3 is the introductory chapter to the expansin superfamily and the process of cell wall remodelling. Post-embryonic plant growth and development is a balanced combination of cell division and cell expansion that dictates the final size and shape of the plant. While cell division serves to increase cell number, cell expansion functions to increase the size of cells. The process of cell expansion in plants is mechanistically very different from animal cells with the added complexity introduced by the presence of a rigid cell wall that encompasses the plasma membrane. Thus, for cell expansion to occur the cell wall structure must be remodeled in a dynamic fashion that involves a complex interplay between loosening of existing wall components accompanied by addition of newly synthesised components to the growing wall. Cell wall loosening largely occurs by alteration of interactions between major components of primary plant cell walls, namely cellulose, hemicellulose and pectin (discussed further in **Chapter 5**).

The alterations are thought to be brought about by several cell wall remodelling enzymes that belong to different families and act upon different components of the cell wall. Well known ones involved in cell wall remodelling are PECTIN METHYL ESTERASE (PME), XYLOGLUCAN TRANSHYDROLASE (XTH) and EXPANSIN families. PMEs affect the consistency of the pectin ground matrix in cell walls through removal of methyl groups by breaking ester bonds. Pectin are cross-linked by calcium ions forming calcium-pectate bridges that stiffen the cell wall and thus reduce cell expansion (Proseus and Boyer, 2006; Derbyshire et al., 2007; Peaucelle et al., 2012). XTH family members bring about wall loosening by two ways: when XYLOGLUCAN ENDOHYDROLASE (XEH) action is involved they break the

bond between two hemicellulose crosslinks; whereas the other family members work through XYLOGLUCAN ENDOTRANSGLUCOSYLASE (XET) action where the hemicellulose crosslink is broken, and one free end re-joins with another free crosslink end within the tissue (Rose et al., 2002; Van Sandt et al., 2007; Park and Cosgrove, 2015). Expansins which are the focus of the study, work in a non-enzymatic manner to modify the non-covalent polysaccharide network that constitute the load-bearing structure of the cell wall (McQueen-Mason and Cosgrove, 1995; Cosgrove, 2000b; Li et al., 2003). EXPANSINs act as a catalyst for acid-dependent growth and aid several basic developmental processes that require cell wall remodelling which is often by promotion of cell expansion or cell elongation. Although we now understand a great deal about the structure of EXPANSIN and its interaction with the plant cell wall, the mechanism by which EXPANSINs unlock the cell wall to bring about its response still remains elusive. In this chapter, we discuss the current knowledge on the evolution and mode-of-action of EXPANSINs, provide a broad overview on their diverse role in a range of developmental processes, and role of hormones in their regulation.

3.1. Size and evolution of the expansin superfamily

Expansins and expansin-like proteins are encoded by a large superfamily of genes and are found in plants, fungi, bacteria, and a few other organisms (Sampedro et al., 2005; Carey and Cosgrove, 2007; Vannerum et al., 2011; Carey et al., 2013; Nikolaidis et al., 2014) (**Figure 3.1 and Table 3.1**). In plants, the expansin superfamily consists of four families: α-expansin (EXPA), β-expansin (EXPB), expansin-like A (EXLA) and expansin-like B (EXLB) (Kende et al., 2004). An additional category for non-plant expansin-like genes

(EXLX) exists for genes that bear homology to Domain 1 and Domain 2 of expansins (see section 3.3 for Domain structure), but are distinct from other existing expansin families (Georgelis et al., 2015). The α-expansins are phylogenetically related to the first discovered cucumber expansins (Cosgrove, 1989a; Cosgrove and Durachko, 1994) and are primarily involved in pH-mediated wall relaxation. The group I grass pollen allergens were later identified based on similar wall extension activity as α-expansins and were classified as β-expansins, characterised by certain amino acid sequence similarity and resemblance of their predicted secondary structure to expansin proteins (Cosgrove et al., 1997; Li and Cosgrove, 2001). The α and β-expansins share about 20% protein sequence similarity and have very similar domain structures. The main difference between the two groups is the polysaccharide they target in the cell wall to bring about their characteristic wall extension activity. The α-expansins are more effective in loosening of dicot walls, while β-expansins are more effective on walls of grass species (Choe and Cosgrove, 2010). A group of expansin-like genes are also classified into the expansin superfamily mainly based on their sequence similarity and expression data from microarrays (Sampedro et al., 2006). However, the majority of these proteins have not been isolated or functionally characterised.

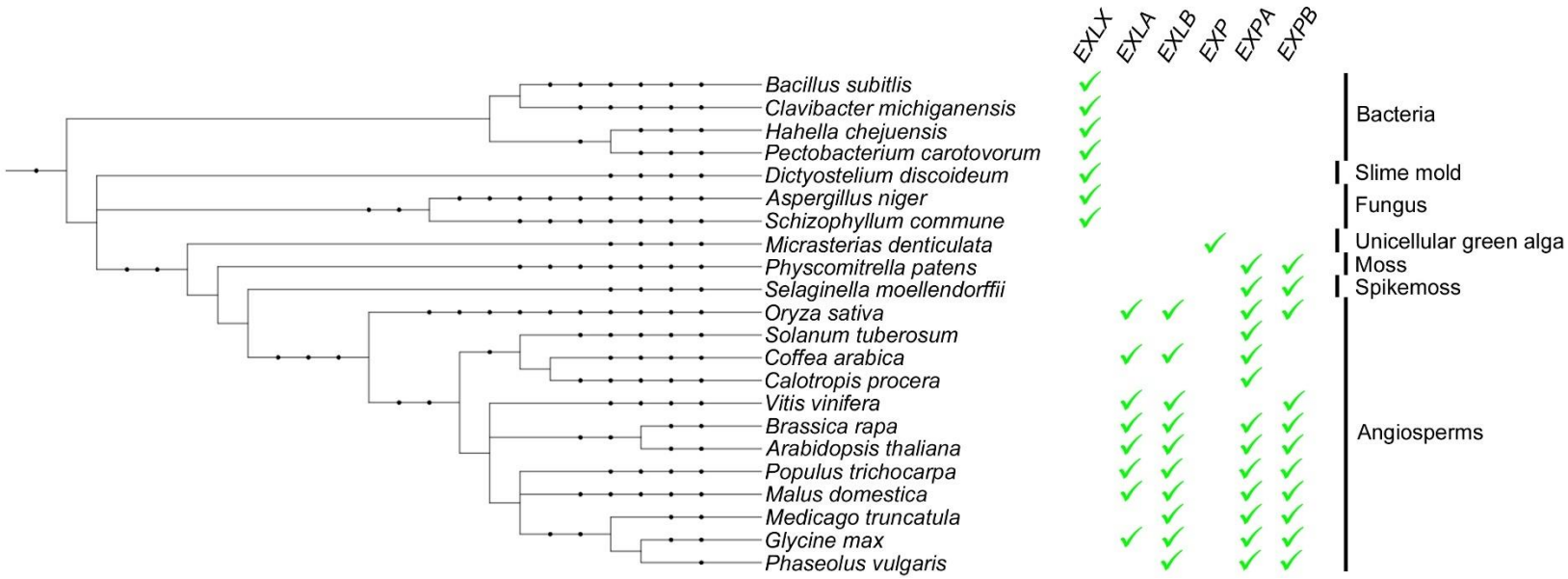


Figure 3.1. A simplified schematic showing the evolution of the EXPANSIN superfamily. Representative species are shown on each branch, the gene families are shown at the top and the phylogenetic classification on the right. The ticks on each branch represent the presence of the indicated gene family in each of the species (see also **Table 1**). The tree presented here was generated using phyloT (phylot.biobyte.de).

Table 3.1. A summary of EXPANSIN gene families identified

Species	Common name	Expansin genes/families identified so far	References
Bacillus subtilis	Hay bacillus or grass bacillus	EXLX	(Kerff et al., 2008)
Pectobacterium carotovorum	Soft rot gram negative bacteria		(Olarte-Lozano et al., 2014)
Clostridium clariflavum			(Lee and Kende, 2001)
Hahella chejuensis			(Lee et al., 2010)
Schizophyllum commune	White-rot fungi		(Tovar-Herrera et al., 2015)
Aspergillus niger			(Georgelis et al., 2014)
Dictyostelium discoideum	Mold		(Darley et al., 2003)
Clavibacter michiganensis	Potato ring rot	2 EXLX	(Laine et al., 2000; Gartemann et al., 2003; Georgelis et al., 2014)
Micrasterias denticulata	Green algae	Only 4 EXPs so far	(Vannerum et al., 2011)
Physcomitrella patens	Moss	Only EXPA and EXPB No EXLA and EXLB	(Carey and Cosgrove, 2007)
Selaginella moellendorffii	Spike moss	Only EXPA and EXPB No EXLA and EXLB	(Carey et al., 2013)
Arabidopsis thaliana	Thale cress	26 EXPA, 6 EXPB, 3 EXLA and 1 EXLB	(Sampedro et al., 2005)
Oryza sativa	Rice	33 EXPA, 6 EXPB, 4 EXLA and 1 EXLB	(Sampedro et al., 2005)
Glycine max	Soy bean	49 EXPA, 9 EXPB, 2 EXLA, 15 EXLB	(Zhu et al., 2014)
Medicago truncatula	Barrel clover	16 EXPA, 1 EXPB, 1 EXLB	(Zhu et al., 2014)
Phaseolus vulgaris	Common bean	25 EXPA, 6 EXPB, 5 EXLB	(Zhu et al., 2014)
Solanum tuberosum	Potato	9 EXPA identified	(Jung et al., 2010)
Populus trichocarpa	Poplar	27 EXPA, 3 EXPB, 2 EXLA, 4 EXLB	(Sampedro et al., 2006)
Vitis vinifera	Grapevine	20 EXPA, 4 EXPB, 1 EXLA, 4 EXLB	(Dal Santo et al., 2013)
Malus x Domestica L. Borkh	Apple	34 EXPA, 1 EXPB, 2 EXLA, 4 EXLB	(Zhang et al., 2014)
Brassica rapa subsp. pekinensis	Chinese cabbage	39 EXPA, 9 EXPB, 2 EXLA, 3 EXLB	(Krishnamurthy et al., 2015)
Anthocephalus chinensis (Rubiaceae)	Bur flower tree	16 EXPA identified so far	(Ouyang et al., 2013)
Coffea arabica	Coffee	9 EXPA, 1 EXLA,1 EXLB	(Budzinski et al., 2011)
Calotropis procera	Kapok tree or rubber bush	EXPA1- 4 identified so far	(Cheema et al., 2010)

Growing genomic resources has helped determine the size of the expansin gene family and its early evolutionary presence (**Figure 3.1 and Table 3.1**). The earliest presence of expansin genes in the green lineage is seen in the green alga *Micrasterias denticulate,* that was found to have expansin-like genes that were closely related to expansins of land plants with suggestive functional resemblance in altering cell wall structure (Vannerum et al., 2011). This provides evidence of the earliest identified presence of an expansin-resembling gene in a unicellular system that precedes land colonisation. Moving on to basal land plants, the moss *Physcomitrella patens* encodes for members of the expansin superfamily, but these bryophytes lacked *EXLA* or *EXLB* family genes similar to the spike moss *Selaginella moellendorffii* where the expansin family was smaller and less diverse (Carey et al., 2013).

The expansin superfamily of the dicot *Arabidopsis thaliana* is described to have 36 genes distributed into 26 *EXPA*s, 6 *EXPB*s, 3 *EXLA*s and one *EXLB* (**Figure 3.1 and Table 3.1**). In the monocot rice (*Oryza sativa*), the superfamily is larger with 56 expansin genes classified into 33 *EXPA*s, 18 *EXPB*, 4 *EXLA* and one *EXLB* (Sampedro et al., 2006). The gene family in soybean has an increased number of genes, which is thought to be through tandem and segmental duplication events, and the genes exhibit wide functional divergence (Zhu et al., 2014). Similarly, gene duplication studies in apple (*Malus x Domestica* L. Borkh) point to a similar development of the gene family through whole-genome and chromosomal-segment duplication events (Zhang et al., 2014). Phylogenetic analysis of grapevine points at expansin genes of grapevine being more closely related to woody species like poplar compared to the genes from Arabidopsis or rice (Dal Santo et al., 2013).

Outside the green lineage, only a few bacterial and fungal species have so far been shown to have the presence of expansin-like genes in their genome (**Figure 3.1 and Table 3.1**). The species associated were often found to colonise or infect the plant in most cases. For instance, a bacterial protein EXLX1 from *Bacillus subtilis* (originally known as YOAJ) (Kerff et al., 2008) has been known to aid colonisation on plant roots. Also SWOLLENIN, from the saprophytic fungus *Trichoderma reesei,* shares sequence homology with expansins and has a similar function (Saloheimo et al., 2002; Brotman et al., 2008; Andberg et al., 2015). They are xenologs of plant expansins that are likely derived from horizontal gene transfer of a eukaryotic plant expansin to prokaryotic bacteria/fungi. The gene transfer seems to have occurred only to certain species that are either closely associated with plants or are plant pathogens (Nikolaidis et al., 2014). Further to the horizontal gene transfer events, the evolution of bacterial EXLX1 and its non-plant homologs is characterized by instances where bacterial expansin genes have autonomously fused to DNA fragments that code for an endoglucanase domain or a carbohydrate binding module domain (Nikolaidis et al., 2014).

3.2. Plant cell wall structure

Cell wall is an important feature of plants that has several biological roles in post-embryonic growth and development such as cell division and cell expansion to dictate the final size and shape of the plant, mechanical strength to the tissues, ion-exchange and defense against microbes (Popper, 2008; Cosgrove, 2014). The primary cell wall of plants is a composite matrix of cellulose microfibrils, hemicelluloses, pectic polysaccharides and cell wall-associated proteins (such as hydroxyproline-rich glycoproteins (HRGP) and

extensins). These are described in depth in **Section 5.1.1.** and **5.1.2.** of **Chapter 5**. The cell wall structure of Angiosperms has been the point of extensive study given its importance as feedstock for biorefineries. More recent studies of ancestral species have shown that there are distinct differences in the wall chemistry between different species within the same taxa as well as evolutionarily early species (Harris and Hartley, 1976; Carpita and Gibeaut, 1993). The differences in cell wall composition were found to correlate with the diversification of the plant taxa reflected in alterations in monomeric sugars (Popper and Fry, 2004). Predominant monosaccharides present in the walls of seeded plants are d-glucose (Glc), d-galactose (Gal), d-mannose (Man), d-xylose (Xyl), l-arabinose (Ara), l-fucose (Fuc), l-rhamnose (Rha) and d-galacturonic acid (GalA). In grass species for instance higher levels of Xyl was observed and lower levels of GalA, Gal and Fuc. These hint at the importance of the monomeric components coming together in altered combinations to form the polysaccharide backbone with diversification of plant species. There seems to be a trend in the characteristics of the cell wall with commonalities traceable through a mix of shared ancestry and convergent evolution. Cellulose is widely distributed right from tunicates, bacteria to the plant kingdom. Xylans are found red algae, chlorophytes onwards to vascular plants with a trend to be distributed in cell wall of photosynthetic species. The same origin of arabinogalactans was observed for from algal lineage suggesting the evolution of wall components being important for the movement and establishment on land (Popper and Tuohy 2010). The presence of expansin-like proteins in bacterial species, mostly through HGT events is suggestive of an adaptive response for the bacteria to interact with higher land plants with evolved cell walls. The presence

of the EXPA and EXPB family of genes from the algal lineage suggests the coevolution of a mechanism to alter cell walls as a means to support growth and coincides with the development of xylan polysaccharides that constitute the wall hemicellulose.

3.3. EXPANSIN structure and action on wall

Expansins are small proteins with molecular weight ranging between 25–27 kDa. In plants, the protein is composed of: i) an N-terminal 'Domain 1' (~120 amino acids long) that shares structural homology to the catalytic domain of family-45 endoglucanases (EG45-like domain), but lacks the β 1,4-glucanase activity characteristic of GH45 enzymes, ii) a C-terminal 'Domain 2' (~98 amino acids long) with presence of three conserved and linearly arranged aromatic residues that exhibits homology to group-2 grass pollen allergens and referred to as the cellulose-binding domain (CBD) and, iii) an amino-terminal signal peptide (~20 amino acids long) (Cosgrove, 2000c; Sampedro and Cosgrove, 2005; Yennawar et al., 2006; Georgelis et al., 2012) (**Figure 3.2A**). The Domain 1 and 2 are essential for binding to cellulose and other polysaccharides to mediate cell wall loosening. The Domain 2 with its three conserved and linearly arranged aromatic residues bears resemblance to a type-A carbohydrate-binding module and is required to bind to hydrophobic surface of cellulose microfibrils for wall loosening action. Another region on Domain 2 is composed of several non-conserved basic residues that promote binding to whole cell walls, but do not promote wall loosening. Extensive studies have contributed to a better understanding of expansin protein structure. An X-ray crystallographic study of ZmEXPB1 from maize (*Zea mays*) showed the presence of the conserved N-terminal Domain 1 (a six-stranded double-ψ β-barrel structure

flanked by short loops and α-helices) with most residues of the catalytic EG45-like site being conserved, and the C-terminal Domain 2 (eight β-strands assembled into two antiparallel β-sheets) that forms a β-sandwich structure packed next to Domain 1. Together they align to form a long shallow grooved surface to which the polysaccharide binds (Yennawar et al., 2006; Andberg et al., 2015).

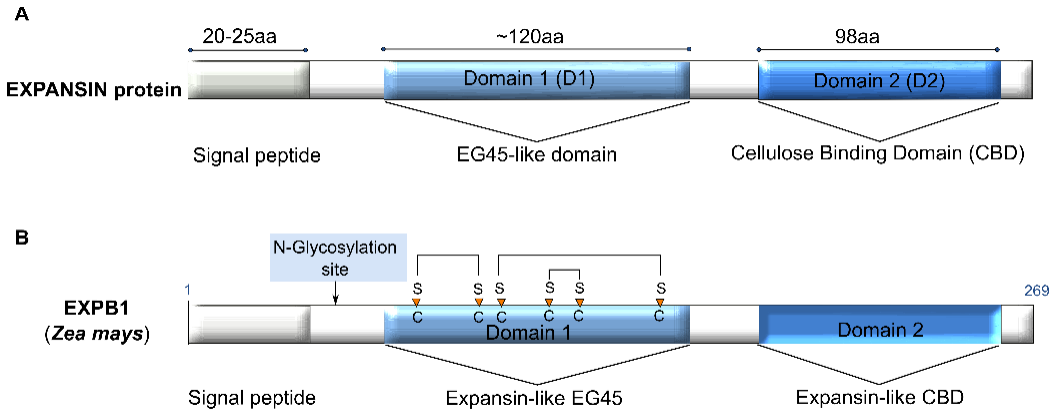


Figure 3.2. A schematic of the EXPANSIN protein with its conserved domains. **(A)** General structure of an EXPANSIN protein with a N-terminal signal peptide that is cleaved when protein enters the endoplasmic reticulum, Domain 1 (D1, light blue) with resemblance to catalytic domain of family-45 endoglucanases (EG45-like) and a C-terminal Cellulose Binding Domain (CBD) 2 (D2, darker blue); **(B)** Maize (*Zea mays*) ZmEXPB1 protein with the conserved Domain 1 and Domain 2. The Domain 1 contains amino acid residues that are N-glycosylated and conserved cysteine residues that are linked by di-sulfide bonds (Yennawar et al., 2006);

The model also suggests the presence of N-linked glycans on Domain 1 that are processed by post translational modification and three disulfide bonds, with the six participating cysteines being highly conserved in both EXPA and EXPB families (Yennawar et al., 2006) (**Figure 3.2B**). The crystal structure of BsEXLX1, an expansin-like protein from *Bacillus subtilis* (a root surface colonising gram positive bacterium), showed similarity in the structure of Domain 1 in the bacterial expansin, but lacked Domain 2 (Kerff et al., 2008). More recently, a comparative homology based modelling approach was used to determine the 3D structure of VpEXPA2, an expansin from *Vasconcellea pubescens* (papaya fruit). This model supports the structural similarity of key features such as the two-domain structure with conserved folds in the two

domains and affinity to cellulose that is typical of expansins (Gaete-Eastman et al., 2009).

While a lot is known about the atomic structure of the protein, the targets that expansins bind to on a plant cell wall and how they bring about their loosening effect have remained a mystery for long. It was originally proposed that expansins disrupt the hydrogen-bonds between cellulose microfibrils and hemicelluloses releasing the wall polymers to move freely in response to mechanical forces generated in a cell due to turgor pressure (McQueen-Mason et al., 1992; Cosgrove, 2000b). Recent studies however are beginning to shed more light on the interaction of expansins with their cell wall targets and their unique mechanism. For example, a combination of dynamic nuclear polarization and enhanced sensitivity based solid-state NMR spectroscopy in combination with differentially labelled Arabidopsis plants (C^{13}) and expansins (^{13}C, ^{15}N), was used to test which cell wall component expansin binds to (Wang et al., 2013). Using ^{13}C-labelled Arabidopsis cell wall and ^{13}C,^{15}N-labeled EXLX1 from *B. subtilis* (recombinantly expressed in *E. coli*), it was observed that expansin targets specific cellulose domains in the cell wall that have a slightly altered cellulose confirmation and that are also enriched in xyloglucans (Georgelis et al., 2011; Wang et al., 2013).

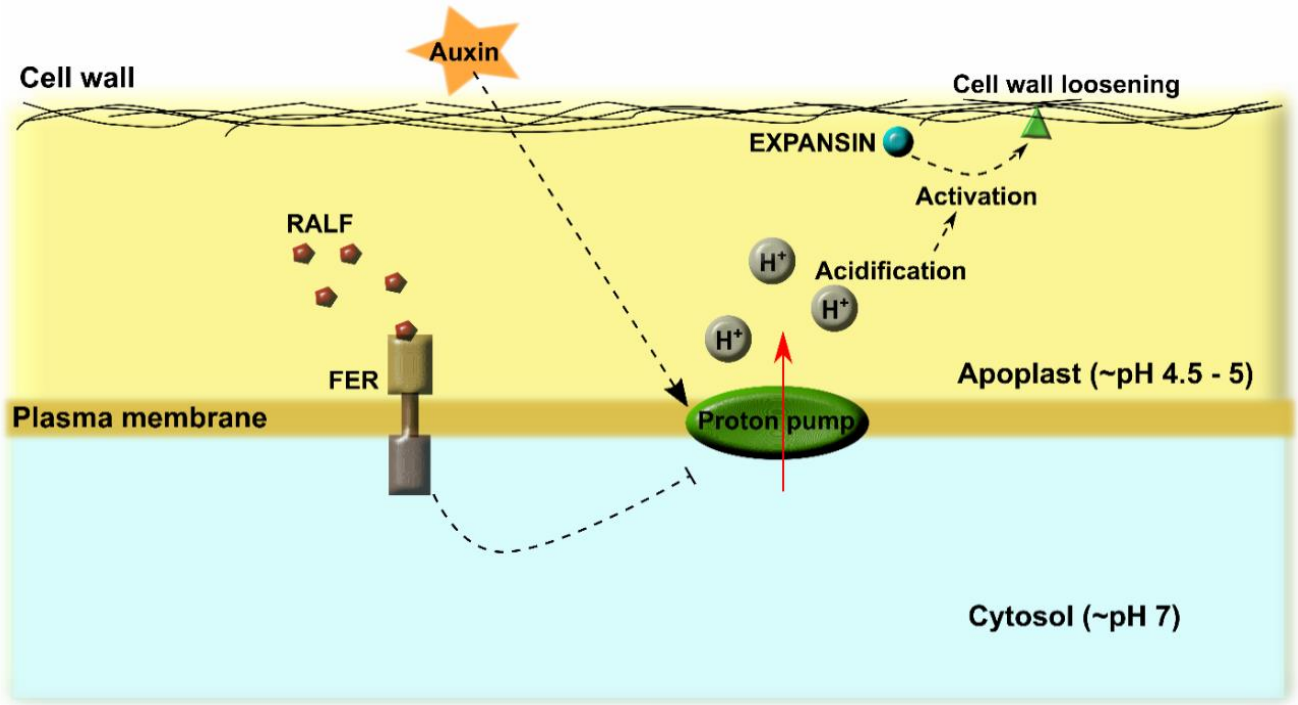


Figure 3.3. A simplified model for EXPANSIN action in a plant cell. FERONIA (FER) is activated by the secretory peptide RAPID ALKALINISATION FACTOR (RALF) (orange) inhibiting H^+-ATPase AHA2 leading to alkalinisation of the extracellular space and inhibition of cell growth. Auxin dependent signalling activates the H^+-ATPase proton pump that leads to accumulation of H^+ ions in the apoplastic space causing acidification, and a drop in pH to the 4.5–5 range that activates EXPANSINs. The activation of EXPANSINs (blue disc to green triangle) leads to its action on the cell wall to bring about cell wall loosening.

The emerging concept is that expansins may act on specific sites on the plant cell wall termed 'biomechanical hotspots', which are characterised by an altered cellulose structure and xyloglucan interaction (Cosgrove, 2014; Park and Cosgrove, 2015). All these developments point to the cell wall structure being far more sophisticated and specialised than originally envisioned. The 'acid-growth' theory points to the importance of acidification (pH ~4.0 – 5.5) of the apoplastic space around the growing cells as a key requirement for activation of expansins (Hager et al., 1971; Cosgrove, 2005) (**Figure 3.3**). However, the molecular mechanism by which the cell initiates changes still remains largely elusive. The plant hormone auxin, critical for plant growth and modulation of various developmental processes, is known to stimulate the activity of the plasma membrane H^+-ATPase causing apoplastic acidification. This triggers protonation of apoplastic auxin that can then diffuse passively into the cell, or in some instances supported by activity of auxin uptake carriers (Raven, 1975; Petrášek and Friml, 2009; Vanneste and Friml, 2009). This auxin transport driven signalling could provide the cue necessary to trigger the activation of expansins and directionality for action within the tissues. A part of this response is seen in stomatal guard cells, where it is known that the activation of a H^+ pump in the plasma membrane leads to creation of an electrochemical gradient across the membrane which results in accumulation of H^+ ions outside of the cell (Edwards et al., 1988). This resultant acidification of the cell wall has been suggested as a possible method by which the expansins are activated to bring about their turgor driven guard cell wall remodelling for stomatal opening and closing (Wei et al., 2011).

3.4. The role of expansins in fundamental developmental events

Expansins act as positive regulators of growth and development (**Figure 3.4**) (Cho and Kende, 1997a). There is growing evidence in various species of the importance of expansins in a wide range of developmental processes and physiological responses, including leaf initiation (Reinhardt et al., 1998a; Pien et al., 2001), leaf development (Sloan et al., 2009; Goh et al., 2012a; Lu et al., 2013), abscission (Cho and Cosgrove, 2000; Belfield et al., 2005b), hypocotyl and coleoptile elongation (Rochange et al., 2001; Gao et al., 2008; Boron et al., 2015), internode elongation (Choi et al., 2003), root growth and development (Lee et al., 2003; Soltys et al., 2012; Ma et al., 2013; Noh et al., 2013), root hair initiation (Baluska et al., 2000; Cho and Cosgrove, 2002; Lin et al., 2011), pollen tube penetration (Cosgrove, 1997a), fruit growth (Brummell et al., 1999a; Rose et al., 2000), fruit ripening (Brummell et al., 1999a; Civello et al., 1999; Brummell et al., 2002; Yoo et al., 2003), fruit softening (Rose et al., 1997; Brummell et al., 1999b; Trivedi and Nath, 2004; Costa et al., 2008), floral development (Ochiai et al., 2010; Harada et al., 2011; Zenoni et al., 2011), submergence response (Cho and Kende, 1997b; Vriezen et al., 2000; Caturla et al., 2002; Colmer et al., 2004), abiotic stress response (Harb et al., 2010; Guo et al., 2011; Lu et al., 2013; Xu et al., 2014b; Yan et al., 2014) and plant-microbial interaction (Hager et al., 1971; Wieczorek et al., 2006; Wieczorek and Grundler, 2006; Fudali et al., 2008).

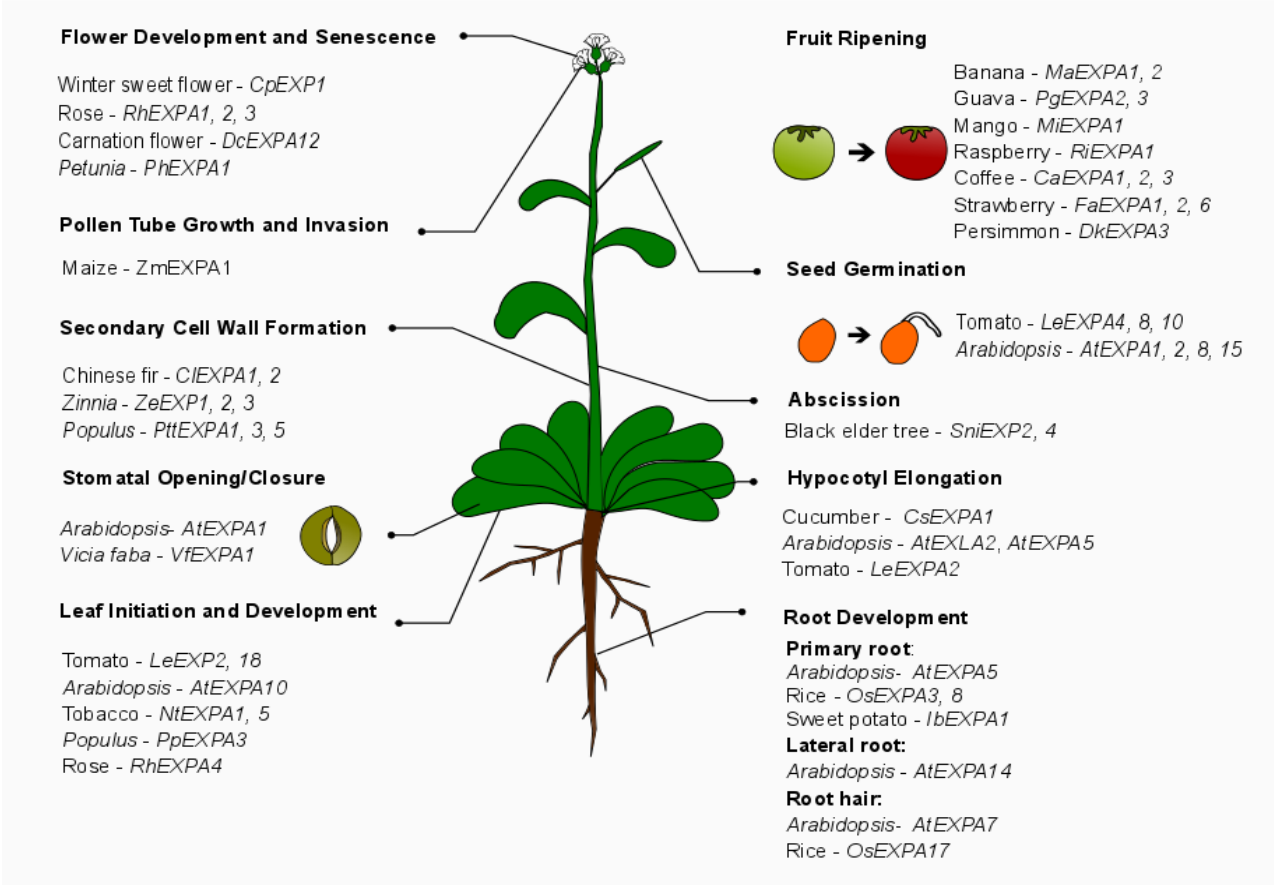


Figure 3.4. Expansins in plant growth and development. The schematic highlights the various processes in plant that contain expansin expression and/or activity.

3.4.1. Root system architecture

The effects of expansins on root development have been studied in crops such as *Glycine max* (soybean) (Lee et al., 2003), *Oryza sativa* (rice) (Wang et al., 2014), *Zea mays* (maize) (Kam et al., 2005), *Hordeum vulgare* (barley) (Kwasniewski et al., 2004; Kwasniewski and Szarejko, 2006), and *Ipomoea batatas* cv. Yulmi (sweet potato) (Noh et al., 2013) (**Figure 4**). In sweet potato, storage root development is accelerated in antisense-*IbEXP1* plants suggesting a negative role for the gene in storage root formation. The response is brought about by the suppression of metaxylem and cambial cell proliferation thereby inhibiting the initial thickening growth of the storage roots (Noh et al., 2013). A study on *Oryza sativa* (rice) identified *OsEXPA3* to be involved in root development. RNAi-mediated silencing of *OsEXPA3* causes suppressed root development with reduced primary root length and lateral root numbers. The root length reduction was found to be linked with decreased vascular cell length suggestive of a role in controlling cell size via regulation of cell elongation. The *OsEXPA3* RNAi plants also have significantly increased cell wall stiffness and changed wall polymer composition. This was measured (indirectly on suspension cell cultures from the calli of *OsEXPA3* RNAi rice plants) by Atomic Force Microscopy (AFM) and Fourier transform infrared spectroscopy (FTIR) analysis and suggests a role in biochemical and mechanical aspects of cell wall loosening (Qiu et al., 2014). Also silencing of *OsEXPA8* results in cell size reduction in the root vascular bundle as well as impaired root hair elongation, reduced root length and formation of lateral roots (Wang et al., 2014). Overexpression of *OsEXPA8* results in increased primary root length with production of more lateral roots and root hairs with decreased wall stiffness (Ma

et al., 2013). *OsEXPA10* was found to be Al-induced specifically in the root tip with strong localisation of OsEXPA10 to cells in the root elongation zone. Knock out of *OsEXPA10* in the absence of Al showed reduced root growth resultant from shorter cortical cell length suggesting its involvement in normal root cell elongation (Che et al., 2016). In Arabidopsis, on independent overexpression of three cell wall remodelling genes [*AtEXPA5,* a pectin methyl esterase inhibitor family protein (PMEI) (At5g62360), and a *CELLULASE* (CEL) (At2g32990)], only the lines overexpressing *AtEXPA5* showed primary roots to elongate faster. On overexpressing *AtEXPA5* together in combination with either PMEI or *CEL*, the offspring produced primary roots that are longer than either of their parents (Xu et al., 2014a). This is an interesting example to show expansins work in combination with other wall related proteins to bring about a developmental effect.

In Arabidopsis, activation of *AtEXPA14* expression by the plant transcription factor LOB DOMAIN-CONTAINING PROTEIN 18/ ASYMMETRIC LEAVES2-LIKE 20 (LBD18/ASL20) promotes lateral root emergence through overlaying layers in primary root possibly through enhancement of cell separation process in the overlaying walls (Lee et al., 2013). The RNAi lines of *EXPA17* show significantly reduced emerged laterals and the opposite effect is observed in the overexpressors (in the presence of auxin) (Lee and Kim, 2013).

3.4.2. Root hair formation

Root hair formation is another process where the role of expansins has been extensively studied (Cho and Cosgrove, 2002). Root hair initiation is marked by the formation of a typical bulge at the basal end of the trichoblasts (root hair

forming epidermal cells). This bulge formation is a targeted cell wall loosening process that is thought to be brought about by a combination of processes that involve alkalinisation of the cytoplasm, acidification of the cell wall, activation of expansins and XET activity (Vissenberg et al., 2001; Cho and Cosgrove, 2002). Arabidopsis *AtEXPA7* and rice *OsEXPA17* are an important factor in root hair formation and elongation. An *AtEXPA7* RNAi line driven by the *EXPA7* promoter displays a 25-48% reduction in root hair length and the lines also exhibit a wide range of lengths (Lin et al., 2011). In rice, mutations in *OsEXPA17* arrest root hair elongation. The defect was partially restorable by complementation of the *Osexpa17* with other root hair related expansins such as *OsEXPA30* or Arabidopsis *AtEXPA7*, which suggests partial conservation of expansin function in root hair development (Yu et al., 2011).

3.4.3. Leaf initiation

Leaves are vital plant photosynthetic organs with leaf morphology having a strong influence on plant productivity. Leaves initiate from the shoot apical meristem and following which the leaf size is determined by a highly spatially and temporally coordinated process of cell division and cell expansion (Donnelly et al., 1999; Tsukaya, 2003; Rodriguez et al., 2014). One of the earliest experiments to demonstrate the role of expansins in leaf initiation and development was in tomato (*Lycopersicon esculentum cv.* Moneymaker), where local application of an expansin protein extract to shoot apical meristem tips led to induction of a leaf-like structure (Fleming et al., 1997; Fleming et al., 1999). It was suggested that expansins cause localised changes to wall extensibility facilitating localised cell bulging that in turn leads to acquisition of ‘primordium identity’, and therefore, leaf primordia initiation (Fleming et al.,

1997). The study also stressed the need for other endogenous signals for completion of the correct leaf structure. Towards this, it was found that the spatiotemporal expression pattern of the expansin genes during organ formation was a key factor (Fleming, 2006). In a study on tobacco vegetative meristems, localised induction of expansin expression enabled leaf primordia induction that went on to produce phenotypically normal leaves (Pien et al., 2001). In this context, in tomato, *LeEXP18* expression corresponds to tissues with high meristematic activity (such as shoot apical meristem, leaf margins, and the procambium), while *LeEXP2* is expressed in expanding tissues (such as maturing stem, leaf and flowers), associating it with cell expansion (Reinhardt et al., 1998b).

Several studies also point to the importance of expansins in later stages of leaf development with expansin-mediated wall extension found to be characteristic to several growing leaves (Keller and Cosgrove, 1995) (**Figure 3.4**). In a study using an inducible promoter system that targets different leaf growth phases, it was found that although expansin gene transcripts were induced at all stages, the effectiveness of expansin protein itself was coincident with the mid phase of leaf growth and influenced by a potential endogenous system (regulatory cofactors) that regulates the efficacy of expansin protein activity (Sloan et al., 2009). The leaf size is regulated by exercising influence on the cell wall rheology seen for instance in a study on Arabidopsis where overexpression of *AtEXPA10* results in plants with larger leaves due to increased petiole cell size, with antisense plants exhibiting reduced acid-induced wall creep (Cho and Cosgrove, 2000). In Arabidopsis plants that

overexpress rose (*Rosa hybrida*) dehydration-induced expansin *RhEXPA4*, the ability of the plant to modulate leaf growth as an adaptive response (compact leaves due to reduced cell size to tolerate drought) is – in part - conferring drought tolerance (Lü et al., 2013). In tobacco (*Nicotiana tabacum*) plants, overexpression of *NtEXPA5* leads to an overall increase in leaf size attributed mainly to increased size of leaf epidermal and parenchyma cells. The increased cell size is mainly induced by cell elongation accompanied by a decrease in the number of cells due to reduced cell divisions, explaining absence of obvious changes in leaf shape. This suggests the presence of a regulatory feedback mechanism that is possibly regulated through transcriptional and/or hormonal signalling in order to maintain the balance between cell size and leaf shape (Kuluev et al., 2013). A temporal regulation of expansin activity in the leaf is suggested by an increase in *NtEXPA1* expression at the terminal buds, young growing leaves and flowers, with cessation of expression once the leaves are fully formed and growth is halted. Transgenic tobacco plants overexpressing *NtEXPA1* display increased length of the leaf blade due to increased size of epidermal and mesophyll cells which is potentially due to activity of NtEXPA1 (Kuluev et al., 2014). It is worth considering that although expansins often seem to exhibit a growth-promoting function in the leaf, they have different roles depending on the developmental stage ranging from supporting the acquisition of leaf primordium identity (although indirect), to being a counterbalance to growth-repression within the leaf at the later stage of development.

3.4.4. Stomatal opening/closing

Stomata – small openings or pores on the leaves – are required for the intake of carbon-dioxide by the plant and the release of oxygen. Their activity requires constant regulation in order to enable the plant to 'breathe'. This very dynamic process is controlled by the contraction and relaxation of the guard cells surrounding the stomatal opening through constant structural changes that take place in the walls of the guard cells. Expansins have been shown to play an important role to facilitate this process (**Figure 3.4**). In Arabidopsis, *AtEXPA1* is expressed in the guard cells and regulates stomatal opening putatively through altering guard cell wall structure (Wei et al., 2011). In transgenic Arabidopsis lines constitutively overexpressing *AtEXPA1,* the elastic modulus of the guard cells is lower, indicative of altered elastic properties of the guard cell wall structure leading to accelerated light-induced opening of the stomata (Zhang et al., 2010; Zhang et al., 2011).

3.4.5. Hypocotyl

The cucumber (*Cucumis sativus*) hypocotyl was one of the first systems where the effect of acid induced 'wall creep' was observed that hinted at the presence of agents in the cell wall that promote this effect (Cosgrove, 1989b) (**Figure 3.4**). Crude proteins isolated from dark-grown cucumber hypocotyls subjected to sequential fractionation led to identification of two proteins (29-30 kDa) later termed 'expansins', that could independently induce wall extension in heat-inactivated growing cell walls (McQueen-Mason et al., 1992; Cosgrove, 2000a). In order to test the effect of increased expansin activity on stimulating growth, recombinant cucumber *CsEXPA1* was expressed under a constitutive

promoter in tomato (*Lycopersicon esculentum* Mill.), which led to complex alterations in the growth of transgenic tomato plants. Increased expansin activity impairs hypocotyl elongation whilst stimulating radial growth of cells, almost suggestive of the growth polarity being affected. Closer examination at a cellular level showed reduced length of epidermal and cortical cells paralleled by an increase in their cell width measured on cross-sections as the cause for alterations in the growth structure of the plants (Rochange et al., 2001). In Arabidopsis plants however, overexpressing *AtEXLA2* increased the length of dark-grown hypocotyls possibly through positive regulation of cell elongation. The hypocotyls also exhibit decreased wall strength suggesting a different mode of action for the *EXPL* family genes towards cell wall modification (Boron et al., 2015). Tomato plants when treated to a combination of auxin coupled with sugar, was found to induce *LeEXPA2* expression to bring about hypocotyl cell elongation (Arru et al., 2008).

3.4.6. Flower development and senescence

Flower opening is an intricate process involving differential expansion of cells in different parts of the flower with the most extreme changes in cell expansion suggested to usually occur in the petals. The modulation of expansin gene expression during flower opening and hormonal cross talk has been studied in order understand the role they might play in the process (Zenoni et al., 2004; Dal Santo et al., 2011; Zenoni et al., 2011) (**Figure 3.4**). For instance, in winter-sweet (*Chimonanthus praecox*) flower, increased *CpEXP1* expression occurs in flower buds during the developmental stages of the bud and in the expanding stages (Ma et al., 2012) similar to the *Mirabilis jalapa,* β-expansin

gene *MjEXPB1* expression level increase (Gookin et al., 2003) and elevated transcript levels of *DcEXPA1* and *DcEXPA2* in carnation flower (*Dianthus caryophyllus*) (Harada et al., 2011). There are instances where expansins have been shown to work alongside other wall remodelling components to bring about their response, or to have different expansins at work in different parts of a developing organ, together orchestrating the developmental process. This was observed in a study on floral development of rose (*Rosa hybrid*) where *RhEXPA1* and *RhXTH1* were increased in the expanding zone at the base of the petal suggested to aid petal expansion, followed by the region exhibiting an increase in *RhEXPA2* and *RhEXPA3* expression as the flower progresses to senescence (Takahashi et al., 2007; Yamada et al., 2009). In *Petunia hybrid, PhEXPA1* is expressed in walls of expanding tissues during corolla development (a collective unit of petals) with down regulation of *PhEXPA1* expression resulting in flowers with smaller petal limbs because of decreased epidermal cell size and cell thickness due to altered crystalline cellulose and pectin deposition (Zenoni et al., 2004; Zenoni et al., 2011). Subcellular localisation studies of PhEXPA1 identified the protein to be localised to the cell wall and cytoplasm. Overexpressing the gene on the other hand causes significant changes in abaxial epidermal cell size with an altered wall polymer composition indicated by reduced pectin and hemicellulose content in the epidermal wall (Dal Santo et al., 2011; Zenoni et al., 2011). It would suggest that expansins are actively expressed during early stages of development from bud to bloom that requires rapid modification of cell wall at the cellular level in a directed manner reflected by the frequently observed expansin transcript and protein localisation patterns.

3.4.7. Pollen tube growth

Germination of pollen on stigma is followed by development of a pollen tube that enters the stigma and grows through the style intracellularly until it reaches the ovary and fertilizes it. β-expansins (grass pollen allergens) have been implicated to aid in invasion of the pollen tube through maternal tissues (Cosgrove, 1997a) and growth of the pollen tube itself (Sella Kapu and Cosgrove, 2010) **(Figure 3.4)**. In maize, ZmEXPB1 facilitates the initial penetration of the pollen tube into the silk and plays an important role in increased growth rate of maize pollen tubes. A maize line having a *Mutator* (*Mu*) transposon insertion in the pollen β-expansin shows loss in competitive growth ability of pollen tubes due to slower growth rate within the style (Valdivia et al. 2007b). The ability to infiltrate the style is suggested to be facilitated by β-expansins through possible weakening of the middle lamella of the cell walls by solubilisation of its wall matrix and increased wall plasticity (Tabuchi et al., 2011). In addition, pollen from maize RNAi lines with reduced β-expansin levels exhibit aggregation of pollen to form clumps, thus with reduced ability to disperse effectively upon anther dehiscence (Valdivia et al., 2009).

3.4.8. Seed germination

Seed germination is a dominant feature in the life of a plant. The embryo of a seed is surrounded by an endosperm layer and a seed coat (testa) and the emerging radicle needs to overcome these constraints to emerge and germinate (Holdsworth et al., 2008; Weitbrecht et al., 2011). Physiologically the constraints in germination are overcome through active cell division and cell expansion of the emerging radicle, which brings back the importance of cell wall

remodelling in yet another key process. Not surprisingly many genes from the expansin family display extensive regulation during early germination (reviewed in Weitbrecht et al., 2011) (**Figure 3.4**). In tomato, expansin transcripts show distinct localisation during seed germination. *LeEXPA8* was found to be expressed in the radicle tip, *LeEXPA10* in both the radicle tip and rest of seed, and *LeEXPA4* localized to the endosperm cap (which correlated with extent of weakening of the endosperm cap tissues following imbibition), all of which suggest specific roles in aid of radicle emergence during seed germination (Chen et al., 2001). In Arabidopsis, *AtEXPA2* is particularly expressed in the seeds and thought to control seed germination by weakening the endosperm layer and related structures surrounding the embryo in a gibberellic acid (GA)-dependent manner (Yan et al., 2014). Three other expansins, *EXPA1*, *EXPA8*, and *EXPA15*, were also shown to exhibit GA-induced expression during seed germination with the expression initiating at the radicle tip followed by its extended progression along embryo axis over time. It is interesting to note that although the radicle tip seems to be the primary site of expansin (and growth promoting gene) expression, the site of expansion is downstream the axis of growth along where the gradient of expression is observed which is attributed to physical arrangement of the cells and other contributing mechanical factors (Bassel et al., 2014).

3.4.9. Fruit

Fruit development is a dynamic process integrating a large number of complex processes in space and time. Expansins have been suggested to be involved at different stages of this process especially during fruit ripening and softening stages in fleshy fruits (Rose et al., 1997; Catala et al., 2000). Fruit

ripening involves textural changes in the fruit that are believed to occur due to cell wall modification by wall remodelling proteins (Brummell et al., 1999b; Brummell and Harpster, 2001). In depth studies on various fruits facilitated by the recent availability of sequenced genomes, show involvement of expansins in the fruit ripening process (**Figure 3.4**). For instance, in banana (*Musa acuminata*) *MaEXPA1* or *MaEXPA2* were shown to be partially transcriptionally activated by the transcription factor MaBSD1 (named after BTF2-like transcription factors, synapse-associated proteins and DOS2-like proteins) to bring about fruit ripening (Ba et al., 2014). In guava (*Psidium guajava* L.), an increased expression of expansin genes was co-incident with fruit ripening, with expression of *PgEXPA2* observed to increase in the fruit from 'Green Stage 2' to 'Overripe Stage 1' and *PgEXPA3* during four stages of fruit ripening with peak intensity at the 'Mature Stage' (Silva et al., 2013). Similarly, in raspberry (*Rubus idaeus*), the highest level of expression of *RiEXPA1* was observed around later stages of the fruit ripening process (Zheng and Hrazdina, 2010). Expression analysis of coffee (*Coffea arabica)* fruits showed accumulation of *CaEXPA1* and *CaEXPA3* transcripts in the perisperm tissue (contributor of coffee bean size) as well as in early stages of pericarp development. Also *CaEXPA2* becomes highly expressed in the pericarp at the later stages during fruit maturation and ripening (Budzinski et al., 2011).

Postharvest ripening is another aspect where expansins have been implied to be involved. Persimmon fruits (*Diospyros kaki* L.) show increased expression level of *DkEXPA3* in the initial 8-day ripening period post-harvest, followed by a gradual decrease in the later stages (Zhang et al., 2012). The deterioration of soft fruits is very often determined by fruit softening rate.

Application of oxalic acid, a reducing agent seems to delay expression of mango fruit (*Mangifera indica* L. cv. Zill) *MiEXPA1* and certain pectolytic enzymes in the peel and flesh suggesting expansins delay the process of softening and ripening during storage (Zheng et al., 2012). Expansin transcript levels have also been shown to relate with variation in firmness of strawberry fruits during ripening (Dotto et al., 2006). In an indirect measure to test the contribution of expansins to ripening, the fruits of strawberries (*Fragaria* x *ananassa* Duch., cv. Camarosa) were heat treated and measured for fruit firmness and expansin gene expression levels. A delay in fruit softening was seen post treatment and it was also observed that the expression of *FaEXP1*, *FaEXP2* and *FaEXP6* was decreased in the treated fruits that could be a potential cause of the delay, although not conclusive enough (Dotto et al., 2011).

3.4.10. Secondary wall formation

Secondary cell walls are laid down once cells mature and cease to grow. They provide strength and mechanical support to plant body, and in case of tracheary elements the deposition of lignified secondary wall, water-proofs the tissues to resist negative pressure during transpiration and enables solute transport (Mellerowicz et al., 2001; Cosgrove and Jarvis, 2012; Zhong and Ye, 2015). Quite a few studies show that expansins are involved in secondary wall formation (**Figure 3.4**). For instance, in Chinese fir (*Cunninghamia lanceolata*)*, ClEXPA1* and *ClEXPA2* are expressed specifically in cambium and in the wood-forming tissues. Independent overexpression of these genes in tobacco plants shows a drastic increase in height and diameter, along with increased size of parenchyma cells of pith and thicker cell walls in xylem of stem due to increased cellulose content (Wang et al., 2011). In *Zinnia elegans*, expansins were found

to be expressed during primary xylem formation; specifically, *ZeEXP1*, *ZeEXP2*, *ZeEXP3* are expressed in a single flank of elongated cells adjacent to protoxylem or metaxylem vessels during development of primary xylem cells. The mRNA of these genes shows differential localisation in the cell at points of potential growth suggesting that they aid the intrusive growth of primary cell wall. The expression of *ZeEXPA1* and *ZeEXPA2* decreases close to secondary cell wall formation while *ZeEXPA3* continues to be expressed suggestive of a coordinated action of expansins in secondary wall development (Im et al., 1999; Im et al., 2000). In hybrid aspen (*Populus tremula* × *Populus tremuloides* Michx), different tissues have differential dominant expression of expansin genes: *PttEXPA1* in the cambial region, *PttEXPA5* in tension wood, and *PttEXPA3* in young leaf. *PttEXPA1* in meristematic (cambial) and radial-expansion zones of stem internodes is suggestive of their aid to intrusively growing tips of differentiating xylem fibers. Overexpression of *PttEXPA1* increases the diameter of the fibers in wood-forming tissues by wall loosening but, does not affect the diameter of the vessel itself enabling symplastic fiber growth in developing wood tissues (Gray-Mitsumune et al., 2004; Gray-Mitsumune et al., 2008).

3.5. Hormonal regulation of plant expansins

Plant hormones play a crucial role in coordinating plant growth and organ development via modulation of fundamental processes such as cell division or cell expansion. Plant hormones have long been implicated in the regulation of expansin gene expression suggested by the presence of classic hormonal regulatory elements in the promoters of most expansin genes (Lee and Kende, 2001). Several plant hormones affect expansin transcript levels (**Figure 3.5**)

and in this context, the role of auxin in regulation of some expansin genes has been well explored (Cosgrove, 1997b; Caderas et al., 2000; Catala et al., 2000; Cosgrove, 2000c). Auxin when coupled with sugar and not on its own was able to induce *LeEXPA2* expression in tomato plants to bring about hypocotyl cell elongation (Arru et al., 2008). Another study that looked at the effect of acetylcholine (a compound that has been ascribed to have similar effects as auxin in plants), found the induction of *LeEXPA2* to be further enhanced in the presence of sugar and alongside auxin (Di Sansebastiano et al., 2014). Auxin also induces *NtEXPA1* and *NtEXPA4* expression in young tobacco leaves located near the terminal bud region. In lower leaves however, brassinosteroids show differential regulation via inhibition of *NtEXPA1* and up-regulation of *NtEXPA4* (Kuluev et al., 2014). When etiolated potato (*Solanum tuberosum*) stems are exposed to auxin, within the first hour the transcript levels of *SlEXPA1*, *SlEXPA3*, *SlEXPA4*, *SlEXPA5* rapidly increase corresponding to the period of cell elongation. Some continue to be expressed while others are down regulated after a point suggesting different roles for the different expansins controlled in part via hormonal regulation (Jung et al., 2010).

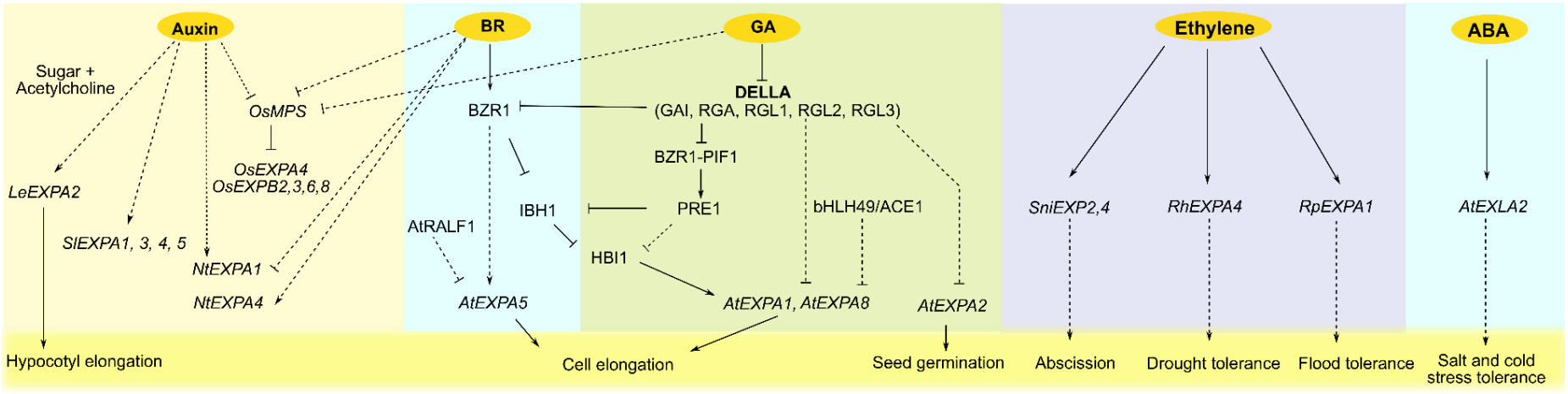


Figure 3.5. Schematic showing a simplified regulatory network of auxin, brassinosteroids (BR), gibberellins (GA), ethylene and abscisic acid (ABA) signalling in regulation of EXPANSIN expression that controls developmental and stress responses in plants.

Brassinosteroid (BR) and gibberellin (GA) are thought to participate in cell growth in part through expansin-mediated loosening of the cell wall (Bai et al., 2012). In Arabidopsis, exogenous application of GA to seeds causes a strong induction of *AtEXPA2* to promote seed germination and to confer salt and osmotic stress tolerance by de-repression of DELLA proteins. All the five DELLAs: GIBBERELLIN INSENSITIVE (GAI), REPRESSOR OF ga1-3 (RGA), RGA-like1 (RGL1), RGL2 and RGL3 were involved in repression of *AtEXP2* to inhibit seed germination, with RGL1 being a key regulator (Arru et al., 2008; Yan et al., 2014). RGL2 was also found to directly bind to the *EXPA8* promoter and down-regulate its expression. This repression inhibits seed germination by exercising a constraint on elongation of the cells (Stamm et al., 2012). *EXPA8* and *EXPA1* are also under direct positive transcriptional control of a bHLH transcription factor HOMOLOG OF BEE2 INTERACTING WITH IBH1 (HBI1) in promoting cell elongation. The antagonistic interaction between two HLH factors, PACLOBUTRAZOL-RESISTANT 1 (PRE1) and ILI1 BINDING bHLH PROTEIN1 (IBH1), and a bHLH factor HBI1 is regulated via GA and brassinosteroid (BR) signalling pathways to regulate cell elongation (Bai et al., 2012). Another bHLH factor, bHLH49/ACTIVATOR FOR CELL ELONGATION1 (ACE1), binds to the G-box on the *EXPA8* promoter and regulates its expression positively to promote cell elongation. In overexpressor lines of *ACE1* increase in the length of cells and not its number are observed. ACE1 acts in cohort with PRE1 to bring about this positive regulation, while its interaction with a different factor IBH1 suppresses its binding to the *EXPA8* promoter turning it into a negative regulator of cell elongation (Ikeda et al., 2012a). BR promotes *AtEXPA5* expression and functions downstream of the transcription

factor BRASSINOZALE-RESISTANT1 (BZR1)-mediated BR signalling (Park et al., 2010) and positively affects root cell elongation. However, this up regulation of *AtEXPA5* is reduced in plants treated with the signalling peptide AtRALF1 that is known to promote cell elongation, even when pre-treated with brassinolide. This suggests an antagonistic relationship between AtRALF1 and BR in regulation of *AtEXPA5* and genes regulating cell expansion (Edwards et al., 1988). In sweet potato, the transcript level of gene *LbEXP1* and three other brassinosteroid (BR)-responsive genes [fatty acid elongase *3-KETOACYL-COA SYNTHASE 1* (*KCS1*), *HAIKU1* and *MINISEED3*] are up-regulated in response to BR treatment again suggesting involvement of BR signalling (Bae et al., 2014). Gibberellin is well known to induce rapid internodal elongation in deep-water rice and four β-expansin genes (*OsEXPB3*, *OsEXPB6*, *OsEXPB11* and *OsEXPB12*) show strong induction at the internodes in response to treatment with gibberellin and also in response to wounding (Jung et al., 2010). An R2R3-type MYB transcription factor in rice, MULTIPASS (OsMPS), binds to the promoter of several rice expansins *OsEXPA4*, *OsEXPB2*, *OsEXPB3, OsEXP6 and OsEXP8,* acting as a negative regulator of cell wall remodelling genes. *OsMPS* expression is down regulated by auxin, BR and GA and up regulated in response to CK, ABA and salt stress. The knock-down mutant *Osmps* shows up regulation of *OsEXPA4*, *OsEXPB3* and *OsEXPB6* with the plants displaying increased size and length of leaf epidermal cells, while overexpression of *OsMPS* shows a decrease (Schmidt et al., 2013).

Fruit softening and abscission involve breakdown of wall material, while expansion involves wall loosening and expansins have been implicated in both of these processes either autonomously or in concert with other factors. In

banana, fruits treated with nitric oxide showed reduced expression of *MaEXP1* which is thought to possibly be through inhibition of ethylene synthesis. This has been associated with delayed fruit pulp softening and also to work in coordination with several other wall degrading enzymes (Yang et al., 2010). Ethylene also down-regulates the expression of *AtEXPA5* and thus plays a role in influencing hypocotyl elongation in Arabidopsis (Son et al., 2012). In black elder tree (*Sambucus nigra*), *SniEXP2* and *SniEXP4* are highly expressed at the leaf abscission zone specifically under ethylene induction. The accumulation of the expansin transcripts is highly specific to ethylene induction and suggestive of expansins' role in ethylene induced cell separation during leaf abscission, although the exact mechanism by which this is brought about is unclear (Belfield et al., 2005a). Treatment with jasmonic acid (JA) is suggested to lead to early flower opening through an increased expression of expansins and *XTHs* in the flower tissues that facilitate acceleration of petal cell wall loosening (Ochiai et al., 2013).

3.6. Future perspectives for expansin research

Expansins are a unique family of proteins that promote controlled cell wall extension and stimulation of stress relaxation in plant cell walls. A striking range of growth, developmental, and physiological processes are regulated by the expansin superfamily with its relatively similar function that is often by promotion of cell expansion or cell elongation. Although most expansins seem to have similar functions, it is still unclear if the different expansins have evolved different approaches depending on type of process they regulate. So far, only few proteins from the different families of expansin superfamily have been the

focus of structural study. Further study of these aspects will help clarify how expansins control such a diverse range of processes. Hormones, transcription factors, and small signalling peptides seem to have a role in regulation of expansins either directly or indirectly. Elucidating the signalling pathways involved in regulation of expansins during plant growth and in response to environmental stimuli is another challenge that warrants further genetic and molecular level studies to gain a better understanding of the expansin superfamily.

A great deal has been understood about the structure of the expansin protein itself and their interaction with specific components of the cell wall. However, the mechanism by which the expansins unlock the cell wall to bring about its response still remains elusive. To unravel this, we first need a more in depth understanding of the structure of the cell wall at the supramolecular level in order to be able to point to the factors in the wall that respond to expansin action. A lot of recent work provides evidence to support the idea of expansins working in cohort with other wall remodelling factors to bring about its wall loosening activity. It is important to understand the function of the protein as a part of multi-enzymatic complex by application of analytical studies that employ computational and theoretical approaches coupled with biochemical and molecular biological data to gain answers on how the expansins interact and therefore, act.

Aims and objectives:

Aims

1) To understand the role of cell wall remodeling genes in early stages of lateral root formation in *Arabidopsis thaliana*

2) Comparative study on cell wall properties of wall mutant's defective in root development and alterations in response to phytohormone auxin

Objectives

1) Meta-analysis to identify cell wall remodeling genes involved in lateral root formation

2) Functional charaterisation of cell wall remodeling gene *EXPANSINA1* with respect to potential role in asymmetric cell divisions during lateral root initiation

3) Develop a method to study the chemical composition of intact cell walls and auxin-mediated alterations to the cell wall composition

4) Comparative study on alterations in cell wall properties of *expa1-1* using confocal Raman microscopy

5) Functional characterisation of transcription factor bHLH49, identified from a study to identify genes involved in asymmetric cell division during lateral root initiation (De Smet et al., 2008)

Chapter 4. *EXPANSINA1* is important for organised cell expansion and asymmetric cell divisions during lateral root initiation in Arabidopsis

4.1. Introduction

Over the last years, many studies point out the importance of cell wall remodelling to enable the emergence of lateral root primordia (Laskowski et al., 2006; Peret et al., 2009a; Aalen et al., 2013; Kumpf et al., 2013; Roycewicz and Malamy, 2014; Vermeer et al., 2014; Vilches-Barro and Maizel, 2015; Wilson et al., 2015; Orman-Ligeza et al., 2016). However, little is understood on how the cell wall is restructured during LR initiation, the interactions and communication between the different layers of the root to accommodate the developing lateral root, and/or the factors that influence these processes. The overarching aim of this PhD was to identify and study novel key regulators of asymmetric cell division (described in detail in **section 4.3.1.**), narrowing down to functional characterisation of a potential candidate from the expansin superfamily. Expansins with their unique ability to promote controlled cell wall extension and stimulation of stress relaxation in plant cell walls (described in detail in **Chapter 3**), form an interesting piece to the puzzle of rapid cell wall restructuring which is fundamental to initiating and growing primordia. This chapter describes the role of *EXPANSINA1* in the process of asymmetric cell division during lateral root formation.

4.2. Results

4.2.1. Meta-analysis to identify cell wall remodelling genes active during lateral root initiation

During lateral root initiation, lateral root founder cells expand radially prior to the first round of asymmetric cell divisions (Vermeer et al., 2014). To investigate the underlying molecular mechanisms associated with radial cell expansion in the pericycle, we probed the differential expression of 406 putative cell wall remodelling genes in TAIR by Gene Ontology (GO) term enrichment analysis (**Supl. Table 4.1.)**. For this, the list of candidates was probed against a transcript profiling dataset (De Smet et al., 2008) that was generated from auxin-induced pericycle cells sorted by Fluorescence-activated cell sorting (FACS). The auxin treatment reflects lateral root initiation with high spatial and temporal resolution. Meta-analysis identified 42 candidates that were differentially regulated in both datasets and therefore are potentially involved in early steps of lateral root initiation (**Supl. Table 4.2.**). Inducibility of these candidate genes by auxin and other plant hormones was confirmed by using available micro-array datasets from Genevestigator (Hruz et al., 2008). We retained 29 candidates for which expression is significantly regulated by auxin (13/29), brassinosteroids (2/29), cytokinin (7/29), abscisic acid (9/29) or salicylic acid (11/29) (**Figure 4.1. and Table 4.1.**). From the meta-analysis data, we decided to focus on *EXPANSINA1* (*EXPA1* - AT1G69530) as the primary candidate for further characterisation.

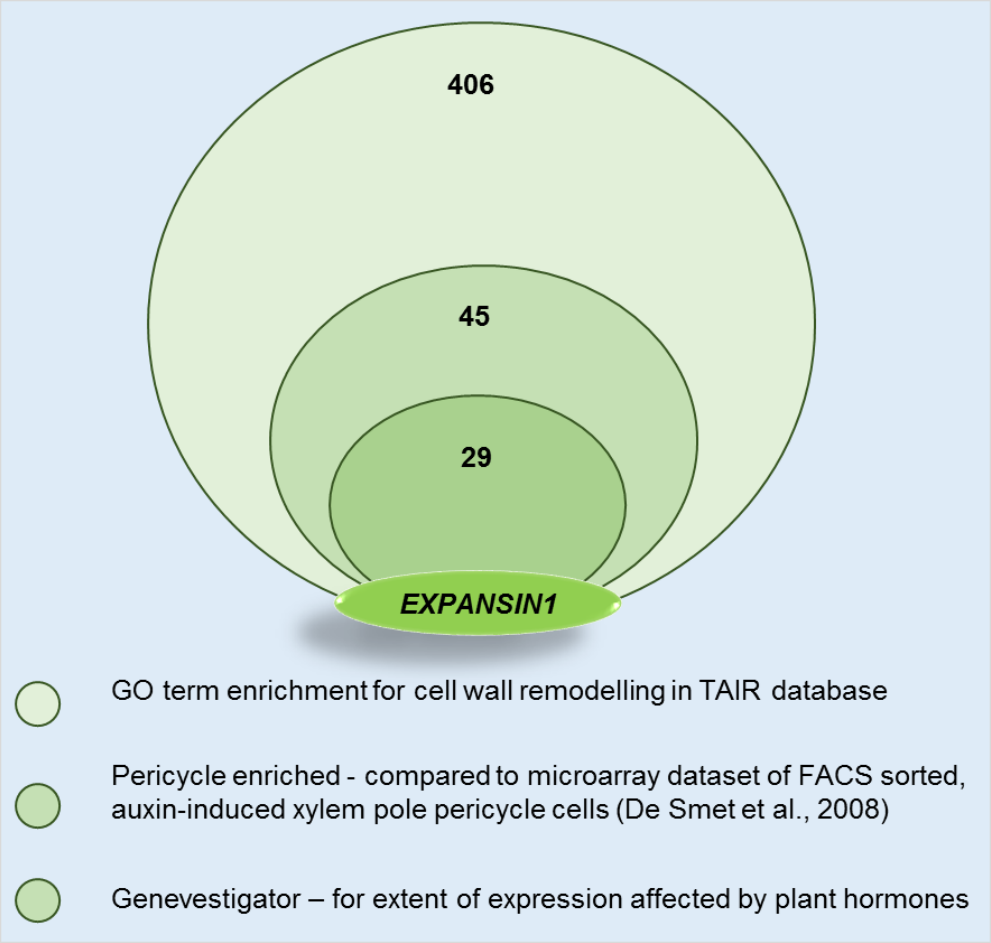


Figure 4.1. Schematic that depicts identification of *EXPA1* following meta-analysis of various cell wall remodelling genes. See also **Supl. Table 4.1. and 4.2.**

Table 4.1. List of genes selected based on differential regulation by hormones in available micro-array datasets from Genevestigator (Hruz et al., 2008).

AGI	Description	BR	ABA	Auxin	SA	Cytokinin
AT4G02290	glycosyl hydrolase 9B13	0	-1	0	0	0
AT5G11720	Glycosyl hydrolases family 31 protein	0	-1	0	0	0
AT1G02640	beta-xylosidase 2	0	-1	0	-1	0
AT4G24780	Pectin lyase-like superfamily protein	0	-1	0	-1	0
AT3G53190	Pectin lyase-like superfamily protein	0	-1	0	-1	0
AT1G02810	Plant invertase/pectin methylesterase inhibitor superfamily	0	0	0	-1	0
AT1G78060	Glycosyl hydrolase family protein	0	0	0	-1	0
AT2G06850	xyloglucan endotransglucosylase/hydrolase 4	0	0	0	-1	0
AT4G23820	Pectin lyase-like superfamily protein	0	0	0	-1	0
AT1G64760	O-Glycosyl hydrolases family 17 protein	0	0	0	-1	0
AT2G19440	O-Glycosyl hydrolases family 17 protein	0	0	0	-1	0
AT2G18800	xyloglucan endotransglucosylase/hydrolase 21	0	0	-1	0	0
AT5G19730	Pectin lyase-like superfamily protein	0	0	-1	0	0
AT5G49360	beta-xylosidase 1	0	0	-1	0	-1
AT4G14130	xyloglucan endotransglucosylase/hydrolase 15	0	1	-1	-1	-1
AT1G04680	Pectin lyase-like superfamily protein	0	-1	1	0	0
AT1G69530	**ExpansinA1**	0		1	0	1
AT1G64390	glycosyl hydrolase 9C2	0	0	1	-1	1
AT4G38210	expansin A20	0	0	1	0	0
AT2G43860	Pectin lyase-like superfamily protein	0	0	1	0	0
AT3G59850	Pectin lyase-like superfamily protein	0	0	1	0	0
AT4G13210	Pectin lyase-like superfamily protein	0	0	1	0	0
AT4G13710	Pectin lyase-like superfamily protein	0	0	1	0	0
AT2G39700	AT2G39700	0	0	1	0	1
AT3G61100	Putative endonuclease or glycosyl hydrolase	0	0	0	0	1
AT3G62460	Putative endonuclease or glycosyl hydrolase	0	0	0	0	1
AT3G62530	ARM repeat superfamily protein	0	0	0	0	1
AT5G09840	Putative endonuclease or glycosyl hydrolase	0	0	0	0	1
AT4G17030	expansin-like B1	0	1	0	0	0
AT5G48070	xyloglucan endotransglucosylase/hydrolase 20	1	0	0	0	0
AT2G18660	plant natriuretic peptide A	1	0	0	1	0
AT5G53370	pectin methylesterase PCR fragment F	0	0	0	1	0
AT1G71380	cellulase 3	0	0	0	0	0

4.2.2. *EXPA1* is expressed in the pericycle during lateral root initiation

To map the *EXPA1* expression pattern during lateral root development, we performed an *in vivo* expression analysis of *pEXPA1::n3xGFP* (provided by De Smet I) by induction of a lateral root via gravitropic root bend technique (Péret et al., 2012). This revealed that *EXPA1* is expressed in the lateral root founder cells (specialised xylem pole pericycle cells) post-nuclear migration, but preceding the asymmetric cell division. Additionally, it is expressed in the small daughter cells following the first formative division and continued to be expressed within the dividing primordia until the later stages of development (**Figure 4.2. a-c**). As the primordium progresses through Stage III, *EXPA1* expression is also detected in the cortical cells overlying the developing lateral root primordium (**Figure 4.2. d**). The gene is also expressed in the columella cells of root tip and epidermal cell layer with an expression pattern that overlaps the region of auxin response in the root tip (**Supl. Figure 4.1**).

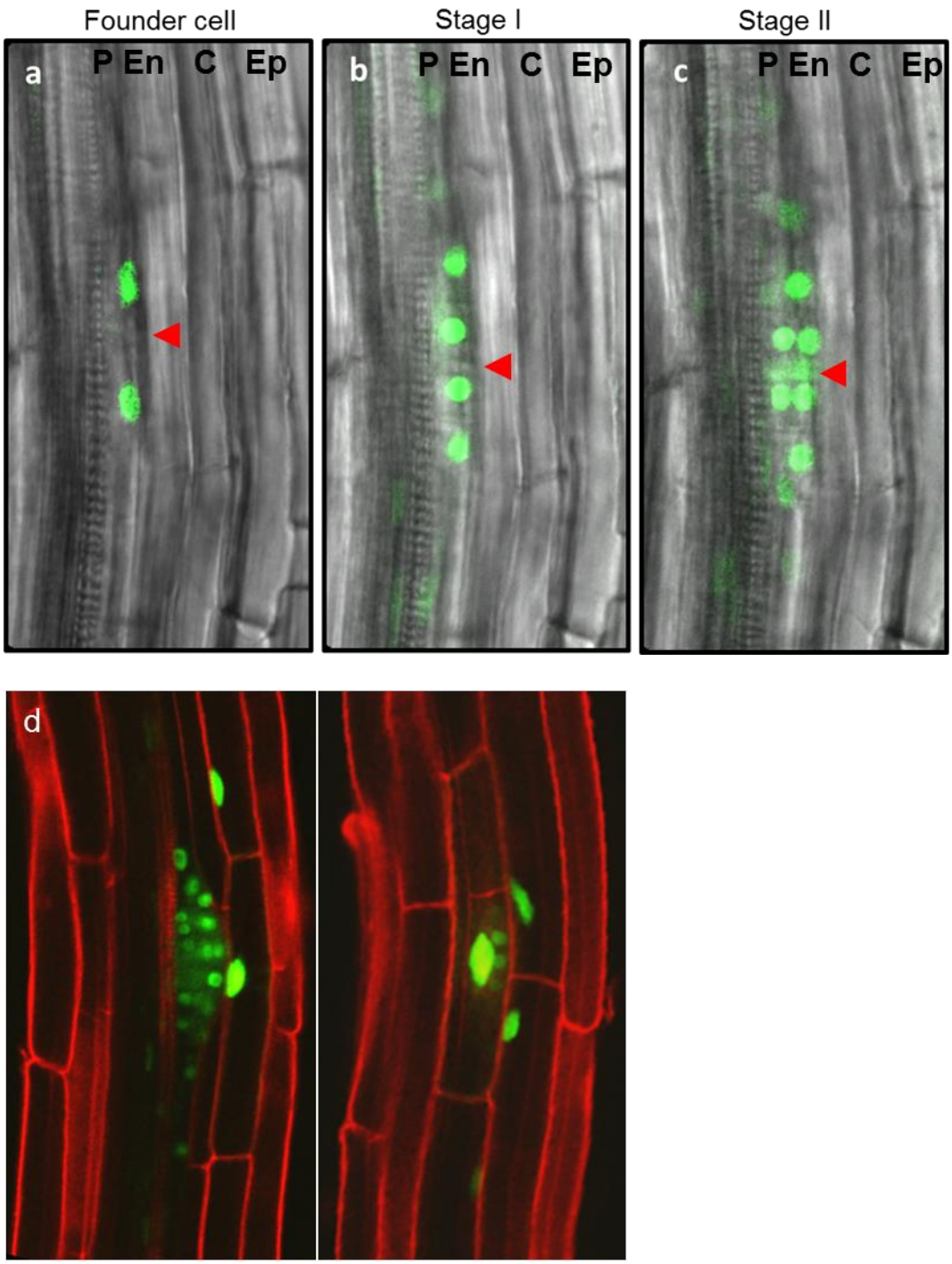


Figure 4.2. *In vivo* expression analysis of *pEXPA1::n3xGFP*. *EXPA1* expression observed in lateral root founder cells post nuclei migration (a), Stage I (b), Stage II (c). Red arrow indicates junction between adjacent pericycle cells that undergo asymmetric cell division; Expression in the cortical cells overlaying the primordia at later stage of development (d) (3 independent replicates).

4.2.3. *EXPA1* is regulated by auxin and is a secondary response downstream of SLR-ARF7-ARF19 module

Auxin is an important regulator of early stages of lateral root development (Overvoorde et al., 2010b). An exogenous auxin treatment time series to measure *EXPA1* expression level 0, 2 and 6hr post 10µM NAA treatment root tissues revealed an increase of *EXPA1* expression upon auxin treatment (**Figure 4.3a**). To assess if the auxin dependent regulation of *EXPA1* was a primary response, we used the protein synthesis inhibitor cycloheximide (CHX) in combination with auxin. Under high auxin levels in cells, early or primary auxin response genes are rapidly induced or repressed via the degradation of auxin/indole-3-acetic acid (AUX/IAA) repressors that de-represses Auxin Response Factors (ARF) in turn activating auxin responsive genes **(Figure 4.3e**) (Abel and Theologis, 1996; Guilfoyle et al., 1998). Primary auxin response genes are direct targets of the AUX/IAA-ARF dimer and do not require *de novo* proteins to activate them. They show induction when treated with auxin in the presence of cycloheximide (CHX), which is a protein synthesis inhibitor. In contrast, secondary auxin responsive genes are not direct targets of AUX/IAA-ARF and are not induced in the presence of CHX. As *EXPA1* expression was not auxin inducible in the presence of CHX, we confirmed *EXPA1* was a secondary response to auxin (**Figure 4.3b**). To assess if *EXPA1* is downstream of the main auxin response module associated with lateral root initiation, namely the SLR−ARF7−ARF19 module (Fukaki et al., 2002b; Fukaki et al., 2005b; Okushima et al., 2005; Okushima et al., 2007b), *EXPA1* expression was analysed in *arf7*, *arf19*, *arf7arf19* and *slr* mutant roots. In all *arf* mutants this signalling module was downregulated, whereas it was constitutively active in

the dominant negative *slr* mutant. In all *arf* mutants *EXPA1* expression was down-regulated, whereas it was upregulated in *slr* (**Figure 4.3c**). In addition, the auxin-dependent up-regulation of *EXPA1* is reduced in *slr* compared to wildtype (**Figure 4.3d**). Overall, *EXPA1* expression is regulated indirectly by auxin and downstream (although likely indirectly) of the SLR-ARF7-ARF19 module.

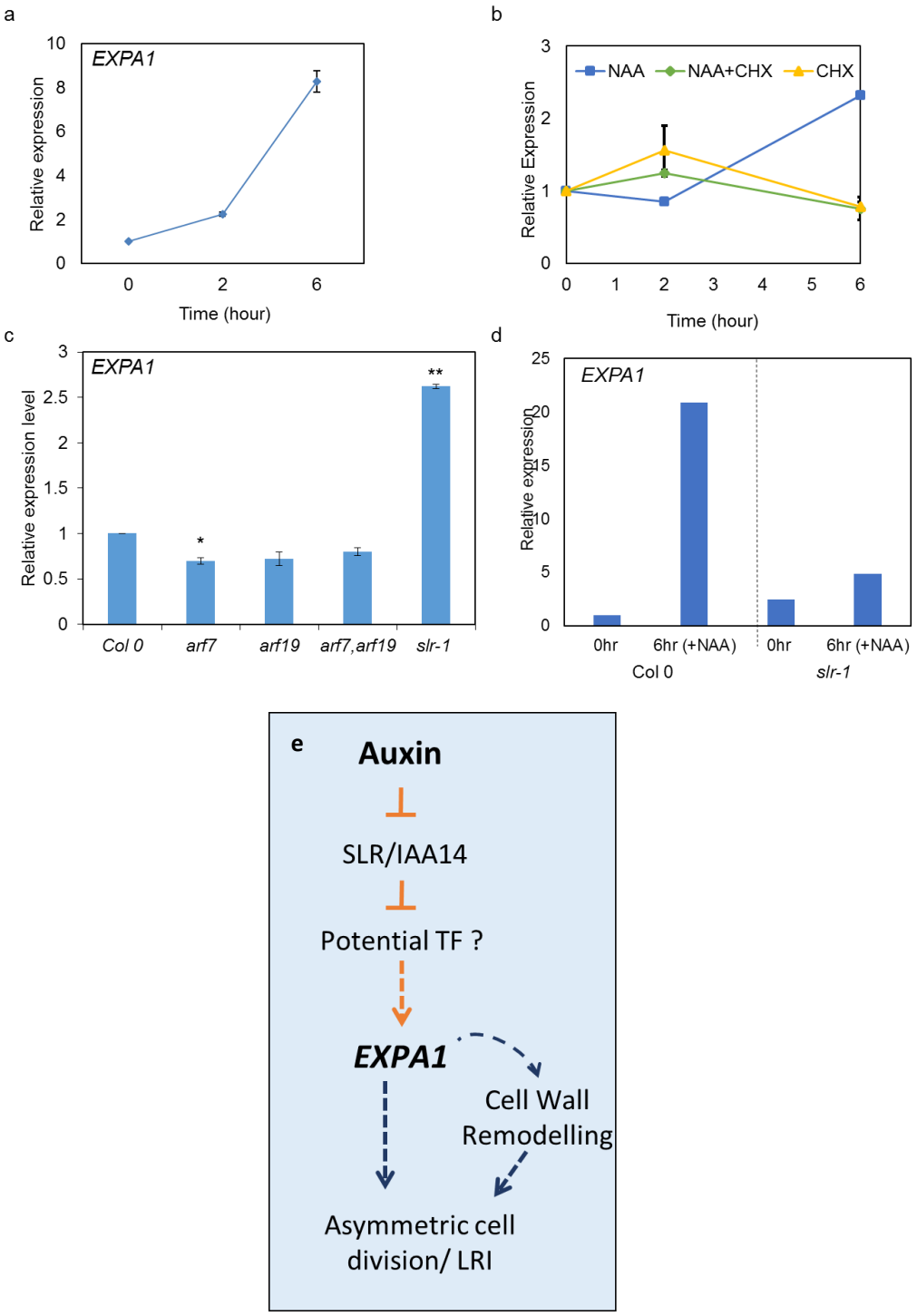


Figure 4.3. 3DPG *Col-0* seedlings analysed for *EXPA1* levels by qRT-PCR. Auxin treatment response time series (a); Expression profile in response to 10µM NAA, 10µM CHX and NAA+CHX 0, 2 and 6 hours post induction (n=3, ±SE) (b); *EXPA1* expression in auxin response mutants (n=2, ±SE, **p<0.001, *p=0.07) (c); Expression profile of *EXPA1* in roots of *slr* compared to *Col-0* at 0hr and 6hr post 10µM NAA treatment (n=1) (d); Schematic of auxin signalling pathway potentially upstream of *EXPA1* during lateral root initiation (e).

4.2.4. *In-vivo* analysis of *pEXPA1::nx3GFP* on auxin treatment

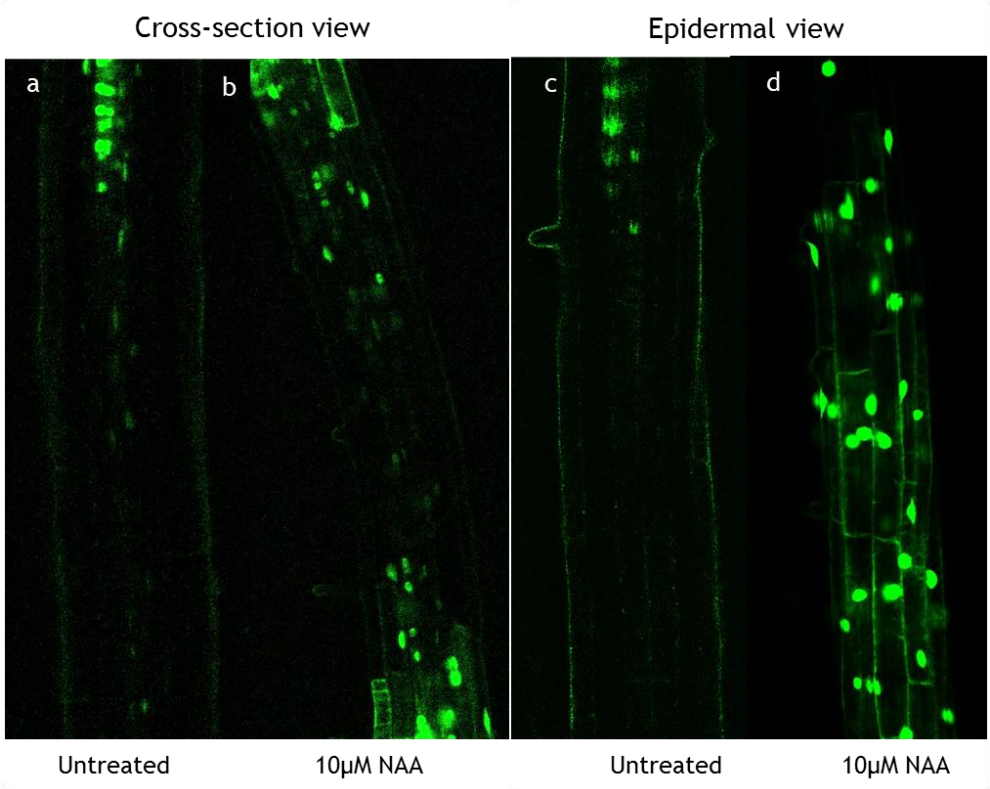


Figure 4.4. Comparison of expression profile of *pEXPA1::n3xGFP* expression in 3DPG roots that are untreated and imaged post gravitropic stimulus (a, c) and post 15hrs 10µM NAA treatment (b, d).

We imaged the roots of 3DPG seedlings of *pEXPA1::n3xGFP* to analyse the differential expression pattern in response to auxin treatment. For untreated samples, the roots were subject to gravitropic lateral root induction and the developing primordium in the bend was imaged. To study the effect of auxin treatment, the roots were exposed to 10µM of a synthetic auxin, NAA (1-naphthaleneacetic acid), and imaged at the differentiation zone 15hrs post induction, when the primordia have undergone the first round of asymmetric cell division (Peret et al., 2012). In the untreated roots, *EXPA1* is mainly expressed in the lateral root primordia with some expression detected in the epidermis (**Figure 4.4. a,c, and Figure 4.2**). Auxin treatment caused strong induction of

EXPA1 transcripts in the vasculature and in the pericycle cell layer, especially in lateral root primordia. The expression is also induced in the cortical and the epidermal layer of the root (**Figure 4.4 b, d**). Increased lateral root induction is a classic response upon auxin treatment and the auxin dependent induction of *EXPA1* expression in the initiating primordia supports the idea of auxin dependent up-regulation of *EXPA1.* The increased expression could also be due to increased lateral primordia induced by auxin that in turn express *EXPA1* driving higher expression levels in the root.

4.2.5. *EXPA1* is involved in pericycle cell expansion during lateral root initiation

To evaluate if *EXPA1* affects lateral root initiation, we analysed an *expa1* T-DNA insertion line (named *expa1-1*). The line was genotyped to confirm homozygosity and used for future phenotypic analysis. The position of the T-DNA insert was identified as 60bp upstream of the start site (ATG) of the *EXPA1* in the 5' UTR region (**Figure 4.5 a**). qRT-PCR analysis shows the line to be a full knock out (**Figure 4.5b**). As only one T-DNA allele was available for the gene, we generated complementation lines to test the rescue of the phenotype (transformed and selected, yet to be analysed).

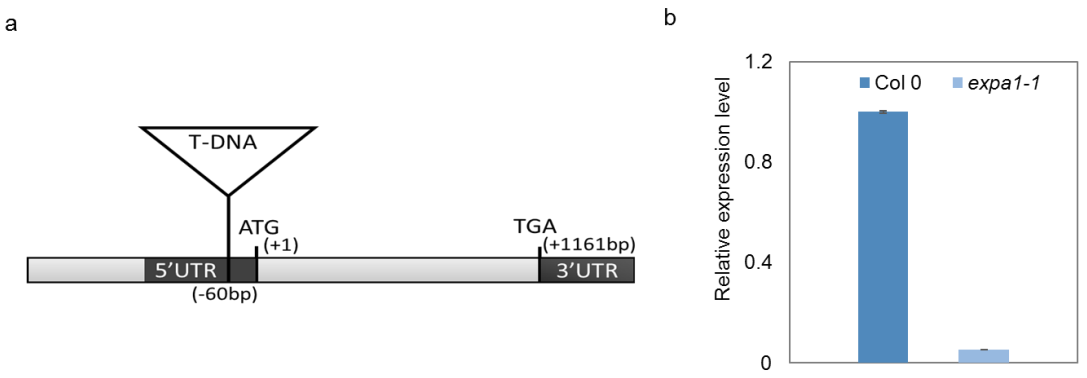


Figure 4.5. T-DNA insertion diagram of *expa1-1* with insert located 60bp upstream of the start site (ATG) in the 5′UTR region of the gene (a); qRT-PCR on *expa1-1* line indicating the T-DNA line was a full knock-out of *EXPANSIN1* expression (b) (n=3 ±SE).

With respect to emerged lateral root density, *expa1-1* did not display a significant difference compared to the wildtype (**Supl. Figure 4.2**). Therefore, to explore a subtler impact on lateral root initiation, we analysed progression through lateral root development stages using the bending assay (**Figure 4.6.a**) (Péret et al., 2012). This revealed a slight, but significant delay in the progression of the lateral root primordia from Stage I to Stage II in *expa1-1* compared to the wild type 18 h post gravitropic stimulus (**Figure 4.6b**). On analysis of roots 42hrs post bend for late emergence defects, in line with the expression pattern in overlying tissues, *expa1-1* exhibits a delay in the progression from Stage V to VI (**Figure 4.6c**) which suggests a potential role in later stages of development of the primordia.

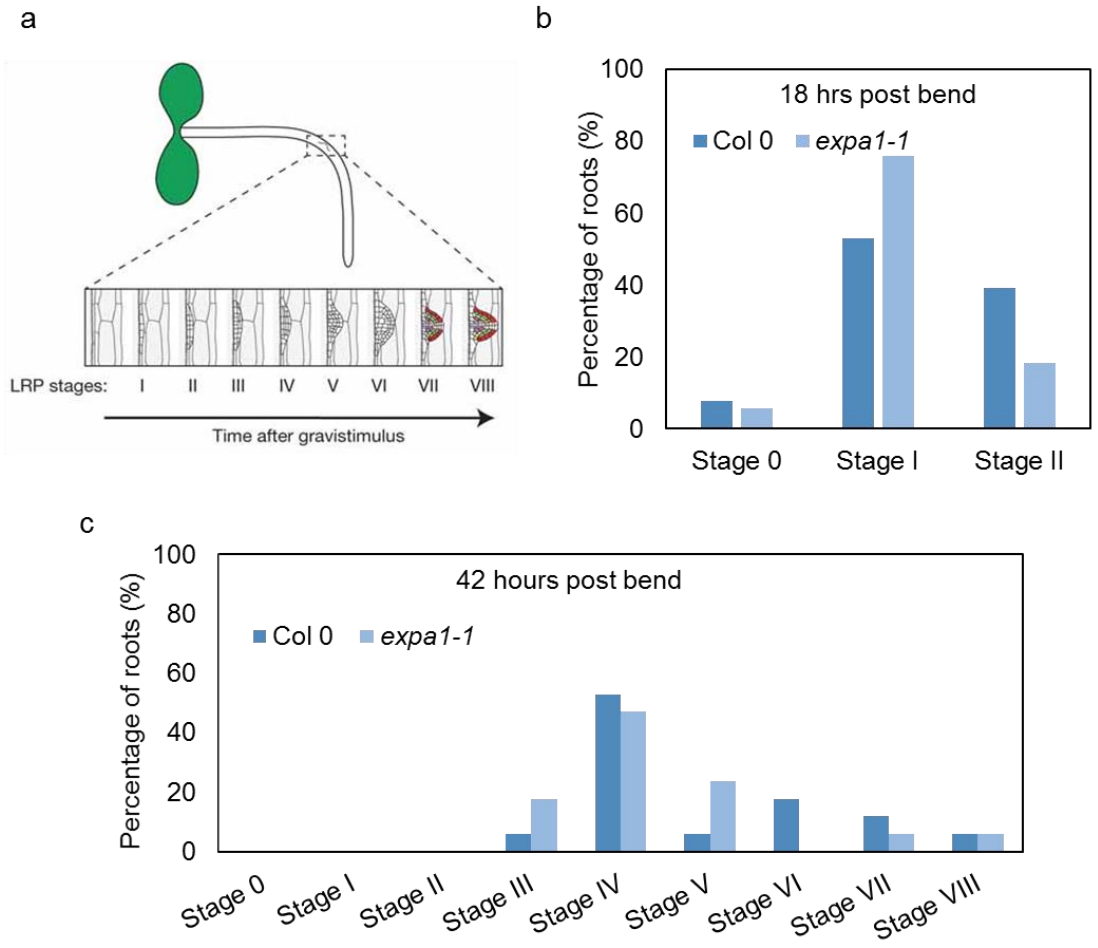


Figure 4.6. Schematic of lateral root bend assay (a); representative data of Col 0 and *expa1-1* analysed 18 hours post bend for early initiation defects (b); 42hrs post-bend for emergence defects (c) (n=3 for all experiments).

To explore if also cell division pattern and pericycle cell size before and/or during lateral root initiation is altered, we introduced plasma membrane marker line *pUBQ10::EYFP:PIP1;2* (referred to as WAVE131YFP*)* WAVE131YFP (Geldner et al., 2009) in *expa1-1* (referred to as *expa1-1 x* WAVE131YFP) and performed a detailed analysis on the early developmental stages of the lateral root primordia. This revealed that 75% of Stage I primordia in *expa1-1* were defective (with divisions that did not fully resemble a typical stage I primordium **Figure 4.7.b**) when compared with the wildtype.

In wildtype, after the first formative division the two small daughter cells are positioned in the center of the early primordium next to each other and large flanking cells at the outer side of the primordium (**Figure 4.7. a**). In the *expa1-1* mutant, in about 75% of the Stage I primordia (**Figure 4.7. b**), show the small daughter cells positioned at the outer side of primordium with loss in the organised structure (**Figure 4.7. b**). The early developmental progression [Stage 0 (pericycle cell on the root bend with no visible sign of division 12 hours post bend) - Stage II] of the lateral root primordia was monitored in the WAVE131YFP and *expa1-1 x* WAVE131YFP from 12hrs post bend. This revealed a transitionary defect in the structure of the Stage I primordia where the primordia initiate with a defective division pattern as shown in representative **Figure 4.7.b**. However, this is compensated by additional divisions that restore the primordia back to an organised Stage II that continues to develop normally thereafter (**Figure 4.8.**). Based on these observations and from recent work that showed that pericycle cells expand radially prior to the first asymmetric cell division (Vermeer et al., 2014) we infer that *EXPA1* plays a role in lateral root initiation possibly through regulation of pericycle cell expansion prior to asymmetric cell division.

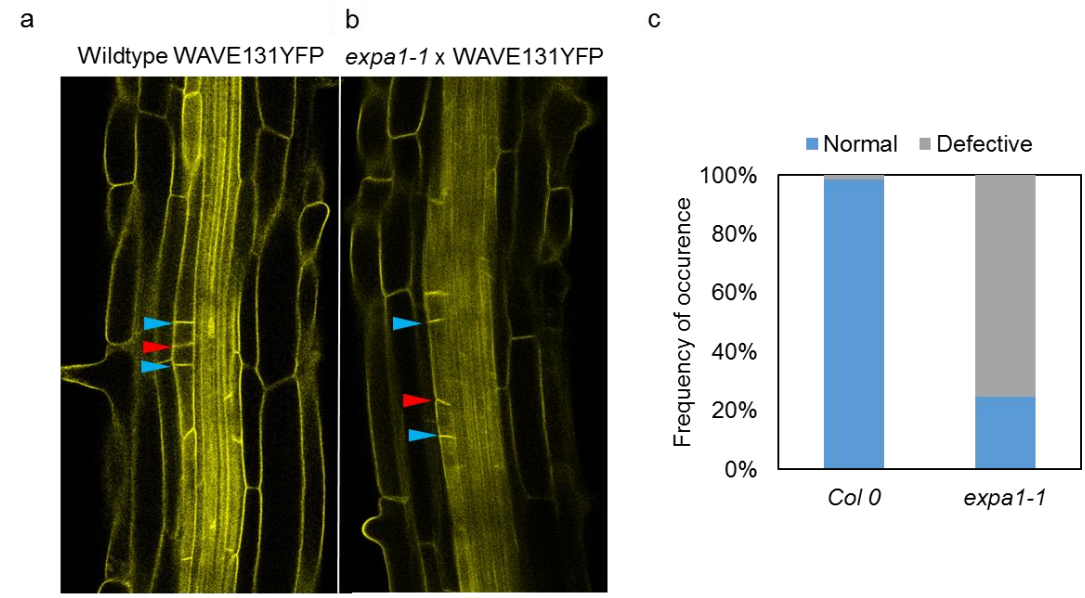


Figure 4.7. Stage I primordia visualised in wildtype (a) and *expa1-1* background (b); Quantification of frequency of occurrence of defective primordia in Col 0 vs *expa1-1* (c) (n=average of 12 roots, 3 replicates).

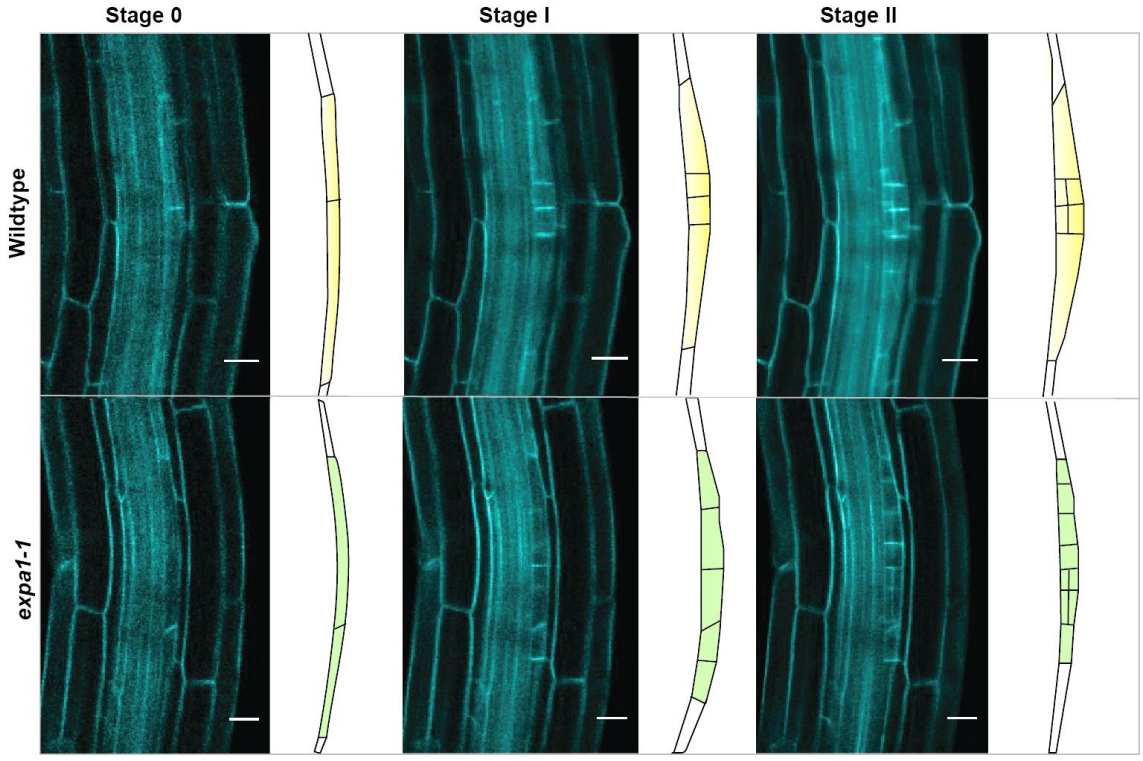


Figure 4.8. Visualisation of lateral root initiation in roots of 3DPG seedlings that were imaged 12hrs gravitropic root bend in wildtype and *expa1-1*. Walls visualised using plasma membrane marker WAVE131YFP

4.2.6. Auxin-mediated pericycle cell expansion during lateral root initiation

Recent work showed that pericycle cells expand radially prior to the first asymmetric cell division (Vermeer et al., 2014). Pericycle cell size maintenance and expansion is not straightforward to capture and measure under regular growth conditions. Therefore, to more easily quantify pericycle cell expansion, a well-established experimental set-up that are routinely used for lateral root transcriptome studies and phenotyping, was applied. First, WAVE131YFP and *expa1-1 x* WAVE131YFP lines were subjected to a lateral root-inducible system that provides a uniform and synchronized population of pericycle cells undergoing lateral root initiation (**Figure 4.9.a**) (Himanen et al., 2002a; Himanen et al., 2004; Vanneste et al., 2005a; De Smet et al., 2008; Geldner et al., 2009). For this, auxin transport was blocked in the pericycle using the auxin transport inhibitor 1-N-naphthylphthalamic acid (NPA), followed by transfer of the seedlings to the synthetic auxin 1-naphthaleneacetic acid (NAA) for 6 hours (**Figure 4.9.a**). The roots were imaged about 400 microns from the root tip in the region where the pericycle cells are fairly uniform sized (**Figure 4.9.b**). Although the curvature of the root surface varies greatly, the surface of the pericycle cells in the longitudinal confocal section is small enough to be locally flattened in 2D without too much cell shape deformation (**Figure 4.9.c**). Measurement of pericycle cell width of NPA grown WAVE131YFP and *expa1-1 x* WAVE131YFP roots revealed that the pericycle cells of *expa1-1 x* WAVE131YFP were significantly wider (~8.1 µm) than WAVE131YFP (~5.5 µm) [Values represent mean ± SE, n= ~21 roots from 3 rounds of experiment, $p<0.001$] (**Figure 4.10.**). To determine the effect of auxin treatment on cell size,

the pericycle cell width was determined post 6hr auxin treatment. The data indicated that the pericycle cells of WAVE131YFP expand radially (~5.5 µm to 7.5 µm, mean± SE, n= 25 roots from 3 rounds of experiment, p<0.001) (**Figure 4.10**), in keeping with a recent work that showed a similar response (Vermeer et al., 2014). The *expa1-1 x* WAVE131YFP however, do not display the radial expansion of pericycle cells upon auxin treatment (~8.1 to ~5.9 µM, mean± SE, n= total 25 roots, 3 replicates) (**Figure 4.10**).

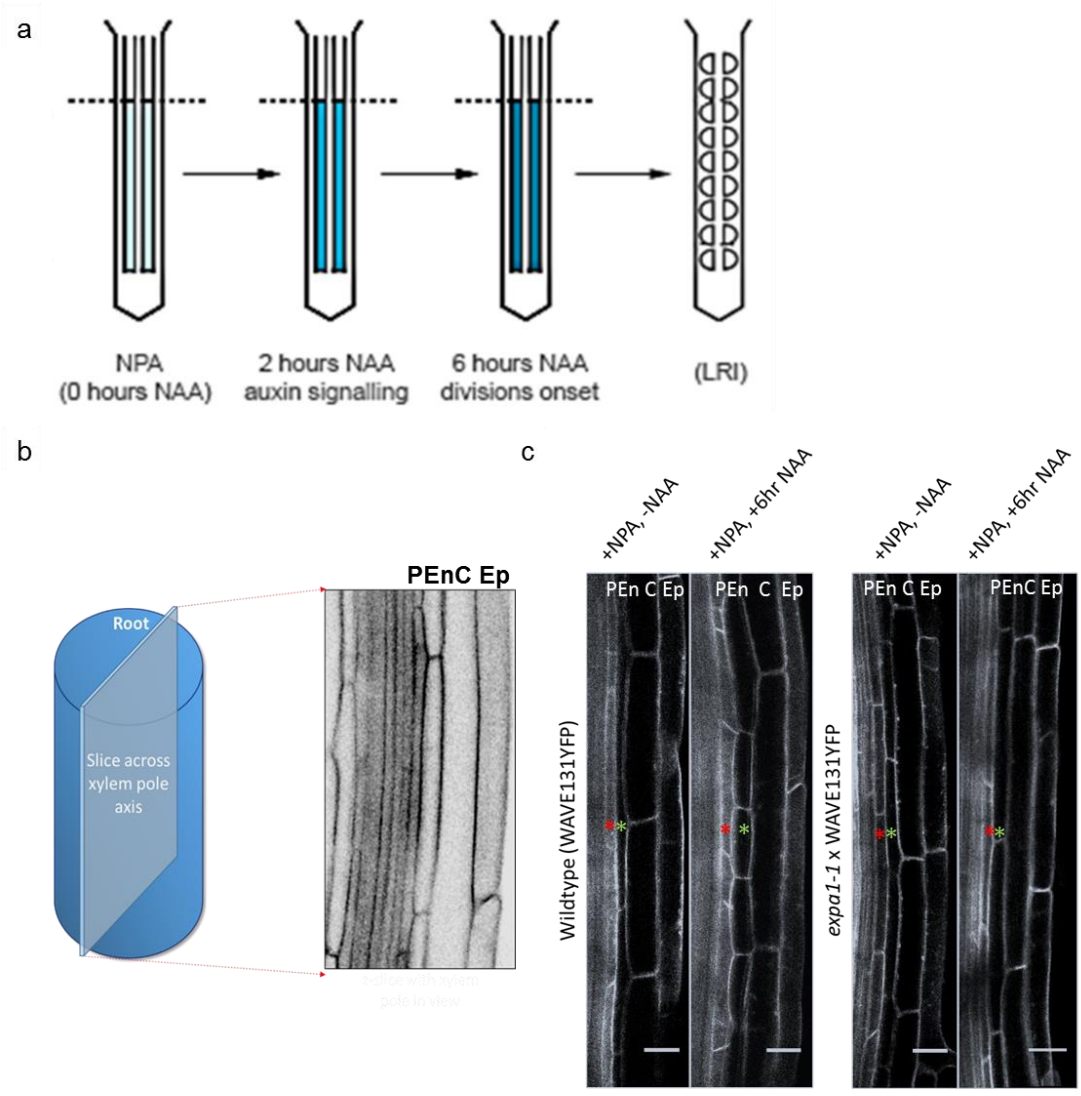


Figure 4.9. Schematic of lateral root induction system (Himanen et al., 2004) (a); illustration of root confocal slice used for cell width measurements (b); representative 2D confocal slices of wildtype and *expa1-1* roots without auxin (+NPA, -NAA) and with auxin treatment (+NPA,+6hrNAA) root used for cell size measurements (c), pericycle cells measured are marked with a red asterix and endodermal with green.

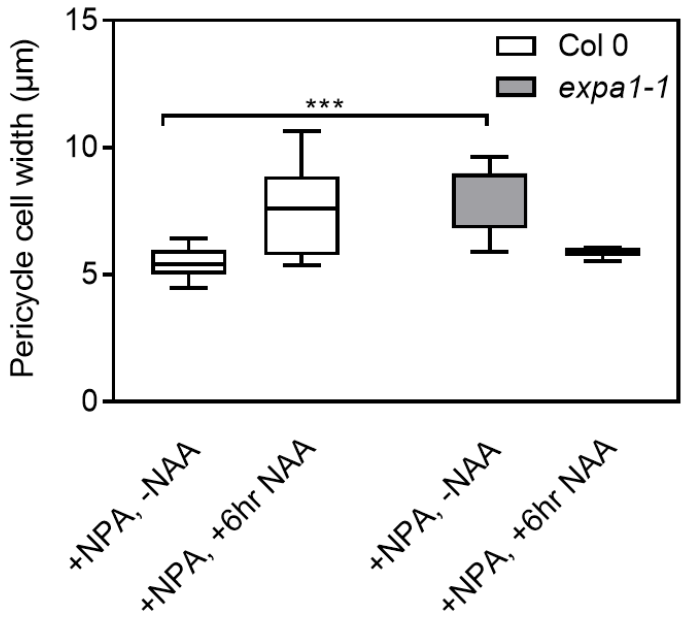


Figure 4.10. Box plot showing distribution of pericycle cell width for *Col-0* (WAVE131YFP) (white boxes) and *expa1-1* (expa1-*1*xWAVE131YFP) (grey boxes). Seedlings were grown on 10µM NPA, and post treatment on 10µM NAA (***p<0.0001 indicates significant difference among means, Unpaired t-test with Turkey's style whisker plot, n=about 21 roots from 3 rounds of experiment).

4.2.7. Auxin mediated cell size changes in overlaying tissue layers

The initiation of new primordia is accompanied by active communication and restructuring of the tissue layers overlaying the pericycle to accommodate the developing primordia. In addition to the cell width changes in the pericycle, we attempted to capture differences in the cell width of the overlaying endodermal, cortex and epidermal cell layer in WAVE131YFP and *expa1-1* x WAVE131YFP in response to auxin. Measurement of endodermal cells width did not show any significant differences under NPA grown (~9.491 – ~8.727, mean± SE, n= total 18 roots from 3 rounds of experiment) and auxin treated conditions (**Figure 4.11. B,b**). In the cortical cells there was no significant differences in cell width under untreated NPA grown condition (~16.31 – ~16.21, mean± SE, n= total 12 roots from 3 rounds of experiment). Auxin treatment widened the cortical cells in WAVE131YFP although the difference was not significant (~16.31 - ~17.55, mean± SE, n= total 12 roots from 3 rounds of experiment). This widening was not reflected in the cortical cells of *expa1-1* x WAVE131YFP (~16.21 - ~13.95, mean± SE, n= total 12 roots from 3 rounds of experiment) (**Figure 4.11. C,b**). However, the cells of *expa1-1* x WAVE131YFP were significantly longer upon auxin treatment (~103.1 - ~ 173.6, *p=0.03, mean± SE, n= total 12 roots from 3 rounds of experiment) (**Figure 4.11. C,a**). Measurement of epidermal cell was technically limited due to insufficient numbers of cells for accurate measurement. From the few cells that were measurable it is hard to draw a reliable conclusion on cell size differences (**Figure 4.11. D,a,b**).

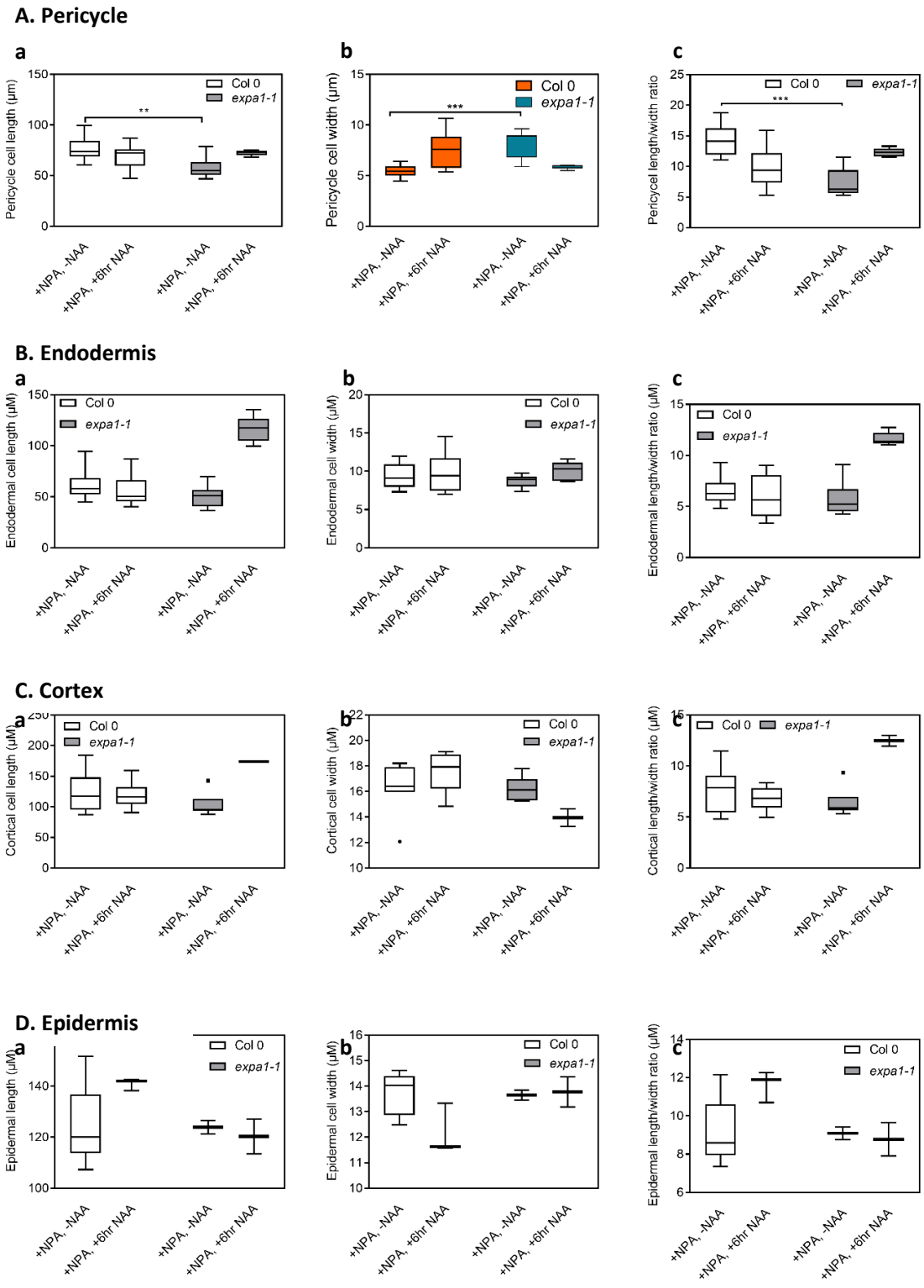


Figure 4.11. Box plots showing the distribution of cell length (a), width (b) and the ration of length/width (c) between *Col-0* (WAVE131YFP) and *expa1-1* (expa1-*1*xWAVE131YFP) for pericycle (A), endodermal (B), cortical (C) and epidermal cells (D). and distribution of cortical cell length (d). Seedlings were germinated and grown on 10µM NPA and a batch post-treated with 10µM NAA for 6 hrs, ***p<0.0001 indicates significant difference among means, Unpaired t-test with Turkey's style whisker plot, n=about 25 roots in total from 3 rounds of experiment).

4.3. Discussion

Asymmetric cell division is important for establishment of cell identity and tissue patterning in developing organs. In dicots, such as Arabidopsis, lateral roots form post-embryonically from a specialised set of xylem pole pericycle cells that divide asymmetrically to form small daughter cells and large flanking cells (De Smet et al., 2008). Very little is understood about the cell wall remodelling that occurs in the pericycle and its overlaying tissues to facilitate the initiation and development of a young primordium. In this study, we performed a meta-analysis of cell wall remodelling that showed differential expression during lateral root initiation and identified *EXPA1* with a strong developmental role.

Expansins act as a catalyst for acid-dependant growth and aid several basic developmental processes that require cell wall remodelling. This is often achieved by promotion of cell expansion or cell elongation (McQueen-Mason and Cosgrove, 1995). The spatial expression pattern of *EXPA1* revealed that it was specifically upregulated in the xylem pole pericycle cells that initiate a lateral root primordium and in the underlying stele (**Figure 4.2.**) with strong induction upon auxin treatment (**Figure 4.4**). Auxin is critical for lateral root initiation and development with different auxin signalling modules acting sequentially to regulate key early developmental steps leading to asymmetric cell division (Dubrovsky et al., 2008; Dubrovsky et al., 2011b; Lavenus et al., 2013a). Basipetal auxin transport is considered to activate the xylem pole pericycle cells to undergo formative divisions (Casimiro et al., 2001). Thus we monitored the auxin dependant regulation of *EXPA1* during lateral root initiation to gain a better insight into their role. Exogenous auxin treatment and auxin-

response mutant expression studies reveal that local regulation of *EXPA1* is downstream of SLR/IAA14-ARF7-ARF19 signalling module (**Figure 4.3.**). This places *EXPA1* in the lateral root developmental window between founder cell nuclear migration and the first round of formative cell division (**Figure 4.12.**). Mutant analysis revealed the importance of *EXPA1* for organised asymmetric cell divisions, observable by the phenotypic defects in the cell arrangement within the lateral root primordium structure (**Figure 4.7.**) and developmental kinetics in the progression from Stage I to Stage II in *expa1-1* (**Figure 4.6.**). The transitional defect in the structure of the Stage I primordium that is amended at the later stages of development could explain the absence of defects in number of emerged lateral roots. Another possibility is that the defective divisions are due to loss in polarity that results in improper founder cell nuclei migration. This could be tested by crossing an early lateral root initiation marker such as *GATA23* (De Rybel et al., 2010a) or *RALFL34* (Murphy et al., 2016) that are expressed before nuclear migration into *expa1-1* and follow the process of nuclear migration and asymmetric cell divisions in 4D. As there was only one T-DNA allele available for *EXPANSINA1*, we generated a complementation line that requires to be phenotyped to assess the recovery of the defects in cell size and organised asymmetric divisions during lateral root initiation.

Analysis of modifications in the early stages of lateral root initiation is challenging because only a few pericycle cells along the root are stimulated to form a lateral root (Laskowski et al., 1995). Hence, we adopted the lateral root induction system with the auxin treatment as a high-throughput means to increase the frequency of lateral root formation for detailed analysis (Himanen et al., 2002a; Himanen et al., 2004). In this system, the auxin transport inhibitor

N-1-naphthylphthalamic acid (NPA) causes auxin to accumulate in the root apex. This leads to reduction in auxin levels required for lateral root initiation in the basal tissue blocking the first transverse division and arrest in lateral root development (Casimiro et al., 2001). The reduced cell length upon auxin treatment (**Supl. Figure 4.3**) is a good indicator of response to auxin treatment as the auxin treatment in the 10µM range is known to cause reduced root length by inhibition of cell elongation.

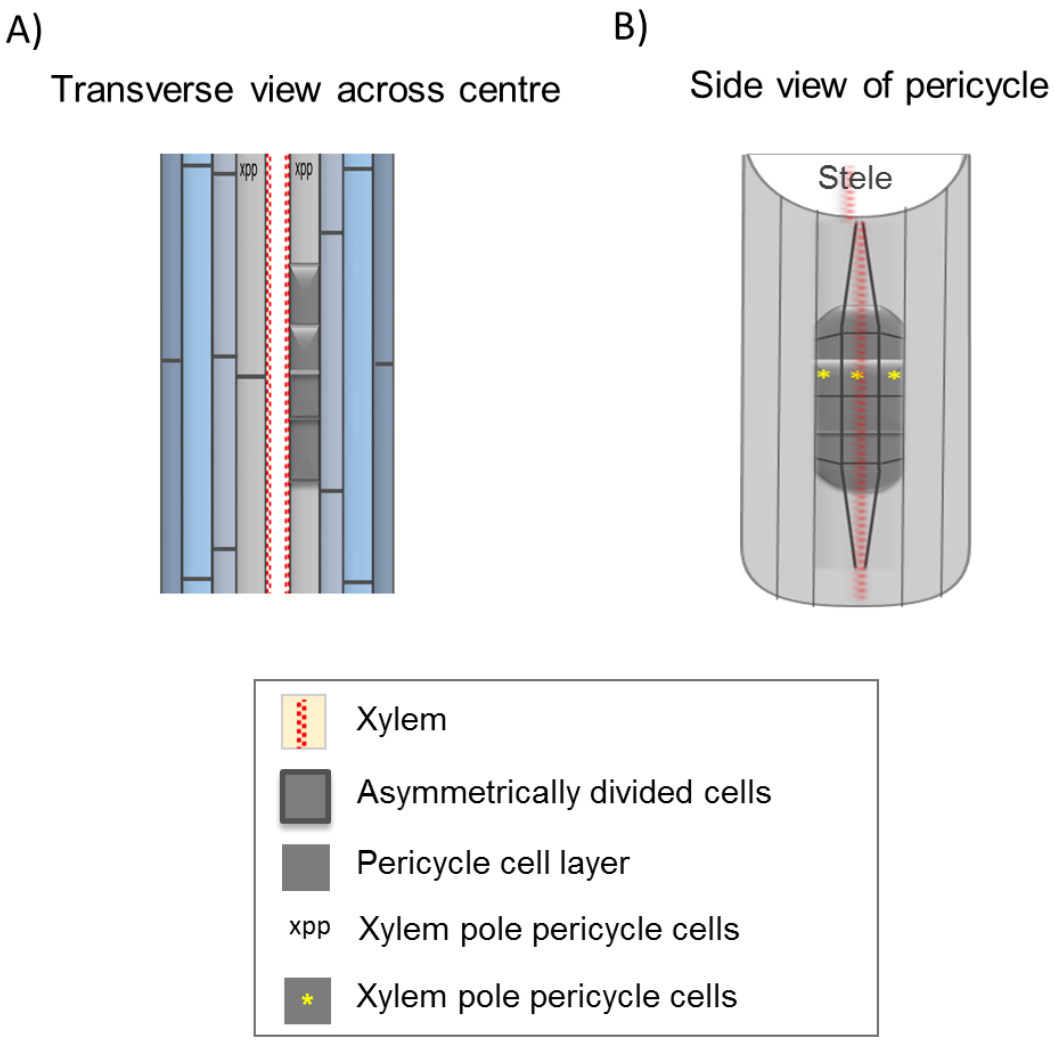


Figure 4.11-1. Schematic of transverse section of the root with the two xylem poles in focus (A); View of the pericycle cell layers involved in asymmetric cell division from the side (B), the three-adjacent xylem pole pericycle cells are marked by the yellow asterix.

We subjected wildtype and *expa1-1* roots that were crossed with a plasma membrane fluorescent marker to the lateral root induction system with the aim to measure the changes in the cell size by imaging the roots in 3D and reducing the data down to 2D for measurement purposes. This approach was selected for the following reasons. Firstly, the cells in the roots with and without auxin induction are not uniformly shaped. Some of the cells are almost rectangular in a cross section while some taper at the edges. These are dictated by the interactions with the adjacent cell layers surrounding a cell, the composition of the cell wall, the developmental phase etc. Therefore, to ensure selection of the pericycle cells specifically involved in lateral root initiation i.e. xylem pole pericycle (XPP) cells, the images were collected with the two xylem tracks in focus (**Figure 4.11-1A**). The lateral root is known to initiate from three adjacent pericycle cells beginning from the central layer followed by the adjacent two to form a whole lateral root (**Figure 4.11-1B**). Keeping this view in focus meant that the xpp cells that were visible for measurement on either side of the xylem track were the ones that would be involved in the asymmetric cell division process. We measured the cell width using 2D confocal z-slices. Cells grow 3 dimensionally with time being the fourth dimension. The cells are bound within a cell wall that maintains the structure and with time and upon receipt of a growth stimulus, the cells increase in size. Our results show that auxin regulates radial expansion of pericycle cells in wildtype roots (**Figure 4.10 b**). This confirms with previous observations on radial expansion of pericycle cells prior to the first asymmetric cell division (Vermeer et al., 2014) (**Figure 4.12.B**) and further, supports the idea of auxin driven cell expansion. In the mutant *expa1-1* however, we observe that this radial expansion was absent in the

pericycle cells (**Figure 4.10 b**). The pericycle cells of *expa1-1* are wider than wildtype when measured in seedlings grown with and without NPA. This indicates that a loss in maintenance of appropriate cell size affects the organised formative division pattern in the pericycle for normal Stage I formation. One explanation could be could be based on the idea that the geometry of the cell affects the orientation of the cell division planes.

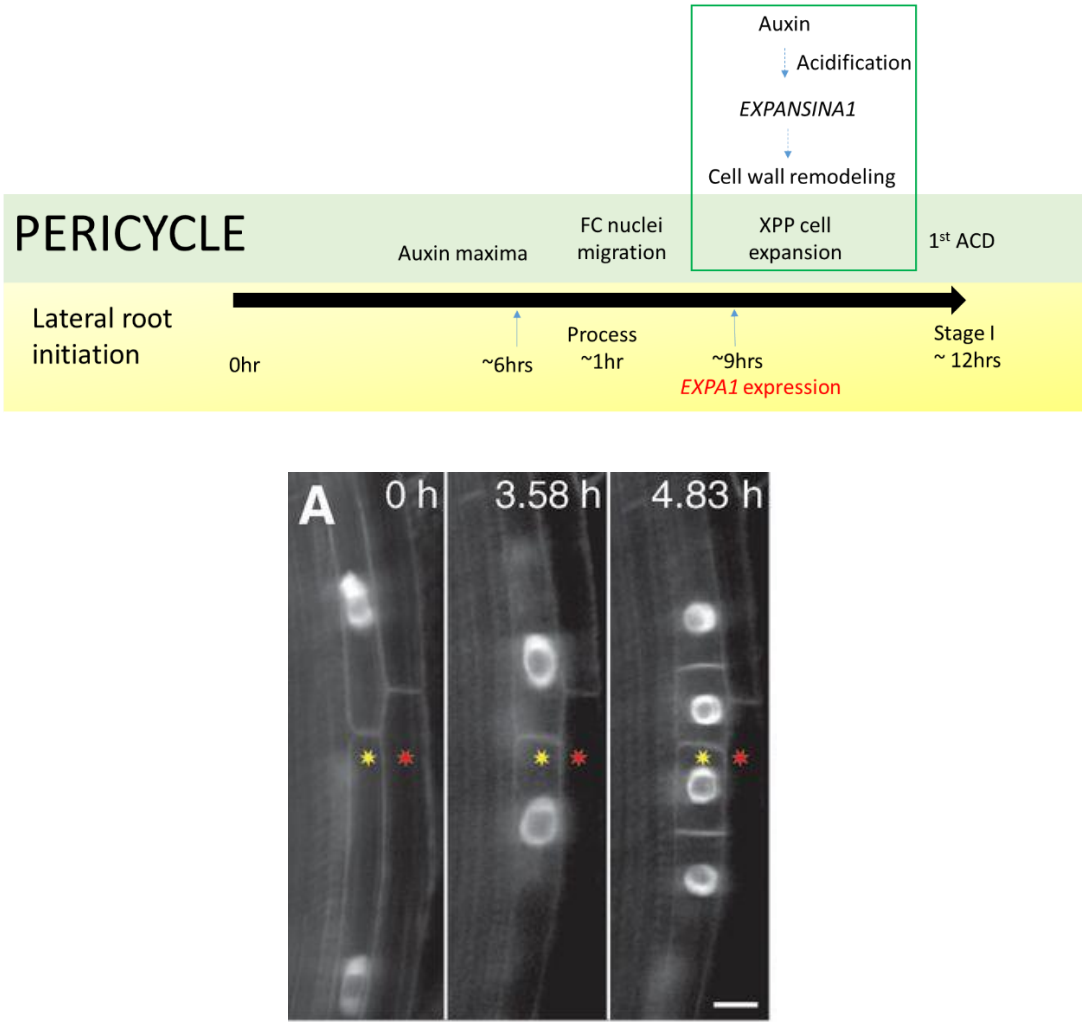


Figure 4.12 A. Schematic timeline of lateral root initiation with approximate times based on literature and observation (Goh et al., 2012b; Vermeer et al., 2014). FC- founder cell; XPP- xylem pole pericycle; ACD- Asymmetric cell division. **B.** Light sheet fluorescence microscopy that showed that pericycle cells swell before formative divisions (Vermeer et al., 2014).

Another explanation could be based on the overall observation on structure of pericycle cells upon NPA treatment. It has been suggested that under normal growth conditions, 'elongated' pericycle cells that exit the meristem have the potential to acquire founder cell identity and undergo formative divisions (Dubrovsky et al., 2000). In our case, the NPA treatment blocks the basipetal auxin transport and redistribution to the pericycle cells important for lateral root initiation. The 10µM dose of NAA is a high concentration of the chemical that is known to inhibit root cell elongation that leads to reduction in cell length in the transition between elongation zone and differentiation zone of the root and thereby reduced overall cell length. On subsequent treatment of the NPA grown seedlings with auxin, the xylem pole pericycle cells in which the cell cycle was blocked, but with cell identity retained, auxin induction causes synchronous activation of cell cycle along the entire length of the root to undergo formative divisions multiple lateral root formation. The pericycle cells swell radially to accommodate the formative divisions and we were able to observe this in out cell size measurements (**Figure 4.10**). In *expa1-1* however, the radial expansion upon auxin induction in the NPA treated seedlings is absent. Instead we observe that the pericycle cells in the NPA treated seedlings are wider than the wildtype cells and upon auxin induction restructure their cell shape to recover wiltype radially expanded cells in preparation for formative division. The cell length/width ratio of the wildtype and *expa1-1* cells are in the same range, but with the cells of *expa1-1* being restructured to meet a size necessary for normal asymmetric cell divisions to occur (**Figure 4.11A-c**). This could explain the delay observable in the transition of the early stages of LRP in the *expa1-1* mutant in the LR bending

assay (**Figure 4.6b**). This suggests that auxin overrides the cell size defect in the pericycle that resets the developmental program for organised asymmetric division and lateral root formation. Taken together our results show that auxin dependent pericycle cell size maintenance by *EXPA1* is important for organised formative divisions.

The presence of *EXPA1* transcripts (**Figure 4.2.d and 4.10b**), as well as similar response to cell size modification upon auxin treatment in the pericycle and cells (**Figure 4.11b, d**) suggest a similarity in the cell cycle machinery in these cell files. A previous study has shown that the average cell cycle time in the meristem for pericycle and cortex cells was similar [estimated by the rate-of-cell production method (Ivanov and Dubrovsky, 1997)]. It would be interesting to explore if there is a multi-step regulatory role for *EXPA1* in lateral root formation. The overlying tissues undergo extensive cell wall remodelling to facilitate emergence. It may well be that step-wise activation of *EXPA1* is triggered in the overlying tissues to enable restructuring of cell wall as the lateral root primordium develops.

Another approach would be to study the tissue specific overexpression in the pericycle using GAL4-enhancer trap line J0121 (Laplaze et al., 2005) that would drive *EXPA1* expression specifically in the pericycle. This would help to further dissect the role of *EXPA1* specific to the pericycle. It would also be valuable to study the translational fusion line *pEXPA1:EXPA1::GFP* (transformed, being selected) to demonstrate the localisation of EXPA1 in the wall. This would help gain an idea about the location in the cell where the protein is active. This brings us to the big question of how do expansins remodel the cell wall? Are the changes a consequence of EXPA1 contributions to

modifications in the cell wall structure? These have been investigated in **Chapter 6**.

4.4. Materials and methods

4.4.1. Plant material

The T-DNA lines for *EXPANSINA1* (AT1G69530) - *expa1-1* (SALK_010506), was obtained from the Nottingham Arabidopsis Stock Centre (NASC) and genotyped to verify homozygosity and tested for loss of expression by qRT-PCR (Appendix 1). Ecotype *Columbia-0* (*Col-0*) was used as the wildtype reference for all the studies. The *UBQ10pro::EYFP:PIP1;2* (WAVE131YFP) line is the plasma membrane marker line described in (Geldner et al., 2009). *pEXPA1::n3xGFP* was generated using a previously published vector backbone (Slane et al., 2014) and an *EXPA1* promoter fragment 1901 base pairs upstream of the start codon. The *pEXPA1::n3xGFP* constructs were transformed into *Agrobacterium sp.* then floral dipped into *Col-0* plants (Clough and Bent, 1998).

4.4.2. Genotyping

Genomic DNA from seedling leaves was extracted using Qiagen Plant DNA extraction kit. Independent plants of the same line were tested by PCR with gene specific primers (Appendix 1) and the SALK T-DNA LbB1.3 primer specially designed to test T-DNA sequence, to determine whether the seed set is heterozygous and/or homozygous for the T-DNA insertion. Homozygous lines were selected from the segregating heterozygous population.

4.4.3. Growth conditions and media

All lines used for analysis, wild-type ecotype - Columbia (*Col-0*), mutants (*expa1-1)* and reporter lines were surface sterilised (70% ethanol for 2 min; 20% bleach for a further 20 min and rinsed off using sterile water with minimum 5 washes), suspended in sterile water and stratified for two days at 4°C. The seeds were then plated and grown on vertical 1/2 MS plates (2.154 g/l MS salts (Duchefa Biochemie MS basal salt mixture without vitamins), 0.1 g/l myo-inositol (Sigma), 0.5g/l MES (Sigma), 10 g/l bacteriological agar (Sigma-Aldrich); pH 5.8 with 1M KOH) at 22 °C under continuous light condition (150 $\mu mol\, m^{-2}\, s^{-1}$). For hormone treatments, the sterilised media was supplemented according to necessity with auxin 10µM NAA (1-Naphthaleneacetic acid), 10µM NPA (1-N-Naphthylphthalamic acid).

4.4.4. Phenotyping

4.4.4.1. Measurement of primary root length and lateral root density

Primary root length and lateral root density measurements were performed on 12 days post germination (12DPG) seedlings. The roots were photographed (using Kodak 3MP camera) and the primary root length measured in Fiji (http://imagej.net/Fiji). Individual roots were observed on a dissecting microscope under 10X magnification, counting lateral roots starting just below the hypocotyl (ignoring adventitious roots) then progressively counting down toward the root tip. All emerged lateral roots were counted for the lateral root density and calculated as number of lateral roots per centimeter of primary root.

4.4.4.2. Lateral root staging

The 12DPG roots post primary root length study were excised to be cleared for staging by treatment with: Methylated ethanol (15 minutes), 60% Ethanol (15 minutes), 40% Ethanol (5 minutes), 20% Ethanol (5 minutes), 10% Ethanol (5 minutes), and finally washed and stored in purified water until further screening. The roots were staged using Leica DM6 B upright microscope (Leica microsystems) with a 40X air lens.

4.4.4.3. Lateral root bending assay

The bending assay was performed on 3DPG seedlings as described in (Péret et al., 2012) by examination of the root bend 18 hours post for early initiation defects and 42hrs post for emergence defects.

4.4.5. Generation of transgenic lines

4.4.5.3. *p35S::EXPA1* overexpressor line generation

For *p35S::EXPA1* line, the coding sequence of *EXPA1* without STOP-codon, and the constitutive 35S promoter were cloned into pEarleyGate 100 by LR recombination with Gateway Cloning® system. pCR8-GW-TOPO® was used as entry vector and the sequence was cloned into two different destination vectors- pEarleyGate100 (35S-Gateway-OCS 3') and pEarleyGate103 (35S-Gateway-GFP-His tag-OCS 3'). The gene sequence was amplified using Phusion® PCR. PCR reaction mix- 31.5µL H2O, 10µL 5× Phusion buffer, 1µL 10mM dNTPs, 2µL gDNA (10ng/µL), 1µL of Forward and 1µL Reverse primer (**Appendix 2**) and 0.5µL Phusion® polymerase enzyme (New England Bio Labs). The PCR was set for 35 cycles under conditions: 98°C 30sec, 98°C 10sec, 54°C 30sec, 72°C 1min 30sec, 72°C

10min, 4°C forever. The amplified product was run on 1% Agarose gel and the band with the amplified product was excised and extracted using GenJet Gel extraction kit and the concentration of the purified product checked using NanoDrop®. The product was then 'A' tailed (**Appendix 2**) and ligated into the donor vector pCR8-GW-TOPO and transformed into chemically competent *E. coli* DH5α cells (**Appendix 3**). Positive colonies were verified using Colony PCR and cultured overnight at 37°C. The amplified plasmids were extracted using ThermoScientific Plasmid Mini Prep kit and sequenced to confirm the cloned sequence using M13 primers. The gene sequence was then recombined into the destination vector by LR reaction using LR colonase enzyme mix and transformed into chemically competent *E.coli* DH5α cells (**Appendix 3**). The post-transformation was repeated as described above to obtain the sequenced positive plasmid. The plasmid was then transfected into Agrobacterium after which it was transformed into *Arabidopsis thaliana* by floral dip method.

4.4.6. qRT–PCR

Total RNA was extracted from roots using a Qiagen® RNeasy plant mini kit. Poly(dT) cDNA was prepared from total RNA using the SuperScript II® Reverse Transcriptase (RT) from Invitrogen®. qPCR was performed using PerfeCTa SYBRGreen® FastMix, Low ROX (Quanta) on Roche LightCycler 480 apparatus. PCR was carried out in 384-well optical reaction plates heated for 1 min to 95°C, followed by 50 cycles of denaturation for 5s at 95°C, annealing for 8s at 60°C and extension for 30s at 72°C. Expression levels were normalized to control gene - Actin. The primers were designed using ROCHE Universal ProbeLibrary Assay Design Center

(http://lifescience.roche.com/webapp/). Primers list of all qPCR primers used in study in **Appendix 1**.

4.4.7. Confocal Imaging

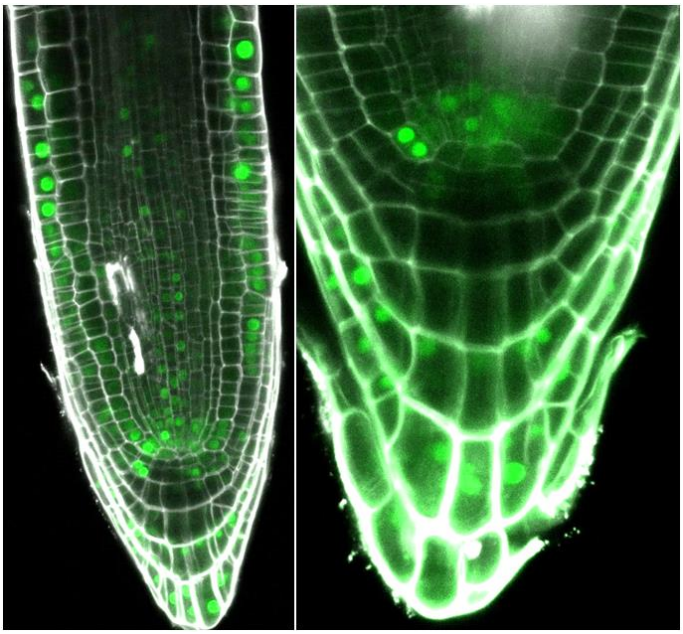
Confocal analysis was performed using Leica TCS-SP5 confocal microscope (Leica, Milton Keynes, UK) and Nikon C2 confocal microscope system. Roots were stained with 10 µg/ml propidium iodide (Sigma) for 2min, rinsed, and mounted in water. Yellow fluorescent protein (YFP) and Green fluorescent protein (GFP) were excited with Argon laser line of wavelength 514nm and 488nm and collected between 525-600nm and 495-600nm respectively. Propidium iodide was excited with HeNe laser of wavelength 488nm and emission range 610-650nm.

4.4.8. Cell measurements

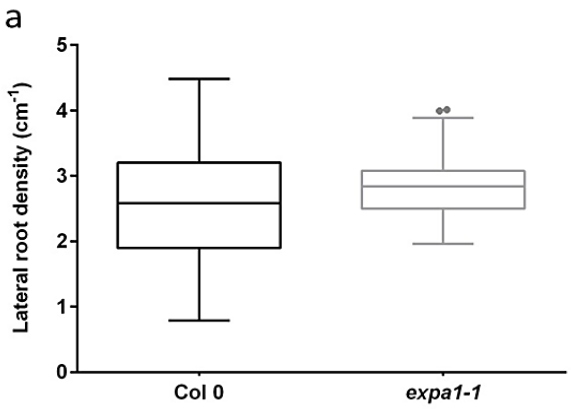
For cell measurements, confocal stacks of 1,024 × 1,024 pixels, with Z slices every 0.5 µm were acquired ~400microns from the root tip with the xylem poles in focus using a 40X air lens. Each stack was processed in Fiji (http://imagej.net/Fiji) (Schindelin et al., 2012) to visualise the Z slice with best focus of xylem poles and the different cell layers at high resolution by conversion into 2D images. The z stacks were processed to one or two 2D images by projecting adjacent Z slices in order visualise the complete cell. Only cells fully in view in the processed 2D images were considered for measurements. For each cell, the 'width' was recorded manually by measuring multiple points along the cells and averaging them out to account for non-uniform cell shapes of the different cell layers. To take into account the differences that can be attributed by thickness of the membrane itself,

the measurements were taken at midpoint to midpoint of the membrane surface.

4.5. Supplementary figures



Supplementary figure 4.1. Expression pattern of *pEXPA1::nx3GFP* in the root tip. Cell wall visualised by propidium iodide staining.



Supplementary figure 4.2. Box plot showing quantification of emerged lateral root densities of Col 0 and *expa1-1.*

4.6. Supplementary tables

Supplementary Table 4.1. List of 406 putative cell wall remodelling genes differentially expressed in the pericycle during lateral root initiation

Gene ID	Gene symbol	Gene description
AT1G01355	AT1G01355	Putative endonuclease or glycosyl hydrolase
AT1G02310	MAN1	Glycosyl hydrolase superfamily protein
AT1G02460	AT1G02460	Pectin lyase-like superfamily protein
AT1G02640	BXL2	beta-xylosidase 2
AT1G02800	CEL2	cellulase 2
AT1G02810	AT1G02810	Plant invertase/pectin methylesterase inhibitor superfamily
AT1G04680	AT1G04680	Pectin lyase-like superfamily protein
AT1G05310	AT1G05310	Pectin lyase-like superfamily protein
AT1G05650	AT1G05650	Pectin lyase-like superfamily protein
AT1G05660	AT1G05660	Pectin lyase-like superfamily protein
AT1G06925	AT1G06925	endonuclease/glycosyl hydrolase
AT1G10050	AT1G10050	glycosyl hydrolase family 10 protein / carbohydrate-binding domain-containing protein
AT1G10550	XTH33	xyloglucan:xyloglucosyl transferase 33
AT1G10640	AT1G10640	Pectin lyase-like superfamily protein
AT1G11310	MLO2	Seven transmembrane MLO family protein
AT1G11370	AT1G11370	Pectin lyase-like superfamily protein
AT1G11545	XTH8	xyloglucan endotransglucosylase/hydrolase 8
AT1G11580	PMEPCRA	methylesterase PCR A
AT1G11590	AT1G11590	Plant invertase/pectin methylesterase inhibitor superfamily
AT1G11820	AT1G11820	O-Glycosyl hydrolases family 17 protein
AT1G11920	AT1G11920	Pectin lyase-like superfamily protein
AT1G12560	EXPA7	expansin A7
AT1G13130	AT1G13130	Cellulase (glycosyl hydrolase family 5) protein
AT1G14420	AT59	Pectate lyase family protein
AT1G14720	XTH28	xyloglucan endotransglucosylase/hydrolase 28
AT1G17150	AT1G17150	Pectin lyase-like superfamily protein
AT1G18310	AT1G18310	glycosyl hydrolase family 81 protein
AT1G19170	AT1G19170	Pectin lyase-like superfamily protein
AT1G19940	GH9B5	glycosyl hydrolase 9B5
AT1G20190	EXPA11	expansin 11
AT1G22880	CEL5	cellulase 5
AT1G23200	AT1G23200	Plant invertase/pectin methylesterase inhibitor superfamily
AT1G23210	GH9B6	glycosyl hydrolase 9B6
AT1G23460	AT1G23460	Pectin lyase-like superfamily protein
AT1G24256	AT1G24256	hypothetical protein
AT1G26770	EXPA10	expansin A10
AT1G27520	AT1G27520	Glycosyl hydrolase family 47 protein
AT1G30080	AT1G30080	Glycosyl hydrolase superfamily protein

AT1G30350	AT1G30350	Pectin lyase-like superfamily protein
AT1G32170	XTH30	xyloglucan endotransglucosylase/hydrolase 30
AT1G32860	AT1G32860	Glycosyl hydrolase superfamily protein
AT1G33220	AT1G33220	Glycosyl hydrolase superfamily protein
AT1G43080	AT1G43080	Pectin lyase-like superfamily protein
AT1G43090	AT1G43090	Pectin lyase-like superfamily protein
AT1G43100	AT1G43100	Pectin lyase-like superfamily protein
AT1G44980	PME7	pectin methylesterase 7
AT1G45191	BGLU1	Glycosyl hydrolase superfamily protein
AT1G48100	AT1G48100	Pectin lyase-like superfamily protein
AT1G48930	GH9C1	glycosyl hydrolase 9C1
AT1G52400	BGLU18	beta glucosidase 18
AT1G56710	AT1G56710	Pectin lyase-like superfamily protein
AT1G60590	AT1G60590	Pectin lyase-like superfamily protein
AT1G62660	AT1G62660	Glycosyl hydrolases family 32 protein
AT1G62980	EXPA18	expansin A18
AT1G64390	GH9C2	glycosyl hydrolase 9C2
AT1G64760	AT1G64760	O-Glycosyl hydrolases family 17 protein
AT1G65310	XTH17	xyloglucan endotransglucosylase/hydrolase 17
AT1G65570	AT1G65570	Pectin lyase-like superfamily protein
AT1G65610	KOR2	Six-hairpin glycosidases superfamily protein
AT1G65680	EXPB2	expansin B2
AT1G65681	EXPB6	beta expansin 6
AT1G66250	AT1G66250	O-Glycosyl hydrolases family 17 protein
AT1G66280	BGLU22	Glycosyl hydrolase superfamily protein
AT1G67750	AT1G67750	Pectate lyase family protein
AT1G69530	EXPA1	expansin A1
AT1G70500	AT1G70500	Pectin lyase-like superfamily protein
AT1G70630	AT1G70630	Nucleotide-diphospho-sugar transferase family protein
AT1G70710	GH9B1	glycosyl hydrolase 9B1
AT1G71380	CEL3	cellulase 3
AT1G75680	GH9B7	glycosyl hydrolase 9B7
AT1G77410	BGAL16	beta-galactosidase 16
AT1G77780	AT1G77780	Glycosyl hydrolase superfamily protein
AT1G77790	AT1G77790	Glycosyl hydrolase superfamily protein
AT1G78060	AT1G78060	Glycosyl hydrolase family protein
AT1G78400	AT1G78400	Pectin lyase-like superfamily protein
AT1G79480	AT1G79480	Carbohydrate-binding X8 domain superfamily protein
AT1G80140	AT1G80140	Pectin lyase-like superfamily protein
AT1G80170	AT1G80170	Pectin lyase-like superfamily protein
AT2G01630	AT2G01630	O-Glycosyl hydrolases family 17 protein
AT2G01850	EXGT-A3	endoxyloglucan transferase A3
AT2G02720	AT2G02720	Pectate lyase family protein
AT2G03090	EXPA15	expansin A15

AT2G04060	AT2G04060	glycosyl hydrolase family 35 protein
AT2G05790	AT2G05790	O-Glycosyl hydrolases family 17 protein
AT2G06850	XTH4	xyloglucan endotransglucosylase/hydrolase 4
AT2G14620	XTH10	xyloglucan endotransglucosylase/hydrolase 10
AT2G14690	AT2G14690	Glycosyl hydrolase superfamily protein
AT2G15450	AT2G15450	Pectin lyase-like superfamily protein
AT2G15460	AT2G15460	Pectin lyase-like superfamily protein
AT2G15470	AT2G15470	Pectin lyase-like superfamily protein
AT2G15560	AT2G15560	Putative endonuclease or glycosyl hydrolase
AT2G16230	AT2G16230	O-Glycosyl hydrolases family 17 protein
AT2G18660	PNP-A	plant natriuretic peptide A
AT2G18800	XTH21	xyloglucan endotransglucosylase/hydrolase 21
AT2G19150	AT2G19150	Pectin lyase-like superfamily protein
AT2G19440	AT2G19440	O-Glycosyl hydrolases family 17 protein
AT2G19890	AT2G19890	hypothetical protein
AT2G20680	MAN2	Glycosyl hydrolase superfamily protein
AT2G20750	EXPB1	expansin B1
AT2G21610	PE11	pectinesterase 11
AT2G23900	AT2G23900	Pectin lyase-like superfamily protein
AT2G26440	AT2G26440	Plant invertase/pectin methylesterase inhibitor superfamily
AT2G26450	AT2G26450	Plant invertase/pectin methylesterase inhibitor superfamily
AT2G26600	AT2G26600	Glycosyl hydrolase superfamily protein
AT2G26620	AT2G26620	Pectin lyase-like superfamily protein
AT2G27500	AT2G27500	Glycosyl hydrolase superfamily protein
AT2G28950	EXPA6	expansin A6
AT2G32860	BGLU33	beta glucosidase 33
AT2G32990	GH9B8	glycosyl hydrolase 9B8
AT2G35610	XEG113	xyloglucanase 113
AT2G36700	AT2G36700	Pectin lyase-like superfamily protein
AT2G36710	AT2G36710	Pectin lyase-like superfamily protein
AT2G36870	XTH32	xyloglucan endotransglucosylase/hydrolase 32
AT2G37640	EXP3	Barwin-like endoglucanases superfamily protein
AT2G39640	AT2G39640	glycosyl hydrolase family 17 protein
AT2G39700	EXPA4	expansin A4
AT2G40310	AT2G40310	Pectin lyase-like superfamily protein
AT2G40610	EXPA8	expansin A8
AT2G43050	ATPMEPCRD	Plant invertase/pectin methylesterase inhibitor superfamily
AT2G43860	AT2G43860	Pectin lyase-like superfamily protein
AT2G43870	AT2G43870	Pectin lyase-like superfamily protein
AT2G43880	AT2G43880	Pectin lyase-like superfamily protein
AT2G43890	AT2G43890	Pectin lyase-like superfamily protein
AT2G44490	PEN2	Glycosyl hydrolase superfamily protein
AT2G44540	GH9B9	glycosyl hydrolase 9B9
AT2G44550	GH9B10	glycosyl hydrolase 9B10

AT2G44560	GH9B11	glycosyl hydrolase 9B11
AT2G44570	GH9B12	glycosyl hydrolase 9B12
AT2G45110	EXPB4	expansin B4
AT2G45220	AT2G45220	Plant invertase/pectin methylesterase inhibitor superfamily
AT2G47030	VGDH1	Plant invertase/pectin methylesterase inhibitor superfamily
AT2G47280	AT2G47280	Pectin lyase-like superfamily protein
AT2G47550	AT2G47550	Plant invertase/pectin methylesterase inhibitor superfamily
AT3G01270	AT3G01270	Pectate lyase family protein
AT3G03220	EXPA13	expansin A13
AT3G04010	AT3G04010	O-Glycosyl hydrolases family 17 protein
AT3G05610	AT3G05610	Plant invertase/pectin methylesterase inhibitor superfamily
AT3G05620	AT3G05620	Plant invertase/pectin methylesterase inhibitor superfamily
AT3G06770	AT3G06770	Pectin lyase-like superfamily protein
AT3G06830	AT3G06830	Plant invertase/pectin methylesterase inhibitor superfamily
AT3G07010	AT3G07010	Pectin lyase-like superfamily protein
AT3G07320	AT3G07320	O-Glycosyl hydrolases family 17 protein
AT3G07820	AT3G07820	Pectin lyase-like superfamily protein
AT3G07830	AT3G07830	Pectin lyase-like superfamily protein
AT3G07840	AT3G07840	Pectin lyase-like superfamily protein
AT3G07850	AT3G07850	Pectin lyase-like superfamily protein
AT3G09540	AT3G09540	Pectin lyase-like superfamily protein
AT3G10114	AT3G10114	pseudogene of glycosyl hydrolase family 81 protein
AT3G10710	RHS12	root hair specific 12
AT3G10720	AT3G10720	Plant invertase/pectin methylesterase inhibitor superfamily
AT3G10890	AT3G10890	Glycosyl hydrolase superfamily protein
AT3G10900	AT3G10900	Glycosyl hydrolase superfamily protein
AT3G13280	AT3G13280	Putative endonuclease or glycosyl hydrolase
AT3G13560	AT3G13560	O-Glycosyl hydrolases family 17 protein
AT3G13750	BGAL1	beta galactosidase 1
AT3G13784	CWINV5	cell wall invertase 5
AT3G14040	AT3G14040	Pectin lyase-like superfamily protein
AT3G14300	ATPMEPCRC	pectinesterase family protein
AT3G15370	EXPA12	expansin 12
AT3G15720	AT3G15720	Pectin lyase-like superfamily protein
AT3G15800	AT3G15800	Glycosyl hydrolase superfamily protein
AT3G16850	AT3G16850	Pectin lyase-like superfamily protein
AT3G17060	AT3G17060	Pectin lyase-like superfamily protein
AT3G19620	AT3G19620	Glycosyl hydrolase family protein
AT3G23640	HGL1	heteroglycan glucosidase 1
AT3G23730	XTH16	xyloglucan endotransglucosylase/hydrolase 16
AT3G23770	AT3G23770	O-Glycosyl hydrolases family 17 protein
AT3G24130	AT3G24130	Pectin lyase-like superfamily protein
AT3G24230	AT3G24230	Pectate lyase family protein
AT3G24330	AT3G24330	O-Glycosyl hydrolases family 17 protein

AT3G24670	AT3G24670	Pectin lyase-like superfamily protein
AT3G25050	XTH3	xyloglucan endotransglucosylase/hydrolase 3
AT3G26130	AT3G26130	Cellulase (glycosyl hydrolase family 5) protein
AT3G26140	AT3G26140	Cellulase (glycosyl hydrolase family 5) protein
AT3G26610	AT3G26610	Pectin lyase-like superfamily protein
AT3G26720	AT3G26720	Glycosyl hydrolase family 38 protein
AT3G27400	AT3G27400	Pectin lyase-like superfamily protein
AT3G27980	AT3G27980	Plant invertase/pectin methylesterase inhibitor superfamily
AT3G29030	EXPA5	expansin A5
AT3G29365	EXPA19	pseudogene of expansin A24
AT3G30540	AT3G30540	Glycosyl hydrolase superfamily protein
AT3G42155	AT3G42155	glycosyl hydrolase family 9 protein
AT3G42160	AT3G42160	Pectin lyase-like superfamily protein
AT3G42590	AT3G42590	transposable_element_gene
AT3G42950	AT3G42950	Pectin lyase-like superfamily protein
AT3G43270	AT3G43270	Plant invertase/pectin methylesterase inhibitor superfamily
AT3G43860	GH9A4	glycosyl hydrolase 9A4
AT3G44070	AT3G44070	Glycosyl hydrolase family 35 protein
AT3G44990	XTH31	xyloglucan endo-transglycosylase-related 8
AT3G45940	AT3G45940	Glycosyl hydrolases family 31 protein
AT3G45960	EXLA3	expansin-like A3
AT3G45970	EXLA1	expansin-like A1
AT3G46570	AT3G46570	Glycosyl hydrolase superfamily protein
AT3G47000	AT3G47000	Glycosyl hydrolase family protein
AT3G47010	AT3G47010	Glycosyl hydrolase family protein
AT3G47040	AT3G47040	Glycosyl hydrolase family protein
AT3G47050	AT3G47050	Glycosyl hydrolase family protein
AT3G47400	AT3G47400	Plant invertase/pectin methylesterase inhibitor superfamily
AT3G48425	AT3G48425	DNAse I-like superfamily protein
AT3G48580	XTH11	xyloglucan endotransglucosylase/hydrolase 11
AT3G48950	AT3G48950	Pectin lyase-like superfamily protein
AT3G49220	AT3G49220	Plant invertase/pectin methylesterase inhibitor superfamily
AT3G49880	AT3G49880	glycosyl hydrolase family protein 43
AT3G52600	CWINV2	cell wall invertase 2
AT3G53190	AT3G53190	Pectin lyase-like superfamily protein
AT3G54470	AT3G54470	uridine 5'-monophosphate synthase / UMP synthase (PYRE-F) (UMPS)
AT3G55140	AT3G55140	Pectin lyase-like superfamily protein
AT3G55430	AT3G55430	O-Glycosyl hydrolases family 17 protein
AT3G55500	EXPA16	expansin A16
AT3G55780	AT3G55780	Glycosyl hydrolase superfamily protein
AT3G56730	AT3G56730	Putative endonuclease or glycosyl hydrolase
AT3G57240	BG3	beta-1,3-glucanase 3
AT3G57270	BG1	beta-1,3-glucanase 1
AT3G57790	AT3G57790	Pectin lyase-like superfamily protein

AT3G59850	AT3G59850	Pectin lyase-like superfamily protein
AT3G60120	BGLU27	beta glucosidase 27
AT3G60570	EXPB5	expansin B5
AT3G60730	AT3G60730	Plant invertase/pectin methylesterase inhibitor superfamily
AT3G60940	AT3G60940	Putative endonuclease or glycosyl hydrolase
AT3G61010	AT3G61010	Ferritin/ribonucleotide reductase-like family protein
AT3G61028	AT3G61028	Putative endonuclease or glycosyl hydrolase
AT3G61090	AT3G61090	Putative endonuclease or glycosyl hydrolase
AT3G61100	AT3G61100	Putative endonuclease or glycosyl hydrolase
AT3G61490	AT3G61490	Pectin lyase-like superfamily protein
AT3G61810	AT3G61810	Glycosyl hydrolase family 17 protein
AT3G62050	AT3G62050	Putative endonuclease or glycosyl hydrolase
AT3G62110	AT3G62110	Pectin lyase-like superfamily protein
AT3G62170	VGDH2	VANGUARD-like protein
AT3G62200	AT3G62200	Putative endonuclease or glycosyl hydrolase
AT3G62210	EDA32	Putative endonuclease or glycosyl hydrolase
AT3G62460	AT3G62460	Putative endonuclease or glycosyl hydrolase
AT3G62710	AT3G62710	Glycosyl hydrolase family protein
AT3G62850	AT3G62850	zinc finger protein-like protein
AT4G00190	PME38	pectin methylesterase 38
AT4G00890	AT4G00890	proline-rich family protein
AT4G01040	AT4G01040	Glycosyl hydrolase superfamily protein
AT4G01630	EXPA17	expansin A17
AT4G01890	AT4G01890	Pectin lyase-like superfamily protein
AT4G02290	GH9B13	glycosyl hydrolase 9B13
AT4G02300	AT4G02300	Plant invertase/pectin methylesterase inhibitor superfamily
AT4G02320	AT4G02320	Plant invertase/pectin methylesterase inhibitor superfamily
AT4G03210	XTH9	xyloglucan endotransglucosylase/hydrolase 9
AT4G03930	AT4G03930	Plant invertase/pectin methylesterase inhibitor superfamily
AT4G08160	AT4G08160	glycosyl hydrolase family 10 protein / carbohydrate-binding domain-containing protein
AT4G09740	GH9B14	glycosyl hydrolase 9B14
AT4G11050	GH9C3	glycosyl hydrolase 9C3
AT4G13080	XTH1	xyloglucan endotransglucosylase/hydrolase 1
AT4G13090	XTH2	xyloglucan endotransglucosylase/hydrolase 2
AT4G13210	AT4G13210	Pectin lyase-like superfamily protein
AT4G13710	AT4G13710	Pectin lyase-like superfamily protein
AT4G13760	AT4G13760	Pectin lyase-like superfamily protein
AT4G14080	MEE48	O-Glycosyl hydrolases family 17 protein
AT4G14130	XTH15	xyloglucan endotransglucosylase/hydrolase 15
AT4G15980	AT4G15980	Plant invertase/pectin methylesterase inhibitor superfamily
AT4G17030	EXLB1	expansin-like B1
AT4G17180	AT4G17180	O-Glycosyl hydrolases family 17 protein
AT4G18180	AT4G18180	Pectin lyase-like superfamily protein
AT4G18340	AT4G18340	Glycosyl hydrolase superfamily protein

AT4G18990	XTH29	xyloglucan endotransglucosylase/hydrolase 29
AT4G19720	AT4G19720	Glycosyl hydrolase family protein with chitinase insertion domain-containing protein
AT4G19730	AT4G19730	Glycosyl hydrolase superfamily protein
AT4G19740	AT4G19740	Glycosyl hydrolase superfamily protein
AT4G19750	AT4G19750	Glycosyl hydrolase family protein with chitinase insertion domain-containing protein
AT4G19760	AT4G19760	Glycosyl hydrolase family protein with chitinase insertion domain-containing protein
AT4G19770	AT4G19770	Glycosyl hydrolase family protein with chitinase insertion domain-containing protein
AT4G19800	AT4G19800	Glycosyl hydrolase family protein with chitinase insertion domain-containing protein
AT4G19820	AT4G19820	Glycosyl hydrolase family protein with chitinase insertion domain-containing protein
AT4G20040	AT4G20040	Pectin lyase-like superfamily protein
AT4G20480	AT4G20480	Putative endonuclease or glycosyl hydrolase
AT4G22080	RHS14	root hair specific 14
AT4G22090	AT4G22090	Pectin lyase-like superfamily protein
AT4G22100	BGLU3	beta glucosidase 2
AT4G23500	AT4G23500	Pectin lyase-like superfamily protein
AT4G23560	GH9B15	glycosyl hydrolase 9B15
AT4G23820	AT4G23820	Pectin lyase-like superfamily protein
AT4G24260	GH9A3	glycosyl hydrolase 9A3
AT4G24780	AT4G24780	Pectin lyase-like superfamily protein
AT4G25810	XTR6	xyloglucan endotransglycosylase 6
AT4G25820	XTH14	xyloglucan endotransglucosylase/hydrolase 14
AT4G26830	AT4G26830	O-Glycosyl hydrolases family 17 protein
AT4G26900	AT-HF	HIS HF
AT4G28250	EXPB3	expansin B3
AT4G28850	XTH26	xyloglucan endotransglucosylase/hydrolase 26
AT4G29360	AT4G29360	O-Glycosyl hydrolases family 17 protein
AT4G30270	XTH24	xyloglucan endotransglucosylase/hydrolase 24
AT4G30280	XTH18	xyloglucan endotransglucosylase/hydrolase 18
AT4G30290	XTH19	xyloglucan endotransglucosylase/hydrolase 19
AT4G30380	AT4G30380	Barwin-related endoglucanase
AT4G30760	AT4G30760	Putative endonuclease or glycosyl hydrolase
AT4G31140	AT4G31140	O-Glycosyl hydrolases family 17 protein
AT4G32370	AT4G32370	Pectin lyase-like superfamily protein
AT4G32375	AT4G32375	Pectin lyase-like superfamily protein
AT4G32380	AT4G32380	pectin lyase superfamily protein
AT4G33220	PME44	pectin methylesterase 44
AT4G33230	AT4G33230	Plant invertase/pectin methylesterase inhibitor superfamily
AT4G33440	AT4G33440	Pectin lyase-like superfamily protein
AT4G33810	AT4G33810	Glycosyl hydrolase superfamily protein
AT4G33820	AT4G33820	Glycosyl hydrolase superfamily protein
AT4G33830	AT4G33830	Glycosyl hydrolase family 10 protein
AT4G33840	AT4G33840	Glycosyl hydrolase family 10 protein

AT4G33850	AT4G33850	pseudogene of Glycosyl hydrolase family 10 protein
AT4G33860	AT4G33860	Glycosyl hydrolase family 10 protein
AT4G34480	AT4G34480	O-Glycosyl hydrolases family 17 protein
AT4G35670	AT4G35670	Pectin lyase-like superfamily protein
AT4G36050	AT4G36050	endonuclease/exonuclease/phosphatase family protein
AT4G37800	XTH7	xyloglucan endotransglucosylase/hydrolase 7
AT4G38210	EXPA20	expansin A20
AT4G38300	AT4G38300	glycosyl hydrolase family 10 protein
AT4G38400	EXLA2	expansin-like A2
AT4G38650	AT4G38650	Glycosyl hydrolase family 10 protein
AT4G38990	GH9B16	glycosyl hydrolase 9B16
AT4G39000	GH9B17	glycosyl hydrolase 9B17
AT4G39010	GH9B18	glycosyl hydrolase 9B18
AT5G01075	AT5G01075	Glycosyl hydrolase family 35 protein
AT5G02260	EXPA9	expansin A9
AT5G04310	AT5G04310	Pectin lyase-like superfamily protein
AT5G04885	AT5G04885	Glycosyl hydrolase family protein
AT5G04960	AT5G04960	Plant invertase/pectin methylesterase inhibitor superfamily
AT5G04970	AT5G04970	Plant invertase/pectin methylesterase inhibitor superfamily
AT5G05290	EXPA2	expansin A2
AT5G07410	AT5G07410	Pectin lyase-like superfamily protein
AT5G07420	AT5G07420	Pectin lyase-like superfamily protein
AT5G07430	AT5G07430	Pectin lyase-like superfamily protein
AT5G09280	AT5G09280	Pectin lyase-like superfamily protein
AT5G09700	AT5G09700	Glycosyl hydrolase family protein
AT5G09730	BXL3	beta-xylosidase 3
AT5G09760	AT5G09760	Plant invertase/pectin methylesterase inhibitor superfamily
AT5G09840	AT5G09840	Putative endonuclease or glycosyl hydrolase
AT5G10560	AT5G10560	Glycosyl hydrolase family protein
AT5G11720	AT5G11720	Glycosyl hydrolases family 31 protein
AT5G12950	AT5G12950	proline-tRNA ligase (DUF1680)
AT5G12960	AT5G12960	proline-tRNA ligase (DUF1680)
AT5G13870	XTH5	xyloglucan endotransglucosylase/hydrolase 5
AT5G13980	AT5G13980	Glycosyl hydrolase family 38 protein
AT5G14650	AT5G14650	Pectin lyase-like superfamily protein
AT5G15110	AT5G15110	Pectate lyase family protein
AT5G15546	AT5G15546	pseudogene of expansin A25
AT5G15870	AT5G15870	glycosyl hydrolase family 81 protein
AT5G16700	AT5G16700	Glycosyl hydrolase superfamily protein
AT5G17200	AT5G17200	Pectin lyase-like superfamily protein
AT5G17500	AT5G17500	Glycosyl hydrolase superfamily protein
AT5G18220	AT5G18220	O-Glycosyl hydrolases family 17 protein
AT5G18990	AT5G18990	Pectin lyase-like superfamily protein
AT5G19730	AT5G19730	Pectin lyase-like superfamily protein

AT5G20250	DIN10	Raffinose synthase family protein
AT5G20390	AT5G20390	Glycosyl hydrolase superfamily protein
AT5G20560	AT5G20560	Glycosyl hydrolase superfamily protein
AT5G20860	AT5G20860	Plant invertase/pectin methylesterase inhibitor superfamily
AT5G20870	AT5G20870	O-Glycosyl hydrolases family 17 protein
AT5G20940	AT5G20940	Glycosyl hydrolase family protein
AT5G20950	AT5G20950	Glycosyl hydrolase family protein
AT5G24318	AT5G24318	O-Glycosyl hydrolases family 17 protein
AT5G26622	AT5G26622	Beta-galactosidase related protein
AT5G26810	AT5G26810	Pectin lyase-like superfamily protein
AT5G27530	AT5G27530	Pectin lyase-like superfamily protein
AT5G27870	AT5G27870	Plant invertase/pectin methylesterase inhibitor superfamily
AT5G28510	BGLU24	beta glucosidase 24
AT5G35640	AT5G35640	Putative endonuclease or glycosyl hydrolase
AT5G39260	EXPA21	expansin A21
AT5G39270	EXPA22	expansin A22
AT5G39280	EXPA23	expansin A23
AT5G39290	EXP26	expansin-A25 protein
AT5G39300	EXPA25	expansin A25
AT5G39310	EXPA24	expansin A24
AT5G39640	AT5G39640	Putative endonuclease or glycosyl hydrolase
AT5G39910	AT5G39910	Pectin lyase-like superfamily protein
AT5G41870	AT5G41870	Pectin lyase-like superfamily protein
AT5G42720	AT5G42720	Glycosyl hydrolase family 17 protein
AT5G43710	AT5G43710	Glycosyl hydrolase family 47 protein
AT5G44830	AT5G44830	Pectin lyase-like superfamily protein
AT5G44840	AT5G44840	Pectin lyase-like superfamily protein
AT5G48070	XTH20	xyloglucan endotransglucosylase/hydrolase 20
AT5G48140	AT5G48140	Pectin lyase-like superfamily protein
AT5G48175	AT5G48175	transmembrane protein
AT5G48900	AT5G48900	Pectin lyase-like superfamily protein
AT5G49215	AT5G49215	Pectin lyase-like superfamily protein
AT5G49360	BXL1	beta-xylosidase 1
AT5G49720	GH9A1	glycosyl hydrolase 9A1
AT5G51490	AT5G51490	Plant invertase/pectin methylesterase inhibitor superfamily
AT5G51500	AT5G51500	Plant invertase/pectin methylesterase inhibitor superfamily
AT5G53370	PMEPCRF	pectin methylesterase PCR fragment F
AT5G55180	AT5G55180	O-Glycosyl hydrolases family 17 protein
AT5G55720	AT5G55720	Pectin lyase-like superfamily protein
AT5G56320	EXPA14	expansin A14
AT5G56590	AT5G56590	O-Glycosyl hydrolases family 17 protein
AT5G57530	XTH12	xyloglucan endotransglucosylase/hydrolase 12
AT5G57540	XTH13	xyloglucan endotransglucosylase/hydrolase 13
AT5G57550	XTH25	xyloglucan endotransglucosylase/hydrolase 25

AT5G57560	TCH4	Xyloglucan endotransglucosylase/hydrolase family protein
AT5G58090	AT5G58090	O-Glycosyl hydrolases family 17 protein
AT5G58480	AT5G58480	O-Glycosyl hydrolases family 17 protein
AT5G61180	AT5G61180	Putative endonuclease or glycosyl hydrolase
AT5G61190	AT5G61190	putative endonuclease or glycosyl hydrolase with C2H2-type zinc finger domain-containing protein
AT5G61680	AT5G61680	Pectin lyase-like superfamily protein
AT5G63180	AT5G63180	Pectin lyase-like superfamily protein
AT5G63225	AT5G63225	Carbohydrate-binding X8 domain superfamily protein
AT5G63230	AT5G63230	Carbohydrate-binding X8 domain superfamily protein
AT5G64450	AT5G64450	NYN domain protein
AT5G64590	AT5G64590	NYN domain protein
AT5G64640	AT5G64640	Plant invertase/pectin methylesterase inhibitor superfamily
AT5G64710	AT5G64710	Putative endonuclease or glycosyl hydrolase
AT5G64790	AT5G64790	O-Glycosyl hydrolases family 17 protein
AT5G65730	XTH6	xyloglucan endotransglucosylase/hydrolase 6
AT5G66150	AT5G66150	Glycosyl hydrolase family 38 protein
AT5G67460	AT5G67460	O-Glycosyl hydrolases family 17 protein

Supplementary Table 4.2. List of cell wall remodelling genes selected from overlay with transcript profiling dataset of FACS sorted auxin-induced pericycle cells

Gene ID	Gene symbol	Gene description
AT1G02640	BXL2	beta-xylosidase 2
AT1G02810	AT1G02810	Plant invertase/pectin methylesterase inhibitor superfamily
AT1G04680	AT1G04680	Pectin lyase-like superfamily protein
AT1G14720	XTH28	xyloglucan endotransglucosylase/hydrolase 28
AT1G64390	GH9C2	glycosyl hydrolase 9C2
AT1G66250	AT1G66250	O-Glycosyl hydrolases family 17 protein
AT1G69530	EXPA1	expansin A1
AT1G71380	CEL3	cellulase 3
AT1G78060	AT1G78060	Glycosyl hydrolase family protein
AT1G80170	AT1G80170	Pectin lyase-like superfamily protein
AT2G01630	AT2G01630	O-Glycosyl hydrolases family 17 protein
AT2G03090	EXPA15	expansin A15
AT2G06850	XTH4	xyloglucan endotransglucosylase/hydrolase 4
AT2G18660	PNP-A	plant natriuretic peptide A
AT2G18800	XTH21	xyloglucan endotransglucosylase/hydrolase 21
AT2G19440	AT2G19440	O-Glycosyl hydrolases family 17 protein
AT2G32990	GH9B8	glycosyl hydrolase 9B8
AT2G39700	EXPA4	expansin A4
AT2G43860	AT2G43860	Pectin lyase-like superfamily protein
AT3G26610	AT3G26610	Pectin lyase-like superfamily protein
AT3G53190	AT3G53190	Pectin lyase-like superfamily protein
AT3G59850	AT3G59850	Pectin lyase-like superfamily protein
AT3G61100	AT3G61100	Putative endonuclease or glycosyl hydrolase
AT3G61490	AT3G61490	Pectin lyase-like superfamily protein
AT3G62050	AT3G62050	Putative endonuclease or glycosyl hydrolase
AT3G62460	AT3G62460	Putative endonuclease or glycosyl hydrolase
AT4G02290	GH9B13	glycosyl hydrolase 9B13
AT4G13210	AT4G13210	Pectin lyase-like superfamily protein
AT4G13710	AT4G13710	Pectin lyase-like superfamily protein
AT4G14130	XTH15	xyloglucan endotransglucosylase/hydrolase 15
AT4G17030	EXLB1	expansin-like B1
AT4G23820	AT4G23820	Pectin lyase-like superfamily protein
AT4G24780	AT4G24780	Pectin lyase-like superfamily protein
AT4G29360	AT4G29360	O-Glycosyl hydrolases family 17 protein
AT4G38210	EXPA20	expansin A20
AT5G09760	AT5G09760	Plant invertase/pectin methylesterase inhibitor superfamily
AT5G09840	AT5G09840	Putative endonuclease or glycosyl hydrolase
AT5G11720	AT5G11720	Glycosyl hydrolases family 31 protein
AT5G19730	AT5G19730	Pectin lyase-like superfamily protein

AT5G48070	XTH20	xyloglucan endotransglucosylase/hydrolase 20
AT5G49360	BXL1	beta-xylosidase 1
AT5G53370	PMEPCRF	pectin methylesterase PCR fragment F

4.7. References

Aalen, R.B., Wildhagen, M., Sto, I.M., and Butenko, M.A. (2013). IDA: a peptide ligand regulating cell separation processes in Arabidopsis. J Exp Bot **64,** 5253-5261.

Abel, S., and Theologis, A. (1996). Early genes and auxin action. Plant Physiology **111,** 9-17.

Casimiro, I., Marchant, A., Bhalerao, R.P., Beeckman, T., Dhooge, S., Swarup, R., Graham, N., Inze, D., Sandberg, G., Casero, P.J., and Bennett, M. (2001). Auxin transport promotes Arabidopsis lateral root initiation. Plant Cell **13,** 843-852.

Clough, S.J., and Bent, A.F. (1998). Floral dip: a simplified method for Agrobacterium-mediated transformation of Arabidopsis thaliana. The Plant journal : for cell and molecular biology **16,** 735-743.

De Smet, I., Vassileva, V., De Rybel, B., Levesque, M.P., Grunewald, W., Van Damme, D., Van Noorden, G., Naudts, M., Van Isterdael, G., De Clercq, R., Wang, J.Y., Meuli, N., Vanneste, S., Friml, J., Hilson, P., Jürgens, G., Ingram, G.C., Inzé, D., Benfey, P.N., and Beeckman, T. (2008). Receptor-Like Kinase ACR4 Restricts Formative Cell Divisions in the Arabidopsis Root. Science **322,** 594-597.

Dubrovsky, J.G., Doerner, P.W., Colón-Carmona, A., and Rost, T.L. (2000). Pericycle Cell Proliferation and Lateral Root Initiation in Arabidopsis. Plant Physiology **124,** 1648-1657.

Dubrovsky, J.G., Sauer, M., Napsucialy-Mendivil, S., Ivanchenko, M.G., Friml, J., Shishkova, S., Celenza, J., and Benková, E. (2008). Auxin acts as a local morphogenetic trigger to specify lateral root founder cells. Proceedings of the National Academy of Sciences **105,** 8790-8794.

Dubrovsky, J.G., Napsucialy-Mendivil, S., Duclercq, J., Cheng, Y., Shishkova, S., Ivanchenko, M.G., Friml, J., Murphy, A.S., and Benkova, E. (2011). Auxin minimum defines a developmental window for lateral root initiation. New Phytol **191,** 970-983.

Fukaki, H., Tameda, S., Masuda, H., and Tasaka, M. (2002). Lateral root formation is blocked by a gain-of-function mutation in the SOLITARY-ROOT/IAA14 gene of Arabidopsis. The Plant journal : for cell and molecular biology **29,** 153-168.

Fukaki, H., Nakao, Y., Okushima, Y., Theologis, A., and Tasaka, M. (2005). Tissue-specific expression of stabilized SOLITARY-ROOT/IAA14 alters lateral root development in Arabidopsis. The Plant journal : for cell and molecular biology **44,** 382-395.

Geldner, N., Denervaud-Tendon, V., Hyman, D.L., Mayer, U., Stierhof, Y.D., and Chory, J. (2009). Rapid, combinatorial analysis of membrane compartments in intact plants with a multicolor marker set. The Plant journal : for cell and molecular biology **59,** 169-178.

Goh, T., Joi, S., Mimura, T., and Fukaki, H. (2012). The establishment of asymmetry in Arabidopsis lateral root founder cells is regulated by LBD16/ASL18 and related LBD/ASL proteins. Development **139,** 883-893.

Guilfoyle, T., Hagen, G., Ulmasov, T., and Murfett, J. (1998). How Does Auxin Turn On Genes? Plant Physiology **118,** 341-347.

Himanen, K., Boucheron, E., Vanneste, S., de Almeida Engler, J., Inze, D., and Beeckman, T. (2002). Auxin-mediated cell cycle activation during early lateral root initiation. Plant Cell **14,** 2339-2351.

Himanen, K., Vuylsteke, M., Vanneste, S., Vercruysse, S., Boucheron, E., Alard, P., Chriqui, D., Van Montagu, M., Inze, D., and Beeckman, T. (2004). Transcript profiling of early lateral root initiation. Proc Natl Acad Sci U S A **101,** 5146-5151.

Hruz, T., Laule, O., Szabo, G., Wessendorp, F., Bleuler, S., Oertle, L., Widmayer, P., Gruissem, W., and Zimmermann, P. (2008). Genevestigator V3: A Reference Expression Database for the Meta-Analysis of Transcriptomes. Advances in Bioinformatics **2008,** 5.

Ivanov, V.B., and Dubrovsky, J.G. (1997). Estimation of the Cell-Cycle Duration in the Root Apical Meristem: A Model of Linkage between Cell-Cycle Duration, Rate of Cell Production, and Rate of Root Growth. International Journal of Plant Sciences **158,** 757-763.

Kumpf, R.P., Shi, C.L., Larrieu, A., Sto, I.M., Butenko, M.A., Peret, B., Riiser, E.S., Bennett, M.J., and Aalen, R.B. (2013). Floral organ abscission peptide IDA and its HAE/HSL2 receptors control cell separation during lateral root emergence. Proc Natl Acad Sci U S A **110,** 5235-5240.

Laplaze, L., Parizot, B., Baker, A., Ricaud, L., Martinière, A., Auguy, F., Franche, C., Nussaume, L., Bogusz, D., and Haseloff, J. (2005). GAL4-GFP enhancer trap lines for genetic manipulation of lateral root development in Arabidopsis thaliana. Journal of Experimental Botany **56,** 2433-2442.

Laskowski, M., Biller, S., Stanley, K., Kajstura, T., and Prusty, R. (2006). Expression profiling of auxin-treated Arabidopsis roots: toward a molecular analysis of lateral root emergence. Plant Cell Physiol **47,** 788-792.

Lavenus, J., Goh, T., Roberts, I., Guyomarc'h, S., Lucas, M., De Smet, I., Fukaki, H., Beeckman, T., Bennett, M., and Laplaze, L. (2013). Lateral root development in Arabidopsis: fifty shades of auxin. Trends Plant Sci.

McQueen-Mason, S.J., and Cosgrove, D.J. (1995). Expansin mode of action on cell walls. Analysis of wall hydrolysis, stress relaxation, and binding. Plant Physiol **107,** 87-100.

Okushima, Y., Fukaki, H., Onoda, M., Theologis, A., and Tasaka, M. (2007). ARF7 and ARF19 regulate lateral root formation via direct activation of LBD/ASL genes in Arabidopsis. Plant Cell **19,** 118-130.

Okushima, Y., Overvoorde, P.J., Arima, K., Alonso, J.M., Chan, A., Chang, C., Ecker, J.R., Hughes, B., Lui, A., Nguyen, D., Onodera, C., Quach, H., Smith, A., Yu, G., and Theologis, A. (2005). Functional genomic analysis of the AUXIN RESPONSE FACTOR gene family members in Arabidopsis thaliana: unique and overlapping functions of ARF7 and ARF19. Plant Cell **17,** 444-463.

Orman-Ligeza, B., Parizot, B., de Rycke, R., Fernandez, A., Himschoot, E., and Van Breusegem, F. (2016). RBOH-mediated ROS production facilitates lateral root emergence in Arabidopsis.

Overvoorde, P., Fukaki, H., and Beeckman, T. (2010). Auxin control of root development. Cold Spring Harb Perspect Biol **2,** a001537.

Peret, B., Larrieu, A., and Bennett, M.J. (2009). Lateral root emergence: a difficult birth. J Exp Bot **60,** 3637-3643.

Péret, B., Li, G., Zhao, J., Band, L.R., Voß, U., Postaire, O., Luu, D.-T., Da Ines, O., Casimiro, I., Lucas, M., Wells, D.M., Lazzerini, L., Nacry, P., King, J.R., Jensen, O.E., Schäffner, A.R., Maurel, C., and Bennett, M.J. (2012). Auxin regulates aquaporin function to facilitate lateral root emergence. Nat Cell Biol **14,** 991-998.

Roycewicz, P.S., and Malamy, J.E. (2014). Cell wall properties play an important role in the emergence of lateral root primordia from the parent root. J Exp Bot **65,** 2057-2069.

Schindelin, J., Arganda-Carreras, I., Frise, E., Kaynig, V., Longair, M., Pietzsch, T., Preibisch, S., Rueden, C., Saalfeld, S., Schmid, B., Tinevez, J.Y., White, D.J., Hartenstein, V., Eliceiri, K., Tomancak, P., and Cardona, A. (2012). Fiji: an open-source platform for biological-image analysis. Nature methods **9,** 676-682.

Slane, D., Kong, J., Berendzen, K.W., Kilian, J., Henschen, A., Kolb, M., Schmid, M., Harter, K., Mayer, U., De Smet, I., Bayer, M., and Jurgens, G. (2014). Cell type-specific transcriptome analysis in the early Arabidopsis thaliana embryo. Development **141,** 4831-4840.

Vanneste, S., De Rybel, B., Beemster, G.T., Ljung, K., De Smet, I., Van Isterdael, G., Naudts, M., Iida, R., Gruissem, W., Tasaka, M., Inze, D., Fukaki, H., and Beeckman, T. (2005). Cell cycle progression in the pericycle is not sufficient for SOLITARY ROOT/IAA14-mediated lateral root initiation in Arabidopsis thaliana. Plant Cell **17,** 3035-3050.

Vermeer, J.E., von Wangenheim, D., Barberon, M., Lee, Y., Stelzer, E.H., Maizel, A., and Geldner, N. (2014). A spatial accommodation by neighboring cells is required for organ initiation in Arabidopsis. Science **343,** 178-183.

Vilches-Barro, A., and Maizel, A. (2015). Talking through walls: mechanisms of lateral root emergence in Arabidopsis thaliana. Curr Opin Plant Biol **23,** 31-38.

Wilson, M.H., Holman, T.J., Sorensen, I., Cancho-Sanchez, E., Wells, D.M., Swarup, R., Knox, J.P., Willats, W.G., Ubeda-Tomas, S., Holdsworth, M., Bennett, M.J., Vissenberg, K., and Hodgman, T.C. (2015). Multi-omics analysis identifies genes mediating the extension of cell walls in the Arabidopsis thaliana root elongation zone. Frontiers in cell and developmental biology **3,** 10.

Chapter 5. Confocal Raman microscopy based imaging of *Arabidopsis* root sections

Work contributions:

Ramakrishna P. – Division of Plant and Crop Sciences, University of Nottingham, UK – Optimised sample preparation and performed the measurements and analysis.

Rance G. - Nottingham Nanoscale and Microscale Research Center, University of Nottingham, UK – Provided training and helped with optimisation of confocal Raman microscope setup and analysis.

5.1. Introduction

Arabidopsis thaliana is widely used as a model organism for basic research in genetics and molecular biology to study the development of various plant organs. A significant amount of this research to understand root biology and its formation is also undertaken using *Arabidopsis* roots as the model system. Study of cellular level changes in live tissues that are embedded under tissue layers is tricky and requires either dissection, fixation or destructive techniques that do not maintain the walls in their natural state. We were interested to study the changes in the plant cell wall in its natural state using a non-invasive and non- destructive techniques and selected confocal Raman microscopy that has been previously used to study composition of wood stems, tomato fruit texture, *Arabidopsis* stem segments and optimise this to be able to probe the cell wall of root sections. In this chapter we present an optimised protocol to section *Arabidopsis* roots and preserve live root segments for confocal Raman analysis and the optimisation of imaging parameters. We also present a basic comparison of differences that we observed in the roots *Arabidopsis* ecotype Columbia and study the differences in wall composition on roots treated with auxin known to induce cell wall remodelling.

5.1.1. Plant Cell Wall Components

The primary cell wall of plants is a composite matrix of cellulose microfibrils, hemicelluloses, pectic polysaccharides and cell wall-associated proteins (such as hydroxyproline-rich glycoproteins (HRGP) and extensins), with the wall being about 0.1-1 µm during early growth. **Cellulose** microfibrils are made up of unbranched (1-4)-β-linked glucose molecules that are linked

together by hydrogen bonding to form microfibrils that are about 3nm in diameter. The cellulose microfibrils bind via non-covalent interactions with other cell wall matrix polysaccharides and form a major constituent of the primary cell wall (**Figure 5.1**). It is one of the most abundant biopolymers on earth and can be as long as 15,000 subunits and its structure enables it to be highly resistant to hydrolysis. Cellulose synthesis involves chain initiation and polymer chain elongation and is synthesised by the CELLULOSE SYNTHASE (CESA) family of proteins. The CESA proteins are located in the cell membrane and due to the large size, the cellulose microfibrils are synthesised near the membrane and released into the extracellular region to be incorporated into growing walls.

Hemicelluloses are branched polysaccharides that are structurally homologous to cellulose due to the (1-4)-β-D-hexosyl residues in their backbone (**Figure 5.1**). Xyloglucan (XyG) is the most commonly found hemicellulose in primary cell walls, while the others that can be found both in primary and secondary walls are arabinoxylan, glucomannan, glucuronoxylan, galactomannan to name a few.

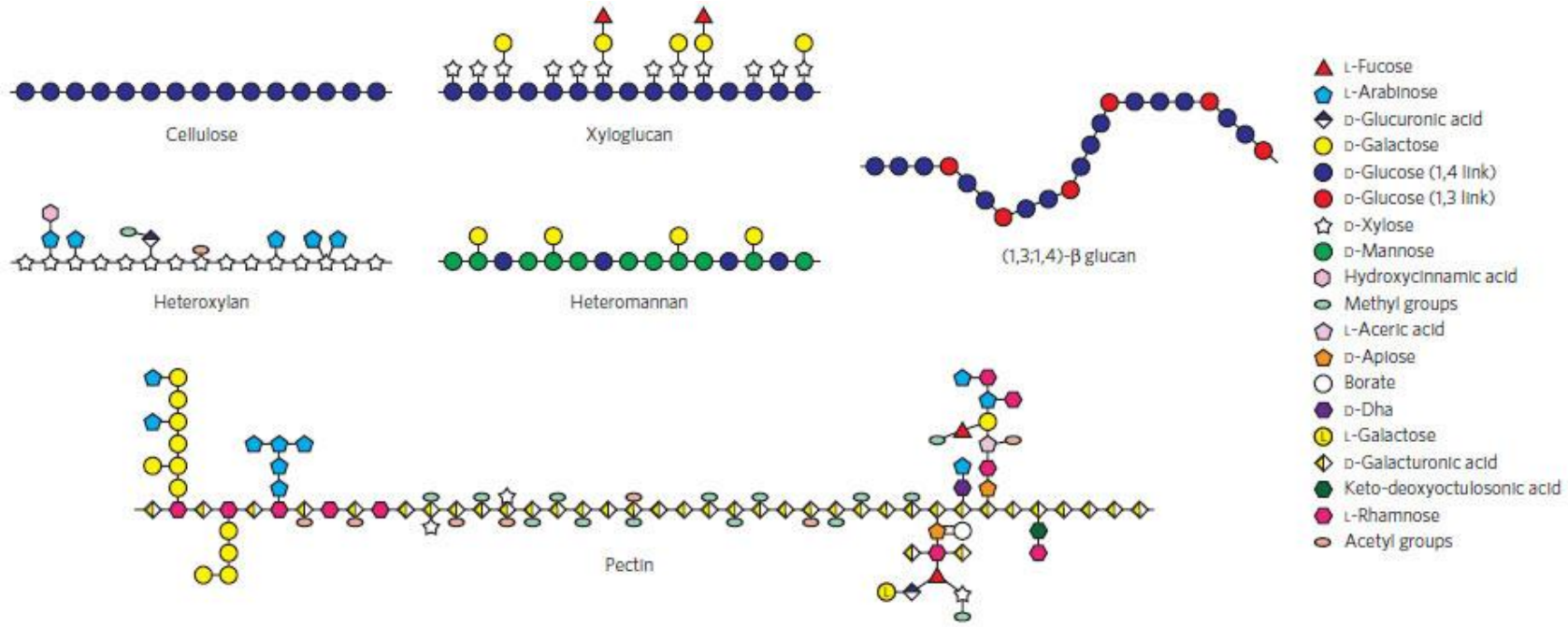


Figure 5.1: Schematic of polysaccharide structures found in plant cell walls. Cellulose, xyloglucan (XyG) and (1,3;1,4)-β-glucan have a glucose (Glc*p*) based backbone; heteroxylan on xylose (Xyl*p*), heteromannan on mannose (Man*p*), pectins based on (1,4)-α-linked chains of galacturonosyl residues (Burton et al., 2010; Doblin et al., 2010)

The hemicelluloses are mainly involved in cross-linking the fibers in the primary cell wall and its branched nature provides the flexibility the cell wall fibers need to form points of contact for cross-links (Rose et al., 2002; Park and Cosgrove, 2015). They are also easily hydrolysed by enzymes or weak acids and bases which makes them the targets for rapid wall modifications during cell growth and development (such as cell elongation and cell expansion) (Van Sandt et al., 2007). **Pectin** are another group of polysaccharides that are enriched in the middle lamella of the cell wall and responsible for cell-to-cell adhesion. They prevent aggregation and collapse of the cellulose network and also determine the porosity of the wall to macromolecules. Pectins are rich in galacturonic acid (GalA) and neutral sugars such as rhamnose, galactose, and arabinose that are often, but not always covalently linked to form macromolecular structures. The three major pectic domains are comprised of: i) Homogalacturonan (HGA) – linear chains of galacturonic acid residues with the carboxyl groups often methyl esterified reducing their ability to form gel. It is the most abundant pectin in primary cell wall; ii) Rhamanogalacturonan-I (RG-I) - alternating residues of galacturonic acid and rhamnose with additional branched side chains that contain other pectin domains; iii) Rhamanogalacturonan-II (RGII) – a complex that contains 11 different sugar residues and forms dimers through borate esters (**Figure 5.1**). The role of pectins has been recently reviewed in (Peaucelle et al., 2012). Once the cells mature and cease enlargement, the spaces in between the matrix can be filled with lignin that leads to formation of the secondary cell wall (Zhong and Ye, 2015). **Lignin** is a an amorphous heteropolymer that is formed by enzyme mediated oxidative coupling of three p-hydroxycinnamyl alcohols to form guaiacyl (G), syringyl (S), and

hydroxyphenyl (H) subunits (Boerjan et al., 2003). They form a hydrophobic heteropolymer that provides the plants with structural support and stiffness and are one of the hardest biopolymers to degrade. All these complex and variable structures interact together to constitute a functional plant cell wall and provide the plant with its shape and the flexibility to accommodate growth.

5.1.2. Primary cell wall interactions and plant growth

Post-embryonic growth and development of plants involves a balanced combination of cell division and cell expansion to dictate the final size and shape of the plant. While cell division serves to increase cell number, cell expansion functions to increase the size of cells. Cell expansion is a mechanistic process that requires remodelling of the cell wall in a dynamic fashion. It involves a complex interplay between loosening of existing wall components accompanied by addition of newly synthesised components to the growing wall. There is still considerable debate on the appropriate model that accurately describes the organisation of the cell wall and its interactions. The literature is rich with hypothetical models to describe the interactions in the cell wall and the structure of the primary cell wall (Cosgrove and Jarvis, 2012; Cosgrove, 2014; Park and Cosgrove, 2015). In the wall of a single cell, individual cellulose microfibrils that range about 5 to 10nm in width (McCann et al., 1990) are arranged 10-30nm apart in loose parallel layers, with the hemicelluloses closely associated with them, and the pectins arranged between them. By dry mass, it is estimated that primary cell walls contain about 40% pectin, 25% cellulose, 20% hemicellulose and about 5% protein and other wall material (**Table 5.1**). However, these compositions vary depending on species and cell type and cannot be considered as standards.

Table 5.1. Polysaccharide composition of cell wall with their primary monomer units based on literature.

Polysaccharide	%composition (dry biomass)	Sugar monomers
Cellulose	15-40%	Glucose
Hemicellulose (primarily xylans)	20-30 %	Xylose
Pectins	30-50%	Galacturonic acid + arabinose, galactose, rhamnose
Other structural proteins (Extensin, HRGP)		

5.1.3. Confocal Raman microscopy

Raman spectroscopy is a vibrational spectroscopy based on the inelastic scattering of light. Micro Raman spectroscopy or Raman microscopy is the same fundamental technique with the only difference being that the collection optics involve a microscope (rather than a fibre optic for example) – and thus this massively improves the spatial resolution. Confocal Raman microscopy is an extension beyond this and uses an aperture/hole to control/restrict the analysis volume and thus this further improves the spatial resolution (particularly the z-resolution). Confocal Raman microscopy provides an '*in situ*', non-destructive chemical analysis and spectroscopic imaging technique that uses the spontaneous inelastic scattering of light to generate spectra unique to a material's molecular composition and state. The technique has the ability to spatially filter and control the volume of the sample that is analysed and does not typically require sample extraction, purification or labelling.

The spectral resolution defines the distance between two pixels on the detector (important for resolving peaks of similar shift in the Raman shift). It is dependent on many factors, including the focal length between the grating and the detector, the groove density of the grating and the wavelength of the excitation laser. The spatial resolution is dependent on the numerical aperture of the objective lens and the size of the confocal hole and defines the minimum distance between two points within a map. Therefore, the importance of the confocal hole is to increase the spatial (x, y and z) resolution and does not affect the spectral resolution (although the instrument used in our study has a long focal length and therefore by definition is a high spectral resolution instrument, it is not a requirement for all confocal instruments to have high spectral resolution). The confocal Raman microscopy utilises the benefits of confocal microscope with Raman spectroscopy to provide molecular (micro or nano-scale) information about the components in the cell at high spectral resolution.

5.1.4. Principle of Raman spectroscopy

Raman spectroscopy is based on the principle of the 'Raman effect' which is a result the of inelastic scattering of light. When a sample is irradiated with monochromatic radiation, the light will interact with the sample by either being reflected, absorbed, or scattered in some manner (**Figure 5.2a**). If the interaction does not lead to any changes in energy level (the energy of the incident radiation is equal to the energy of scattered light) of the molecule, it is referred to as Rayleigh or elastic scattering. If the radiation interacts with the molecule, it causes short-lived distortions in the electron cloud that create

molecular vibrations which results in a change in the energy of the scattered light and this is referred to as inelastic scattering or the 'Stokes Raman effect' (**Figure 5.2b**).

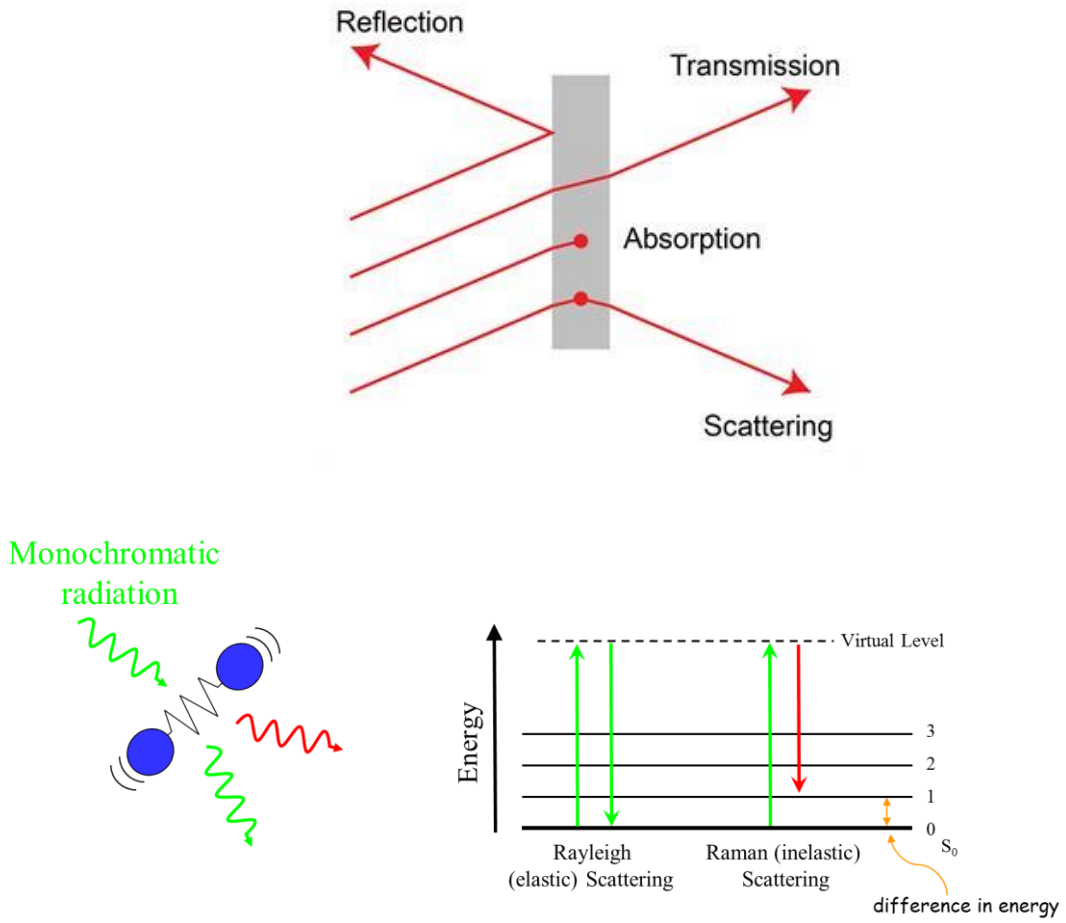


Figure 5.2. Schematic of light interactions with a surface (a); Schematic of Raman Effect that Raman spectroscopy is based on (b).

The change in wavelength of the scattered photon helps provide chemical and structural information of the material being analysed in the form of a spectra. The vibrational energies of molecules are sensitive to features such as the atomic mass, molecular structure and geometry, bond strength, bond order, or general influence of non-covalent interactions on bond energies of the molecule. The Raman scattering is a very weak effect with only about 1 in 10^7 photons becoming Raman scattered. The spectra contain information

about the vibrational modes of the molecule and sharp spectral features allow for identification of the molecule by its spectrum. Raman spectroscopy has been used to explore changes in the molecular composition of cell walls of *Arabidopsis* stem sections (Schmidt et al., 2010), in secondary cell wall of black spruce (Agarwal, 2006) and *Poplar* (Gierlinger and Schwanninger, 2006).

5.2 Results

5.2.1. Optimisation of sample preparation for *Arabidopsis* roots by confocal Raman microscopy

A detailed protocol has been described for imaging of plant cell walls by confocal Raman microscopy for young tree wall material (Gierlinger et al., 2012). We optimised this protocol to image transverse sections of *Arabidopsis* roots. The main challenge was to obtain high quality, fresh root cross sections as a reflection of the plants true native state. *Arabidopsis* roots of young seedlings are very fragile and can be easily damaged by extensive handling. Hence, we developed an embedding method that places the least strain on the root tissue and allows sectioning.

5.2.1.1. Embedding media optimisation

The samples were embedded in different concentrations of Agarose (2.5%, 4%, and 5%) and bacteriological agar (2.5%, 4%, and 5%) to test for the condition that produces stable, easy to handle root cross sections. The 4% bacteriological agar sections had the best embedding property and produced sections that were stable in their contact with the roots. The consistency of the 4% bacteriological agar media was flexible and easier to handle sample orientation at cooled down temperature of 40 ºC. Hence, this was chosen as

the medium to embed the sample in. The preparation of agar is a critical step and care had to be taken to prevent air gaps that could hinder the sample preparation and its stability in the embedded agar block.

5.2.1.2. Embedding procedure

1.5ml Eppendorf tubes are used as molds to embed the sample**.** A drop of water at the base of the tube helped easy release of the agar block**.** 1-2ml agar, maintained at 60 ºC was pipetted into the tube and allowed to cool for a few seconds. The sample is slid into the agar and oriented perpendicular to the orientation of sectioning using a dissection needle such that cross sections of the root are obtained. The sample is allowed to set either by placing them overnight at 4ºC or in cold water for an hour minimum. The agar block was then removed from the Eppendorf and the excess was trimmed off from either ends. The surface of the block was blot dried on tissue or blotting paper to remove moisture and enable better adhesion between block and glue.

5.2.1.3. Vibratome sectioning

Transverse root cross sections were prepared using Leica VT 1000S Vibratome. The sample is attached onto the specimen mounting disc using sufficient mounting material (superglue) in the right orientation. Allow to dry for 30 mins and the sample is ready for sectioning. The surface onto which specimen is attached must be clean, dry and free from residual adhesives from previous applications. The mounting disc is slotted into the holder of the Vibratome bath. The section thickness was set to 100 microns. Thinner sections were unstable and the root samples were frequently lost post-sectioning.

Samples are floated in distilled water and picked up and moved to a slide using a paintbrush or disposable inoculation loop. The loop provides a stable round surface to pick the sample without breakage. The sample was covered with a glass coverslip and sealed to prevent evaporation.

5.2.2. Optimised Confocal Raman imaging of *Arabidopsis* root sections

The challenge faced with imaging *Arabidopsis* roots for our analysis was to be able to exclusively probe the protoxylem pericycle cell junction of the live root sections. In the previous section, we have described the optimisation of agarose embedding and sectioning protocol that was developed to enable this. In this section, we move on to analyse wildtype Col 0 roots to determine the chemical composition differences in the pericycle cell wall. The key steps in confocal Raman spectroscopic analysis are:

i) Sample preparation
ii) Data acquisition
iii) Data analysis

5.2.2.1. Sample preparation

Arabidopsis Col 0 (wildtype) seedlings were germinated and grown for 72hrs post germination on 10µM NPA. The root sections were take roughly about 400 microns upward from the root tip. The roots were embedded in 4% bacteriological agar media (Sigma-Aldrich) and 100-micron transverse root sections were prepared by Vibratome (Leica VT 1000S Vibratome). The sections were placed in D_2O (Sigma-Aldrich) on glass microscope slides and covered with glass cover slips. The edges of the cover slips were sealed with nail paint onto the glass slides to prevent evaporation of D_2O. *Critical steps*: i) Ensure material never dries; ii) It is important to have a flat or uniform surface

with intact cell wall. Samples are screened on a light microscope before the main analysis. In addition, we acquired the Raman spectra of individual wall polysaccharides that are commercially available to generate a reference spectrum for comparison. Microcrystalline cellulose powder (~20µm) (Sigma Aldrich), Azo-Xyloglucan (tamarind, purity >95%) from Megazyme and Pectin from citrus peel (Galacturonic acid >74%) from Sigma Aldrich were used to collect the Raman spectrum.

5.2.2.2. Data acquisition

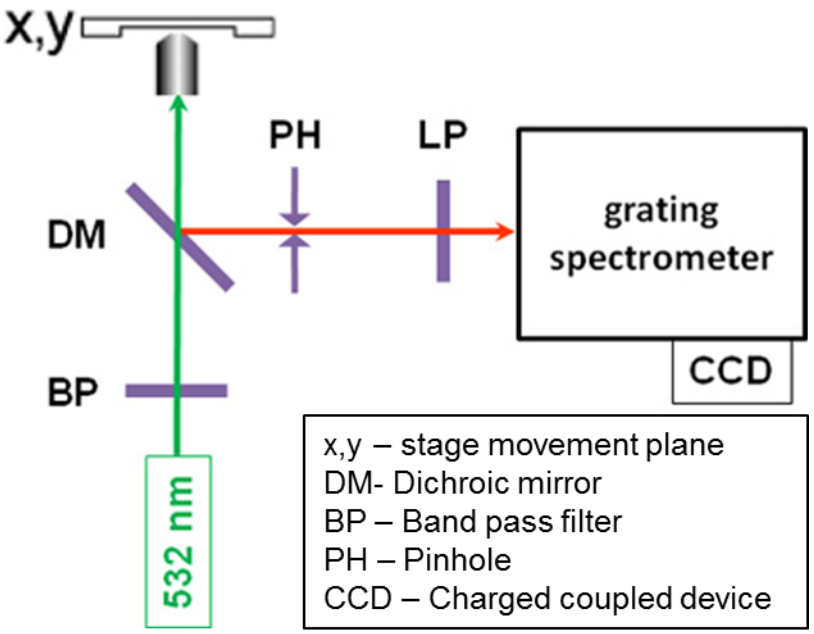


Figure 5.3. Schematic of confocal Raman instrument setup.

Raman spectroscopy and imaging was performed using a Horiba LabRAM HR microscope equipped with a piezoelectric scan stage (Märzhäuser, Germany) using either a 532nm or 785nm laser, a 100x air objective (Nikon, NA = 0.9) and 600lines mm^{-1} grating. Point spectra of approximately 1 micron spatial resolution were acquired by focusing on the point of interest on the sample. The integration time of 120s was fixed for each scan and a single spectrum at each point was recorded within the range of

1000-3600 cm^{-1}. Raman spectrum of the reference materials were collected to use as basis for comparative post-analysis. Xyloglucan and pectin pure compounds had a high level of fluorescence and were therefore photobleached for 30mins before reference spectra acquisition with the 785nm laser, 60s integration time. Cellulose did not exhibit high background fluorescence and the spectra was acquired without photobleaching. The point spectra of the samples were then processed with LabSpec 6 software (Horiba Scientific).

5.2.2.3. Data analysis

To extract relevant information from the acquired spectra, the spectra were pre-processed and subsequently analysed. The relative intensity and energy of a particular peak in a Raman spectrum can be used to identify a specific molecular vibration or functional group and thus aid with structural confirmation of the material under examination. Raman instruments with CCD detectors occasionally pick up spikes caused by cosmic rays. By increasing the number of accumulations that detects the false peak these could be eliminated it from the final resultant spectrum. Sample fluorescence is one of the major hindrances to Raman spectroscopy of plant materials. The issue of fluorescence was overcome in two steps. Samples that produced signal above 10,000 counts were bleached for ~5 mins before the final spectra were acquired. The second step involved application of baseline correction algorithm to eliminate the fluorescence background. For our analysis, we baseline corrected individual spectra with a local polynomial fit of the data and subsequently smoothed using the DeNoise filter embedded in LabSpec 6 software (Horiba Scientific, UK). Single point spectra were acquired at multiple points of the pericycle cell junction and averaged to obtain the final cumulated

spectrum for comparative analysis. *Peak comparison study:* For each spectrum obtained, each point represents one value of the corresponding pixel in the image. The spectral map was obtained by integrating the intensities under the curve for the regions that correspond to a specific compound of interest. For point spectrum, the area under the curve was calculated for the range that showed enrichment of peaks i.e., between 1100-1800 and 2800-3200$cm^{-1.}$ This helped eliminating the interference signal from the glass slide and D_2O. The amount and scattering strength of bands that correspond to a cellulose, hemicellulose and pectin content were assigned to the different peaks on the spectra. The intensity of the peaks was then compared to infer the difference in distribution of cell wall polysaccharides at the imaged point of interest.

5.2.3. Raman spectra of pure wall compounds for reference

The relative intensity and energy of a particular peak in a Raman spectrum can be used to identify a specific molecular vibration or functional group and thus aid with structural confirmation of the material under examination. In our study, we determined the Raman spectra of extracted cell wall compounds cellulose, xyloglucan and pectin, that are available commercially (**Figure 5.4.**) The peaks were observed at points that have been previously assigned to a particular vibrational mode based on literature (Sene et al., 1994; Schulz and Baranska, 2007; Gierlinger et al., 2008; Chylińska et al., 2014). Key spectral peaks have been assigned as follows: Cellulose – 1093, 1121, 1378, 2895 and 2897 cm^{-1}; xyloglucan - 1256, 1465 and 2897 cm^{-1} and pectins - 1420, 1750 and 2948 cm^{-1} (**Table 5.2**). The peaks in a Raman spectra have been shown to be sensitive to the orientation of the microfibril. For instance, the peaks at 1121 and 1098 cm^{-1} correspond to the symmetric and

asymmetric stretching mode of COC glycosidic bond of cellulose (Gierlinger et al., 2008). This could be explored in the future by using a polarizing lens to be able to know more in depth about the orientation of the compound. Polysaccharides sometimes show overlapping bands due to similar base chemical backbone with differences being a property of the attached functional groups. For example, the vibrational peak of (C=O) band at 1742cm^{-1} could be assigned to both hemicellulose and pectin as they both contain carbonyl functionality and cannot be used to uniquely identify these molecules (Schulz and Baranska, 2007; Lacayo et al., 2010). However, the vibrations are also affected by various other factors and hence although both the compounds may contain the (C=O) functional group, the differences may lay in their vibrational energies.

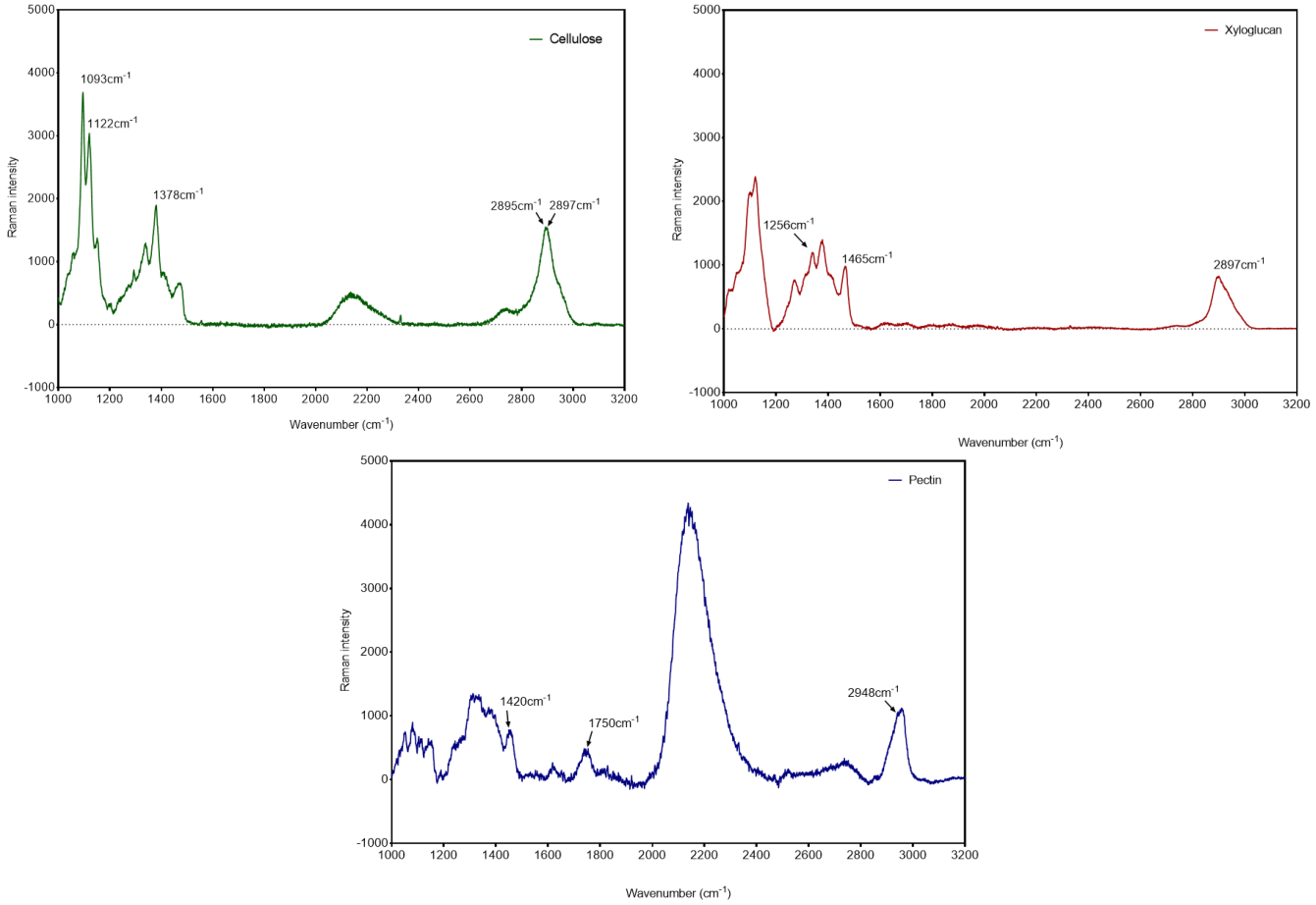


Figure 5.4. Raman spectra of commercially available cell wall compounds- cellulose, xyloglucan and pectin. Peaks assigned based on literature (**Table 5.2**)

Table 5.2. Table of bands of Raman spectra assigned to cell wall polysaccharides based on literature

Raman wavenumber (cm^{-1})	Vibrational mode assigned	Compound origin
2952	C-H	Pectin
2930	C-H	Hemicellulose
2895	C-H	Cellulose
1742	C=O	Pectin, Hemicellulose
1730		
1420	COO^-	Pectin (PGA)
1378	HCC, HCO, HOC	Cellulose
1360	CH bending	
1332	Aliphatic O-H	Syringyl – lignin
1294	C-C stretch of coniferyl alcohol	
1270		Guaicyl
1256	CH, COH	Hemicellulose
1121	COC (glycosidic, symmetric)	Cellulose
1098	COC (glycosidic, asymmetric)	Cellulose
971	CH2	Cellulose
854	COC	Pectin
817	COH	Pectin
478	COC (glycosidic)	Pectin
380	CCC	Cellulose

5.2.4. Differences detected in Raman spectra of *Arabidopsis* roots

Point spectra of two distinct points at the junction between adjacent xylem pole pericycle cells were acquired and compared for differences in spectral band intensities and abundance (**Figure 5.5**).

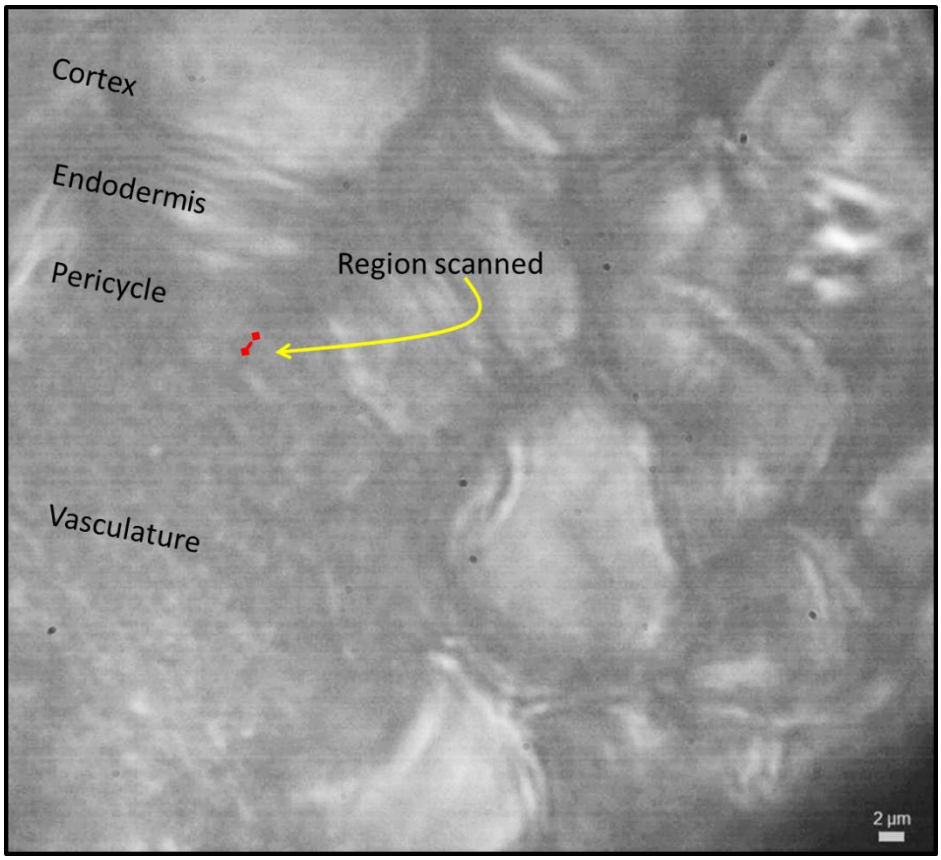


Figure 5.5. Representative cross section of *Arabidopsis* root slice viewed under 100X magnification used for confocal Raman spectroscopic analysis. The red line represents the region where point spectrum was acquired from two adjacent points and averaged out for analysis.

The spectral peaks of wildtype Col-0 root cross section acquired before and after treatment from three different points at the xylem pole pericycle junctions, were compared to determine if there was consistency in the observed spectral pattern and reproducibility of peaks. The different points within each root considered here as a replicate were then averaged out for the treated and untreated to compare for differences in their spectral peaks. Due to background

fluorescence issue and fluctuations in the bands at low wavenumbers we were unable to discriminate Raman features from those associated with fluorescence for the region below 1000 cm^{-1}.

Figure 5.6. shows the average Raman spectrum of *Arabidopsis* root cross sections in D_2O. We can assign the major Raman bands to functional groups likely associated with primary cell wall polymers – cellulose hemicellulose and pectin – based on the comparison with the peaks in the reference spectra shown in **Figure 5.4**. On comparing for differences in wall polysaccharide composition upon auxin treatment, we could uncover strong differences in the regions that are known to be enriched with bands in cellulose-hemicellulose and a few bands of pectin. The region between 2820 – 2935 cm^{-1} showed differences in the relative shape and intensity of peaks which could be a consequence of treatment and which could infer corresponding structural changes the cell wall. At this point however, given that we acquire point spectrum that we have averaged out to compare, it presents only very basic differences and does not help us gain a broader spatial distribution of wall polymers in this instance.

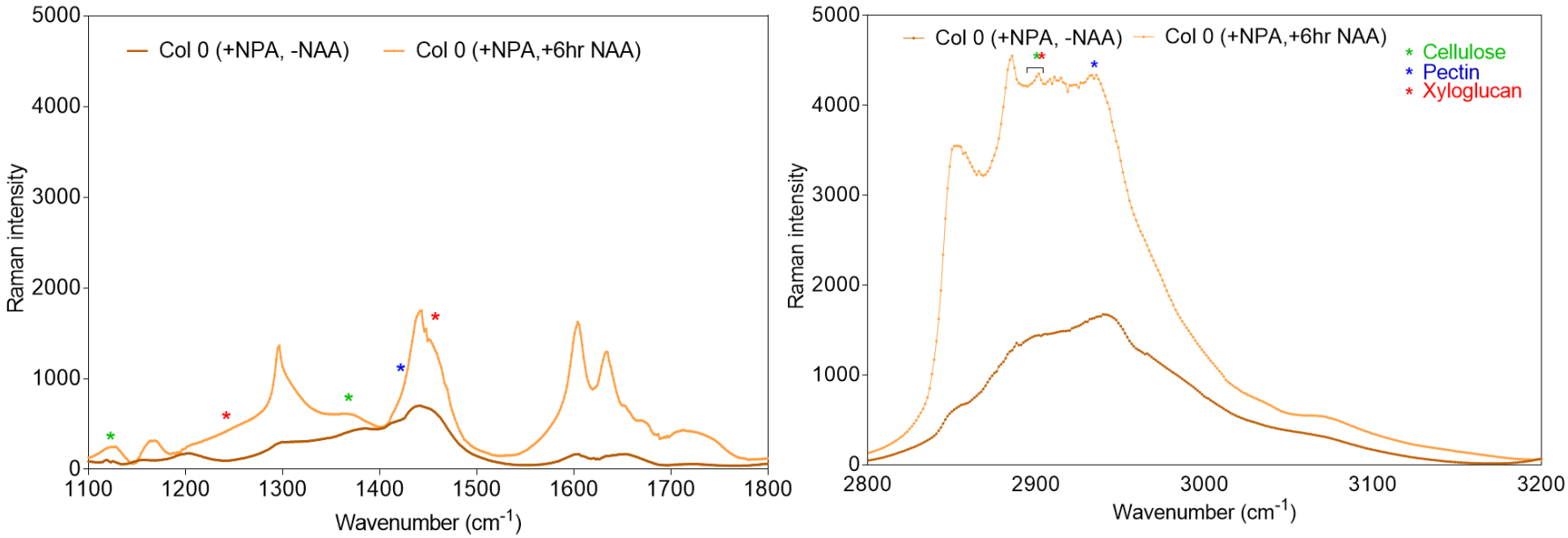


Figure 5.6. Average Raman spectrum at the xylem pole pericycle cell junction of Col 0 roots under untreated (i.e. 10µM NPA grown) and post 6hr 10µM NAA treatment condition. Spectra split into the range 1100-1800 cm^{-1} and 2800-3200 cm^{-1} to eliminate noise from glass slide and D_2O. The asterix are color coded corresponding to the compound that has a distinct spectral band assigned to the wavenumber from literature. (n=4 roots/line, graph represent average of all roots).

Single spectra and analysis of bands was able to help us understand the differences molecular structure of the wall. However, it has its disadvantages when it came to hemicelluloses as it is unable to distinguish between cellulose and hemicellulose due to overlapping bands. A chemometric analysis such as vertex component analysis (VCA) and/or multivariate cluster analysis might help to resolve the different components of the wall in greater depth (Gierlinger et al., 2012; Gierlinger, 2014). Another step would be to generate Raman maps of a larger area of the root section instead of point spectra. This has been tried in tomato fruits to study the polymer composition at the cell wall corners (Chylińska et al., 2014). This would help gain a broader picture of the changes across difference wall junctions.

5.2.5. Advantages and disadvantages of the techniques

Advantages

- The techniques provides chemical composition data for the region of interest at micro/nano scale
- It is a non-destructive techniques so the sample can be reanalysed
- It is also possible to analyse samples with aqueous solutions which is useful for live-tissue imaging
- All material exhibit Raman scattering, some more than the others, and some idenitifed and characterised better than the others. The well known wall polymers have been characterised and assigned a peak (**Table 5.2**)
- The use of a polarising, birefringement element has the potential to distinguish the orientation of the chemical bonds. This would mean it is capable of idenntification of orientation of the wall fibres for example orientation of the cellulose fibres (which is important for to understand the area or direction of growth in the cell wall)

- There are higher resoulution Raman systems that are capable of prividing greater spectral resolution than explored in the current work. These systems can help look at sample stress and holds potential for studies on mechanical properties

Disadvantages

- The technique is not high-throughput for studies on *Arabidopsis* roots at least at present. *Arabidopsis* roots are delicate structures that require careful handling to prevent damage during sample preparation. The sections used in the study need to be a uniform flat surface with the thinner section being better making it tricy to handle. Hence, requires skilled personnel for sample preparation

- Photoluminescence can mask Raman effect. To overcome this one of the approaches would be to switch to a different excitation wavelength (such as from 532nm to 785nm used in our case for some samples with high fluorescence background)

- There are several new combinations of wall molecules formed in a growing cell wall that are dynamic and hard to capture with the current ability of the Raman spectroscopy set-up. Time-point based spectra or maps are the only posible current measurements which can sometimes be subject to varaibility based on the state of a plant compared to another

- The glassware can mask some of the spectra. A potential solution ot thios is to use metal microscopes. However, in the case of live-tissue that we use in the study, we depend on transmittance of light through the sample to locate and chemically image the sample so this is not feasible for our purpose

- Alternatively, quartz or Calcium fluoride (CaF_2)slides could be used as they have a weaker Raman sinal and less intrusive optical properties. CaF_2 also offers lower absorption of light and higher transmission, low refractive index and hence can be used to couple with UV/IR based application

Chapter 6. A comparative study on cell wall properties of *Arabidopsis* roots and wall mutant *expa1-1*

Work contributions:

Ramakrishna P. – Division of Plant and Crop Sciences, University of Nottingham, UK – Designed the experiment, grew, and treated the plant material and provided the samples for the monosaccharide analysis, performed the Raman spectroscopy.

Moirangthem K. - Division of Nutritional Sciences, University of Nottingham, UK - Performed the monosaccharide analysis on plant root material.

Rance G. – Nottingham Nanoscale and Microscale Research Center, University of Nottingham, UK - Guidance to optimise and perform the Raman spectroscopic analysis

6.1. Introduction

Plant cell walls have evolved in their structure and composition to fit specific roles in the diverse plant kingdom. The sessile nature of plants requires them to have strong defense mechanisms to deal with animal, fungal, bacterial and viral attack and the plants have evolved a rigid polysaccharide support in the form of a cell wall, that provides shape, tensile strength and protection to the plant and also helps the cell develop turgor pressure to maintain the pressure of the cell contents. Due to the added complexity introduced by the presence of a rigid cell wall, the process of cell division and expansion in plants is mechanistically very different from that observed in animal cells. These processes require dynamic remodeling of cell wall which is an interplay between loosening of existing wall components accompanied by addition of newly synthesised components to the growing wall.

In **Chapter 4** we showed that *EXPA1* is important for maintenance of pericycle cell size in an auxin-dependent manner for organised asymmetric cell divisions during lateral root initiation. The *expa1-1* mutants display radially expanded cells with a transitionary defect in the kinetics of lateral root primordia initiation and in the structure of Stage I primordia. In this chapter, we explore the possibility that the defects observed are due to loss in the dynamic wall remodelling property that is characteristic of expansins. The 'acid-growth' theory points to the importance of acidification (pH ~4.0 – 5.5) of the apoplastic space around the growing cells as a key requirement for activation of expansins (Hager et al., 1971; Cosgrove, 2005). Hence, we studied the remodeling of the cell wall in response to auxin treatment to gain a better understanding of the role of *EXPA1* in mediating changes to xylem pole pericycle cells.

To do this, we first adopted a crude approach where we analysed whole roots of the mutant to obtain a monosaccharide profile of the cell walls under normal growth and auxin induced growth condition. **Table 5.1** provides a general simplified % composition of the different polysaccharides and their monomeric constituents in dried primary cell wall of plants based on literature. These were the components that we were largely interested to analyse in this study. Following this, we probed then used the lateral root induction system described in **Chapter 4** to study cell size differences in the pericycle cell wall to induce lateral root formation, and probed for specific differences in the pericycle cell wall composition using confocal Raman microscopy. This would help us understand the defects in *expa1-1* are as a consequence of differences in the restructuring of the cell wall.

6.2. Results

6.2.1. Monosaccharide compositional analysis of whole roots of *Arabidopsis* by HPAEC-PAD

Combining the potential of expansins to be activated in acidic pH, as well as the rapid wall modification responses that auxin confers to cell wall, we chose to: i) Quantify the hydrolysis products of whole roots of wildtype and *expa1-1* as a first step to understand differences in the monosaccharide composition of the cell wall; ii) We then exposed the roots to auxin to trigger dynamic alterations to the structure of the cell wall and then analysed the treated roots in a similar manner for differences in monosaccharide composition. The profiling was performed using a modified protocol of Saeman hydrolysis (Saeman et al., 1945) to hydrolyse the roots that breaks down the cellulose and hemicellulose polymers of the cell walls from their bound complexes to monomeric sugars and analysed them using high performance anion exchange chromatography (HPAEC) with Pulsed Amperometric Detection (PAD). Different polysaccharides have different rates of degradation. For instance, microcrystalline cellulose requires stronger hydrolysis, the xylose yield declines after an hour of hydrolysis while the glucose peaks after 2 hours (Bittner et al., 1989). Hence, we used sulphuric acid in a two-step hydrolysis process (Saeman et al., 1945) with treatment for two different concentration of acid, durations and temperatures to ensure hydrolysis of the majority of the wall components into their monomer sugar units for detection. After hydrolysis, the sample is diluted (1:100 in 10mM NaOH) and the monosaccharides are separated by HPAEC and detected by PAD. The degradation of arabinose and

galactose monomers in the hydrolysis process was corrected for with correction factor based on estimated % recovery of standard sugars (**Figure 6.1.**).

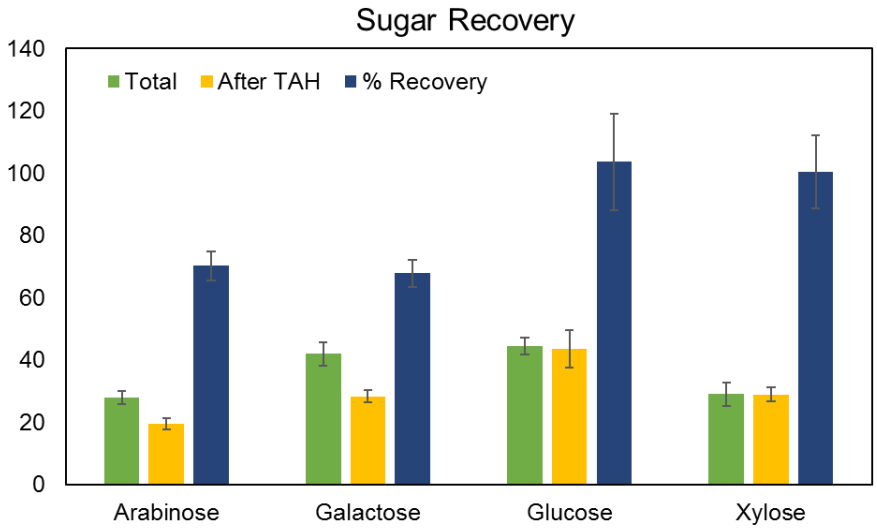


Figure 6.1. Estimation of recovery of sugars following total acid hydrolysis (TAH). (Values represent ±SD, n=6)

6.2.1.1. *expa1-1* roots exhibit reduced levels of galactose compared to wildtype

The monomeric sugar profile of 7DPG whole roots of Col 0 revealed that glucose was the most abundant monomer in the primary walls of the roots followed by galactose, arabinose and xylose (**Figure 6.2.**). In order to identify if the mutation in *EXPA1* affected the composition of the cell wall we compared the monosaccharide profile of *EXPA1* with wildtype. This revealed that the glucose monomer levels in *expa1-1* were similar to that of wildtype. However, the galactose composition was significantly reduced in *expa1-1* (**Figure 6.2.**), while the composition of arabinose and xylose remained unchanged.

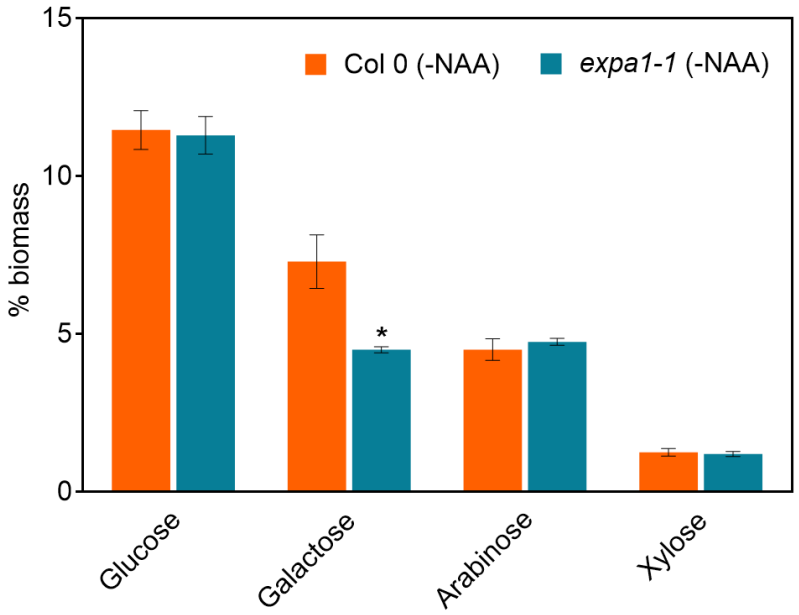


Figure 6.2. Representative graph of 2 biological replicates of monosaccharide profiling of 10DPG roots of Col 0 and *expa1-1*. Graph represents ±SE; *p<0.01; (n=2)

6.2.1.2. Auxin treatment induces alterations in composition of cell walls of *Arabidopsis* roots

Time course studies of auxin-induced changes in wall composition were performed by exposing 7DPG roots of Col 0 and expa1-1 to 10µM NAA (1-napthaleneacetic acid) treatment for 6hrs. The concentration of auxin and duration of treatment were maintained to match the conditions applied in the lateral root induction system for pericycle cell size measurements (as described in **Chapter 4**). Analysis of the monosaccharide profile upon auxin treatment revealed that glucose remained the abundant monosaccharide in the cell wall of wildtype roots, followed by galactose, arabinose and xylose. The % composition of glucose in the roots was significantly reduced in the auxin treated roots when compared to the untreated (**Figure 6.3.**). In *expa1-1*, the levels of glucose remained unchanged upon auxin treatment. However, the galactose levels were significantly increased in the treated roots of *expa1-1* compared to untreated (**Figure 6.3.**). On comparing the differences induced by auxin on wall composition of wildtype and *expa1-1*, we observed that the glucose levels of wildtype roots were significantly lower than *expa1-1* (**Figure 6.4.a**). This can also be viewed as an absence of change in the glucose levels in *expa1-1* upon auxin treatment. With respect to the galactose levels, we observe that the auxin treatment restores the galactose composition in *expa1-1* to the wildtype levels (**Figure 6.4.b**).

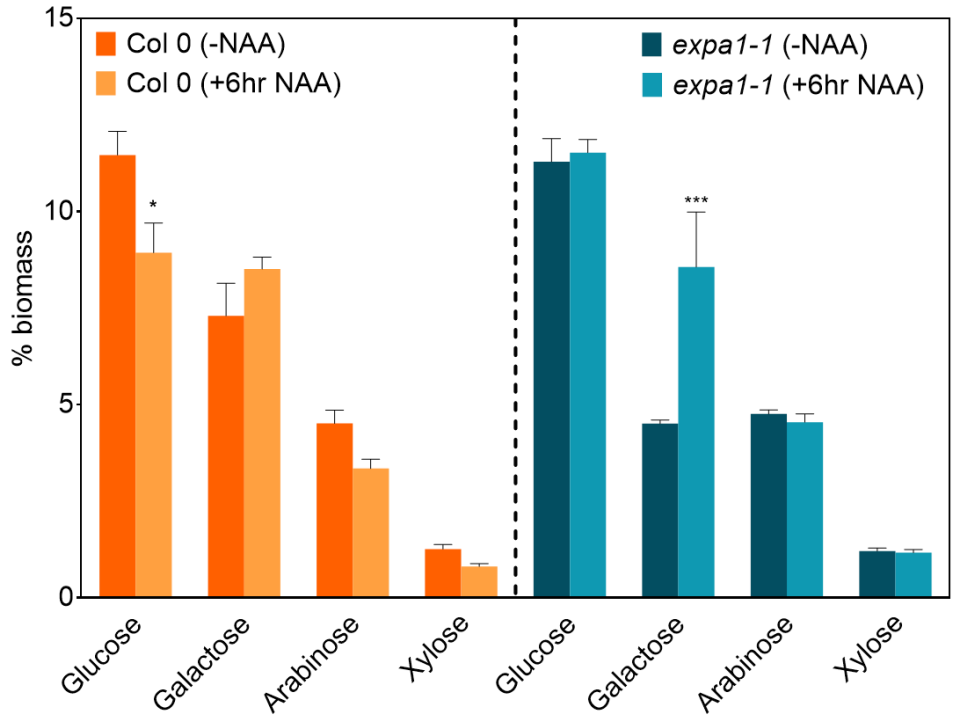


Figure 6.3. Monosaccharide composition profile of 10DPG Col 0 and *expa1-1* roots under untreated (-NAA) and post 10µM NAA treatment (+6hr NAA) conditions. Graphs represent ±SE; *p<0.01; ***p<0.0001; n=2.

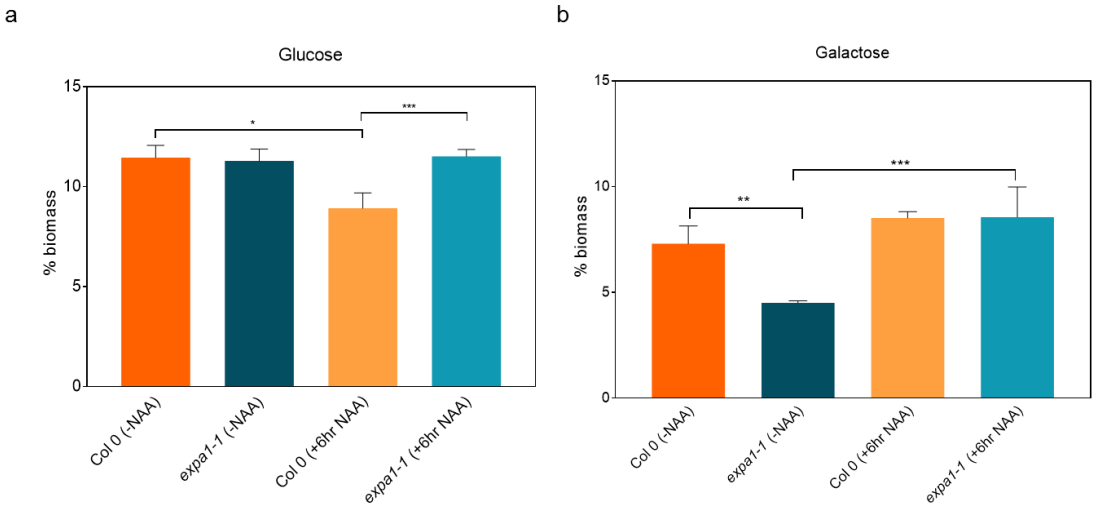


Figure 6.4. Composition of Glucose (a) and Galactose (b) in 10DPG roots of Col 0 and *expa1-1* under untreated (-NAA) and post 10µM NAA treatment (+6hr NAA) conditions. Graphs represent ±SE; *p<0.01; **p<0.001, ***p<0.0001; n=2.

6.2.2. Chemical analysis of pericycle cell wall composition of *expa1-1* by confocal Raman microscopy

To obtain a better understanding of the role of *EXPANSINA1* in modification of cell wall architecture in the specialised xylem pole pericycle cells of the roots, we performed confocal Raman spectroscopy on adjacent pericycle cell wall junctions of the mutant *expa1-1* and compared for differences with the control (**Figure 5.5**).

The growth set-up described previously (**Section 4.2.6.**) for the pericycle cell measurement was used for consistency in the analysis conditions. The same was repeated for roots that were induced on 10µM NAA and analysed for differences post treatment. Point spectra of two distinct points at the junction between adjacent xylem pole pericycle cells were acquired and compared for differences in spectral band intensities and abundance. The spectral peaks for each line and treatment were compared for consistency in spectral pattern and reproducibility of peaks in the different replicates and these were then averaged out to study for differences in spectral peaks.

Due to background fluorescence in the root sample and the fluctuations in the bands at low wavenumbers we were unable to get distinct spectra for the region below 1000 cm^{-1}. Several of the distinct bands for pectin have been reported in the 200-900 cm^{-1} region especially one at 854 cm^{-1}. This was a drawback in our analysis as we anticipated differences in the pectin levels in the cell walls from our monosaccharide profile analysis. However, there have been some reports with bands in the spectral range our analysis was performed in (1000-3600 cm^{-1}) and we have interpreted our results based on this.

6.2.2.1. Chemical composition of root xylem pole pericycle cell wall

First, we compare the composition of the pericycle cell wall in wildtype Col 0 roots and *expa1-1* under untreated conditions to see if there were inherent differences. **Figure 6.6** represents the differences in the Raman spectra of the pericycle cell wall junction before treatment. The characteristic peaks assigned to reference pure compounds from literature (**Figure 5.4**) was evident at some points such as 1122 and 1378 cm^{-1} for cellulose, 1256 and 1465 cm^{-1} for xylogucans, 1420 and 2948 cm^{-1} that corresponds to pectin (**Table 5.2**). The region between 2820-2935 cm^{-1} are enriched with bonds that correspond to cellulose some of which overlaps with xyloglucans and therefore difficult to resolve and assign to a specific compound. Overall on comparison, there are no striking differences between the mutant *expa1-1* and wildtype. The slight difference in profile that we observe may be due to differences from altered interactions in the polysaccharide wall. Although, it is difficult to interpret this without more detailed chemometric analysis.

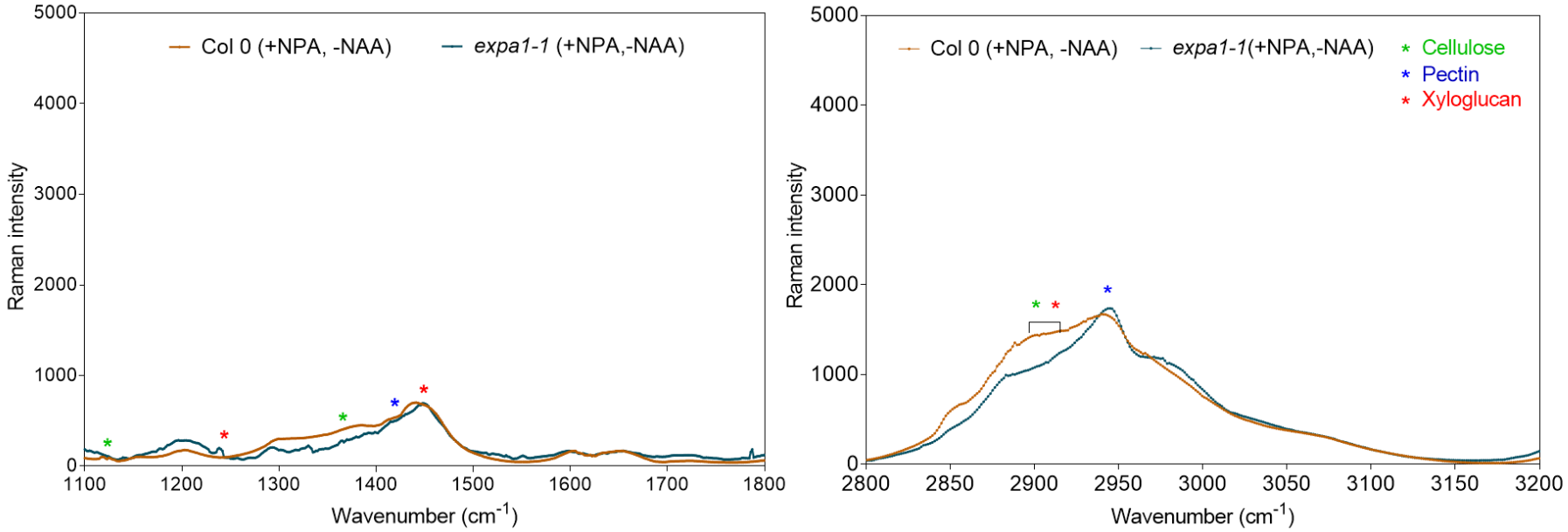


Figure 6.6. Average Raman spectrum at the xylem pole pericycle cell junction of Col 0 and *expa1-1* roots under untreated conditions (i.e. 10µM NPA grown). Spectra split into the range 1100-1800 cm^{-1} and 2800-3200 cm^{-1} to eliminate noise from glass slide and D_2O. The asterix are color coded corresponding to the compound that has a distinct spectral band assigned to the wavenumber from literature. (n=4 roots/line, graph represent average of all roots).

6.2.2.2. Auxin induced differences in composition of root xylem pole pericycle cell wall

To keep in line with the analysis on effect of auxin on pericycle cell expansion and the effect on the alterations in the wall of the mutant *expa1-1* we then compared the untreated roots to the ones post 6hr auxin induction (10µM NAA). Upon auxin treatment in the wildtype roots we observe that there are strong differences in the intensities of the Raman bands (**Figure 6.7**). The peaks show a uniform increase in their intensity accompanied by appearance of new distinct peaks that are unassigned to any particular compound. There is an increase in intensity of the band at 1420 cm^{-1} and 1456 cm^{-1} that related to pectins and xyloglucans respectively, suggesting alterations in their composition in the wall. The most striking feature is the pattern and modifications in the intensity levels of cellulose and hemicellulose (xyloglucan) overlapping region between 2820-2935 cm^{-1} along with the band that relates to pectin at ~2948 cm^{-1}. The change in the pattern of the spectra and peaks of the bands suggest strong modifications by differences in the levels of pectins, cellulose and xyloglucans in the wall.

We then compared the differences in band intensities of *expa1-1* relative to the levels in wildtype upon treatment (**Figure 6.7**). The treated *expa1-1* roots show a similar spectral profile to wildtype. However, the intensity of the peaks was reduced and the mutants do not see the same strong level of changes in the intensity of the peaks. The striking differences observed in the wildtype in the region between 2820-2935 cm^{-1} corresponding to cellulose and xyloglucan and the shift in the pectin band at ~2948 cm^{-1} was partially distinguishable.

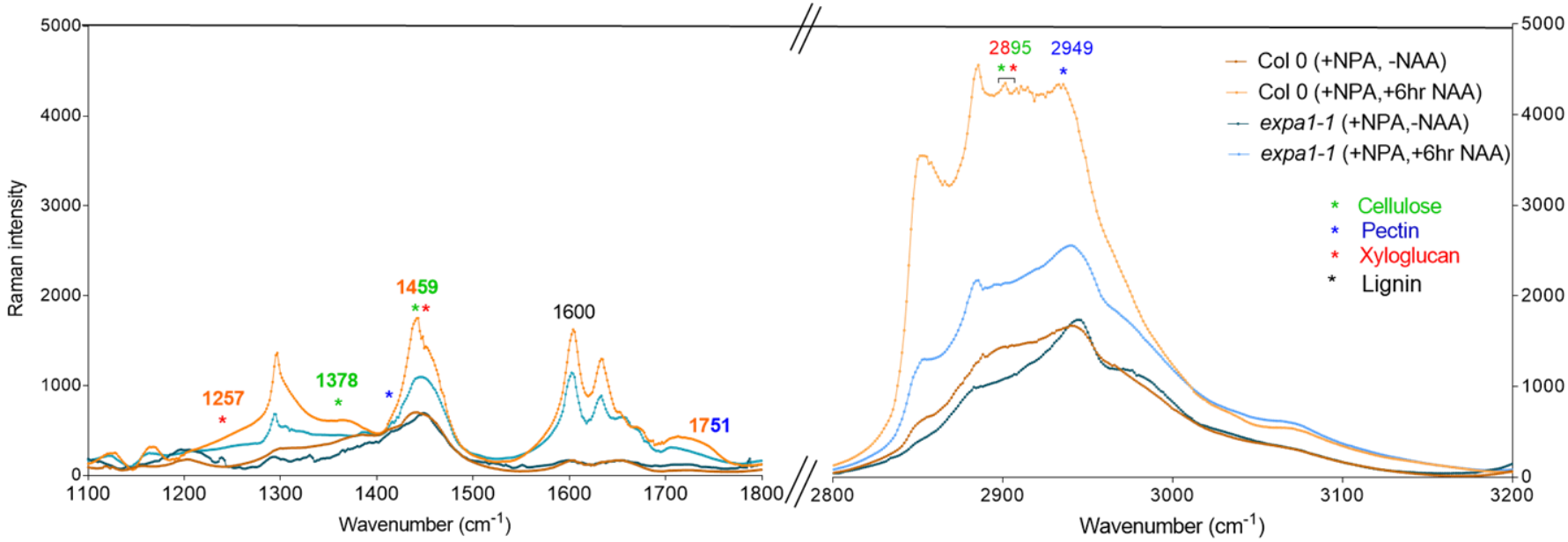


Figure 6.7. Average Raman spectrum at the xylem pole pericycle cell junction of Col 0 and *expa1-1* roots under untreated (i.e. 10µM NPA grown) and post 6hr 10µM NAA treatment condition. Spectra between 1800-2800 cm^{-1} spans the reference spectra from D_2O and was used for normalization of all the spectra. The asterix are color coded corresponding to the compound that has a distinct spectral band assigned to the wavenumber from literature. (n=4 roots/line, graph represent average of all roots).

6.3. Discussion

The cell wall structure and its organisation has a strong influence on the growth and development of cells and regulation of cellular processes. This is reflected in a number of cell wall mutants that display alterations in cell morphology and related developmental processes (Roudier et al., 2005; Cavalier et al., 2008; Park and Cosgrove, 2012; Xiao et al., 2016). **Chapter 4** describes the defects observed in *expa1-1* mutants and the importance of *EXPA1* for cell size maintenance and organised asymmetric cell divisions. In this chapter, we take the next step to understand the mechanism by which *EXPA1* brings about its regulatory effects. Expansins are known for their non-enzymatic wall loosening activity that is activated by acidic pH. They are thought to act on loadbearing biomechanical hotspots that are located at specific sites of the plant cell wall. These hotspots are characterised by an altered interaction of cellulose and xyloglucans that is thought to act as the buffer zone in the wall that provides the flexibility needed for rapid wall modifications (Cosgrove, 2014; Park and Cosgrove, 2015). In addition, according to the 'acid growth' theory, auxin-mediated apoplastic acidification is known to promote biomechanical modification of the cell wall (Hager et al., 1971; Loescher and Nevins, 1972). This has been hypothesised to be via activation of expansins to mediate cell wall loosening. It is however, unclear which of the two – auxin or acidification – has a preferential influence on the activation of expansins or there is the possibility that they may have independent means to activate expansins depending the type of modification required (rapid wall loosening responses) or the developmental process involved (signalling based organ development). Auxin is well known for its role

in lateral root initiation (Lavenus et al., 2013a) and hence, the most obvious choice of treatment to investigate the means by which *EXPA1* elicits its effect on the pericycle walls during lateral root initiation.

6.3.1. Monosaccharide profile and wall composition

First, we analysed the monomeric sugar content of the whole roots of *expa1-1* and wildtype Col 0 to evaluate if the mutation had any large-scale effects on the roots. Then we compared for difference and in the monomeric sugar content by stimulation of cell wall remodelling with auxin. The monomeric sugar composition analysis provides a monosaccharide profile of the hydrolysed plant cell walls with the help of a highly sensitive HPAEC-PAD to identify monomers. The profile provides an overview of the monomeric sugar composition of the roots from which we can deduce differences in composition of the cell wall. For our analysis, we focus on four main sugars – glucose, galactose, arabinose and xylose that form the basic building blocks of the most abundant polysaccharide of the primary cell wall. In this study, we used dried root material and hence we are able to estimate the relative amount of each sugar monomer that constitutes the wall biomass. The wall composition estimated from this analysis has been interpreted as being indicative of the sugar content and not absolute. This was to take into account the dynamic nature of the cell walls and polysaccharide structure variation from plant to plant.

Our data shows reduced levels of galactose in *expa1-1* which may be due to alterations in the pectin composition of the root cell walls (**Figure 6.2**). This is suggested by the higher levels of arabinose compared to xylose seen in the wildtype roots that suggest that the high galactose levels may be

contributed by pectin polysaccharide side chains rather than hemicelluloses, and this being altered in *expa1-1*. This idea could be strengthened by an assay on the Galacturonic acid levels in the wildtype and *expa1-1* roots to determine the pectin levels in the roots and help to understand the cause for the differences in galactose levels. Other sugars such as xylose and arabinose were also detected in the analyses, but did not show significant differences in their levels under our conditions. There were other unidentifiable and unresolved peaks in the chromatogram that could potentially constitute other cell wall sugar residues or other wall constituents (**Supl. Figure 6.2.**). However, for our study we restricted the analysis to the four major sugars – glucose, galactose, arabinose and xylose based on the standards we used for detection (**Supl. Figure 6.1.**).

Auxin is also known to increase the levels of galacturonic acid (Loescher and Nevins, 1972). Upon auxin treatment, we observed a drop in the glucose levels in the wildtype roots (**Figure 6.4.a**). The glucose levels in *expa1-1* however, remain unchanged. This suggests that the auxin treatment modifies the cell wall sugar composition largely via alterations to the glucose monomer based polysaccharides of the cell wall. These modifications are either absent or do not occur in the *expa1-1* roots, reflected by the unchanged glucose levels of *expa1-1* roots upon auxin treatment. Auxin has been known to have a two-step role in the cell wall remodelling process. It is known that auxin can cause:

i) **Rapid changes to the cell wall by apoplastic acidification that activates wall loosening agents like expansin to enable expansive growth (Rayle and Cleland, 1992)**

ii) The advanced response involves activation of cell wall synthesis machinery that leads to utilisation of glucose monomers to build the wall microfibrils

A 6hr treatment can be considered as sufficient duration to induce the cell wall synthesis machinery and cell cycle for division. This is reflected in the wildtype where we observe a drop in the glucose levels suggestive of utilisation of the monomers to synthesize a wall. It is important to bear in mind that these changes are at the level of whole roots and that different zone and tissues of the root would respond differently to the auxin treatment. If we consider our scenario of expansive growth of pericycle cells to accommodate asymmetric cell division, the pericycle cells are embedded deep within the primary root. Any specific effects that *EXPA1* might have in the pericycle especially during lateral root initiation would be diluted down in this assay of whole roots. The benefit of the monosaccharide profile is that it has provided a clue that expansin action may be related to the pectin distribution in the cell wall. To overcome the shortcoming of this assay regarding lack of tissue specificity, we employed confocal Raman microscopy, which is discussed in the following section.

Interestingly, auxin treatment restores the galactose levels in *expa1-1* to wildtype levels before treatment (**Figure 6.4 b**) which may reflect alterations in the pectin polysaccharides of the wall. Pectin are often considered the glue that holds the wall components together. It was reported that, suppression of both a polygalacturonase (that depolymerises pectin) and an expansin was shown to increase the firmness of tomato fruits (Powell et al., 2003). This suggests a link between auxin mediated expansin action and the state of pectins in the cell wall. It would be interesting explore the link between expansin and pectins in

maintenance of cell size and integrity by characterising some pectin mutants to analyse if they have defects with respect to root development.

6.3.2. Raman spectrum based differences in chemical composition of the pericycle cell wall

Raman imaging helps gain insight into the composition of the cell wall at targeted region of interest at high-spatial resolution, without the need to label or stain the sample. We were not able to uncover differences in the cell wall composition in wildtype and *expa1-1* mutants at the pericycle junction. On auxin treatment however, we were able to see strong differences in the cell wall polysaccharide composition. The spectra had many characteristic bands that were broadened when compared to the reference spectrum of the pure compounds (**Figure 6.6. and 6.7**). Expansins are known to cause alteration in the interactions of cellulose microfibrils with other wall components. These additional and broadened peaks could reflect auxin-induced interactions between cell wall polymers that deviate from the pure reference cell wall components. In addition, enhanced peak intensities in the regions enriched with bands for cellulose and pectin suggest an enrichment of these. It has been shown that the cell walls of the lateral root primordia are more methyl esterified than the ones of the overlying tissue and hence less easily degraded by pectin lyases (Laskowski et al., 2006). The expression of *EXPA1*, pectin methyl esterase (*PME1*), and the pectin lyases *PLA1* and *PLA2*, are upregulated during lateral root emergence under auxin treated conditions (Laskowski et al., 2006). Alterations in the methyl-esterification of pectins in the shoot apical meristem of Arabidopsis was shown to affect flower primordia formation and cause strong defects in phyllotactic pattern (Peaucelle et al., 2008). The altered

pectin bands in the Raman analysis of *expa1-1* suggest modification to the pectin levels that was induced upon auxin treatment. This is interesting as the active remodelling in the walls upon auxin treatment would require modification in the adhesive properties of the pericycle cell wall especially in the pectic polymers. This is reflected on the large-scale in the whole roots as well with the recovered galactose levels in *expa1-1* based on the monosaccharide profile. It is tempting to suggest that expansins may possibly play a role in altering the cell wall structure via changing in pectin levels. Oversimplification would be: Lower levels of pectin in *expa1-1* upon auxin treatment - less adhesive wall microfibrils - loss in cell wall strength - wider pericycle cells – perturbed asymmetric cell divisions. This could be tested by analysing the cell wall structure of pericycle cells. Additionally, pectin mutants such as the ones describe above *pla1, pla2, pme1* could be analysed for defects in lateral root formation. It would also be interesting to label the root sections with antibodies specific to different cell wall polymer epitopes to visualise their distribution in the root tissues.

Our data support the idea that *EXPA1* is important for the dynamic wall remodelling responses during lateral root development, and is triggered by a cue, which in this case was the auxin treatment. This suggests that the auxin dependent modification of the cell wall was reduced in the absence of *EXPA1* in the pericycle cell walls (**Figure 6.7**).

Single spectra and analysis of bands helped us understand the differences in molecular structure of the wall. However, this approach has its disadvantages when it came to hemicelluloses as it is unable to distinguish between cellulose and hemicellulose due to overlapping bands. A chemometric

analysis such as vertex component analysis (VCA) and/or multivariate cluster analysis might help to resolve the different components of the wall in greater depth (Gierlinger et al., 2012; Gierlinger, 2014). The multivariate analysis (MVA) is only possible for data sets e.g. maps, where there will be variability in the contribution of specific components to the resultant spectrum, rather than single point spectra. For single point spectra, we could attempt Classic Least Squares (CLS) analysis. However, for a good model, we would need to have reference spectra of all possible components in the cell wall, even those present in tiny quantities, which in a complex biological system is near impossible. The potential approach that this work can be extended to is to generate Raman maps of a larger area of the root section instead of point spectra. Similar mapping has been performed on cell wall of tomato fruits to study the polymer composition at the cell wall corners (Chylińska et al., 2014). This would help gain a broader picture of the changes across difference wall junctions. It would for instance, be interesting to study the difference between the pericycle and endodermal wall junction given the extensive remodeling of the endodermis to accommodate an expanding pericycle that develops into a primordium.

It may be that expansins are regulated at atleast two levels: First, auxin induces the expression of *EXPA1*. Second, EXPANSINs are activated by acidification. This acidification in the cell wall is induced by auxin carriers, which are polarly localised in the plasma membrane. This leads to polar cell wall acidification and subsequent polar cell expansion. This could be explored further by crossing auxin transport markers such as PIN3 into the mutant and study the directionality of auxin transport during lateral root initiation (Swarup et al., 2008a; Peret et al., 2013).

6.4. Materials and methods

6.4.1. Sample preparation for hydrolysis

7DPG seedlings of Col 0 and *expa1-1* grown on 1/2MS and grown at 22 °C under continuous light condition (150 µmol m^{-2} s^{-1}) were used for this analysis. For auxin treatment, the 7DPG seedlings were treated with 10µM NAA in liquid 1/2MS medium for 6 hours followed by five washes in distilled water. The samples were then separated into leaf fractions by cutting them at the base of the hypocotyl and into root fraction. These fractions were air dried at 37^0C for two days and subject to sugar composition analysis.

6.4.2. Saeman hydrolysis

30mg of tissue post drying was subject to a modified protocol of Saeman hydrolysis (Saeman et al., 1945). 12M sulphuric acid (1 ml) was added to 30mg of sample and incubated for 1 hour at 37°C. This was then diluted with 11ml MilliQ® water and incubated for a further 2 hours at 100°C.

6.4.3. HPAEC-PAD

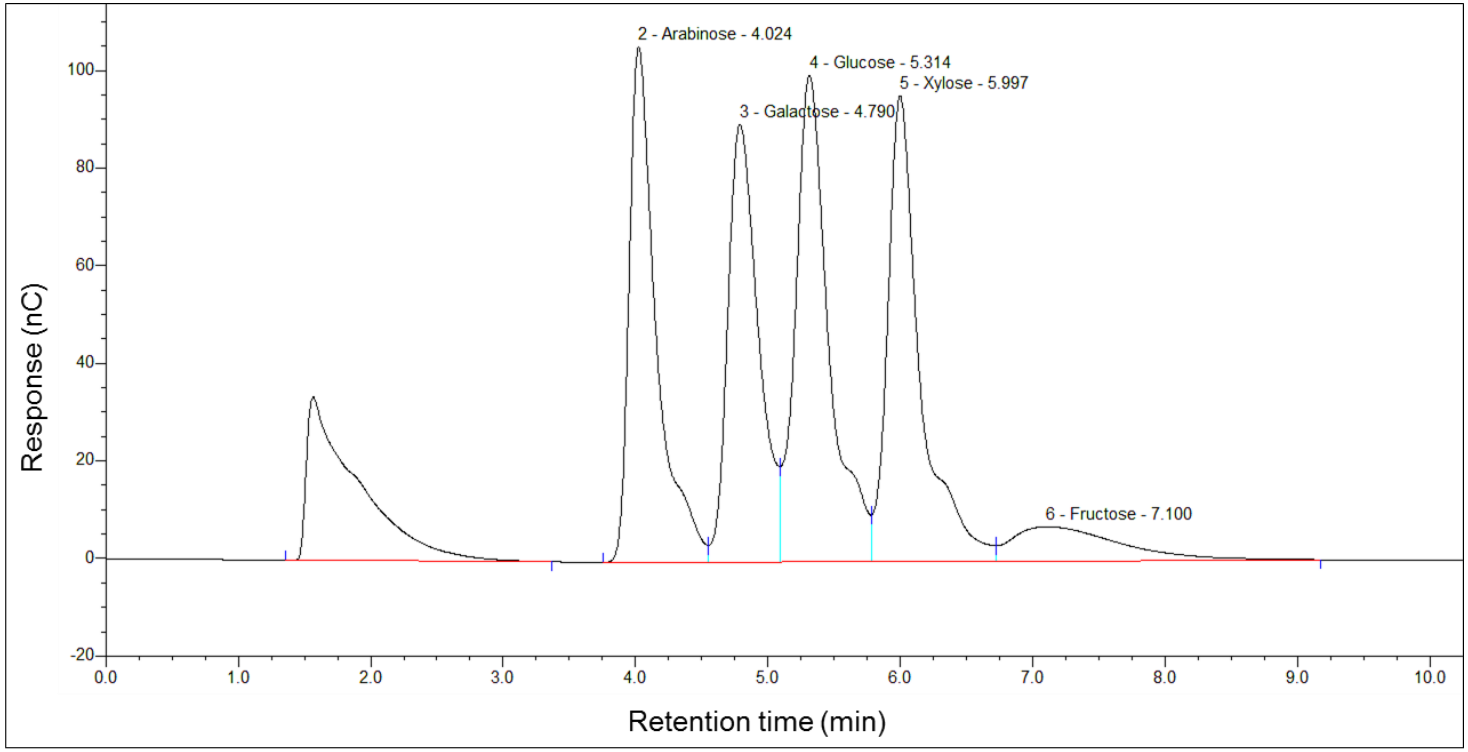
The hydrolysate was analysed with High-Performance Anion Exchange Chromatography (HPAEC) (Dionex® ICS-3000) comprised of a high-pressure GD 50 gradient pump, an analytical column (Carbopac® PA20, 4mm×250 mm) and a pulsed amperometric detector (PAD). 10mM NaOH was used as the mobile phase and the column was flushed with 200mM NaOH between runs. All chromatographic analyses were carried out at 30°C with a flow rate of 1.0mLmin^{-1}. Samples were diluted 1:100 in 10mM NaOH and centrifuged at

4472G for 10 minutes before loading to Dionex® vials. Sugar standards ranged from 0.250 to 2 g L^{-1} of arabinose, galactose, glucose and xylose.

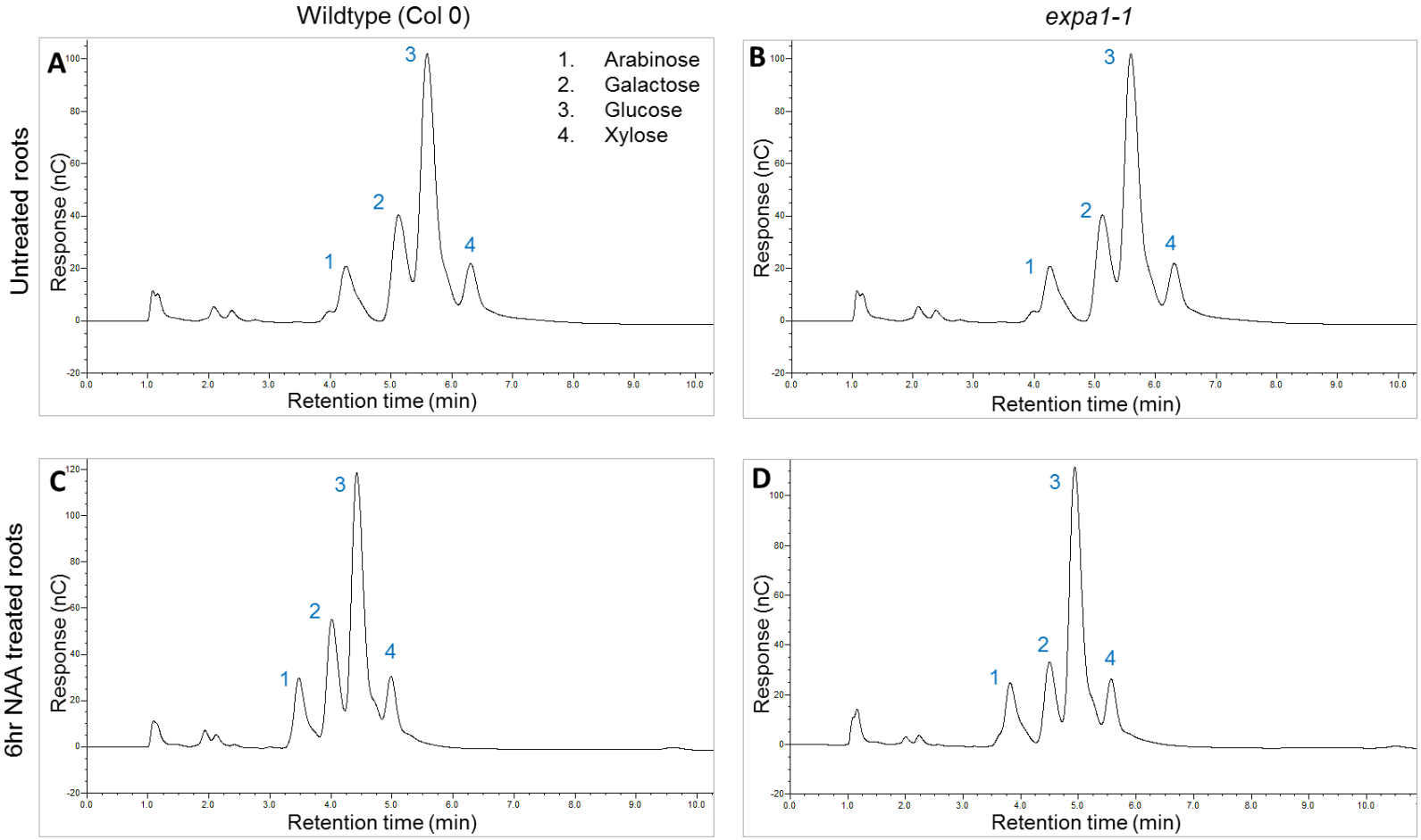
6.4.4. Confocal Raman microscopy

The optimised method and analysis are described in full detail in **Chapter 6**.

6.5. Supplementary figures



Supplementary figure 6.1. Chromatogram of monomeric sugar standards analysed by HPAEC-PAD analysis.



Supplementary figure 6.2. Representative chromatogram of the separated sugars in untreated wildtype Col 0 (A) and *expa1-1* mutant (B); 6hr 10µM NAA treated roots of Col 0 (c) and *expa1-1* (D).

6.6. References

Cavalier, D.M., Lerouxel, O., Neumetzler, L., Yamauchi, K., Reinecke, A., Freshour, G., Zabotina, O.A., Hahn, M.G., Burgert, I., Pauly, M., Raikhel, N.V., and Keegstra, K. (2008). Disrupting two Arabidopsis thaliana xylosyltransferase genes results in plants deficient in xyloglucan, a major primary cell wall component. Plant Cell **20,** 1519-1537.

Chylińska, M., Szymańska-Chargot, M., and Zdunek, A. (2014). Imaging of polysaccharides in the tomato cell wall with Raman microspectroscopy. Plant Methods **10,** 1-9.

Cosgrove, D.J. (2005). Growth of the plant cell wall. Nat Rev Mol Cell Biol **6,** 850-861.

Cosgrove, D.J. (2014). Re-constructing our models of cellulose and primary cell wall assembly. Curr Opin Plant Biol **22,** 122-131.

Gierlinger, N. (2014). Revealing changes in molecular composition of plant cell walls on the micron-level by Raman mapping and vertex component analysis (VCA). Frontiers in Plant Science **5,** 306.

Gierlinger, N., Keplinger, T., and Harrington, M. (2012). Imaging of plant cell walls by confocal Raman microscopy. Nature protocols **7,** 1694-1708.

Hager, A., Menzel, H., and Krauss, A. (1971). [Experiments and hypothesis concerning the primary action of auxin in elongation growth]. Planta **100,** 47-75.

Laskowski, M., Biller, S., Stanley, K., Kajstura, T., and Prusty, R. (2006). Expression profiling of auxin-treated Arabidopsis roots: toward a molecular analysis of lateral root emergence. Plant Cell Physiol **47,** 788-792.

Lavenus, J., Goh, T., Roberts, I., Guyomarc'h, S., Lucas, M., De Smet, I., Fukaki, H., Beeckman, T., Bennett, M., and Laplaze, L. (2013). Lateral root development in Arabidopsis: fifty shades of auxin. Trends Plant Sci.

Li, Z.-C., Durachko, D., and Cosgrove, D. (1993). An oat coleoptile wall protein that induces wall extension in vitro and that is antigenically related to a similar protein from cucumber hypocotyls. Planta **191,** 349-356.

Loescher, W., and Nevins, D.J. (1972). Auxin-induced Changes in Avena Coleoptile Cell Wall Composition. Plant Physiology **50,** 556-563.

McQueen-Mason, S.J., and Cosgrove, D.J. (1995). Expansin mode of action on cell walls. Analysis of wall hydrolysis, stress relaxation, and binding. Plant Physiol **107,** 87-100.

Park, Y.B., and Cosgrove, D.J. (2012). Changes in cell wall biomechanical properties in the xyloglucan-deficient xxt1/xxt2 mutant of Arabidopsis. Plant Physiol **158,** 465-475.

Park, Y.B., and Cosgrove, D.J. (2015). Xyloglucan and its interactions with other components of the growing cell wall. Plant Cell Physiol **56,** 180-194.

Peaucelle, A., Louvet, R., Johansen, J.N., Höfte, H., Laufs, P., Pelloux, J., and Mouille, G. (2008). Arabidopsis Phyllotaxis Is Controlled by the Methyl-Esterification Status of Cell-Wall Pectins. Current Biology **18,** 1943-1948.

Peret, B., Middleton, A.M., French, A.P., Larrieu, A., Bishopp, A., Njo, M., Wells, D.M., Porco, S., Mellor, N., Band, L.R., Casimiro, I., Kleine-Vehn, J., Vanneste, S., Sairanen, I., Mallet, R., Sandberg, G., Ljung, K., Beeckman, T., Benkova, E., Friml, J., Kramer, E., King, J.R., De Smet, I., Pridmore, T., Owen, M., and Bennett, M.J. (2013). Sequential induction of auxin efflux and influx carriers regulates lateral root emergence. Mol Syst Biol **9,** 699.

Powell, A.L.T., Kalamaki, M.S., Kurien, P.A., Gurrieri, S., and Bennett, A.B. (2003). Simultaneous Transgenic Suppression of LePG and LeExp1 Influences Fruit Texture and Juice Viscosity in a Fresh Market Tomato Variety. Journal of Agricultural and Food Chemistry **51,** 7450-7455.

Rayle, D.L., and Cleland, R.E. (1992). The Acid Growth Theory of auxin-induced cell elongation is alive and well. Plant Physiol **99,** 1271-1274.

Roudier, F., Fernandez, A.G., Fujita, M., Himmelspach, R., Borner, G.H., Schindelman, G., Song, S., Baskin, T.I., Dupree, P., Wasteneys, G.O., and Benfey, P.N. (2005). COBRA, an Arabidopsis extracellular glycosyl-phosphatidyl inositol-anchored protein, specifically controls highly anisotropic expansion through its involvement in cellulose microfibril orientation. Plant Cell **17,** 1749-1763.

Saeman, J.F., Bubl, J.L., and Harris, E.E. (1945). Quantitative Saccharification of Wood and Cellulose. Industrial & Engineering Chemistry Analytical Edition **17,** 35-37.

Swarup, K., Benkova, E., Swarup, R., Casimiro, I., Peret, B., Yang, Y., Parry, G., Nielsen, E., De Smet, I., Vanneste, S., Levesque, M.P., Carrier, D., James, N., Calvo, V., Ljung, K., Kramer, E., Roberts, R., Graham, N., Marillonnet, S., Patel, K., Jones, J.D.G., Taylor, C.G., Schachtman, D.P., May, S., Sandberg, G., Benfey, P., Friml, J., Kerr, I., Beeckman, T., Laplaze, L., and Bennett, M.J. (2008). The auxin influx carrier LAX3 promotes lateral root emergence. Nat Cell Biol **10,** 946-954.

Xiao, C., Zhang, T., Zheng, Y., Cosgrove, D.J., and Anderson, C.T. (2016). Xyloglucan Deficiency Disrupts Microtubule Stability and Cellulose Biosynthesis in Arabidopsis, Altering Cell Growth and Morphogenesis. Plant Physiology **170,** 234-249.

Chapter 7. A role for *bHLH49* in *Arabidopsis* lateral root development

7.1. Introduction

Transcription factors (TF) have long been known as important regulators of cell identity and differentiation as shown by several studies. For example in *Arabidopsis thaliana* SHORTROOT (SHR) controls of radial patterning and maintenance of stem cells in the root meristem (Nakajima et al., 2001); CAPRICE (CPC) regulates fate determination of hair-forming cells (Wada et al., 2002);DEFICIENS (DEF) and GLOBULOSA (GLO) control organ identity in the flower (Perbal et al., 1996). These are a just a few examples of many that point at the importance of TFs as key regulators that control the on/off switch of cellular programs in the plants at the right time, and at the right place to pattern developing organs. We were interested in transcription factors that potentially play a role in asymmetric cell division and cell identity establishment in lateral root development.

A previous studies identified key regulatory components that control asymmetric cell division during lateral root initiation by transcript profiling of Fluorescent Assisted Cell Sorting (FACS) of pericycle cells that were induced with auxin to initiate lateral roots (De Smet et al., 2008). bHLH49 was selected from a potential list of transcription factors that showed differential regulation upon auxin treatment. Interestingly, bHLH49 also came up in a Yeast One Hybrid screen on the promoter of *RAPID ALKALINISATION FACTOR LIKE 34* (*RALFL34*), that encodes a small signalling peptide shown to regulate formative cell division during lateral root initiation (Murphy et al., 2016). bHLH49 has also been suggested to dimerise with an antagonistic HLH factor, IBH1 that is a part of the transcriptional complex that activates *EXPANSIN1* (described in **Chapter 4** and **5**) to regulate cell elongation (Bai et al., 2012; Ikeda et al., 2012b). In this

chapter, we describe the follow-up studies on *bHLH49* as a transcriptional regulator and its potential role in lateral root development.

7.2. Results and discussion

7.2.1. *bHLH49* is specifically activated in the lateral root founder cells at primordia initiation

To investigate when and where *bHLH49* is expressed in root development, we examined the expression pattern in *Arabidopsis* lateral roots using a promoter fusion line *pBLHL49::nx3GFP* (kindly provided by T. Radoeva and D. Weijers). In order to visualise the exact developmental time point at which the expression if *bHLH49* is activated I used the lateral root bend assay where the seedlings are grown vertically for 3DPG followed by a 90^0 gravitropic stimulus that induces a lateral root on the outside of the bend (Péret et al., 2012). *bHLH49* transcripts were expressed in the small daughter cells of Stage I lateral root primordia after the first anticlinal asymmetric cell division (**Figure 7.1. a,b**). The gene continues to be expressed in the actively dividing cells of the lateral root primordia throughout its later stages of development as well in the cortical cells overlying the primordium (**Figure 7.1. d**).

Further to this, to investigate if the localisation of the translated bHLH49 protein matched the localisation of the transcript, we looked at the expression pattern of the translational fusion line *pBHLH49:BHLH49::sYFP* (kindly provided by T. Radoeva and D. Weijers) in the developing lateral roots. As expected, the protein was localised in nucleus and detected in the lateral root primordia (**Figure 7.2. a**). In addition, bHLH49 had a strong endodermal expression pattern along the length of the root (**Figure 7.2. b**).

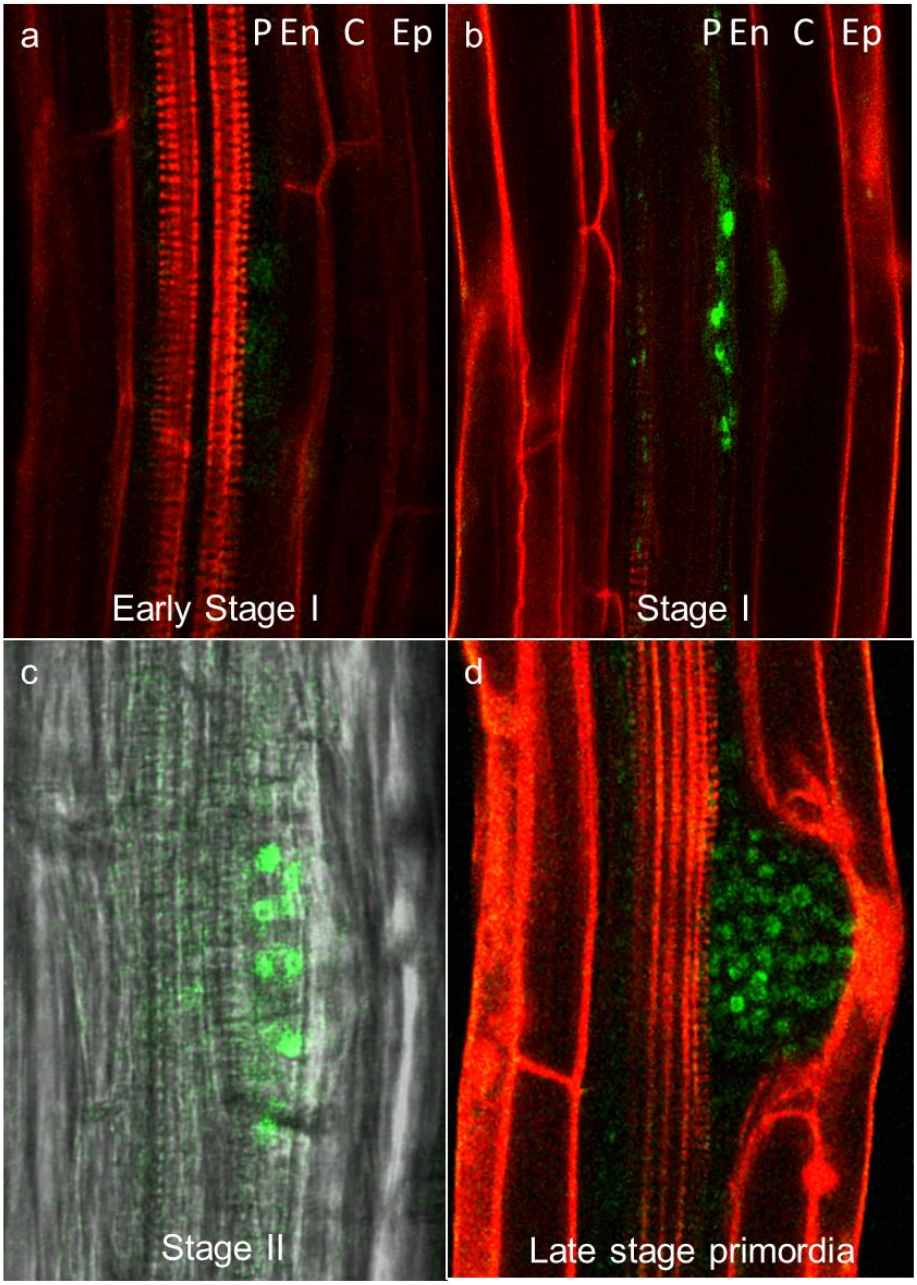


Figure 7.1. Expression profile of *pBHLH49::nx3GFP* visualised in the lateral root. Stage I (a,b), Stage II (c), and later stage primordia (d). P- Pericycle, En – Endodermis, C- Cortex and Ep -Epidermal cell layer. Cell walls visualised by Propidium Iodide staining (red).

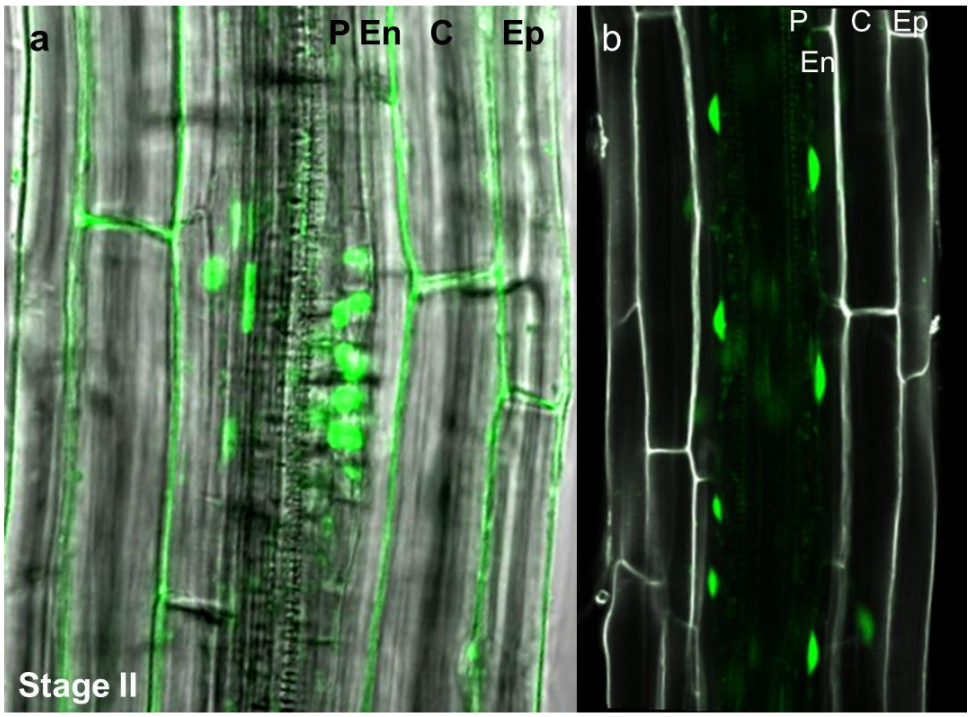


Figure 7.2. Expression profile of *pBHLH49:BHLH49::sYFP* (represented in green) visualised in the lateral root. Stage II (merged with bright field image) (a), and the strong endodermal expression (cell walls visualised by Propidium Iodide staining - represented in grey) (b). P- Pericycle, En – Endodermis, C- Cortex and Ep -Epidermal cell layer.

7.2.2. *bHLH49* is required during early stages of lateral root primordia formation

To determine the role of *bHLH49* in root development, I obtained a SALK T-DNA mutant line (named *bhlh49-1*) that was verified as a homozygous knock-out of *bHLH49* by qRT-PCR (**Figure 7.3. a**). On phenotyping the mutant for differences in primary root length and emerged lateral root density, we do not observe any significant differences in either (**Figure 7.3. c,d**). To investigate if the absence of a root development phenotype was due to redundancy from the large bHLH gene family, a double mutant with its close family homolog *bhlh76* (kindly provided by T. Radoeva and D. Weijers) was assessed. Phenotypic

analysis of the *blhl49,76* double mutant showed significant reduction in the primary root length and lateral root density (**Figure 7.3. e,f**). In contrast to *bHLH49*, *bHLH76* is only weakly expressed during lateral root initiation, induced during the first round of asymmetric cell divisions and then continues to be highly expressed, but weaker than *bHLH49*, throughout lateral root development and emergence (Voß et al., 2015; Figure. 7.1b). Taking into account the early presence of *bHLH49* transcripts during lateral root formation (**Figure 6.1.**), we employed the lateral root bend assay on the *bhlh49-1* mutant to test if this might help detect early initiation defects. Examination of *bhlh49-1* roots 18hrs post-bend showed a delay in the developmental progression of the lateral root primordia from Stage I to Stage II (**Figure 7.3. b**).

Additionally, we phenotyped an overexpressor line driven by *RPS5A* (*RIBOSOMAL PROTEIN S5A*) promoter that is strongly expressed in dividing cells (Weijers et al., 2001) - *pRPS5A::bHLH49* (kindly provided by T. Radoeva and D. Weijers) for differences in primary root length and lateral root density, but found no significant changes in either (**Figure 7.4. a,b**). The roots of the overexpressors were cleared and examined for morphological defects or differences in the distribution of the lateral root primordia. This showed that there were more early stage primordia (between stage I-III) distributed at more frequent intervals along the root compared to wild type as shown by the representative images in **Figure 7.4. c**. They were considered defective if observed within one visual field of a 40X objective. This suggests that bHLH49 may regulate the distribution of lateral roots along the root. However, this requires further quantification of the defect to confirm this.

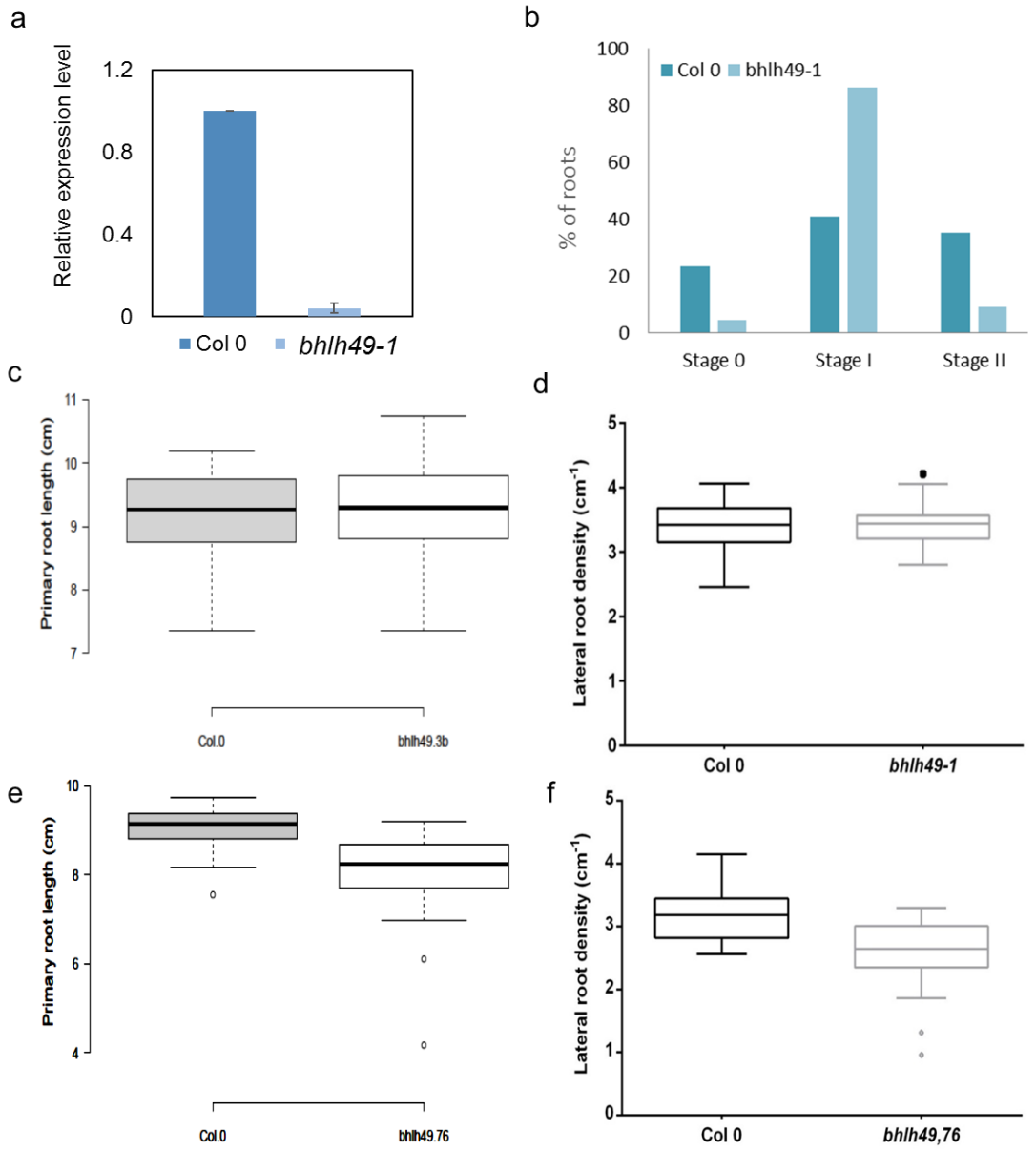


Figure 7.3. qRT-PCR that shows *bhlh49-1* as a knockout line (n=3; ±SE) (a); Lateral root bend assay of *bhlh49-1* (n=2) (b); Box plots that shows the distribution of primary root length (c) and lateral root density/cm of the root (d) in Col 0 and *bhlh49-1* (n=3), and double mutant *bhlh49,76* (n=2) (e,f).

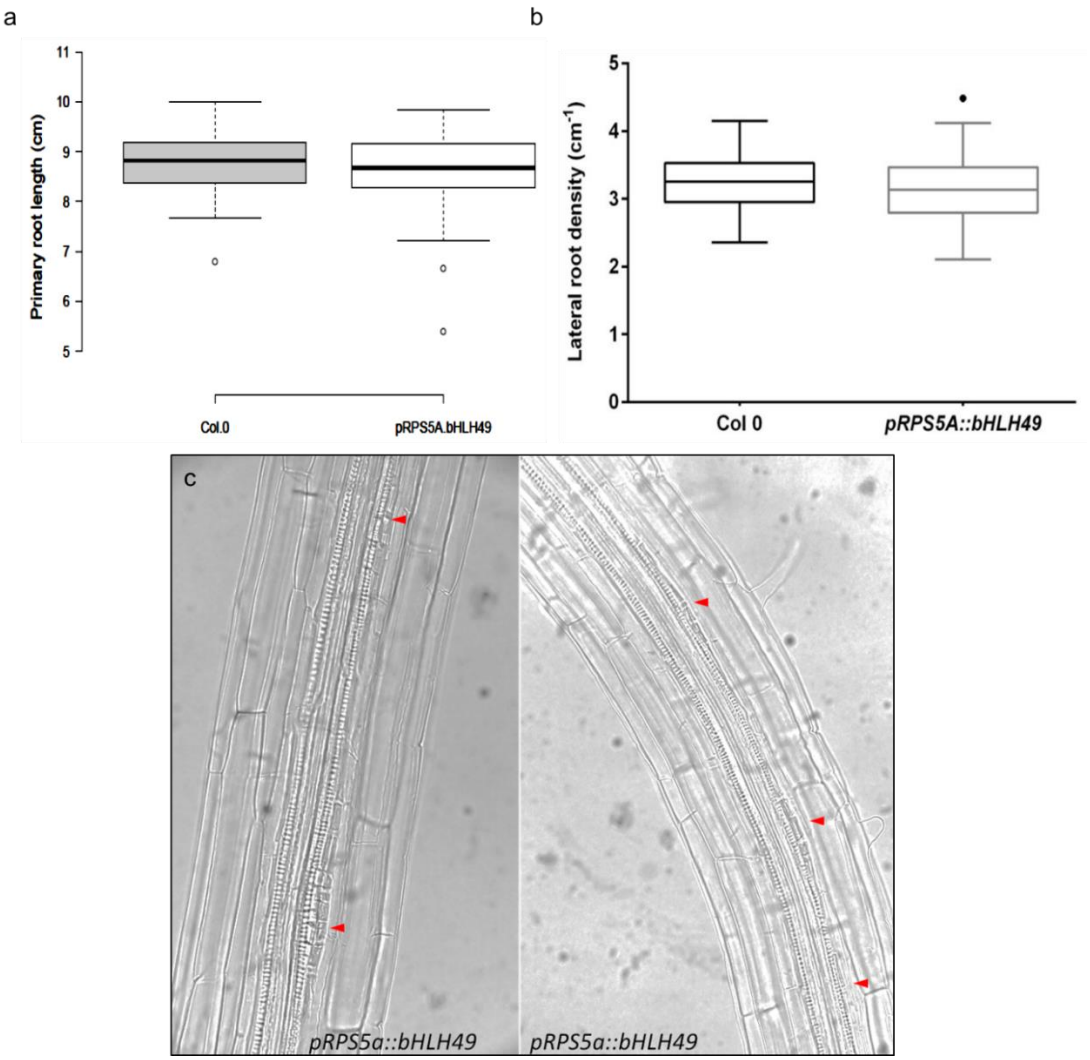


Figure 7.4. Box plots that show the distribution of primary root length (a) and lateral root density/cm of the root (b) in Col-0 and *pRPS5a::bHLH49* (n=2); Representative DIC images of close Stage I primordia and unusually positioned lateral roots in the overexpressor *pRPS5a::bHLH49* line (c). The red arrowhead indicates the points where lateral roots are observed.

7.2.3. Role of auxin in regulation of *bHLH49* and root growth

To study the role auxin in regulation of *bHLH49*, we conducted a time course of exogenous auxin treatment to determine if the expression of the genes was altered upon auxin treatment. We performed qRT-PCR to detect transcript level changes of *bHLH49* expression specifically in the roots following treatment with auxin (10µM NAA) after 0, 2, and 6hrs (**Figure 7.5. a**). *bHLH49* expression was downregulated within 2 hours of auxin treatment. The rapid downregulation within two hours suggested that the gene was directly regulated by auxin. The next step was to determine for certain if the down regulation was a direct, or and indirect effect of auxin. To test this, we used a protein synthesis inhibitor, cycloheximide (10µM CHX), in combination with auxin (10µM NAA) treatment and measured the *bHLH49* expression in the roots at 0, 2 and 6hr time post treatment. We observed the expected downregulation of *bHLH49* expression levels upon auxin treatment (**Figure 7.5. b**). The downregulation was lost when treated with the combination of both auxin and CHX. This suggests that *bHLH49* is a secondary auxin response gene, as its auxin induced repression is dependent on protein synthesis of an intermediate transcription factor. To determine if *bHLH49* functions downstream of the SLR/IAA14 pathway, we studied the expression levels of *bHLH49* in these auxin response mutant backgrounds. We observe that *bHLH49* expression is reduced in the auxin response mutants' background (**Figure 7.5. c**).

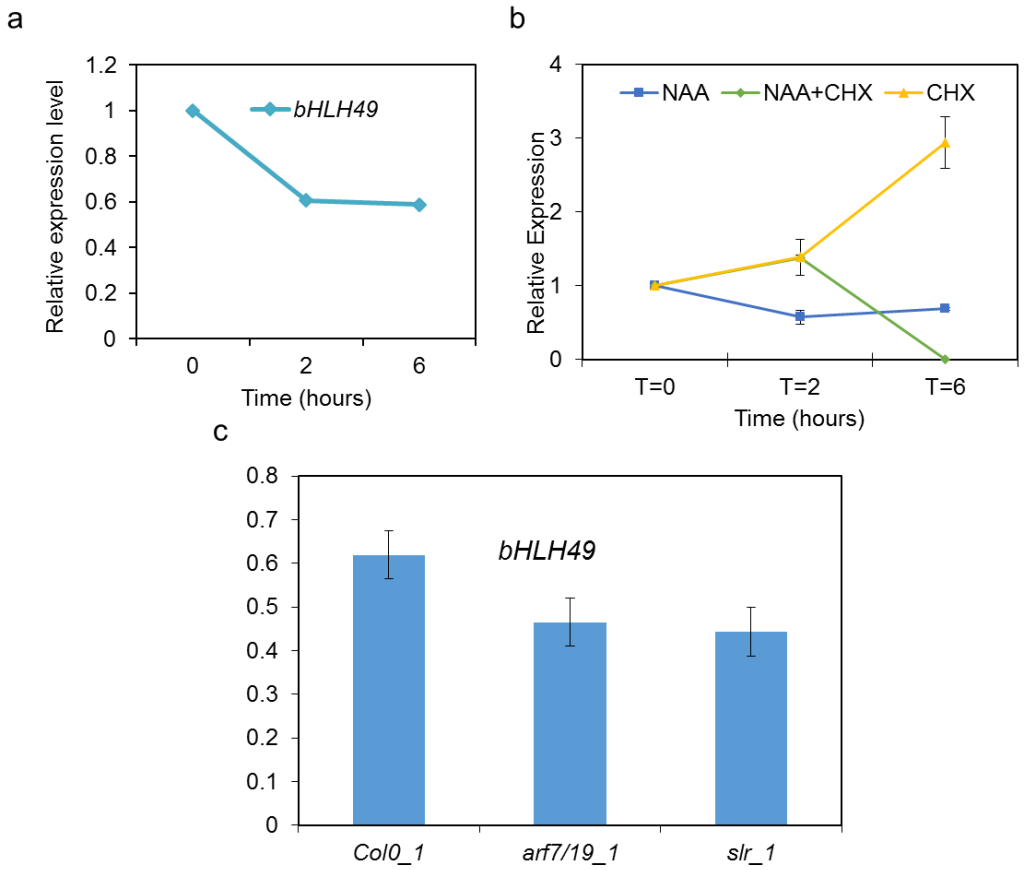


Figure 7.5. qRT-PCR of 3DPG Col-0 roots analysed for *bHLH49* levels. Auxin treatment response time series (a); Expression profile in response to 10µM NAA, 10µM CHX and NAA+CHX 0, 2 and 6 hours post induction (n=2, ±SE) (b); *bHLH49* expression in auxin response mutants (n=2, ±SE) (c).

7.2.4. *bHLH49* as a potential transcriptional regulator

To identify potential TFs that putatively interact with the *RALFL34* promoter, we performed a Yeast One Hybrid (Y1H) analysis of *RALFL34* (400bp) and *EXPA1* (1Kb) promoter with a stele enrich library of TFs that included pericycle cells (Gaudinier et al., 2011; Murphy et al., 2016). This provided a set of 27 transcription factors with the potential to bind to the *RALFL34* promoter (**Table 7.1.**). On comparing these candidates with FACS profiles of the above-mentioned transcriptomic dataset (De Smet et al., 2008), we chose the basic helix-loop-helix transcription factor bHLH49 (AT1G68920) for further functional characterisation. *bHLH49* was early down regulated in pericycle cells on auxin induction. *EXPA1* and *RALFL34* showed an opposite profile to *bHLH49* in this dataset suggesting bHLH49 might function as a repressor (De Smet et al., 2008) (**Figure 7.6. a**). In addition, *bHLH49* is highly expressed throughout the lateral root development process (Voß et al., 2015) (**Figure 7.6. b**). This suggested a potential role for *bHLH49* in regulation of lateral root initiation and development which we decided to explore further.

Table 7.1. List of genes identified by Yeast One Hybrid analysis of *RALFL34* (400bp) promoter (Murphy et al., 2016).

Accession no.	Gene Description	Promoter *RALFL34* 400bp
AT2G23290	ATMYB70 - Member of the R2R3 factor gene family.	
AT4G17460	HAT1, Encodes a class II HD-ZIP protein	
AT3G15210	ATERF4	
AT5G44210	ATERF9	
AT1G28370	ATERF11	
AT1G47870	E2FC	
AT1G68840	ATRAV2, EDF2, ETHYLENE RESPONSE DNA BINDING FACTOR 2	
AT5G51190	Encodes a member of the ERF subfamily B-3 of ERF/AP2 TF family.	
AT5G53290	CRF3, encodes a member of the ERF subfamily B-5 of ERF/AP2 TF family	
AT1G68920	BHLH49	
AT3G23030	IAA2	
AT1G04100	IAA10	
AT5G10510	PLT3 - PLETHORA 3	
AT1G56170	"NUCLEAR FACTOR Y, SUBUNIT C2", ATHAP5B	
AT1G51600	GATA28	
AT2G36930	zinc finger (C2H2 type) family protein	
AT3G57480	zinc finger (C2H2 type, AN1-like) family protein	
AT1G21910	DREB26 - DEHYDRATION RESPONSE ELEMENT-BINDING PROTEIN 26	
AT2G44730	Alcohol dehydrogenase transcription factor Myb/SANT-like family protein	
AT1G61730	DNA-binding storekeeper protein-related transcriptional regulator	
AT5G13790	AGL15 member of the MADS domain family of regulatory factors	
AT2G18060	Encodes a NAC-domain transcription factor, VND1	
AT4G28500	NAC domain containing protein 73, SND2	
AT3G54390	sequence-specific DNA binding transcription factors	
AT5G05610	AL1, Encodes a member of the Alfin1-like family of nuclear-localized PHD	
AT1G34370	ATSTOP1 -SENSITIVE TO PROTON RHIZOTOXICITY 1	

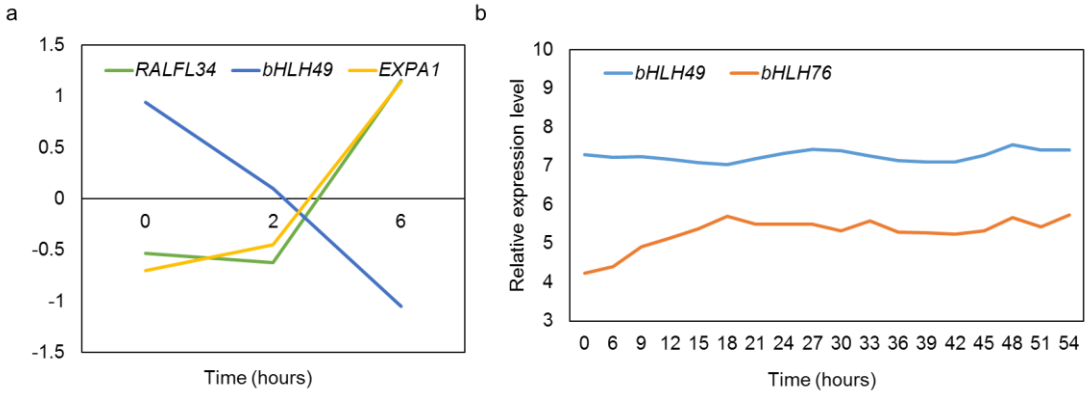


Figure 7.6. FACS profile of *bHLH49*, *RALFL34* and *EXPA1* from the transcript profiling dataset of pericycle cells induced by auxin to form lateral roots (De Smet et al., 2008) (a); Expression profile of *bHLH49* and *bHLH76* in lateral root transcriptomic time course dataset in log2 scale (Voß et al., 2015) (b).

7.2.5. bHLH49 mediated regulation of cell wall remodelling genes

The auxin-dependent downregulation of *bHLH49* (Figure 6.6. a) was a response that was also observed in *RALFL34* (Murphy et al., 2016). Given the contrasting FACS profile of *bHLH49* (**Figure 7.6. a**), and potential regulation of *RALFL34* suggested by Y1H analysis (**Table 7.1.**) we looked further into the ability of *bHLH49* to regulate two cell wall remodelling genes of our interest – *RALFL34* and *EXPA1.* We first performed *in silico* analysis of the two gene promoters (**Section 7.2.5.1**) followed by an *in planta* transient protoplast assay to study the nature of regulation (**Section 7.2.5.2.**).

7.2.5.1. *In silico* promoter analysis of *RALFL34* and *EXPA1* promoter

The DNA binding bHLH TFs are typically known to bind to either an E-box (5'-CANNTG-3') or G-box (5'-CACGTG-3') or a combination of these sequences on the promoter (Toledo-Ortiz et al., 2003). It has been suggested that presence of more than two E-boxes or at least one E-box and one G-box increases the probability of a bHLH interaction with the given promoter. Both *RALFL34* and *EXPA1* promoters were screened for presence of E-box and G-box sequences. Screening the 2.1Kb promoter of *EXPA1* showed the presence of 8 E-box sites and 1 G-Box (**Figure 7.7. a**). Screening the 1.2Kb *RALFL34* promoter showed presence of 5 E-box sites and absence of G-box sites (**Figure 7.7. b**). This suggest both promoters are targeted by bHLH transcription factors.

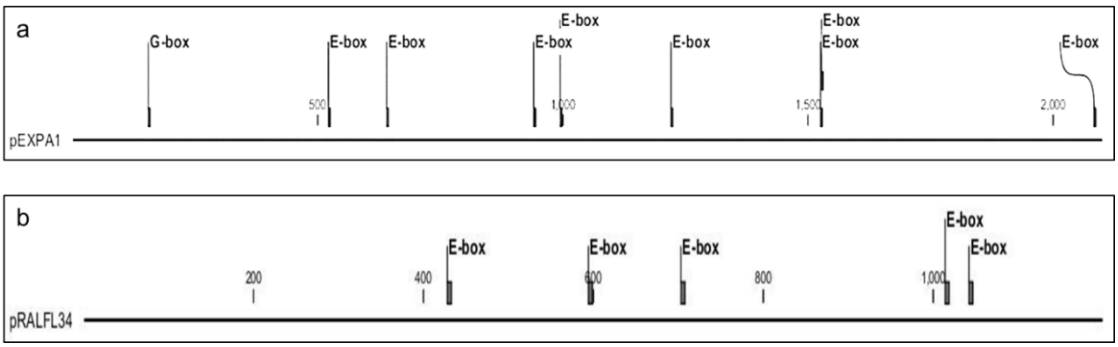


Figure 7.7. *In silico* promoter analysis of *EXPA1* (2.1Kb) and *RALFL34* (1.2Kb) promoter that marks the E-box and G-box sites generated using CLC Genomics Workbench, Qiagen.

7.2.5.2. Protoplast assay to test bHLH49 mediated regulation of *RALFL34* and *EXPA1*

To determine if bHLH49 is able to regulate *RALFL34* expression *in planta*, we performed an *in vivo* assay with a protoplast system which monitors gene expression quantitatively by activation of a luciferase (LUC) reporter (Lau et al., 2011; Vanden Bossche et al., 2013). The close phylogenetic homologue, *bHLH76* was included in the assay to take into account redundancy of the gene family and the possibility of dimerization necessary for an active regulatory machinery. The results show that was not able to induce expression of *pRALFL34::LUC* in this transient system (**Figure 7.8. a**). Also, no significant regulation of *pEXPA1::LUC* expression by bHLH49 and bHLH76 could be shown (**Figure 7.8. b**).

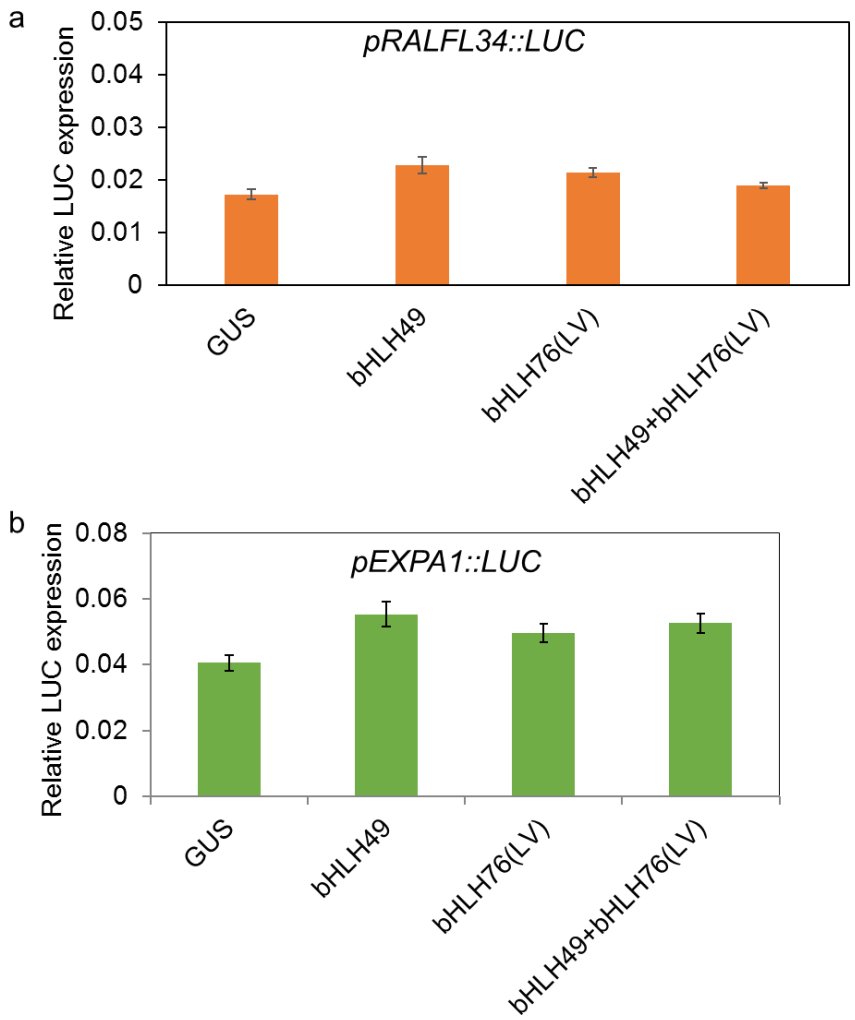


Figure 7.8. Luciferase (LUC) activity upon co-expression of *pRALFL34::LUC* and GUS (control) or bHLH49 in protoplasts (a) and the same for *pEXPA1::LUC* (b). Luciferase assay was performed three times, each time with eight biological replicates. The graph shows the average of all 24 data points ±SE.

7.3. Discussion

7.3.1. *bHLH49* and lateral root development

The lateral root associated expression of *bHLH49* suggests an early role for the gene in lateral root development (**Figure 7.1.**). Indeed, *bhlh49-1* displays a lateral root developmental delay in the early stages (Stage I to Stage II) and the *bhlh49,76* double mutant shows reduced lateral root density. In addition, the increased presence of early Stage I and Stage II primordia along the root in the overexpressor line suggests *bHLH49* is required for controlling positioning of the lateral root primordia along the root, possibly by repressing lateral root initiation. Further phenotyping of the *bhlh76* and *blhl49,76* using the lateral root bending assay and would help distinguish the contribution of the bHLH76 to the reduced lateral root density and primary root phenotype. Together these data argue for a role of bHLH49 and possibly bHLH76 in regulating lateral root spacing and development. However, a more detailed analysis of the phenotype is needed to understand how and when bHLH49 contributes to lateral root formation.

Cell type specific marker genes such as *SHORTROOT* (Nakajima et al., 2001) or *GATA23* (De Rybel et al., 2010) could be employed to drive ectopic gene expression that may help explain the mutant phenotypes observed in the loss and gain of function lines. As lateral roots are primed in the primary root basal meristem by spatial oscillations of auxin responsive gene expression (Moreno-Risueno et al., 2010a), it would be interesting to use the auxin response reporter *DR5::LUC*. This would allow to distinguish if these auxin response oscillations are perturbed or if the lateral spacing defect appears later

in development. The strong endodermal expression of bHLH49 protein is intriguing as the reorganisation of the endodermis is important to facilitate the accommodation of the developing primordia (Vermeer et al., 2014). If *bHLH49* regulates lateral root developmental genes in the endodermal layer, this could involve processes like the primordium having to break and pass through the endodermal-casparian strip barrier and could be explored further.

Given the auxin dependent repression of *bHLH49,* and the importance of auxin feedback from the pericycle into the endodermis (Marhavý et al., 2013), it would be interesting to study the expression of *bHLH49* in *pCASP1:shy2-2* lines that are specifically disrupted in their endodermal auxin response. Taken together, although this study does not give definite answers about the mechanism of *bHLH49* action, it does provide preliminary evidence to help define the role of *bHLH49* in early lateral root development.

7.3.2. *bHLH49*-mediated transcriptional regulation

The bHLH family of genes are conserved in all eukaryotes, and represents one of the largest families of transcription factors that play a key role in a number of developmental processes (Heim et al., 2003; Toledo-Ortiz et al., 2003; Carretero-Paulet et al., 2010). The *Arabidopsis* genome contains 167 bHLHs that are classified into 28 subfamilies based on their bHLH domain sequence (with the exception of 3 factors) and bHLH49 belongs to subfamily 25 that have high level of sequence homology (25%-61%) (Heim et al., 2003; Li et al., 2006b).

This study demonstrates a role for *bHLH49* during early lateral root development with nuclear localisation of bHLH49 (**Figure 7.2.**) suggestive of its role as transcription factor. bHLH49 (also referred to as ACTIVATOR OF CELL ELONGATION 1), was shown to regulate cell elongation in leaves through direct activation of an expansin *EXPA8* (Bai et al., 2012; Ikeda et al., 2012a). Here, two cell wall remodelling genes were identified as putative targets of bHLH49 by Yeast 1 Hybrid: *RALFL34* acts through regulation of cell elongation, and *EXPA1* promotes cell expansion and elongation through cell wall loosening. As I was interested to test their potential regulation by bHLH49, the putative interaction of bHLH49 with the promoter of *RALFL34* and *EXPA1* was explored using an *in planta* transient protoplast assay. However, no significant regulatory relationship could be confirmed (**Figure 7.8.**). This may be due to several reasons: For instance, bHLH factors have been well known to heterodimerise with other bHLH TFs to form a working transcriptional complex. bHLH49 has been shown to be a part of a complex tri-antagonistic bHLH system that competitively regulates cell elongation (Ikeda et al., 2012b). It may be possible that we do not have all the components of the protein complex machinery required for the interaction to mediate regulation of *RALFL34* or *EXPA1*. The need for a cofactor for complex formation was partially tested in the protoplast assay where we included the closely related homolog bHLH76 in the interaction, but this showed no difference in the regulation. This raises the question of whether bHLH49 requires homodimerisation or heterodimerisation with other bHLH factors to form an active complex which could be tested by *in vivo* protein-protein interaction assay such as FRET-FLIM based (Llères et al., 2001) or Co-Immunoprecipitation techniques.

7.3.3. Auxin-mediated control of *bHLH49* expression

Auxin which is a key regulator of lateral root formation, negatively regulates *bHLH49* expression (**Figure 7.5**). The SLR-ARF7-ARF19 dependent signalling module is essential for transcriptional activation of genes that control lateral root formation (Lavenus et al., 2013a). The lack of change in expression levels in the auxin response mutants *slr-1 and arf7,arf19* suggests that the regulation of *bHLH49* might potentially be through a different auxin-signalling pathway, such as BODENLOS (BDL)/IAA12-MONOPTEROS (MP)/ARF5–dependent pathway (De Smet et al., 2010). It would be interesting to test *bdl/iaa12* and *mp/arf5* mutants for deviations in *bHLH49* expression to try and identify the potential auxin signalling module upstream of *bHLH49*. It would be interesting to study the profile of *bHLH49* transcript and post-translated protein levels in real-time in the lateral roots by combining the lateral root bend assay with exogenous auxin treatment. This would provide *in vivo* evidence of the auxin-mediated downregulation. The observations suggest that *bHLH49* forms a part of the regulatory network controlled by auxin to regulate lateral root development.

It might also be interesting to explore brassinosteroid (BR) or gibberellin (GA)-dependent signalling as bHLH49-mediated activation of *EXPA8* to bring about cell elongation in leaves, was identified downstream of the GA-BR mediated hormonal regulation pathway (Bai et al., 2012; Ikeda et al., 2012b). There may well be potential hormonal-cross talk in regulation of the developmental process or an alternate hormone regulated pathway that regulates bHLH49-mediated response in lateral root development, through an auxin-independent pathway. The GA dependent response of *bHLH49* could be

explored further through a study of *bHLH49* expression in GA response mutants and phenotyping for differences in lateral root development upon exogenous treatment with the hormone. We also performed ChIP-qPCR to test the interaction of bHLH49 with the *RALFL34* and *EXPA1* promoter, but were unable to gain consistent results (data not shown). It might be worth performing ChIP-seq to identify the potential targets of bHLH49 *in planta*.

7.4. Materials and methods

7.4.1. Plant materials

Arabidopsis thaliana ecotype Columbia (Col 0) was used throughout this study. The two T-DNA insertion alleles for *bHLH49* (AT1G68920) used in this study *bhlh49-1, bhlh49-2* (SALK_081687, SALK_087424.22.10.x) were obtained from NASC and genotyped to verify homozygosity. The *bhlh49,76*, *pRPS5a::bHLH49*, *bHLH49::nx3GFP* and *pbHLH49::bHLH49:sYFP* lines were kindly provided by Tatyana Radoeva and Dolf Weijers (Wageningen University and Research Centre, Netherlands).

7.4.2. Growth conditions and media

The growth conditions were the same as previously described in Section 4.4.3 of Chapter 4.

7.4.3. Genotyping

The T-DNA alleles were genotyped using the following primers: as described in Section 4.4.2.

7.4.4. Phenotypic analysis

Refer to Section 4.4.4.1. for primary root length and lateral root density measurement; 4.4.4.2. for lateral root staging and 4.4.4.3. for lateral root bending assay.

7.4.5. qRT-PCR

Refer to Section 4.4.6. for the protocol. The primers used for the analysis were: BHLH49_F: CCTCTACCTCATGGATTCATGC, BHLH49_R:

GGATCACATTTTGCAAATCACC. All qRT-PCR experiments were performed in three biological replicates (unless otherwise specified) with 3 technical repeats, and the data presented as means ±SE.

7.4.6. Microscopic analysis

Lateral roots were staged on a Leica DMRB microsystem using differential interference contrast (DIC). Fluorescent seedlings were analysed on a Nikon confocal microscope utilizing both an Argon 488 laser and a 514 HeNe laser at ×20 and ×40 magnifications. For more details on confocal imaging refer to Section 4.4.7.

7.4.7. Transient activity assays

BY-2 protoplast assays were performed at VIB (Ghent, Belgium) as described in (Vanden Bossche et al., 2013), using reporter (*LucTrap*, encoding firefly luciferase) and effector constructs (*pJIT60*).

7.5. References

Bai, M.Y., Fan, M., Oh, E., and Wang, Z.Y. (2012). A triple helix-loop-helix/basic helix-loop-helix cascade controls cell elongation downstream of multiple hormonal and environmental signaling pathways in Arabidopsis. Plant Cell **24,** 4917-4929.

Carretero-Paulet, L., Galstyan, A., Roig-Villanova, I., Martínez-García, J.F., Bilbao-Castro, J.R., and Robertson, D.L. (2010). Genome-Wide Classification and Evolutionary Analysis of the bHLH Family of Transcription Factors in Arabidopsis, Poplar, Rice, Moss, and Algae. Plant Physiology **153,** 1398-1412.

De Smet, I., Vassileva, V., De Rybel, B., Levesque, M.P., Grunewald, W., Van Damme, D., Van Noorden, G., Naudts, M., Van Isterdael, G., De Clercq, R., Wang, J.Y., Meuli, N., Vanneste, S., Friml, J., Hilson, P., Jürgens, G., Ingram, G.C., Inzé, D., Benfey, P.N., and Beeckman, T. (2008). Receptor-Like Kinase ACR4 Restricts Formative Cell Divisions in the Arabidopsis Root. Science **322,** 594-597.

De Smet, I., Lau, S., Voß, U., Vanneste, S., Benjamins, R., Rademacher, E.H., Schlereth, A., De Rybel, B., Vassileva, V., Grunewald, W., Naudts, M., Levesque, M.P., Ehrismann, J.S., Inzé, D., Luschnig, C., Benfey, P.N., Weijers, D., Van Montagu, M.C.E., Bennett, M.J., Jürgens, G., and Beeckman, T. (2010). Bimodular auxin response controls organogenesis in Arabidopsis. Proceedings of the National Academy of Sciences **107,** 2705-2710.

Gaudinier, A., Zhang, L., Reece-Hoyes, J.S., Taylor-Teeples, M., Pu, L., Liu, Z., Breton, G., Pruneda-Paz, J.L., Kim, D., Kay, S.A., Walhout, A.J.M., Ware, D., and Brady, S.M. (2011). Enhanced Y1H assays for Arabidopsis. Nat Meth **8,** 1053-1055.

Heim, M.A., Jakoby, M., Werber, M., Martin, C., Weisshaar, B., and Bailey, P.C. (2003). The Basic Helix–Loop–Helix Transcription Factor Family in Plants: A Genome-Wide Study of Protein Structure and Functional Diversity. Molecular biology and evolution **20,** 735-747.

Ikeda, M., Fujiwara, S., Mitsuda, N., and Ohme-Takagi, M. (2012a). A triantagonistic basic helix-loop-helix system regulates cell elongation in Arabidopsis. Plant Cell **24,** 4483-4497.

Lau, S., De Smet, I., Kolb, M., Meinhardt, H., and Jurgens, G. (2011). Auxin triggers a genetic switch. Nat Cell Biol **13,** 611-615.

Lavenus, J., Goh, T., Roberts, I., Guyomarc'h, S., Lucas, M., De Smet, I., Fukaki, H., Beeckman, T., Bennett, M., and Laplaze, L. (2013). Lateral root development in Arabidopsis: fifty shades of auxin. Trends Plant Sci.

Li, X., Duan, X., Jiang, H., Sun, Y., Tang, Y., Yuan, Z., Guo, J., Liang, W., Chen, L., Yin, J., Ma, H., Wang, J., and Zhang, D. (2006). Genome-wide analysis of basic/helix-loop-helix transcription factor family in rice and Arabidopsis. Plant Physiol **141,** 1167-1184.

Llères, D., Swift, S., and Lamond, A.I. (2001). Detecting Protein-Protein Interactions In Vivo with FRET using Multiphoton Fluorescence Lifetime Imaging Microscopy (FLIM). In Current Protocols in Cytometry (John Wiley & Sons, Inc.

Marhavý, P., Vanstraelen, M., De Rybel, B., Zhaojun, D., Bennett, M.J., Beeckman, T., and Benková, E. (2013). Auxin reflux between the endodermis and pericycle promotes lateral root initiation. The EMBO Journal **32,** 149-158.

Moreno-Risueno, M.A., Van Norman, J.M., Moreno, A., Zhang, J., Ahnert, S.E., and Benfey, P.N. (2010). Oscillating Gene Expression Determines Competence for Periodic Arabidopsis Root Branching. Science **329,** 1306-1311.

Murphy, E., Vu, L.D., Van den Broeck, L., Lin, Z., Ramakrishna, P., van de Cotte, B., Gaudinier, A., Goh, T., Slane, D., Beeckman, T., Inzé, D., Brady, S.M., Fukaki, H., and De Smet, I. (2016). RALFL34 regulates formative cell divisions in Arabidopsis pericycle during lateral root initiation. Journal of Experimental Botany.

Nakajima, K., Sena, G., Nawy, T., and Benfey, P.N. (2001). Intercellular movement of the putative transcription factor SHR in root patterning. Nature **413,** 307-311.

Perbal, M.C., Haughn, G., Saedler, H., and Schwarz-Sommer, Z. (1996). Non-cell-autonomous function of the Antirrhinum floral homeotic proteins DEFICIENS and GLOBOSA is exerted by their polar cell-to-cell trafficking. Development **122,** 3433-3441.

Péret, B., Li, G., Zhao, J., Band, L.R., Voß, U., Postaire, O., Luu, D.-T., Da Ines, O., Casimiro, I., Lucas, M., Wells, D.M., Lazzerini, L., Nacry, P., King, J.R., Jensen, O.E., Schäffner, A.R., Maurel, C., and Bennett, M.J. (2012). Auxin regulates aquaporin function to facilitate lateral root emergence. Nat Cell Biol **14,** 991-998.

Toledo-Ortiz, G., Huq, E., and Quail, P.H. (2003). The Arabidopsis Basic/Helix-Loop-Helix Transcription Factor Family. The Plant Cell Online **15,** 1749-1770.

Vanden Bossche, R., Demedts, B., Vanderhaeghen, R., and Goossens, A. (2013). Transient expression assays in tobacco protoplasts. Methods in molecular biology (Clifton, N.J.) **1011,** 227-239.

Vermeer, J.E., von Wangenheim, D., Barberon, M., Lee, Y., Stelzer, E.H., Maizel, A., and Geldner, N. (2014). A spatial accommodation by neighboring cells is required for organ initiation in Arabidopsis. Science **343,** 178-183.

Voß, U., Wilson, M.H., Kenobi, K., Gould, P.D., Robertson, F.C., Peer, W.A., Lucas, M., Swarup, K., Casimiro, I., Holman, T.J., Wells, D.M., Péret, B., Goh, T., Fukaki, H., Hodgman, T.C., Laplaze, L., Halliday, K.J., Ljung, K., Murphy, A.S., Hall, A.J., Webb, A.A.R., and Bennett, M.J. (2015). The circadian clock rephases during lateral root organ initiation in Arabidopsis thaliana. Nature Communications **6,** 7641.

Wada, T., Kurata, T., Tominaga, R., Koshino-Kimura, Y., Tachibana, T., Goto, K., Marks, M.D., Shimura, Y., and Okada, K. (2002). Role of a positive regulator of root hair development, CAPRICE, in Arabidopsis root epidermal cell differentiation. Development **129,** 5409-5419.

Weijers, D., Franke-van Dijk, M., Vencken, R.J., Quint, A., Hooykaas, P., and Offringa, R. (2001). An Arabidopsis Minute-like phenotype caused by a semi-dominant mutation in a RIBOSOMAL PROTEIN S5 gene. Development **128,** 4289-4299.

Chapter 8. Conclusions and future work

Lateral roots are a key component of the root system and help anchor the plant in soil and mediate acquisition of water and nutrients. In most dicots, such as *Arabidopsis*, lateral roots initiate post-embryonically from a specialised set of xylem pole pericycle cells termed ‘founder cells’. These cells go through a coordinated series of asymmetric cell divisions that gives rise to daughter cells with different identities that drive morphogenesis and patterning of the lateral root primordia (Malamy and Benfey, 1997; De Smet et al., 2006b; Peret et al., 2009b; De Smet, 2012a). The cell wall plays a key role by providing structure to the tissues and being flexible to restructuring to accommodate growth. Very little is understood about the molecular components that drive the spatial coordination of these tightly controlled divisions and cell geometries in the initiating lateral root. The aim of this work was to gain a better insight into this process and identify potential molecular components that may be involved.

8.1. Conclusions - Bringing it all together

In the research presented here, we identified *EXPANSINA1* (*EXPA1*) as a potential candidate that regulates early lateral root initiation. *EXPA1* was found to be expressed in the lateral root founder cells prior to asymmetric cell division suggestive of a role in early lateral root initiation. Examination of the loss of function line of *expa1-1* showed that the early fundamental asymmetric divisions were perturbed in the mutant with a resultant delay in the progression of a nascent lateral root primordia from Stage I to Stage II. This clearly indicated that the gene *EXPA1* has an important role to play for organised asymmetric cell divisions. To delve deeper into understanding the function of the gene, the first logical step was to study if the cell size of the lateral root founder cells that go on to form a lateral root were affected in the mutant driven by the idea that

expansins are important for cell wall remodeling and the absence of one would point to defects in this process. Therefore, we went on to measure the cell width of the specialised lateral root founder cells using the technique of lateral root induction system (LRIS) to have a larger pool of cells in the lateral root formation process than normally found in a root. Although a non-natural lateral root formation system, the LRIS is an effective method to enhance the overall pool of lateral root forming cells to carry out measurable cell size studies. In addition, we also observe that *EXPA1* is an auxin responsive gene likely downstream of SLR-ARF7-ARF19 (**Figure 4.3**). We measured the cell size of pericycle, endodermal and a few representative cortical and epidermal cells. The key cell layer that is responsive to auxin and lateral root formation is the pericycle. The cells are 3-dimensional objects and it is difficult to measure the actual cell size accurately in 2D. For this we have taken precautions in out measurement parameters and based our conclusions on the overall trend rather than fixed numbers. Thus, the key observations from the cell size studies point that the pericycle cells of *expa1-1* do not undergo the radial expansion in the same way as in wildtype roots. The pericycle cells of *expa1-1* are radially wider when grown in auxin deprived condition and upon auxin treatment, they restructure themselves to match the size and shape of pericycle cells of wildtype roots. This indicates two possibilities, first that the defect in the pericycle cells could be inherent from their emergence from the quiescent center of the root that goes on to reflect in the cell size as root development progresses. Secondly, auxin being an important cue to coordinate the restructuring of the cell size via activation of other cell wall remodeling genes to ensure the defect due to absence of *EXPA1* is corrected and normal formative divisions progress. The

first could be true given that the *EXPA1* is expressed in the initial just above the quiescent center and in the elongation zone of the root (**Supl. Figure 4.1**) and its absence leads to no significant defects in the primary root, but that is more strongly reflected as the lateral root development progresses. For the second possibility, it is possible that auxin may trigger other expansins to be expressed in the absence of *EXPA1* for instance, a close homolog *EXPA15* was found to be upregulated in the *expa1-1* in whole roots (**Figure 8.1 A, C**) and with a similar profile as *EXPA1* in the FACS assay on auxin stimulated asymmetrically dividing pericycle cells in a LRIS (De Smet et al., 2008) (**Figure 8.1B**). Therefore, it is worth exploring the role of *EXPA15* and its potential role in correcting the cell size defects in the absence of *EXPA1* and rectifying the inability to undergo normal organized formative divisions. Hence, we show that *EXPA1* is important for maintenance of pericycle cell size for organised asymmetric cell divisions. We also report here that auxin induces *EXPA1* expression, and analysis of auxin response mutant's places *EXPA1* regulation (although likely indirectly) of the SLR-ARF7-ARF19 module.

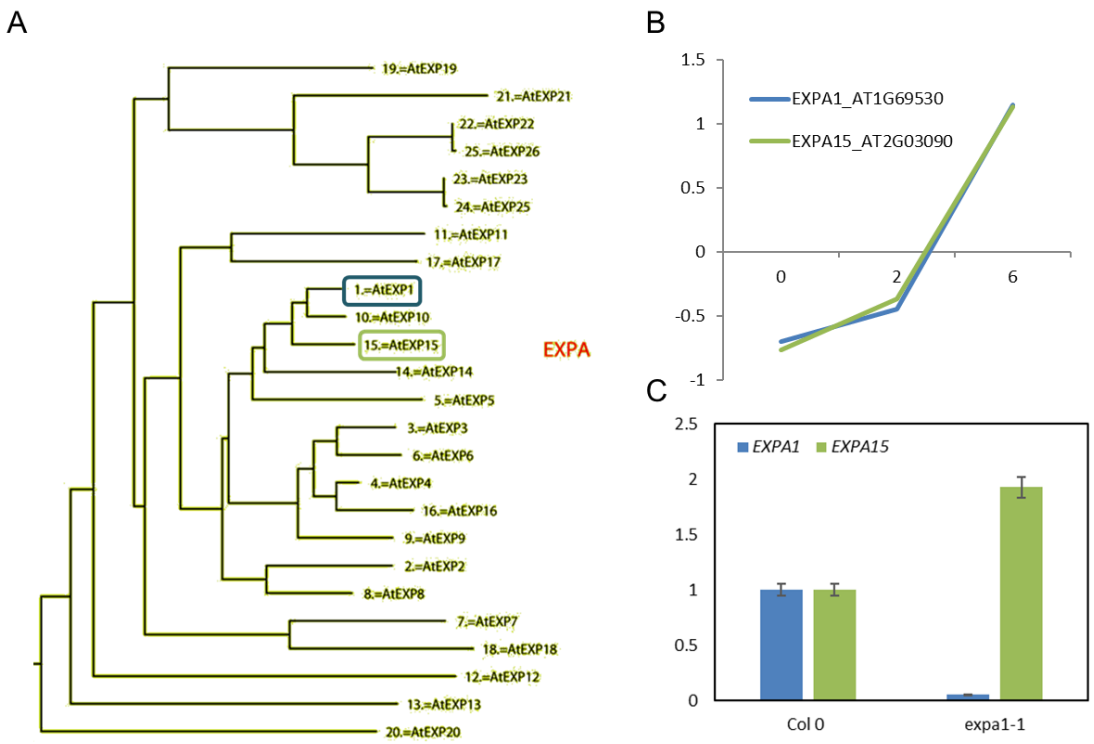


Figure 8.1. Phylogenetic tree of EXPA family of genes with *EXPA1* and close homolog *EXPA15* highlighted (Modified from schematic from Expansin Central website:http://www.personal.psu.edu/fsl/ExpCentral/index.htm)(A); Expression profile of *EXPA1* and *EXPA15* in the FACS dataset (De Smet et al., 2008) (B); qRT-PCR based expression level of *EXPA15* in roots of *expa1-1* with expression levels normalized to 1 in Col 0 (C) (n=3).

Cell size studies on the overlaying layers shows a few interesting differences especially in the endodermal cell layer. The cells of the NPA grown seedlings for both wildtype and expa1-1 did not have significant differences in either their length or width. However, auxin seemed to uncover differences in the cell size with the endodermal cells of *expa1-1* becoming longer than wildtype when treated with auxin, with no differences in their cell width. The endodermal cells of *expa1-1* are overall larger than wildtype with the main contributing factor for the size being an increased cell length. Auxin accumulation in the pericycle cell is known to be channeled by a reflux pathway into the primordia with the help of PIN3 (from the PIN family of auxin efflux carrier proteins is part of the polar auxin transport machinery that determines

the direction of the auxin flow) to aid LRP development (Wiśniewska et al., 2006; Marhavý P et al., 2013). In the case of *expa1-1*, we can speculate that the larger endodermal cells may be due to the increased auxin levels in the endodermal cells that leads to inhibition of cell division and promotion of cell elongation resulting in increased cell lengths. *EXPA1* is not expressed in the endodermal layer, but it is in the cortical cells. The cortical and epidermal cells do show differences in cell size upon auxin treatment, but the data is not conclusive given the small number of cells measured.

We then went on to explore if the defects in cell size are due to alterations in the cell wall brought about by the action of EXPANSINs. To do this we applied a combination of whole root analysis and point measurements to uncover cell-wall processes underpinning lateral root development: 1) a crude whole root extract of cell wall analysed for differences in the overall sugar polymer levels with and without the auxin treatment; ii) A more targeted approach by application of confocal Raman spectroscopy to the junction of pericycle cells subject to the LRIS. In the first method, the whole root plant cell wall digests were analysed by chromatography and four key sugar monomers were analysed- glucose, galactose, arabinose and xylose. These monomers are breakdown products of key cell wall polymers such as cellulose, xyloglucan and pectins. This showed that there was an increase in the levels of galactose and a drop in the glucose levels in the *expa1-1* mutant suggesting differences in the interactions between the cell wall polymers upon auxin treatment. Auxin has long been known to loosen the rigid cell wall network of cellulose fibers and matrix polysaccharides by stimulating the transport of H^+ ions into the cell wall, decreasing the wall pH (Valent and Albersheim, 1974). Expansins on the other

hand are known to be activated in the cell wall in acidic pH and alter the hydrogen bonding between the matrix polysaccharides that link the cellulose fibers together (Cosgrove, 2005). Thus, from the monosaccharide data of the untreated wildtype and *expa1-1* roots wherein there is a reduction in the galactose monomers in the root, it could be speculated that the pectin sidechains containing galactose monomers are not released upon digestion due to absence of active *EXPA1*. Upon auxin treatment however, structure of the cell wall is modified leading to an altered composition of monosaccharides upon digestion of the auxin treated walls. This suggests that the absence of *EXPA1* alters the structural properties of the cell wall which in turn affects the viscoelastic properties of the cell (such as cell expansion) that drives development. It could be considered that the cell wall of the auxin treated roots undergo dynamic remodeling of the wall polymers. The main source of glucans and galactans are from the xyloglucans and pectic polysaccharide sidechains. These differences in the levels of glucose and galactose upon auxin may be possibly due to alteration in the state of interaction of the xyloglucans and pectins in the wall as the levels of these compounds are known to be modified as the root matures from cell wall compound epitope labelling studies (Wilson et al., 2015). This needs to be further validated with a more comprehensive profiling of the cell wall using different extraction techniques to isolate cellulose, xyloglucan and pectin rich fractions and infer from their distribution such as the one used in (Wilson et al., 2015) (**Figure 8.2**). In their study of the different zones of the root by using cell wall epitope specific antibodies, it was found that the AGPs were found to be present in higher levels from the elongation zone onwards towards the mature parts of the root. Xyloglucans were highest in the

root elongation zone and their presence becoming more evident as the root matures. Similar pattern was observed for the homogalacturonans associated with pectins (Wilson et al., 2015) (**Figure 8.2B**). These data therefore suggest that the interaction in the cell wall of the *expa1-1* roots is certainly altered upon auxin treatment.

The targeted approach using confocal Raman spectroscopy supports the localised changes in the chemical composition of the cell wall upon auxin treatment. There is an enrichment in the signal of the chemical bonds between the cell wall compounds in the pericycle cell wall junction that could be reflective of novel interactions among the components of the cell wall. Enriched HOC and CH bonds correspond to alterations in cellulose and xyloglucans respectively in pericycle cell wall of *expa1-1* upon auxin treatment. Taking the whole root analysis and the pericycle specific changes it is interesting to note that there are differences observable in the two levels of study that reflects the complex nature of the cell wall along the root. The whole root data suggests altered interactions between cellulose and pectin based compounds of the root cell wall. Given that we have used 7 days post germination roots, they have a fair distribution of meristematic, elongating, lateral root, secondary cell wall forming tissue to consider. The interesting changes reflected are upon auxin treatment with the auxin responsive tissue being more active than the others and this is somethings we must consider in the interpretation. With the data so far, we can interpret that *EXPA1* being a part of an auxin driven machinery to bring about alteration to the wall composition. In our developmental system, this is reflected as *EXPA1* being needed for maintenance of cell wall integrity and in turn cell size.

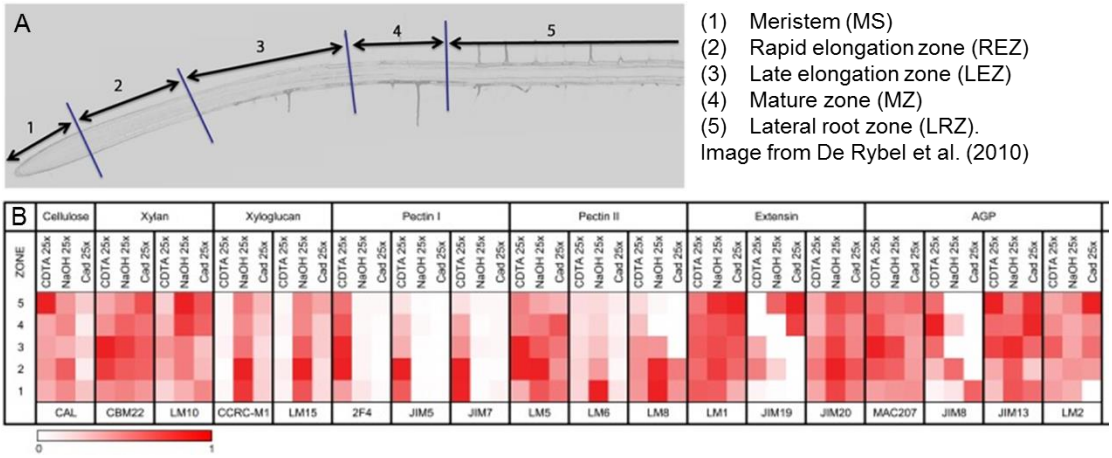


Figure 8.2. Schematic of root zones used in the study by Wilson et al., 2015 for multiohmic analysis of roots to identify cell wall remodeling genes (A); Epitope intensities for different root zones with results for each antibody (B) (Wilson et al., 2015).

The confocal Raman spectroscopy is often used in the analysis of lignin composition in the cell wall of woody species or fruit development. This is the first instance the technique has been optimised and applied to the study of *Arabidopsis* roots. This is a challenging task given the fragile nature of *Arabidopsis* roots when they are young. The plant material is also a large source of fluorescence due to high concentration of aromatic compounds that pose a challenge in acquisition of a Raman spectra. Given the nature of the system under study, the pericycle cell layer that is the source of lateral root formation, is present below three distinct cell layers – epidermis, cortex and endodermis, that makes it challenging to apply topical studies such as Atomic Force Microscopy, Electron Microscopy to understand local changes in the cell wall. Coupling of the confocal set-up to gain micron level resolution to study chemical properties at the point of interest through Raman spectroscopy was thus an interesting option to explore to understand the chemical alteration in the cell wall and interpret the relevance developmentally. Hence, we developed an optimised method to perform confocal Raman microscopy on *Arabidopsis*

root sections and applied the method to analyse *expa1-1* for cell wall compositional differences. The techniques could be applied to study other cell wall mutants to gain new insights into the structure of cell wall. The advantages are the specificity it provides in terms of are of interest under study. However, it is also important to consider that the Raman spectra reflects the chemical state of the plant cell wall and the current understanding of the complexes that a cell wall is comprised of is not fully understood yet. Also, for more detailed analysis of the cell wall composition by Raman, a better understanding of the different interactions/bonds between the cell wall polymers and therefore, their characteristic Raman spectra is necessary to draw better conclusion from the present data.

To summarise the main finding of this research, we show that auxin dependent regulation of *EXPA1* plays an important role in pericycle cell size maintenance and is required for organised asymmetric cell division. Taking into account the current understanding in the literature of the lateral root formation process, the acid growth theory of auxin driven wall loosening, the cell wall extension capacity of expansin, we propose the following model for the role of *EXPANSINA1* in driving alteration to pericycle cell wall to aid the asymmetric cell division and therefore in lateral root initiation in *Arabidopsis thaliana* (**Figure 8.3**).

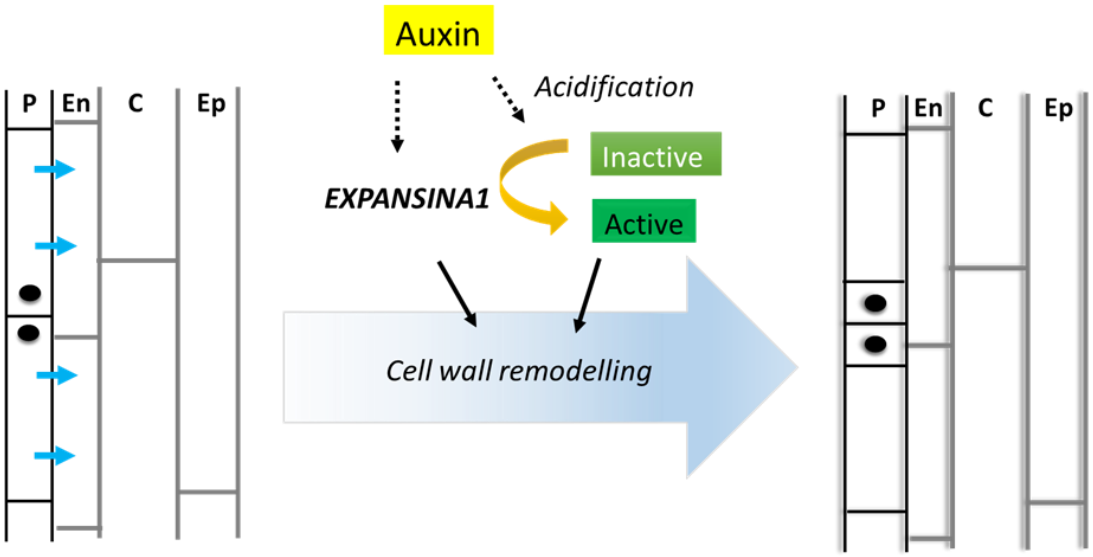


Figure 8.3. Schematic model for role of *EXPA1* in lateral root formation

The study also presents preliminary evidence to help define the role of *bHLH49* in early lateral root development. Loss- and gain-of-function phenotypes suggest a role for *bHLH49* in regulation of lateral root spacing and development that could possibly be via repression of lateral root initiation along the root. We also observe auxin driven downregulation of *bHLH49* that suggests it forms a part of the regulatory network controlled by auxin to regulate lateral root development. bHLH49 has a potential role in the transcriptional regulation of genes involved in early lateral root development from the preliminary evidence shown in this work. Further study into the functional role and potential interactors would help gain a clearer picture on its function.

8.2. Future perspectives

The study provides a strong clue about the connection between the auxin mediated response in the cell wall and the action of expansin reflected by differences in cellulose and pectin levels based on monosaccharide and Raman

analysis. It would be interesting investigate this further by generation of detailed Raman mapping of the different root tissues and application of multivariate methods to gain a more in depth understanding of the chemical composition of the wall polymers and their distribution. The technique also holds potential to perform several interesting analyses on the cell type specific wall architecture for instance, to study the interaction of the casparian strip with the endodermal cell wall, pollen composition, fruit cell wall composition, differences in the cell wall properties of flower petal etc. In addition to the chemical map generated from Raman, it would be useful to support this with cell specific immunolocalisation of cell wall polymers using antibodies to epitopes of major cell wall glycan's. The differences detected in *expa1-1* in the monosaccharide analysis could be followed up with a more detailed profiling of the cell wall glycan's using high-throughput glycan microarrays under dynamic wall remodeling conditions. This would also help in separating the different cellulosic, xyloglucan and pectin fractions to better understand the interplay between them in the wall. Application of the study to a dynamic system such as upon auxin treatment may help uncover modifications in the interactions that could help increase our understanding on the function of expansins in the wall. Although the confocal Raman imaging presented here was developed for study of *Arabidopsis* roots, it can easily be transferred to the study of other root systems with slight modifications. Other root systems such as tomato, rice, wheat, or maize may be easier to section than *Arabidopsis* and could be studied by this method. The main thing that may prove challenging would be the spectrum acquisition itself as some of these specimens have high auto fluorescence that could be overcome by optimisation of acquisition parameters

and post-processing. To support the cell wall chemistry data with information on mechanical properties, it may be worth exploring the possibility to apply a combination of confocal Raman with AFM as the instruments have been developed now to couple the two techniques together.

In terms of lateral root initiation, given acidic pH induced activity of expansins, it would be very interesting to test the response of altered pH on cell size and lateral root development. pH rhodo dyes are commercially available. However, for study of an internal tissue layer such as pericycle that is under study, the dye must first overcome the barriers of overlaying cell layers and penetration through the caparian strip to be able to be absorbed into the pericycle layer and then reflect the dynamic alterations. Another interesting observation that could be pursued would be the expression pattern in the overlying cortical cell layers that suggests a potential role for *EXPA1* at the later stages of primordia development. It would be interesting to follow this up to determine if the gene has a multi-step role possibly to help emergence suggested by the lateral root staging data (**Figure 4.6. c**). We have preliminary data that suggests *EXPA10,* a close homolog of *EXPA1*, shows lateral root formation defects. Double mutant analysis would help overcome redundancy issues and establish a stronger role for the expansins in lateral root development. In terms of the EXPA1 protein, it would be highly interesting to study its localisation in the cell to get a better picture of where the protein is active, and study its dynamics in response to hormone treatment in real-time by 4D imaging. It would be interesting to carry out pericycle cell specific induction of *EXPA1* to isolate the role of the gene more specifically to the pericycle and eliminate any other effects that may dilute its response in lateral

root formation and provide a more pronounced effect. The EXPA1 could be crossed in the *slr-1* (*solitary root*) mutant that does not produce any lateral roots to test if the cell size changes are reflects in the pericycle of the *slr* mutant. This would also help place *EXPA1* in the pathway either downstream or not of SLR. Cell-type specific overexpression of EXPA1 can be carried out nder the promoter of *LBD18* (expressed specifically in LR initiating cells with defect in nuclear migration) or *CASP/SHY* (in the endodermis), to see if this has an effect in the lateral root development. Given the expression of *EXPA1* in the initials above the quiescent center of the root (**Supl. Figure 4.1**), it would be interesting to use whole root imaging technique such as Light Sheet Microscopy to image the differences in the development of the pericycle cell layer from the QC upwards as a form of cell lineage analysis to capture alterations in the transition of the cells as they progress through the developmental stages.

References

Aalen, R.B., Wildhagen, M., Sto, I.M., and Butenko, M.A. (2013). IDA: a peptide ligand regulating cell separation processes in Arabidopsis. J Exp Bot **64,** 5253-5261.

Abel, S., and Theologis, A. (1996). Early genes and auxin action. Plant Physiology **111,** 9-17.

Agarwal, U.P. (2006). Raman imaging to investigate ultrastructure and composition of plant cell walls: distribution of lignin and cellulose in black spruce wood (Picea mariana). Planta **224,** 1141-1153.

Andberg, M., Penttilä, M., and Saloheimo, M. (2015). Swollenin from Trichoderma reesei exhibits hydrolytic activity against cellulosic substrates with features of both endoglucanases and cellobiohydrolases. Bioresource Technology **181,** 105-113.

Arru, L., Rognoni, S., Poggi, A., and Loreti, E. (2008). Effect of sugars on auxin-mediated LeEXPA2 gene expression. Plant Growth Regul **55,** 11-20.

Ba, L.-j., Shan, W., Xiao, Y.-y., Chen, J.-y., Lu, W.-j., and Kuang, J.-f. (2014). A ripening-induced transcription factor MaBSD1 interacts with promoters of MaEXP1/2 from banana fruit. Plant Cell Reports**,** 1-8.

Bae, J.M., Kwak, M.S., Noh, S.A., Oh, M.J., Kim, Y.S., and Shin, J.S. (2014). Overexpression of sweetpotato expansin cDNA (IbEXP1) increases seed yield in Arabidopsis. Transgenic research **23,** 657-667.

Bai, M.Y., Fan, M., Oh, E., and Wang, Z.Y. (2012). A triple helix-loop-helix/basic helix-loop-helix cascade controls cell elongation downstream of multiple hormonal and environmental signaling pathways in Arabidopsis. Plant Cell **24,** 4917-4929.

Baluska, F., Salaj, J., Mathur, J., Braun, M., Jasper, F., Samaj, J., Chua, N.H., Barlow, P.W., and Volkmann, D. (2000). Root hair formation: F-actin-dependent tip growth is initiated by local assembly of profilin-supported F-actin meshworks accumulated within expansin-enriched bulges. Developmental biology **227,** 618-632.

Bassel, G.W., Stamm, P., Mosca, G., Barbier de Reuille, P., Gibbs, D.J., Winter, R., Janka, A., Holdsworth, M.J., and Smith, R.S. (2014). Mechanical constraints imposed by 3D cellular geometry and arrangement modulate growth patterns in the Arabidopsis embryo. Proceedings of the National Academy of Sciences **111,** 8685-8690.

Beeckman, T., Burssens, S., and Inzé, D. (2001). The peri-cell-cycle in Arabidopsis. J Exp Bot **52,** 403-411.

Belfield, E.J., Ruperti, B., Roberts, J.A., and McQueen-Mason, S. (2005a). Changes in expansin activity and gene expression during ethylene-promoted leaflet abscission in Sambucus nigra. Journal of Experimental Botany **56,** 817-823.

Belfield, E.J., Ruperti, B., Roberts, J.A., and McQueen-Mason, S. (2005b). Changes in expansin activity and gene expression during ethylene-promoted leaflet abscission in Sambucus nigra. Journal of experimental botany **56,** 817-823.

Benková, E., Ivanchenko, M.G., Friml, J., Shishkova, S., and Dubrovsky, J.G. (2009). A morphogenetic trigger: is there an emerging concept in plant developmental biology? Trends in Plant Science **14,** 189-193.

Benková, E., Michniewicz, M., Sauer, M., Teichmann, T., Seifertová, D., Jürgens, G., and Friml, J. (2003). Local, Efflux-Dependent Auxin Gradients as a Common Module for Plant Organ Formation. Cell **115,** 591-602.

Berckmans, B., Vassileva, V., Schmid, S.P., Maes, S., Parizot, B., Naramoto, S., Magyar, Z., Alvim Kamei, C.L., Koncz, C., Bogre, L., Persiau, G., De Jaeger, G., Friml, J., Simon, R., Beeckman, T., and De Veylder, L. (2011). Auxin-dependent cell cycle reactivation through transcriptional regulation of Arabidopsis E2Fa by lateral organ boundary proteins. The Plant cell **23,** 3671-3683.

Bielach, A., Podlešáková, K., Marhavý, P., Duclercq, J., Cuesta, C., Müller, B., Grunewald, W., Tarkowski, P., and Benková, E. (2012). Spatiotemporal Regulation of Lateral Root Organogenesis in Arabidopsis by Cytokinin. The Plant Cell Online **24,** 3967-3981.

Bishopp, A., Help, H., El-Showk, S., Weijers, D., Scheres, B., Friml, J., Benková, E., Mähönen, Ari P., and Helariutta, Y. (2011). A Mutually Inhibitory Interaction between Auxin and Cytokinin Specifies Vascular Pattern in Roots. Current Biology **21,** 917-926.

Boerjan, W., Ralph, J., and Baucher, M. (2003). LIGNIN BIOSYNTHESIS. Annual Review of Plant Biology **54,** 519-546.

Boron, A.K., Van Loock, B., Suslov, D., Markakis, M.N., Verbelen, J.P., and Vissenberg, K. (2015). Over-expression of AtEXLA2 alters etiolated arabidopsis hypocotyl growth. Annals of botany **115,** 67-80.

Brady, S.M., Orlando, D.A., Lee, J.-Y., Wang, J.Y., Koch, J., Dinneny, J.R., Mace, D., Ohler, U., and Benfey, P.N. (2007). A High-Resolution Root Spatiotemporal Map Reveals Dominant Expression Patterns. Science **318,** 801-806.

Brotman, Y., Briff, E., Viterbo, A., and Chet, I. (2008). Role of swollenin, an expansin-like protein from Trichoderma, in plant root colonization. Plant Physiol **147,** 779-789.

Brummell, D.A., and Harpster, M.H. (2001). Cell wall metabolism in fruit softening and quality and its manipulation in transgenic plants. Plant Mol Biol **47,** 311-340.

Brummell, D.A., Harpster, M.H., and Dunsmuir, P. (1999a). Differential expression of expansin gene family members during growth and ripening of tomato fruit. Plant Mol Biol **39,** 161-169.

Brummell, D.A., Howie, W.J., Ma, C., and Dunsmuir, P. (2002). Postharvest fruit quality of transgenic tomatoes suppressed in expression of a ripening-related expansin. Postharvest Biol Tec **25,** 209-220.

Brummell, D.A., Harpster, M.H., Civello, P.M., Palys, J.M., Bennett, A.B., and Dunsmuir, P. (1999b). Modification of expansin protein abundance in tomato fruit alters softening and cell wall polymer metabolism during ripening. Plant Cell **11,** 2203-2216.

Budzinski, I.G., Santos, T.B., Sera, T., Pot, D., Vieira, L.G., and Pereira, L.F. (2011). Expression patterns of three alpha-expansin isoforms in Coffea arabica during fruit development. Plant biology **13,** 462-471.

Burton, R.A., Gidley, M.J., and Fincher, G.B. (2010). Heterogeneity in the chemistry, structure and function of plant cell walls. Nat Chem Biol **6,** 724-732.

Caderas, D., Muster, M., Vogler, H., Mandel, T., Rose, J.K., McQueen-Mason, S., and Kuhlemeier, C. (2000). Limited correlation between expansin gene expression and elongation growth rate. Plant Physiol **123,** 1399-1414.

Carey, R.E., and Cosgrove, D.J. (2007). Portrait of the expansin superfamily in Physcomitrella patens: comparisons with angiosperm expansins. Annals of botany **99,** 1131-1141.

Carey, R.E., Hepler, N.K., and Cosgrove, D.J. (2013). Selaginella moellendorffii has a reduced and highly conserved expansin superfamily with genes more closely related to angiosperms than to bryophytes. BMC plant biology **13,** 4.

Carpita, N.C., and Gibeaut, D.M. (1993). Structural models of primary cell walls in flowering plants: Consistency of molecular structure with the physical properties of the walls during growth. Plant Journal **3,** 1-30.

Carretero-Paulet, L., Galstyan, A., Roig-Villanova, I., Martínez-García, J.F., Bilbao-Castro, J.R., and Robertson, D.L. (2010). Genome-Wide Classification and Evolutionary Analysis of the bHLH Family of Transcription Factors in Arabidopsis, Poplar, Rice, Moss, and Algae. Plant Physiology **153,** 1398-1412.

Casimiro, I., Beeckman, T., Graham, N., Bhalerao, R., Zhang, H., Casero, P., Sandberg, G., and Bennett, M.J. (2003). Dissecting Arabidopsis lateral root development. Trends in Plant Science **8,** 165-171.

Casimiro, I., Marchant, A., Bhalerao, R.P., Beeckman, T., Dhooge, S., Swarup, R., Graham, N., Inze, D., Sandberg, G., Casero, P.J., and Bennett, M. (2001). Auxin transport promotes Arabidopsis lateral root initiation. Plant Cell **13,** 843-852.

Catala, C., Rose, J.K., and Bennett, A.B. (2000). Auxin-regulated genes encoding cell wall-modifying proteins are expressed during early tomato fruit growth. Plant Physiol **122,** 527-534.

Caturla, M., Chaparro, C., Schroeyers, K., and Holsters, M. (2002). Suppression subtractive hybridization to enrich low-abundance and submergence-enhanced transcripts of adventitious root primordia of Sesbania rostrata. Plant Science **162,** 915-921.

Cavalier, D.M., Lerouxel, O., Neumetzler, L., Yamauchi, K., Reinecke, A., Freshour, G., Zabotina, O.A., Hahn, M.G., Burgert, I., Pauly, M., Raikhel, N.V., and Keegstra, K. (2008). Disrupting two Arabidopsis thaliana xylosyltransferase genes results in plants deficient in xyloglucan, a major primary cell wall component. Plant Cell **20,** 1519-1537.

Celenza, J.L., Grisafi, P.L., and Fink, G.R. (1995). A pathway for lateral root formation in Arabidopsis thaliana. Genes & Development **9,** 2131-2142.

Chang, L., Ramireddy, E., and Schmülling, T. (2013). Lateral root formation and growth of Arabidopsis is redundantly regulated by cytokinin metabolism and signalling genes. J Exp Bot.

Che, J., Yamaji, N., Shen, R.F., and Ma, J.F. (2016). An Al-inducible expansin gene, OsEXPA10 is involved in root cell elongation of rice. The Plant journal : for cell and molecular biology.

Cheema, H.M.N., Bashir, A., Khatoon, A., Iqbal, N., Zafar, Y., and Malik, K.A. (2010). Molecular characterization and transcriptome profiling of expansin genes isolated from Calotropis procera fibers. Electron J Biotechn **13**.

Chen, F., Dahal, P., and Bradford, K.J. (2001). Two tomato expansin genes show divergent expression and localization in embryos during seed development and germination. Plant Physiol **127,** 928-936.

Cho, H.T., and Kende, H. (1997a). Expression of expansin genes in rice is correlated with growth. Plant Physiology **114,** 810-810.

Cho, H.T., and Kende, H. (1997b). Expansins in deepwater rice internodes. Plant Physiol **113,** 1137-1143.

Cho, H.T., and Cosgrove, D.J. (2000). Altered expression of expansin modulates leaf growth and pedicel abscission in Arabidopsis thaliana. Proc Natl Acad Sci U S A **97,** 9783-9788.

Cho, H.T., and Cosgrove, D.J. (2002). Regulation of root hair initiation and expansin gene expression in Arabidopsis. Plant Cell **14,** 3237-3253.

Choe, H.-T., and Cosgrove, D. (2010). Expansins as Agents in Hormone Action. In Plant Hormones, P. Davies, ed (Springer Netherlands), pp. 262-281.

Choi, D., Lee, Y., Cho, H.T., and Kende, H. (2003). Regulation of expansin gene expression affects growth and development in transgenic rice plants. Plant Cell **15,** 1386-1398.

Chylińska, M., Szymańska-Chargot, M., and Zdunek, A. (2014). Imaging of polysaccharides in the tomato cell wall with Raman microspectroscopy. Plant Methods **10,** 1-9.

Civello, P.M., Powell, A.L., Sabehat, A., and Bennett, A.B. (1999). An expansin gene expressed in ripening strawberry fruit. Plant Physiol **121,** 1273-1280.

Clough, S.J., and Bent, A.F. (1998). Floral dip: a simplified method for Agrobacterium-mediated transformation of Arabidopsis thaliana. The Plant journal : for cell and molecular biology **16,** 735-743.

Colmer, T.D., Peeters, A.J., Wagemaker, C.A., Vriezen, W.H., Ammerlaan, A., and Voesenek, L.A. (2004). Expression of alpha-expansin genes during root acclimations to O2 deficiency in Rumex palustris. Plant Mol Biol **56,** 423-437.

Cosgrove, D.J. (1989a). Characterization of long-term extension of isolated cell walls from growing cucumber hypocotyls. Planta **177,** 121-130.

Cosgrove, D.J. (1989b). Characterization of long-term extension of isolated cell walls from growing cucumber hypocotyls. Planta **177,** 121-130.

Cosgrove, D.J. (1997a). Creeping walls, softening fruit, and penetrating pollen tubes: the growing roles of expansins. Proc Natl Acad Sci U S A **94,** 5504-5505.

Cosgrove, D.J. (1997b). Cellular mechanisms underlying growth asymmetry during stem gravitropism. Planta **203,** S130-135.

Cosgrove, D.J. (2000a). Loosening of plant cell walls by expansins. Nature **407,** 321-326.

Cosgrove, D.J. (2000b). Expansive growth of plant cell walls. Plant physiology and biochemistry : PPB / Societe francaise de physiologie vegetale **38,** 109-124.

Cosgrove, D.J. (2000c). Loosening of plant cell walls by expansins. Nature **407,** 321-326.

Cosgrove, D.J. (2005). Growth of the plant cell wall. Nat Rev Mol Cell Biol **6,** 850-861.

Cosgrove, D.J. (2014). Re-constructing our models of cellulose and primary cell wall assembly. Curr Opin Plant Biol **22,** 122-131.

Cosgrove, D.J., and Durachko, D.M. (1994). Autolysis and extension of isolated walls from growing cucumber hypocotyls. J Exp Bot **45,** 1711-1719.

Cosgrove, D.J., and Jarvis, M.C. (2012). Comparative structure and biomechanics of plant primary and secondary cell walls. Frontiers in Plant Science **3,** 204.

Cosgrove, D.J., Bedinger, P., and Durachko, D.M. (1997). Group I allergens of grass pollen as cell wall-loosening agents. Proc Natl Acad Sci U S A **94,** 6559-6564.

Costa, F., Van de Weg, W.E., Stella, S., Dondini, L., Pratesi, D., Musacchi, S., and Sansavini, S. (2008). Map position and functional allelic diversity of Md-Exp7, a new putative expansin gene associated with fruit softening in apple (Malus x domestica Borkh.) and pear (Pyrus communis). Tree Genet Genomes **4,** 575-586.

Dal Santo, S., Fasoli, M., Cavallini, E., Tornielli, G.B., Pezzotti, M., and Zenoni, S. (2011). PhEXPA1, a Petunia hybrida expansin, is involved in cell wall metabolism and in plant architecture specification. Plant Signal Behav **6,** 2031-2034.

Dal Santo, S., Vannozzi, A., Tornielli, G.B., Fasoli, M., Venturini, L., Pezzotti, M., and Zenoni, S. (2013). Genome-wide analysis of the expansin gene superfamily reveals grapevine-specific structural and functional characteristics. PloS one **8,** e62206.

Darley, C.P., Li, Y., Schaap, P., and McQueen-Mason, S.J. (2003). Expression of a family of expansin-like proteins during the development of Dictyostelium discoideum. FEBS Letters **546,** 416-418.

De Rybel, B., Audenaert, D., Xuan, W., Overvoorde, P., Strader, L.C., Kepinski, S., Hoye, R., Brisbois, R., Parizot, B., Vanneste, S., Liu, X., Gilday, A., Graham, I.A., Nguyen, L., Jansen, L., Njo, M.F., Inzé, D., Bartel, B., and Beeckman, T. (2012). A role for the root cap in root branching revealed by the non-auxin probe naxillin. Nature Chemical Biology **8,** 798-805.

De Rybel, B., Vassileva, V., Parizot, B., Demeulenaere, M., Grunewald, W., Audenaert, D., Van Campenhout, J., Overvoorde, P., Jansen, L., Vanneste, S., Möller, B., Wilson, M., Holman, T., Van Isterdael, G.,

Brunoud, G., Vuylsteke, M., Vernoux, T., De Veylder, L., Inzé, D., Weijers, D., Bennett, M.J., and Beeckman, T. (2010a). A Novel Aux/IAA28 Signaling Cascade Activates GATA23-Dependent Specification of Lateral Root Founder Cell Identity. Current Biology **20,** 1697-1706.

De Rybel, B., Vassileva, V., Parizot, B., Demeulenaere, M., Grunewald, W., Audenaert, D., Van Campenhout, J., Overvoorde, P., Jansen, L., Vanneste, S., Moller, B., Wilson, M., Holman, T., Van Isterdael, G., Brunoud, G., Vuylsteke, M., Vernoux, T., De Veylder, L., Inze, D., Weijers, D., Bennett, M.J., and Beeckman, T. (2010b). A Novel Aux/IAA28 Signaling Cascade Activates GATA23-Dependent Specification of Lateral Root Founder Cell Identity. Current Biology **20,** 1697-1706.

De Smet, I. (2012a). Lateral root initiation: one step at a time. New Phytol **193,** 867-873.

De Smet, I. (2012b). Lateral root initiation: one step at a time. New Phytologist **193,** 867-873.

De Smet, I., and Beeckman, T. (2011). Asymmetric cell division in land plants and algae: the driving force for differentiation. Nat Rev Mol Cell Biol **12,** 177-188.

De Smet, I., Vanneste, S., Inze, D., and Beeckman, T. (2006a). Lateral root initiation or the birth of a new meristem. Plant molecular biology **60,** 871-887.

De Smet, I., Vanneste, S., Inze, D., and Beeckman, T. (2006b). Lateral root initiation or the birth of a new meristem. Plant Mol Biol **60,** 871-887.

De Smet, I., Tetsumura, T., De Rybel, B., Frey, N.F.D., Laplaze, L., Casimiro, I., Swarup, R., Naudts, M., Vanneste, S., Audenaert, D., Inze, D., Bennett, M.J., and Beeckman, T. (2007). Auxin-dependent regulation of lateral root positioning in the basal meristem of Arabidopsis. Development **134,** 681-690.

De Smet, I., Vassileva, V., De Rybel, B., Levesque, M.P., Grunewald, W., Van Damme, D., Van Noorden, G., Naudts, M., Van Isterdael, G., De Clercq, R., Wang, J.Y., Meuli, N., Vanneste, S., Friml, J., Hilson, P., Jürgens, G., Ingram, G.C., Inzé, D., Benfey, P.N., and Beeckman, T. (2008). Receptor-Like Kinase ACR4 Restricts Formative Cell Divisions in the Arabidopsis Root. Science **322,** 594-597.

De Smet, I., Lau, S., Voß, U., Vanneste, S., Benjamins, R., Rademacher, E.H., Schlereth, A., De Rybel, B., Vassileva, V., Grunewald, W., Naudts, M., Levesque, M.P., Ehrismann, J.S., Inzé, D., Luschnig, C., Benfey, P.N., Weijers, D., Van Montagu, M.C.E., Bennett, M.J., Jürgens, G., and Beeckman, T. (2010). Bimodular auxin response

controls organogenesis in Arabidopsis. Proceedings of the National Academy of Sciences **107,** 2705-2710.

Derbyshire, P., McCann, M.C., and Roberts, K. (2007). Restricted cell elongation in Arabidopsis hypocotyls is associated with a reduced average pectin esterification level. BMC plant biology **7,** 31.

Di Sansebastiano, G.P., Fornaciari, S., Barozzi, F., Piro, G., and Arru, L. (2014). New insights on plant cell elongation: a role for acetylcholine. International journal of molecular sciences **15,** 4565-4582.

DiDonato, R.J., Arbuckle, E., Buker, S., Sheets, J., Tobar, J., Totong, R., Grisafi, P., Fink, G.R., and Celenza, J.L. (2004). Arabidopsis ALF4 encodes a nuclear-localized protein required for lateral root formation. The Plant Journal **37,** 340-353.

Ditengou, F.A., Tealea, W.D., Kochersperger, P., Flittner, K.A., Kneuper, I., van der Graaff, E., Nziengui, H., Pinosa, F., Li, X.G., Nitschke, R., Laux, T., and Palme, K. (2008). Mechanical induction of lateral root initiation in Arabidopsis thaliana. Proceedings of the National Academy of Sciences of the United States of America **105,** 18818-18823.

Doblin, M.S., Pettolino, F., and Bacic, A. (2010). Plant cell walls: the skeleton of the plant world. Functional Plant Biology **37,** 357-381.

Donnelly, P.M., Bonetta, D., Tsukaya, H., Dengler, R.E., and Dengler, N.G. (1999). Cell cycling and cell enlargement in developing leaves of Arabidopsis. Developmental biology **215,** 407-419.

Dotto, M.C., Martinez, G.A., and Civello, P.M. (2006). Expression of expansin genes in strawberry varieties with contrasting fruit firmness. Plant physiology and biochemistry : PPB / Societe francaise de physiologie vegetale **44,** 301-307.

Dotto, M.C., Pombo, M.A., Martinez, G.A., and Civello, P.M. (2011). Heat treatments and expansin gene expression in strawberry fruit. Sci Hortic-Amsterdam **130,** 775-780.

Dubrovsky, J., Rost, T., Colón-Carmona, A., and Doerner, P. (2001). Early primordium morphogenesis during lateral root initiation in Arabidopsis thaliana. Planta **214,** 30-36.

Dubrovsky, J.G., Doerner, P.W., Colón-Carmona, A., and Rost, T.L. (2000). Pericycle Cell Proliferation and Lateral Root Initiation in Arabidopsis. Plant Physiology **124,** 1648-1657.

Dubrovsky, J.G., Soukup, A., Napsucialy-Mendivil, S., Jeknic, Z., and Ivanchenko, M.G. (2009). The lateral root initiation index: an integrative measure of primordium formation. Ann Bot-London **103,** 807-817.

Dubrovsky, J.G., Sauer, M., Napsucialy-Mendivil, S., Ivanchenko, M.G., Friml, J., Shishkova, S., Celenza, J., and Benková, E. (2008). Auxin

acts as a local morphogenetic trigger to specify lateral root founder cells. Proceedings of the National Academy of Sciences **105,** 8790-8794.

Dubrovsky, J.G., Napsucialy-Mendivil, S., Duclercq, J., Cheng, Y., Shishkova, S., Ivanchenko, M.G., Friml, J., Murphy, A.S., and Benkova, E. (2011a). Auxin minimum defines a developmental window for lateral root initiation. New Phytologist **191,** 970-983.

Dubrovsky, J.G., Napsucialy-Mendivil, S., Duclercq, J., Cheng, Y., Shishkova, S., Ivanchenko, M.G., Friml, J., Murphy, A.S., and Benkova, E. (2011b). Auxin minimum defines a developmental window for lateral root initiation. New Phytol **191,** 970-983.

Edwards, M.C., Smith, G.N., and Bowling, D.J.F. (1988). Guard Cells Extrude Protons Prior to Stomatal Opening—A Study using Fluorescence Microscopy and pH Micro-electrodes. Journal of Experimental Botany **39,** 1541-1547.

FAO. (2009). FAO's Director-General on How to Feed the World in 2050. Population and Development Review **35,** 837-839.

FAO. (2014). The State of Food and Agriculture.

Fernandez, A., Hilson, P., and Beeckman, T. (2013a). GOLVEN peptides as important regulatory signalling molecules of plant development. J Exp Bot.

Fernandez, A., Drozdzecki, A., Hoogewijs, K., Nguyen, A., Beeckman, T., Madder, A., and Hilson, P. (2013b). Transcriptional and Functional Classification of the GOLVEN/ROOT GROWTH FACTOR/CLE-Like Signaling Peptides Reveals Their Role in Lateral Root and Hair Formation. Plant physiology **161,** 954-970.

Fleming, A.J. (2006). The co-ordination of cell division, differentiation and morphogenesis in the shoot apical meristem: a perspective. J Exp Bot **57,** 25-32.

Fleming, A.J., McQueen-Mason, S., Mandel, T., and Kuhlemeier, C. (1997). Induction of Leaf Primordia by the Cell Wall Protein Expansin. Science **276,** 1415-1418.

Fleming, A.J., Caderas, D., Wehrli, E., McQueen-Mason, S., and Kuhlemeier, C. (1999). Analysis of expansin-induced morphogenesis on the apical meristem of tomato. Planta **208,** 166-174.

Fortin, M.C., Pierce, F.J., and Poff, K.L. (1989). The pattern of secondary root formation in curving roots of Arabidopsis thaliana (L.) Heynh. Plant, Cell & Environment **12,** 337-339.

Fudali, S., Sobczak, M., Janakowski, S., Griesser, M., Grundler, F.M., and Golinowski, W. (2008). Expansins are among plant cell wall modifying

agents specifically expressed during development of nematode-induced syncytia. Plant Signal Behav **3,** 969-971.

Fukaki, H., and Tasaka, M. (2009). Hormone interactions during lateral root formation. Plant molecular biology **69,** 437-449.

Fukaki, H., Tameda, S., Masuda, H., and Tasaka, M. (2002a). Lateral root formation is blocked by a gain-of-function mutation in the SOLITARY-ROOT/IAA14 gene of Arabidopsis. The Plant Journal **29,** 153-168.

Fukaki, H., Tameda, S., Masuda, H., and Tasaka, M. (2002b). Lateral root formation is blocked by a gain-of-function mutation in the SOLITARY-ROOT/IAA14 gene of Arabidopsis. The Plant journal : for cell and molecular biology **29,** 153-168.

Fukaki, H., Nakao, Y., Okushima, Y., Theologis, A., and Tasaka, M. (2005a). Tissue-specific expression of stabilized SOLITARY-ROOT/IAA14 alters lateral root development in Arabidopsis. The Plant Journal **44,** 382-395.

Fukaki, H., Nakao, Y., Okushima, Y., Theologis, A., and Tasaka, M. (2005b). Tissue-specific expression of stabilized SOLITARY-ROOT/IAA14 alters lateral root development in Arabidopsis. The Plant journal : for cell and molecular biology **44,** 382-395.

Gaete-Eastman, C., Figueroa, C.R., Balbontin, C., Moya, M., Atkinson, R.G., Herrera, R., and Moya-Leon, M.A. (2009). Expression of an ethylene-related expansin gene during softening of mountain papaya fruit (Vasconcellea pubescens). Postharvest Biol Tec **53,** 58-65.

Gao, Q., Zhao, M., Li, F., Guo, Q., Xing, S., and Wang, W. (2008). Expansins and coleoptile elongation in wheat. Protoplasma **233,** 73-81.

Gartemann, K.H., Kirchner, O., Engemann, J., Grafen, I., Eichenlaub, R., and Burger, A. (2003). Clavibacter michiganensis subsp. michiganensis: first steps in the understanding of virulence of a Gram-positive phytopathogenic bacterium. Journal of biotechnology **106,** 179-191.

Gaudinier, A., Zhang, L., Reece-Hoyes, J.S., Taylor-Teeples, M., Pu, L., Liu, Z., Breton, G., Pruneda-Paz, J.L., Kim, D., Kay, S.A., Walhout, A.J.M., Ware, D., and Brady, S.M. (2011). Enhanced Y1H assays for Arabidopsis. Nat Meth **8,** 1053-1055.

Geldner, N., Denervaud-Tendon, V., Hyman, D.L., Mayer, U., Stierhof, Y.D., and Chory, J. (2009). Rapid, combinatorial analysis of membrane compartments in intact plants with a multicolor marker set. The Plant journal : for cell and molecular biology **59,** 169-178.

Geldner, N., Richter, S., Vieten, A., Marquardt, S., Torres-Ruiz, R.A., Mayer, U., and Jürgens, G. (2004). Partial loss-of-function alleles reveal a role

for GNOM in auxin transport-related, post-embryonic development of Arabidopsis. Development **131,** 389-400.

Georgelis, N., Yennawar, N.H., and Cosgrove, D.J. (2012). Structural basis for entropy-driven cellulose binding by a type-A cellulose-binding module (CBM) and bacterial expansin. Proc Natl Acad Sci U S A **109,** 14830-14835.

Georgelis, N., Nikolaidis, N., and Cosgrove, D.J. (2014). Biochemical analysis of expansin-like proteins from microbes. Carbohydrate polymers **100,** 17-23.

Georgelis, N., Nikolaidis, N., and Cosgrove, D.J. (2015). Bacterial expansins and related proteins from the world of microbes. Applied microbiology and biotechnology **99,** 3807-3823.

Georgelis, N., Tabuchi, A., Nikolaidis, N., and Cosgrove, D.J. (2011). Structure-function analysis of the bacterial expansin EXLX1. The Journal of biological chemistry **286,** 16814-16823.

Gierlinger, N. (2014). Revealing changes in molecular composition of plant cell walls on the micron-level by Raman mapping and vertex component analysis (VCA). Frontiers in Plant Science **5,** 306.

Gierlinger, N., Sapei, L., and Paris, O. (2008). Insights into the chemical composition of Equisetum hyemale by high resolution Raman imaging. Planta **227,** 969-980.

Gierlinger, N., Keplinger, T., and Harrington, M. (2012). Imaging of plant cell walls by confocal Raman microscopy. Nature protocols **7,** 1694-1708.

Goh, H.H., Sloan, J., Dorca-Fornell, C., and Fleming, A. (2012a). Inducible repression of multiple expansin genes leads to growth suppression during leaf development. Plant Physiol **159,** 1759-1770.

Goh, T., Joi, S., Mimura, T., and Fukaki, H. (2012b). The establishment of asymmetry in Arabidopsis lateral root founder cells is regulated by LBD16/ASL18 and related LBD/ASL proteins. Development **139,** 883-893.

Gookin, T.E., Hunter, D.A., and Reid, M.S. (2003). Temporal analysis of alpha and beta-expansin expression during floral opening and senescence. Plant Science **164,** 769-781.

Gray-Mitsumune, M., Blomquist, K., McQueen-Mason, S., Teeri, T.T., Sundberg, B., and Mellerowicz, E.J. (2008). Ectopic expression of a wood-abundant expansin PttEXPA1 promotes cell expansion in primary and secondary tissues in aspen. Plant biotechnology journal **6,** 62-72.

Gray-Mitsumune, M., Mellerowicz, E.J., Abe, H., Schrader, J., Winzell, A., Sterky, F., Blomqvist, K., McQueen-Mason, S., Teeri, T.T., and Sundberg, B. (2004). Expansins abundant in secondary xylem belong

to subgroup A of the alpha-expansin gene family. Plant Physiol **135,** 1552-1564.

Guilfoyle, T., Hagen, G., Ulmasov, T., and Murfett, J. (1998). How Does Auxin Turn On Genes? Plant Physiology **118,** 341-347.

Guo, W., Zhao, J., Li, X., Qin, L., Yan, X., and Liao, H. (2011). A soybean beta-expansin gene GmEXPB2 intrinsically involved in root system architecture responses to abiotic stresses. The Plant journal : for cell and molecular biology **66,** 541-552.

Hager, A., Menzel, H., and Krauss, A. (1971). [Experiments and hypothesis concerning the primary action of auxin in elongation growth]. Planta **100,** 47-75.

Harada, T., Torii, Y., Morita, S., Onodera, R., Hara, Y., Yokoyama, R., Nishitani, K., and Satoh, S. (2011). Cloning, characterization, and expression of xyloglucan endotransglucosylase/hydrolase and expansin genes associated with petal growth and development during carnation flower opening. J Exp Bot **62,** 815-823.

Harb, A., Krishnan, A., Ambavaram, M.M., and Pereira, A. (2010). Molecular and physiological analysis of drought stress in Arabidopsis reveals early responses leading to acclimation in plant growth. Plant Physiol **154,** 1254-1271.

Harris, P.J., and Hartley, R.D. (1976). Detection of bound ferulic acid in cell walls of the Gramineae by ultraviolet fluorescence microscopy. Nature **259,** 508-510.

Heim, M.A., Jakoby, M., Werber, M., Martin, C., Weisshaar, B., and Bailey, P.C. (2003). The Basic Helix–Loop–Helix Transcription Factor Family in Plants: A Genome-Wide Study of Protein Structure and Functional Diversity. Molecular biology and evolution **20,** 735-747.

Herder, G.D., Van Isterdael, G., Beeckman, T., and De Smet, I. (2010). The roots of a new green revolution. Trends in Plant Science **15,** 600-607.

Himanen, K., Boucheron, E., Vanneste, S., de Almeida Engler, J., Inze, D., and Beeckman, T. (2002a). Auxin-mediated cell cycle activation during early lateral root initiation. Plant Cell **14,** 2339-2351.

Himanen, K., Boucheron, E., Vanneste, S., de Almeida Engler, J., Inzé, D., and Beeckman, T. (2002b). Auxin-Mediated Cell Cycle Activation during Early Lateral Root Initiation. The Plant Cell Online **14,** 2339-2351.

Himanen, K., Vuylsteke, M., Vanneste, S., Vercruysse, S., Boucheron, E., Alard, P., Chriqui, D., Van Montagu, M., Inze, D., and Beeckman, T. (2004). Transcript profiling of early lateral root initiation. Proc Natl Acad Sci U S A **101,** 5146-5151.

Hofhuis, H., Laskowski, M., Du, Y., Prasad, K., Grigg, S., Pinon, V., and Scheres, B. (2013). Phyllotaxis and Rhizotaxis in Arabidopsis Are Modified by Three PLETHORA Transcription Factors. Current Biology **23,** 956-962.

Holdsworth, M., Bentsink, L., and Soppe, W. (2008). Molecular networks regulating Arabidopsis seed maturation, after-ripening, dormancy and germination. New Phytol **179,** 33 - 54.

Hruz, T., Laule, O., Szabo, G., Wessendorp, F., Bleuler, S., Oertle, L., Widmayer, P., Gruissem, W., and Zimmermann, P. (2008). Genevestigator V3: A Reference Expression Database for the Meta-Analysis of Transcriptomes. Advances in Bioinformatics **2008,** 5.

Ikeda, M., Fujiwara, S., Mitsuda, N., and Ohme-Takagi, M. (2012a). A Triantagonistic Basic Helix-Loop-Helix System Regulates Cell Elongation in Arabidopsis. The Plant cell **24,** 4483-4497.

Ikeda, M., Fujiwara, S., Mitsuda, N., and Ohme-Takagi, M. (2012b). A triantagonistic basic helix-loop-helix system regulates cell elongation in Arabidopsis. Plant Cell **24,** 4483-4497.

Ikeyama, Y., Tasaka, M., and Fukaki, H. (2010). RLF, a cytochrome b(5)-like heme/steroid binding domain protein, controls lateral root formation independently of ARF7/19-mediated auxin signaling in Arabidopsis thaliana. Plant Journal **62,** 865-875.

Im, K., Cosgrove, D.J., and Jones, A.M. (1999). Novel subcellular localization of Zinnia elegans expansin (ZeExp) mRNAs-ZeExp1 and 3 mRNA goes north while ZeExp2 mRNA goes south. Mol Biol Cell **10,** 294a-294a.

Im, K.H., Cosgrove, D.J., and Jones, A.M. (2000). Subcellular localization of expansin mRNA in xylem cells. Plant Physiol **123,** 463-470.

Ivanov, V.B., and Dubrovsky, J.G. (1997). Estimation of the Cell-Cycle Duration in the Root Apical Meristem: A Model of Linkage between Cell-Cycle Duration, Rate of Cell Production, and Rate of Root Growth. International Journal of Plant Sciences **158,** 757-763.

Jung, J., O'Donoghue, E.M., Dijkwel, P.P., and Brummell, D.A. (2010). Expression of multiple expansin genes is associated with cell expansion in potato organs. Plant Science **179,** 77-85.

Jurado, S., Diaz-Trivino, S., Abraham, Z., Manzano, C., Gutierrez, C., and del Pozo, J.c. (2008). SKP2A protein, an F-box that regulates cell division, is degraded via the ubiquitin pathway. Plant signaling & behavior **3,** 810-812.

Jurado, S., Abraham, Z., Manzano, C., López-Torrejón, G., Pacios, L.F., and Del Pozo, J.C. (2010). The Arabidopsis Cell Cycle F-Box Protein SKP2A Binds to Auxin. The Plant Cell Online **22,** 3891-3904.

Kajala, K., Ramakrishna, P., Fisher, A., Bergmann, D.C., De Smet, I., Sozzani, R., Weijers, D., and Brady, S.M. (2014). Omics and modelling approaches for understanding regulation of asymmetric cell divisions in arabidopsis and other angiosperm plants. Annals of botany.

Kam, M.J., Yun, H.S., Kaufman, P.B., Chang, S.C., and Kim, S.K. (2005). Two expansins, EXP1 and EXPB2, are correlated with the growth and development of maize roots. J Plant Biol **48,** 304-310.

Keller, E., and Cosgrove, D.J. (1995). Expansins in growing tomato leaves. The Plant Journal **8,** 795-802.

Kende, H., Bradford, K., Brummell, D., Cho, H.T., Cosgrove, D., Fleming, A., Gehring, C., Lee, Y., McQueen-Mason, S., Rose, J., and Voesenek, L.A. (2004). Nomenclature for members of the expansin superfamily of genes and proteins. Plant Mol Biol **55,** 311-314.

Kerff, F., Amoros, A., Herman, R., Sauvage, E., Petrella, S., Filee, P., Charlier, P., Joris, B., Tabuchi, A., Nikolaidis, N., and Cosgrove, D.J. (2008). Crystal structure and activity of Bacillus subtilis YoaJ (EXLX1), a bacterial expansin that promotes root colonization. P Natl Acad Sci USA **105,** 16876-16881.

Krishnamurthy, P., Hong, J.K., Kim, J.A., Jeong, M.J., Lee, Y.H., and Lee, S.I. (2015). Genome-wide analysis of the expansin gene superfamily reveals Brassica rapa-specific evolutionary dynamics upon whole genome triplication. Molecular genetics and genomics : MGG **290,** 521-530.

Kuluev, B.R., Safiullina, M.G., Kniazev, A.V., and Chemeris, A.V. (2013). [Effect of ectopic expression of NtEXPA5 gene on cell size and growth of organs of transgenic tobacco plants]. Ontogenez **44,** 34-41.

Kuluev, B.R., Knyazev, A.V., Nikonorov, Y.M., and Chemeris, A.V. (2014). Role of the expansin genes NtEXPA1 and NtEXPA4 in the regulation of cell extension during tobacco leaf growth. Russ J Genet+ **50,** 489-497.

Kumpf, R.P., Shi, C.L., Larrieu, A., Sto, I.M., Butenko, M.A., Peret, B., Riiser, E.S., Bennett, M.J., and Aalen, R.B. (2013). Floral organ abscission peptide IDA and its HAE/HSL2 receptors control cell separation during lateral root emergence. Proc Natl Acad Sci U S A **110,** 5235-5240.

Kurup, S., Runions, J., Köhler, U., Laplaze, L., Hodge, S., and Haseloff, J. (2005). Marking cell lineages in living tissues. The Plant Journal **42,** 444-453.

Kwasniewski, M., and Szarejko, I. (2006). Molecular cloning and characterization of beta-expansin gene related to root hair formation in barley. Plant Physiol **141,** 1149-1158.

Kwasniewski, M., Mizeracka, J., and Szarejko, I. (2004). Identification of Regulatory Elements in the Promoter of Barley Beta-Expansin Gene by Comparative Genome Analysis. Acta Physiol Plant **26,** 56-57.

Lacayo, C.I., Malkin, A.J., Holman, H.Y., Chen, L., Ding, S.-Y., Hwang, M.S., and Thelen, M.P. (2010). Imaging cell wall architecture in single Zinnia elegans tracheary elements. Plant Physiol **154**.

Laine, M.J., Haapalainen, M., Wahlroos, T., Kankare, K., Nissinen, R., Kassuwi, S., and Metzler, M.C. (2000). The cellulase encoded by the native plasmid of Clavibacter michiganensis ssp. sepedonicus plays a role in virulence and contains an expansin-like domain. Physiological and Molecular Plant Pathology **57,** 221-233.

Laplaze, L., Parizot, B., Baker, A., Ricaud, L., Martinière, A., Auguy, F., Franche, C., Nussaume, L., Bogusz, D., and Haseloff, J. (2005). GAL4-GFP enhancer trap lines for genetic manipulation of lateral root development in Arabidopsis thaliana. Journal of Experimental Botany **56,** 2433-2442.

Laplaze, L., Benkova, E., Casimiro, I., Maes, L., Vanneste, S., Swarup, R., Weijers, D., Calvo, V., Parizot, B., Herrera-Rodriguez, M.B., Offringa, R., Graham, N., Doumas, P., Friml, J., Bogusz, D., Beeckman, T., and Bennett, M. (2007). Cytokinins Act Directly on Lateral Root Founder Cells to Inhibit Root Initiation. The Plant Cell Online **19,** 3889-3900.

Laskowski, M. (2013). Lateral root initiation is a probabilistic event whose frequency is set by fluctuating levels of auxin response. J Exp Bot **64,** 2609-2617.

Laskowski, M., Biller, S., Stanley, K., Kajstura, T., and Prusty, R. (2006). Expression profiling of auxin-treated Arabidopsis roots: toward a molecular analysis of lateral root emergence. Plant Cell Physiol **47,** 788-792.

Laskowski, M., Grieneisen, V.A., Hofhuis, H., ten Hove, C.A., Hogeweg, P., Maree, A.F.M., and Scheres, B. (2008). Root System Architecture from Coupling Cell Shape to Auxin Transport. Plos Biol **6,** 2721-2735.

Laskowski, M.J., Williams, M.E., Nusbaum, H.C., and Sussex, I.M. (1995). Formation of lateral root meristems is a two-stage process. Development **121,** 3303-3310.

Lau, S., De Smet, I., Kolb, M., Meinhardt, H., and Jurgens, G. (2011). Auxin triggers a genetic switch. Nat Cell Biol **13,** 611-615.

Lavenus, J., Goh, T., Roberts, I., Guyomarc'h, S., Lucas, M., De Smet, I., Fukaki, H., Beeckman, T., Bennett, M., and Laplaze, L. (2013a). Lateral root development in Arabidopsis: fifty shades of auxin. Trends Plant Sci.

Lavenus, J., Goh, T., Roberts, I., Guyomarc'h, S., Lucas, M., De Smet, I., Fukaki, H., Beeckman, T., Bennett, M., and Laplaze, L. (2013b). Lateral root development in Arabidopsis: fifty shades of auxin. Trends in Plant Science **18,** 450-458.

Lee, D.K., Ahn, J.H., Song, S.K., Choi, Y.D., and Lee, J.S. (2003). Expression of an expansin gene is correlated with root elongation in soybean. Plant Physiol **131,** 985-997.

Lee, H.J., Lee, S., Ko, H.J., Kim, K.H., and Choi, I.G. (2010). An expansin-like protein from Hahella chejuensis binds cellulose and enhances cellulase activity. Molecules and cells **29,** 379-385.

Lee, H.W., and Kim, J. (2013). EXPANSINA17 up-regulated by LBD18/ASL20 promotes lateral root formation during the auxin response. Plant Cell Physiol **54,** 1600-1611.

Lee, H.W., Kim, M.J., Kim, N.Y., Lee, S.H., and Kim, J. (2013). LBD18 acts as a transcriptional activator that directly binds to the EXPANSIN14 promoter in promoting lateral root emergence of Arabidopsis. Plant Journal **73,** 212-224.

Lee, Y., and Kende, H. (2001). Expression of β-Expansins Is Correlated with Internodal Elongation in Deepwater Rice. Plant Physiology **127,** 645-654.

Li, L.C., and Cosgrove, D.J. (2001). Grass group I pollen allergens (beta-expansins) lack proteinase activity and do not cause wall loosening via proteolysis. European journal of biochemistry / FEBS **268,** 4217-4226.

Li, X., Mo, X., Shou, H., and Wu, P. (2006a). Cytokinin-Mediated Cell Cycling Arrest of Pericycle Founder Cells in Lateral Root Initiation of Arabidopsis. Plant and Cell Physiology **47,** 1112-1123.

Li, X., Duan, X., Jiang, H., Sun, Y., Tang, Y., Yuan, Z., Guo, J., Liang, W., Chen, L., Yin, J., Ma, H., Wang, J., and Zhang, D. (2006b). Genome-wide analysis of basic/helix-loop-helix transcription factor family in rice and Arabidopsis. Plant Physiol **141,** 1167-1184.

Li, Y., Jones, L., and McQueen-Mason, S. (2003). Expansins and cell growth. Curr Opin Plant Biol **6,** 603-610.

Lin, C., Choi, H.S., and Cho, H.T. (2011). Root hair-specific EXPANSIN A7 is required for root hair elongation in Arabidopsis. Molecules and cells **31,** 393-397.

Llères, D., Swift, S., and Lamond, A.I. (2001). Detecting Protein-Protein Interactions In Vivo with FRET using Multiphoton Fluorescence Lifetime Imaging Microscopy (FLIM). In Current Protocols in Cytometry (John Wiley & Sons, Inc.

Loescher, W., and Nevins, D.J. (1972). Auxin-induced Changes in Avena Coleoptile Cell Wall Composition. Plant Physiology **50,** 556-563.

Lu, P., Kang, M., Jiang, X., Dai, F., Gao, J., and Zhang, C. (2013). RhEXPA4, a rose expansin gene, modulates leaf growth and confers drought and salt tolerance to Arabidopsis. Planta **237,** 1547-1559.

Lucas, M., Godin, C., Jay-Allemand, C., and Laplaze, L. (2008). Auxin fluxes in the root apex co-regulate gravitropism and lateral root initiation. J Exp Bot **59,** 55-66.

Lucas, M., Kenobi, K., von Wangenheim, D., Voβ, U., Swarup, K., De Smet, I., Van Damme, D., Lawrence, T., Péret, B., Moscardi, E., Barbeau, D., Godin, C., Salt, D., Guyomarc'h, S., Stelzer, E.H.K., Maizel, A., Laplaze, L., and Bennett, M.J. (2013). Lateral root morphogenesis is dependent on the mechanical properties of the overlaying tissues. Proceedings of the National Academy of Sciences **110,** 5229-5234.

Lynch, J.P. (2007). Roots of the Second Green Revolution. Australian Journal of Botany **55,** 493-512.

Lü, P., Kang, M., Jiang, X., Dai, F., Gao, J., and Zhang, C. (2013). RhEXPA4, a rose expansin gene, modulates leaf growth and confers drought and salt tolerance to Arabidopsis. Planta **237,** 1547-1559.

Ma, J., Li, Z., Wang, B., Sui, S.Z., and Li, M.Y. (2012). Cloning of an Expansin Gene from Chimonanthus praecox Flowers and Its Expression in Flowers Treated with Ethephon or 1-Methylcyclopropene. Hortscience **47,** 1472-1477.

Ma, N., Wang, Y., Qiu, S., Kang, Z., Che, S., Wang, G., and Huang, J. (2013). Overexpression of OsEXPA8, a root-specific gene, improves rice growth and root system architecture by facilitating cell extension. PloS one **8,** e75997.

Malamy, J.E., and Benfey, P.N. (1997). Organization and cell differentiation in lateral roots of Arabidopsis thaliana. Development **124,** 33-44.

Manzano, C., Ramirez-Parra, E., Casimiro, I., Otero, S., Desvoyes, B., De Rybel, B., Beeckman, T., Casero, P., Gutierrez, C., and C. del Pozo, J. (2012). Auxin and Epigenetic Regulation of SKP2B, an F-Box That Represses Lateral Root Formation. Plant physiology **160,** 749-762.

Marhavy, P., Vanstraelen, M., De Rybel, B., Ding, Z.J., Bennett, M.J., Beeckman, T., and Benkova, E. (2013). Auxin reflux between the endodermis and pericycle promotes lateral root initiation. Embo Journal **32,** 149-158.

Marhavý, P., Vanstraelen, M., De Rybel, B., Zhaojun, D., Bennett, M.J., Beeckman, T., and Benková, E. (2013). Auxin reflux between the

endodermis and pericycle promotes lateral root initiation. The EMBO Journal **32,** 149-158.

McCann, M.C., Wells, B., and Roberts, K. (1990). Direct visualization of cross-links in the primary plant cell wall. Journal of Cell Science **96,** 323-334.

McQueen-Mason, S., Durachko, D.M., and Cosgrove, D.J. (1992). Two endogenous proteins that induce cell wall extension in plants. Plant Cell **4,** 1425-1433.

McQueen-Mason, S.J., and Cosgrove, D.J. (1995). Expansin mode of action on cell walls. Analysis of wall hydrolysis, stress relaxation, and binding. Plant Physiol **107,** 87-100.

Mellerowicz, E.J., Baucher, M., Sundberg, B., and Boerjan, W. (2001). Unravelling cell wall formation in the woody dicot stem. Plant Mol Biol **47,** 239-274.

Meng, L., Buchanan, B.B., Feldman, L.J., and Luan, S. (2012). CLE-like (CLEL) peptides control the pattern of root growth and lateral root development in Arabidopsis. Proceedings of the National Academy of Sciences **109,** 1760-1765.

Moreno-Risueno, M.A., Van Norman, J.M., Moreno, A., Zhang, J., Ahnert, S.E., and Benfey, P.N. (2010a). Oscillating Gene Expression Determines Competence for Periodic Arabidopsis Root Branching. Science **329,** 1306-1311.

Moreno-Risueno, M.A., Van Norman, J.M., Moreno, A., Zhang, J.Y., Ahnert, S.E., and Benfey, P.N. (2010b). Oscillating Gene Expression Determines Competence for Periodic Arabidopsis Root Branching. Science **329,** 1306-1311.

Mravec, J., Kubeš, M., Bielach, A., Gaykova, V., Petrášek, J., Skůpa, P., Chand, S., Benková, E., Zažímalová, E., and Friml, J. (2008). Interaction of PIN and PGP transport mechanisms in auxin distribution-dependent development. Development **135,** 3345-3354.

Murphy, E., Vu, L.D., Van den Broeck, L., Lin, Z., Ramakrishna, P., van de Cotte, B., Gaudinier, A., Goh, T., Slane, D., Beeckman, T., Inzé, D., Brady, S.M., Fukaki, H., and De Smet, I. (2016). RALFL34 regulates formative cell divisions in Arabidopsis pericycle during lateral root initiation. Journal of Experimental Botany.

Muto, H., Watahiki, M.K., Nakamoto, D., Kinjo, M., and Yamamoto, K.T. (2007). Specificity and Similarity of Functions of the Aux/IAA Genes in Auxin Signaling of Arabidopsis Revealed by Promoter-Exchange Experiments among MSG2/IAA19, AXR2/IAA7, and SLR/IAA14. Plant physiology **144,** 187-196.

Nakajima, K., Sena, G., Nawy, T., and Benfey, P.N. (2001). Intercellular movement of the putative transcription factor SHR in root patterning. Nature **413,** 307-311.

Nikolaidis, N., Doran, N., and Cosgrove, D.J. (2014). Plant expansins in bacteria and fungi: evolution by horizontal gene transfer and independent domain fusion. Molecular biology and evolution **31,** 376-386.

Noh, S.A., Lee, H.S., Kim, Y.S., Paek, K.H., Shin, J.S., and Bae, J.M. (2013). Down-regulation of the IbEXP1 gene enhanced storage root development in sweetpotato. J Exp Bot **64,** 129-142.

Norman Earnst. Borlaug. (1970). The green revolution, peace and humanity.

Ochiai, M., Matsumoto, S., and Yamada, K. (2013). Methyl jasmonate treatment promotes flower opening of cut Eustoma by inducing cell wall loosening proteins in petals. Postharvest Biol Tec **82,** 1-5.

Ochiai, M., Takagaki, N., Takahashi, R., Fujitani, C., and Yamada, K. (2010). Role of Expansin and XTH during Rose Flower Opening. Acta Hortic **870,** 273-278.

Okumura, K., Goh, T., Toyokura, K., Kasahara, H., Takebayashi, Y., Mimura, T., Kamiya, Y., and Fukaki, H. (2013). GNOM/FEWER ROOTS is Required for the Establishment of an Auxin Response Maximum for Arabidopsis Lateral Root Initiation. Plant and Cell Physiology **54,** 406-417.

Okushima, Y., Fukaki, H., Onoda, M., Theologis, A., and Tasaka, M. (2007a). ARF7 and ARF19 Regulate Lateral Root Formation via Direct Activation of LBD/ASL Genes in Arabidopsis. The Plant Cell Online **19,** 118-130.

Okushima, Y., Fukaki, H., Onoda, M., Theologis, A., and Tasaka, M. (2007b). ARF7 and ARF19 regulate lateral root formation via direct activation of LBD/ASL genes in Arabidopsis. Plant Cell **19,** 118-130.

Okushima, Y., Overvoorde, P.J., Arima, K., Alonso, J.M., Chan, A., Chang, C., Ecker, J.R., Hughes, B., Lui, A., Nguyen, D., Onodera, C., Quach, H., Smith, A., Yu, G., and Theologis, A. (2005). Functional genomic analysis of the AUXIN RESPONSE FACTOR gene family members in Arabidopsis thaliana: unique and overlapping functions of ARF7 and ARF19. Plant Cell **17,** 444-463.

Olarte-Lozano, M., Mendoza-Nunez, M.A., Pastor, N., Segovia, L., Folch-Mallol, J., and Martinez-Anaya, C. (2014). PcExl1 a novel acid expansin-like protein from the plant pathogen Pectobacterium carotovorum, binds cell walls differently to BsEXLX1. PloS one **9,** e95638.

Orman-Ligeza, B., Parizot, B., de Rycke, R., Fernandez, A., Himschoot, E., and Van Breusegem, F. (2016). RBOH-mediated ROS production facilitates lateral root emergence in Arabidopsis.

Ouyang, K.X., Liu, M.Q., Pian, R.Q., Liu, S.S., and Chen, X.Y. (2013). Isolation and analysis of alpha-expansin genes in the tree Anthocephalus chinensis (Rubiaceae). Genetics and molecular research : GMR **12,** 1061-1073.

Overvoorde, P., Fukaki, H., and Beeckman, T. (2010a). Auxin Control of Root Development. Cold Spring Harbor Perspectives in Biology **2**.

Overvoorde, P., Fukaki, H., and Beeckman, T. (2010b). Auxin control of root development. Cold Spring Harb Perspect Biol **2,** a001537.

Parizot, B., De Rybel, B., and Beeckman, T. (2010). VisuaLRTC: A New View on Lateral Root Initiation by Combining Specific Transcriptome Data Sets. Plant physiology **153,** 34-40.

Parizot, B., Roberts, I., Raes, J., Beeckman, T., and De Smet, I. (2012). In silico analyses of pericycle cell populations reinforce their relation with associated vasculature in Arabidopsis. Philosophical Transactions of the Royal Society B: Biological Sciences **367,** 1479-1488.

Parizot, B., Laplaze, L., Ricaud, L., Boucheron-Dubuisson, E., Bayle, V., Bonke, M., De Smet, I., Poethig, S.R., Helariutta, Y., Haseloff, J., Chriqui, D., Beeckman, T., and Nussaume, L. (2008). Diarch Symmetry of the Vascular Bundle in Arabidopsis Root Encompasses the Pericycle and Is Reflected in Distich Lateral Root Initiation. Plant physiology **146,** 140-148.

Park, C.H., Kim, T.W., Son, S.H., Hwang, J.Y., Lee, S.C., Chang, S.C., Kim, S.H., Kim, S.W., and Kim, S.K. (2010). Brassinosteroids control AtEXPA5 gene expression in Arabidopsis thaliana. Phytochemistry **71,** 380-387.

Park, Y.B., and Cosgrove, D.J. (2012). Changes in cell wall biomechanical properties in the xyloglucan-deficient xxt1/xxt2 mutant of Arabidopsis. Plant Physiol **158,** 465-475.

Park, Y.B., and Cosgrove, D.J. (2015). Xyloglucan and its interactions with other components of the growing cell wall. Plant Cell Physiol **56,** 180-194.

Peaucelle, A., Braybrook, S., and Hofte, H. (2012). Cell wall mechanics and growth control in plants: the role of pectins revisited. Front Plant Sci **3,** 121.

Peaucelle, A., Louvet, R., Johansen, J.N., Höfte, H., Laufs, P., Pelloux, J., and Mouille, G. (2008). Arabidopsis Phyllotaxis Is Controlled by the

Methyl-Esterification Status of Cell-Wall Pectins. Current Biology **18,** 1943-1948.

Perbal, M.C., Haughn, G., Saedler, H., and Schwarz-Sommer, Z. (1996). Non-cell-autonomous function of the Antirrhinum floral homeotic proteins DEFICIENS and GLOBOSA is exerted by their polar cell-to-cell trafficking. Development **122,** 3433-3441.

Peret, B., Larrieu, A., and Bennett, M.J. (2009a). Lateral root emergence: a difficult birth. J Exp Bot **60,** 3637-3643.

Peret, B., De Rybel, B., Casimiro, I., Benkova, E., Swarup, R., Laplaze, L., Beeckman, T., and Bennett, M.J. (2009b). Arabidopsis lateral root development: an emerging story. Trends Plant Sci **14,** 399-408.

Peret, B., Middleton, A.M., French, A.P., Larrieu, A., Bishopp, A., Njo, M., Wells, D.M., Porco, S., Mellor, N., Band, L.R., Casimiro, I., Kleine-Vehn, J., Vanneste, S., Sairanen, I., Mallet, R., Sandberg, G., Ljung, K., Beeckman, T., Benkova, E., Friml, J., Kramer, E., King, J.R., De Smet, I., Pridmore, T., Owen, M., and Bennett, M.J. (2013). Sequential induction of auxin efflux and influx carriers regulates lateral root emergence. Mol Syst Biol **9,** 699.

Petrášek, J., and Friml, J. (2009). Auxin transport routes in plant development. Development **136,** 2675-2688.

Pien, S., Wyrzykowska, J., McQueen-Mason, S., Smart, C., and Fleming, A. (2001). Local expression of expansin induces the entire process of leaf development and modifies leaf shape. Proc Natl Acad Sci U S A **98,** 11812-11817.

Popper, Z.A. (2008). Evolution and diversity of green plant cell walls. Current Opinion in Plant Biology **11,** 286-292.

Popper, Z.A., and Fry, S.C. (2004). Primary cell wall composition of pteridophytes and spermatophytes. New Phytologist **164,** 165-174.

Powell, A.L.T., Kalamaki, M.S., Kurien, P.A., Gurrieri, S., and Bennett, A.B. (2003). Simultaneous Transgenic Suppression of LePG and LeExp1 Influences Fruit Texture and Juice Viscosity in a Fresh Market Tomato Variety. Journal of Agricultural and Food Chemistry **51,** 7450-7455.

Proseus, T.E., and Boyer, J.S. (2006). Periplasm turgor pressure controls wall deposition and assembly in growing Chara corallina cells. Annals of botany **98,** 93-105.

Péret, B., De Rybel, B., Casimiro, I., Benková, E., Swarup, R., Laplaze, L., Beeckman, T., and Bennett, M.J. (2009). Arabidopsis lateral root development: an emerging story. Trends in Plant Science **14,** 399-408.

Péret, B., Li, G., Zhao, J., Band, L.R., Voß, U., Postaire, O., Luu, D.-T., Da Ines, O., Casimiro, I., Lucas, M., Wells, D.M., Lazzerini, L., Nacry, P.,

King, J.R., Jensen, O.E., Schäffner, A.R., Maurel, C., and Bennett, M.J. (2012). Auxin regulates aquaporin function to facilitate lateral root emergence. Nat Cell Biol **14,** 991-998.

Qiu, S., Ma, N., Che, S., Wang, Y., Peng, X., Zhang, G., Wang, G., and Huang, J. (2014). Repression of OsEXPA3 Expression Leads to Root System Growth Suppression in Rice. Crop Sci. **54,** 2201-2213.

Rasmussen, C.G., Humphries, J.A., and Smith, L.G. (2011). Determination of Symmetric and Asymmetric Division Planes in Plant Cells. Annual Review of Plant Biology **62,** 387-409.

Raven, J.A. (1975). TRANSPORT OF INDOLEACETIC ACID IN PLANT CELLS IN RELATION TO pH AND ELECTRICAL POTENTIAL GRADIENTS, AND ITS SIGNIFICANCE FOR POLAR IAA TRANSPORT. New Phytologist **74,** 163-172.

Rayle, D.L., and Cleland, R.E. (1992). The Acid Growth Theory of auxin-induced cell elongation is alive and well. Plant Physiol **99,** 1271-1274.

Reinhardt, D., Wittwer, F., Mandel, T., and Kuhlemeier, C. (1998a). Localized upregulation of a new expansin gene predicts the site of leaf formation in the tomato meristem. The Plant cell **10,** 1427-1437.

Reinhardt, D., Wittwer, F., Mandel, T., and Kuhlemeier, C. (1998b). Localized Upregulation of a New Expansin Gene Predicts the Site of Leaf Formation in the Tomato Meristem. The Plant Cell **10,** 1427-1437.

Ren, H., Santner, A., Pozo, J.C.d., Murray, J.A.H., and Estelle, M. (2008). Degradation of the cyclin-dependent kinase inhibitor KRP1 is regulated by two different ubiquitin E3 ligases. The Plant Journal **53,** 705-716.

Rochange, S.F., Wenzel, C.L., and McQueen-Mason, S.J. (2001). Impaired growth in transgenic plants over-expressing an expansin isoform. Plant Mol Biol **46,** 581-589.

Rodriguez, R.E., Debernardi, J.M., and Palatnik, J.F. (2014). Morphogenesis of simple leaves: regulation of leaf size and shape. Wiley Interdisciplinary Reviews: Developmental Biology **3,** 41-57.

Rogg, L.E., Lasswell, J., and Bartel, B. (2001). A Gain-of-Function Mutation in IAA28 Suppresses Lateral Root Development. The Plant Cell Online **13,** 465-480.

Rose, J.K., Lee, H.H., and Bennett, A.B. (1997). Expression of a divergent expansin gene is fruit-specific and ripening-regulated. Proc Natl Acad Sci U S A **94,** 5955-5960.

Rose, J.K., Braam, J., Fry, S.C., and Nishitani, K. (2002). The XTH family of enzymes involved in xyloglucan endotransglucosylation and endohydrolysis: current perspectives and a new unifying nomenclature. Plant Cell Physiol **43,** 1421-1435.

Rose, J.K., Cosgrove, D.J., Albersheim, P., Darvill, A.G., and Bennett, A.B. (2000). Detection of expansin proteins and activity during tomato fruit ontogeny. Plant Physiol **123,** 1583-1592.

Roudier, F., Fernandez, A.G., Fujita, M., Himmelspach, R., Borner, G.H., Schindelman, G., Song, S., Baskin, T.I., Dupree, P., Wasteneys, G.O., and Benfey, P.N. (2005). COBRA, an Arabidopsis extracellular glycosyl-phosphatidyl inositol-anchored protein, specifically controls highly anisotropic expansion through its involvement in cellulose microfibril orientation. Plant Cell **17,** 1749-1763.

Roycewicz, P.S., and Malamy, J.E. (2014). Cell wall properties play an important role in the emergence of lateral root primordia from the parent root. J Exp Bot **65,** 2057-2069.

Saeman, J.F., Bubl, J.L., and Harris, E.E. (1945). Quantitative Saccharification of Wood and Cellulose. Industrial & Engineering Chemistry Analytical Edition **17,** 35-37.

Saloheimo, M., Paloheimo, M., Hakola, S., Pere, J., Swanson, B., Nyyssönen, E., Bhatia, A., Ward, M., and Penttilä, M. (2002). Swollenin, a Trichoderma reesei protein with sequence similarity to the plant expansins, exhibits disruption activity on cellulosic materials. European Journal of Biochemistry **269,** 4202-4211.

Sampedro, J., and Cosgrove, D.J. (2005). The expansin superfamily. Genome Biol **6,** 242.

Sampedro, J., Carey, R.E., and Cosgrove, D.J. (2006). Genome histories clarify evolution of the expansin superfamily: new insights from the poplar genome and pine ESTs. Journal of plant research **119,** 11-21.

Sampedro, J., Lee, Y., Carey, R.E., DePamphilis, C., and Cosgrove, D.J. (2005). Use of genomic history to improve phylogeny and understanding of births and deaths in a gene family. The Plant Journal **44,** 409-419.

Sanz, L., Dewitte, W., Forzani, C., Patell, F., Nieuwland, J., Wen, B., Quelhas, P., De Jager, S., Titmus, C., Campilho, A., Ren, H., Estelle, M., Wang, H., and Murray, J.A.H. (2011). The Arabidopsis D-Type Cyclin CYCD2;1 and the Inhibitor ICK2/KRP2 Modulate Auxin-Induced Lateral Root Formation. The Plant Cell Online **23,** 641-660.

Schindelin, J., Arganda-Carreras, I., Frise, E., Kaynig, V., Longair, M., Pietzsch, T., Preibisch, S., Rueden, C., Saalfeld, S., Schmid, B., Tinevez, J.Y., White, D.J., Hartenstein, V., Eliceiri, K., Tomancak, P., and Cardona, A. (2012). Fiji: an open-source platform for biological-image analysis. Nature methods **9,** 676-682.

Schmidt, M., Schwartzberg, A.M., Carroll, A., Chaibang, A., Adams, P.D., and Schuck, P.J. (2010). Raman imaging of cell wall polymers in

Arabidopsis thaliana. Biochemical and biophysical research communications **395,** 521-523.

Schmidt, R., Schippers, J.H., Mieulet, D., Obata, T., Fernie, A.R., Guiderdoni, E., and Mueller-Roeber, B. (2013). MULTIPASS, a rice R2R3-type MYB transcription factor, regulates adaptive growth by integrating multiple hormonal pathways. The Plant journal : for cell and molecular biology **76,** 258-273.

Schulz, H., and Baranska, M. (2007). Identification and quantification of valuable plant substances by IR and Raman spectroscopy. Vibrational Spectroscopy **43,** 13-25.

Sella Kapu, N.U., and Cosgrove, D.J. (2010). Changes in growth and cell wall extensibility of maize silks following pollination. Journal of Experimental Botany **61,** 4097-4107.

Sene, C., McCann, M.C., Wilson, R.H., and Grinter, R. (1994). Fourier-Transform Raman and Fourier-Transform Infrared Spectroscopy (An Investigation of Five Higher Plant Cell Walls and Their Components). Plant Physiol **106,** 1623-1631.

Silva, A.I.R., Palenius, H.G.N., Guzman, G.H., Solis, A.G.A., Pina, C.G., and Dominguez, J.F.M. (2013). Ripening-related cDNAs in guava fruit (Psidium guajava L.). characterization and expression analysis. Rev Fitotec Mex **36,** 117-125.

Slane, D., Kong, J., Berendzen, K.W., Kilian, J., Henschen, A., Kolb, M., Schmid, M., Harter, K., Mayer, U., De Smet, I., Bayer, M., and Jurgens, G. (2014). Cell type-specific transcriptome analysis in the early Arabidopsis thaliana embryo. Development **141,** 4831-4840.

Sloan, J., Backhaus, A., Malinowski, R., McQueen-Mason, S., and Fleming, A.J. (2009). Phased control of expansin activity during leaf development identifies a sensitivity window for expansin-mediated induction of leaf growth. Plant Physiol **151,** 1844-1854.

Soltys, D., Rudzinska-Langwald, A., Gniazdowska, A., Wisniewska, A., and Bogatek, R. (2012). Inhibition of tomato (Solanum lycopersicum L.) root growth by cyanamide is due to altered cell division, phytohormone balance and expansin gene expression. Planta **236,** 1629-1638.

Son, S.H., Chang, S.C., Park, C.H., and Kim, S.K. (2012). Ethylene negatively regulates EXPA5 expression in Arabidopsis thaliana. Physiol Plant **144,** 254-262.

Stamm, P., Ravindran, P., Mohanty, B., Tan, E., Yu, H., and Kumar, P. (2012). Insights into the molecular mechanism of RGL2-mediated inhibition of seed germination in Arabidopsis thaliana. BMC plant biology **12,** 179.

Swarup, K., Benkova, E., Swarup, R., Casimiro, I., Peret, B., Yang, Y., Parry, G., Nielsen, E., De Smet, I., Vanneste, S., Levesque, M.P., Carrier, D., James, N., Calvo, V., Ljung, K., Kramer, E., Roberts, R., Graham, N., Marillonnet, S., Patel, K., Jones, J.D.G., Taylor, C.G., Schachtman, D.P., May, S., Sandberg, G., Benfey, P., Friml, J., Kerr, I., Beeckman, T., Laplaze, L., and Bennett, M.J. (2008a). The auxin influx carrier LAX3 promotes lateral root emergence. Nat Cell Biol **10,** 946-954.

Swarup, K., Benkova, E., Swarup, R., Casimiro, I., Peret, B., Yang, Y., Parry, G., Nielsen, E., De Smet, I., Vanneste, S., Levesque, M.P., Carrier, D., James, N., Calvo, V., Ljung, K., Kramer, E., Roberts, R., Graham, N., Marillonnet, S., Patel, K., Jones, J.D.G., Taylor, C.G., Schachtman, D.P., May, S., Sandberg, G., Benfey, P., Friml, J., Kerr, I., Beeckman, T., Laplaze, L., and Bennett, M.J. (2008b). The auxin influx carrier LAX3 promotes lateral root emergence. Nat Cell Biol **10,** 946-954.

Tabuchi, A., Li, L.C., and Cosgrove, D.J. (2011). Matrix solubilization and cell wall weakening by beta-expansin (group-1 allergen) from maize pollen. The Plant journal : for cell and molecular biology **68,** 546-559.

Takahashi, R., Fujitani, C., Yamaki, S., and Yamada, K. (2007). Analysis of the cell wall loosening proteins during rose flower opening. Proceedings of the International Conference on Quality Management in Supply Chains of Ornamentals **755,** 483-488.

Tatematsu, K., Kumagai, S., Muto, H., Sato, A., Watahiki, M.K., Harper, R.M., Liscum, E., and Yamamoto, K.T. (2004). MASSUGU2 Encodes Aux/IAA19, an Auxin-Regulated Protein That Functions Together with the Transcriptional Activator NPH4/ARF7 to Regulate Differential Growth Responses of Hypocotyl and Formation of Lateral Roots in Arabidopsis thaliana. The Plant Cell Online **16,** 379-393.

Tian, Q., and Reed, J.W. (1999). Control of auxin-regulated root development by the Arabidopsis thaliana SHY2/IAA3 gene. Development **126,** 711-721.

Toledo-Ortiz, G., Huq, E., and Quail, P.H. (2003). The Arabidopsis Basic/Helix-Loop-Helix Transcription Factor Family. The Plant Cell Online **15,** 1749-1770.

Tovar-Herrera, O.E., Batista-García, R.A., Sánchez-Carbente, M.d.R., Iracheta-Cárdenas, M.M., Arévalo-Niño, K., and Folch-Mallol, J.L. (2015). A Novel Expansin Protein from the White-Rot Fungus Schizophyllum commune. PloS one **10,** e0122296.

Trivedi, P.K., and Nath, P. (2004). MaExp1, an ethylene-induced expansin from ripening banana fruit. Plant Science **167,** 1351-1358.

Tsukaya, H. (2003). Organ shape and size: a lesson from studies of leaf morphogenesis. Curr Opin Plant Biol **6,** 57-62.

Uehara, T., Okushima, Y., Mimura, T., Tasaka, M., and Fukaki, H. (2008). Domain II Mutations in CRANE/IAA18 Suppress Lateral Root Formation and Affect Shoot Development in Arabidopsis thaliana. Plant and Cell Physiology **49,** 1025-1038.

UNDP. (2016). UNDP support to the implementation of the 2030 agenda for sustainable development.

Valdivia, E.R., Stephenson, A.G., Durachko, D.M., and Cosgrove, D. (2009). Class B beta-expansins are needed for pollen separation and stigma penetration. Sexual plant reproduction **22,** 141-152.

Van Damme, D., De Rybel, B., Gudesblat, G., Demidov, D., Grunewald, W., De Smet, I., Houben, A., Beeckman, T., and Russinova, E. (2011). Arabidopsis α Aurora Kinases Function in Formative Cell Division Plane Orientation. The Plant Cell Online **23,** 4013-4024.

Van Norman, J.M., Xuan, W., Beeckman, T., and Benfey, P.N. (2013). To branch or not to branch: the role of pre-patterning in lateral root formation. Development **140,** 4301-4310.

Van Sandt, V.S., Suslov, D., Verbelen, J.P., and Vissenberg, K. (2007). Xyloglucan endotransglucosylase activity loosens a plant cell wall. Annals of botany **100,** 1467-1473.

Vanden Bossche, R., Demedts, B., Vanderhaeghen, R., and Goossens, A. (2013). Transient expression assays in tobacco protoplasts. Methods in molecular biology (Clifton, N.J.) **1011,** 227-239.

Vannerum, K., Huysman, M.J., De Rycke, R., Vuylsteke, M., Leliaert, F., Pollier, J., Lutz-Meindl, U., Gillard, J., De Veylder, L., Goossens, A., Inze, D., and Vyverman, W. (2011). Transcriptional analysis of cell growth and morphogenesis in the unicellular green alga Micrasterias (Streptophyta), with emphasis on the role of expansin. BMC plant biology **11,** 128.

Vanneste, S., and Friml, J. (2009). Auxin: A Trigger for Change in Plant Development. Cell **136,** 1005-1016.

Vanneste, S., De Rybel, B., Beemster, G.T., Ljung, K., De Smet, I., Van Isterdael, G., Naudts, M., Iida, R., Gruissem, W., Tasaka, M., Inze, D., Fukaki, H., and Beeckman, T. (2005a). Cell cycle progression in the pericycle is not sufficient for SOLITARY ROOT/IAA14-mediated lateral root initiation in Arabidopsis thaliana. Plant Cell **17,** 3035-3050.

Vanneste, S., De Rybel, B., Beemster, G.T.S., Ljung, K., De Smet, I., Van Isterdael, G., Naudts, M., Iida, R., Gruissem, W., Tasaka, M., Inzé, D., Fukaki, H., and Beeckman, T. (2005b). Cell Cycle Progression in the

Pericycle Is Not Sufficient for SOLITARY ROOT/IAA14-Mediated Lateral Root Initiation in Arabidopsis thaliana. The Plant Cell Online **17,** 3035-3050.

Vanneste, S., Coppens, F., Lee, E., Donner, T.J., Xie, Z., Van Isterdael, G., Dhondt, S., De Winter, F., De Rybel, B., Vuylsteke, M., De Veylder, L., Friml, J., Inze, D., Grotewold, E., Scarpella, E., Sack, F., Beemster, G.T.S., and Beeckman, T. (2011). Developmental regulation of CYCA2s contributes to tissue-specific proliferation in Arabidopsis. The EMBO journal **30,** 3430-3441.

Vermeer, J.E., von Wangenheim, D., Barberon, M., Lee, Y., Stelzer, E.H., Maizel, A., and Geldner, N. (2014). A spatial accommodation by neighboring cells is required for organ initiation in Arabidopsis. Science **343,** 178-183.

Vilches-Barro, A., and Maizel, A. (2015). Talking through walls: mechanisms of lateral root emergence in Arabidopsis thaliana. Curr Opin Plant Biol **23,** 31-38.

Vissenberg, K., Fry, S.C., and Verbelen, J.P. (2001). Root hair initiation is coupled to a highly localized increase of xyloglucan endotransglycosylase action in Arabidopsis roots. Plant Physiol **127,** 1125-1135.

Voß, U., Wilson, M.H., Kenobi, K., Gould, P.D., Robertson, F.C., Peer, W.A., Lucas, M., Swarup, K., Casimiro, I., Holman, T.J., Wells, D.M., Péret, B., Goh, T., Fukaki, H., Hodgman, T.C., Laplaze, L., Halliday, K.J., Ljung, K., Murphy, A.S., Hall, A.J., Webb, A.A.R., and Bennett, M.J. (2015). The circadian clock rephases during lateral root organ initiation in Arabidopsis thaliana. Nature Communications **6,** 7641.

Vriezen, W.H., De Graaf, B., Mariani, C., and Voesenek, L.A. (2000). Submergence induces expansin gene expression in flooding-tolerant Rumex palustris and not in flooding-intolerant R. acetosa. Planta **210,** 956-963.

Wada, T., Kurata, T., Tominaga, R., Koshino-Kimura, Y., Tachibana, T., Goto, K., Marks, M.D., Shimura, Y., and Okada, K. (2002). Role of a positive regulator of root hair development, CAPRICE, in Arabidopsis root epidermal cell differentiation. Development **129,** 5409-5419.

Wang, G., Gao, Y., Wang, J., Yang, L., Song, R., Li, X., and Shi, J. (2011). Overexpression of two cambium-abundant Chinese fir (Cunninghamia lanceolata) alpha-expansin genes ClEXPA1 and ClEXPA2 affect growth and development in transgenic tobacco and increase the amount of cellulose in stem cell walls. Plant biotechnology journal **9,** 486-502.

Wang, T., Park, Y.B., Caporini, M.A., Rosay, M., Zhong, L., Cosgrove, D.J., and Hong, M. (2013). Sensitivity-enhanced solid-state NMR detection

of expansin's target in plant cell walls. Proc Natl Acad Sci U S A **110,** 16444-16449.

Wang, Y., Ma, N.N., Qiu, S.C., Zou, H.Y., Zang, G.C., Kang, Z.H., Wang, G.X., and Huang, J.L. (2014). Regulation of the alpha-expansin gene OsEXPA8 expression affects root system architecture in transgenic rice plants. Mol Breeding **34,** 47-57.

Wei, P.C., Zhang, X.Q., Zhao, P., and Wang, X.C. (2011). Regulation of stomatal opening by the guard cell expansin AtEXPA1. Plant Signal Behav **6,** 740-742.

Weijers, D., Franke-van Dijk, M., Vencken, R.J., Quint, A., Hooykaas, P., and Offringa, R. (2001). An Arabidopsis Minute-like phenotype caused by a semi-dominant mutation in a RIBOSOMAL PROTEIN S5 gene. Development **128,** 4289-4299.

Weitbrecht, K., Muller, K., and Leubner-Metzger, G. (2011). First off the mark: early seed germination. J Exp Bot **62,** 3289 - 3309.

Wieczorek, K., and Grundler, F.M. (2006). Expanding nematode-induced syncytia: the role of expansins. Plant Signal Behav **1,** 223-224.

Wieczorek, K., Golecki, B., Gerdes, L., Heinen, P., Szakasits, D., Durachko, D.M., Cosgrove, D.J., Kreil, D.P., Puzio, P.S., Bohlmann, H., and Grundler, F.M. (2006). Expansins are involved in the formation of nematode-induced syncytia in roots of Arabidopsis thaliana. The Plant journal : for cell and molecular biology **48,** 98-112.

Wilmoth, J.C., Wang, S., Tiwari, S.B., Joshi, A.D., Hagen, G., Guilfoyle, T.J., Alonso, J.M., Ecker, J.R., and Reed, J.W. (2005). NPH4/ARF7 and ARF19 promote leaf expansion and auxin-induced lateral root formation. The Plant Journal **43,** 118-130.

Wilson, M.H., Holman, T.J., Sorensen, I., Cancho-Sanchez, E., Wells, D.M., Swarup, R., Knox, J.P., Willats, W.G., Ubeda-Tomas, S., Holdsworth, M., Bennett, M.J., Vissenberg, K., and Hodgman, T.C. (2015). Multi-omics analysis identifies genes mediating the extension of cell walls in the Arabidopsis thaliana root elongation zone. Frontiers in cell and developmental biology **3,** 10.

Xiao, C., Zhang, T., Zheng, Y., Cosgrove, D.J., and Anderson, C.T. (2016). Xyloglucan Deficiency Disrupts Microtubule Stability and Cellulose Biosynthesis in Arabidopsis, Altering Cell Growth and Morphogenesis. Plant Physiology **170,** 234-249.

Xu, P., Cai, X.T., Wang, Y., Xing, L., Chen, Q., and Xiang, C.B. (2014a). HDG11 upregulates cell-wall-loosening protein genes to promote root elongation in Arabidopsis. J Exp Bot **65,** 4285-4295.

Xu, Q., Xu, X., Shi, Y., Xu, J., and Huang, B. (2014b). Transgenic Tobacco Plants Overexpressing a Grass <italic>PpEXP1</italic> Gene Exhibit Enhanced Tolerance to Heat Stress. PloS one **9,** e100792.

Yadav, S.R., Bishopp, A., and Helariutta, Y. (2010). Plant Development: Early Events in Lateral Root Initiation. Current Biology **20,** R843-R845.

Yamada, K., Takahashi, R., Fujitani, C., Mishima, K., Yoshida, M., Joyce, D.C., and Yamaki, S. (2009). Cell Wall Extensibility and Effect of Cell-Wall-Loosening Proteins during Rose Flower Opening. J Jpn Soc Hortic Sci **78,** 242-251.

Yan, A., Wu, M., Yan, L., Hu, R., Ali, I., and Gan, Y. (2014). AtEXP2 is involved in seed germination and abiotic stress response in Arabidopsis. PloS one **9,** e85208.

Yang, E., Yang, S.Y., Lu, W.J., Chen, J.Y., Qu, H.X., Jiang, Y.M., Joyce, D.C., and Duan, X.W. (2010). Effect of nitric oxide on the sensitivity of banana fruit slices to ethylene. J Hortic Sci Biotech **85,** 17-22.

Yennawar, N.H., Li, L.C., Dudzinski, D.M., Tabuchi, A., and Cosgrove, D.J. (2006). Crystal structure and activities of EXPB1 (Zea m 1), a beta-expansin and group-1 pollen allergen from maize. Proc Natl Acad Sci U S A **103,** 14664-14671.

Yoo, S.D., Gao, Z.F., Cantini, C., Loescher, W.H., and van Nocker, S. (2003). Fruit ripening in sour cherry: Changes in expression of genes encoding expansins and other cell-wall-modifying enzymes. J Am Soc Hortic Sci **128,** 16-22.

Yu, Z.M., Kang, B., He, X.W., Lv, S.L., Bai, Y.H., Ding, W.N., Chen, M., Cho, H.T., and Wu, P. (2011). Root hair-specific expansins modulate root hair elongation in rice. Plant Journal **66,** 725-734.

Zenoni, S., Fasoli, M., Tornielli, G.B., Dal Santo, S., Sanson, A., de Groot, P., Sordo, S., Citterio, S., Monti, F., and Pezzotti, M. (2011). Overexpression of PhEXPA1 increases cell size, modifies cell wall polymer composition and affects the timing of axillary meristem development in Petunia hybrida. New Phytol **191,** 662-677.

Zenoni, S., Reale, L., Tornielli, G.B., Lanfaloni, L., Porceddu, A., Ferrarini, A., Moretti, C., Zamboni, A., Speghini, A., Ferranti, F., and Pezzotti, M. (2004). Downregulation of the Petunia hybrida alpha-expansin gene PhEXP1 reduces the amount of crystalline cellulose in cell walls and leads to phenotypic changes in petal limbs. Plant Cell **16,** 295-308.

Zhang, S., Xu, R., Gao, Z., Chen, C., Jiang, Z., and Shu, H. (2014). A genome-wide analysis of the expansin genes in Malus x Domestica. Molecular genetics and genomics : MGG **289,** 225-236.

Zhang, X.-Q., Wei, P.-C., Xiong, Y.-M., Yang, Y., Chen, J., and Wang, X.-C. (2010). Overexpression of the Arabidopsis α-expansin gene AtEXPA1 accelerates stomatal opening by decreasing the volumetric elastic modulus. Plant Cell Reports **30,** 27-36.

Zhang, X.Q., Wei, P.C., Xiong, Y.M., Yang, Y., Chen, J., and Wang, X.C. (2011). Overexpression of the Arabidopsis alpha-expansin gene AtEXPA1 accelerates stomatal opening by decreasing the volumetric elastic modulus. Plant Cell Rep **30,** 27-36.

Zhang, Z.K., Fu, R.S., Huber, D.J., Rao, J.P., Chang, X.X., Hu, M.J., Zhang, Y., and Jiang, N.N. (2012). Expression of Expansin Gene (CDK-Exp3) and Its Modulation by Exogenous Gibberellic Acid During Ripening and Softening of Persimmon Fruit. Hortscience **47,** 378-381.

Zheng, D.S., and Hrazdina, G. (2010). Cloning and characterization of an expansin gene, RiEXP1, and a 1-aminocyclopropane-1-carboxylic acid synthase gene, RiACS1 in ripening fruit of raspberry (Rubus idaeus L.). Plant Science **179,** 133-139.

Zheng, X.L., Jing, G.X., Liu, Y., Jiang, T.J., Jiang, Y.M., and Li, J.R. (2012). Expression of expansin gene, MiExpA1, and activity of galactosidase and polygalacturonase in mango fruit as affected by oxalic acid during storage at room temperature. Food Chem **132,** 849-854.

Zhong, R., and Ye, Z.-H. (2015). Secondary Cell Walls: Biosynthesis, Patterned Deposition and Transcriptional Regulation. Plant and Cell Physiology **56,** 195-214.

Zhu, Y., Wu, N., Song, W., Yin, G., Qin, Y., Yan, Y., and Hu, Y. (2014). Soybean (Glycine max) expansin gene superfamily origins: segmental and tandem duplication events followed by divergent selection among subfamilies. BMC plant biology **14,** 93.

Appendices

Appendix 1: Table of T-DNA lines used in study

Gene	Accession no.	Line	Background	Mutagen
EXPA1	AT1G69530	SALK_010506	Col 0	T-DNA Insertion (Exon)
BHLH49	AT1G68920	SALK_081687	Col 0	T-DNA Insertion (Exon)

Appendix 2: List of primers used in study

Genotyping primers

Gene	Accession no.	Left primer	Right primer
EXPA1	AT1G69530	CAAAGCAGACCACTATGACCC	TGTTCGGTAAGGCGTTGTTAG
BHLH49	AT1G68920	TTGGGCAAACTCTTTGGTATG	TGGCGTTGTAGTGATTGTACG

Primers for *35S::EXPA1::GFP* line

Left primer	Right primer
ATGGCTCTTGTCACCTTC	AGCACTCGAAGCACCACTTC

Primers for translational fusion line *pEXPA1::EXPA1::GFP* (-STOP codon)

Left primer	Right primer
TTCCAAATATAGCATTGGACCGT	AGCACTCGAAGCACCACTT

Primers for translational fusion line *pEXPA1::EXPA1::GFP* (+STOP codon)

Left primer	Right primer
TTCCAAATATAGCATTGGACCGT	AGCACTCGAAGCACCACTT

qPCR primers

Gene	Left primer	Right primer
EXPA1	GATGTCAAGAAACTGGGGACA	GAAAGACCAGCCTGCGTTAG
IAA19	TGATGTACCTTGGGGGATGT	TGAACCAGCTCCTTGCTTCT
bHLH49	CCTCTACCTCATGGATTCATGC	GGATCACATTTTGCAAATCACC
RALFL34	TGGCAGCTTCGTCTCTCAA	TGGAGAGAAATGAAAGTGAGAAGAG

Appendix 3: 'A' tailing of PCR product

Purified PCR product 16.1µl, 10X Taq buffer 2 µl, MgCl2 (50mM) 1 µl, dATP (10mM) 0.4 µl and Taq polymerase 0.5 µl in a 1.5ml microfuge tube. Incubate at 70°C for 30 sec.

Appendix 4: Transformation of chemically competent *E.coli* cells

The chemically competent *E. coli DH5α* cells were thawed on ice. 6µL of the reaction mixture was added and incubated on ice for 30 min. Cells were heat shocked at 42°C for 45sec and transferred on ice for 5min, then 200µL room temp SOC was added to each sample that was then incubated at 37°C, 220 rpm for 1 hour 30 min. They were then plated on LB agar plated containing antibiotics.